OLIGOMERIZATION AND CATALYTIC KETONIZATION IN THE MIXALCO™ PROCESS

A Dissertation

by

SEBASTIAN ANIBAL TACO VASQUEZ

Submitted to the Office of Graduate and Professional Studies of
Texas A&M University
in partial fulfillment of the requirements for the degree of

DOCTOR OF PHILOSOPHY

Chair of Committee,	Mark T. Holtzapple
Committee Members,	Mahmoud El-Halwagi
	Charles Glover
	Sergio Capareda
Head of Department,	M. Nazmul Karim

December 2013

Major Subject: Chemical Engineering

ABSTRACT

This research describes the zeolite use in the oligomerization and catalytic ketonization steps of the MixAlco™ process. In this dissertation, the following six products associated with the MixAlco™ process were studied: acetic acid, mixed acids, acetone, mixed ketones, isopropanol, and mixed alcohols. The effect of the temperature (*T*), weight hourly space velocity (WHSV), type of catalyst, feed composition, and pressure (*P*) were studied.

For the isopropanol and mixed alcohol reactions, the following conditions were used: HZSM-5 (280, moles of silica per mole of alumina = 280), *T* = 300–510°C, WHSV = 0.5–11.5 h^{-1}, and *P* = 101, 5000, and 8000 kPa. The temperature, WHSV, and pressure affect the type of reaction that occurs: *n*-merization, disproportionation, and cracking.

For acetone, the following conditions were used: HZSM-5 (80), *T* = 305–415°C, WHSV = 1.3–11.8 h^{-1}, and *P* = 101 kPa. For mixed ketone, the effect of temperature (*T* = 400–590 °C) was evaluated at *P* = 101 kPa and WHSV = 1.9 h^{-1}. HZSM-5 rapidly deactivated during the ketone reaction.

Medium-molecular-weight olefins (1-hexene, 1-octene and 1-decene) were dimerized using Beta (25) zeolite catalyst in a batch reactor. For the dimerization reaction, the following conditions were used: Beta (25), *T* = 170–270°C, *t* = 7 h, and *P* = 101 kPa. The maximum conversion achieved was 57%.

For the catalytic ketonization of acetic acid and mixed acids, the following conditions were used: ZrO_2 catalyst, *T* = 300–410°C, WHSV = 2.5–8.5 h^{-1}, and *P* = 101

kPa. Acetic acid conversion was 100% at low WHSV and temperatures over 400°C. For mixed acids, maximum conversion was 95%.

This study describes the pilot plant and reports results from an 11-month production campaign transforming paper and chicken manure into gasoline and jet fuel. In total, 100 L of jet fuel were obtained.

Finally, an integrated approach to obtain gasoline and jet fuel in the MixAlco™ process using LINGO optimization software is presented.

DEDICATION

This work is dedicated to my awesome mother, Rina.

ACKNOWLEDGEMENTS

I especially want to thank my advisor, Dr. Mark Holtzapple, for his guidance during my studies at Texas A&M. Under his supervision, he has encouraged me greatly. I admire him for his wide understanding of science and technology, and also his kindness and sincerity. As well, I admire his perseverance and words of encouragement. It would have been impossible to complete this work without his inspiration and support.

I was delighted to interact with Dr. John Dunkleman. He was always accessible and willing to help me with this project. He has provided assistance in numerous ways such as fixing the equipment, suggesting new ideas for the project, and providing support. As well, during all this time, we have become good friends.

I would like to thank my thesis committee members Dr. Mahmoud El-Halwagi, Dr. Charles Glover, and Dr. Sergio Capareda for their helpful comments and suggestions. I extend my appreciation to Dr. Melinda Wales for all her support in running the lab.

I am grateful for all the members of my laboratory group (Austin Bond, Swades K. Chaudhurib, Michael Landoll). They have always been kind and willing to help me at all times. I specially want to thank my student workers: David Graf, Emmanuel Nieves, Felipe Huertas, Jia Wen Yu, Lilibeth Orozco, Patty Lynn, Rodrigo Beneddetti, Sami Abassi, and Sebastian Carmona.

I am forever indebted to my parents and my sister for their understanding, endless patience, and encouragement when it was most required. I am so grateful to my mother Rina who encouraged me and cared for me all my life.

Furthermore, Pastor Clyde Wilton has always been a constant source of encouragement during my graduate studies. “The ways of the Lord are always the best” and “love is always the superior way” are among his teachings that gave me a new perspective on life.

Last, but not least, thanks be to my Lord Jesus Christ. He, who through his spirit, gave me strength and peace during all my life.

TABLE OF CONTENTS

Page

LIST OF FIGURES

Page

LIST OF TABLES

Page

1. INTRODUCTION AND LITERATURE REVIEW

High global demand for fuels and the depletion of fossil fuels have motivated research into renewable fuels. Lignocellulosic biomass is one of the most abundant and sustainable sources of liquid fuels. One option for converting lignocellulosic biomass to liquid fuels is the MixAlco™ Process (Figure 1-1), which uses the following steps: pretreatment, fermentation, descumming, dewatering, ketonization, alcoholization, and oligomerization.[1–3] Depending how many steps are employed, the final product is ketones, alcohols, or hydrocarbons. Potential biomass feedstocks include municipal solid waste, animal manure, and energy crops.[4–8]

The MixAlco™ process is a version of the carboxylate platform that does not require sterilization to obtain fuels.[9] Using a fermentation process similar to that which occurs in the rumen of cattle, the biomass is converted to mixed acids (e.g., acetic, propionic, butyric acid). Using a buffer (e.g., calcium carbonate), these acids are neutralized to their corresponding carboxylate salts, which are subsequently chemically transformed into a variety of industrial chemicals (e.g., acetone, isopropanol) or fuels (e.g., gasoline, jet fuel).

Many options exist, such as the production of liquid hydrocarbons from tar sands, shale, coal, or natural gas. All of these options are based on fossil fuels, which are a finite resource. Further, the combustion of fossil fuels accumulates carbon dioxide into the atmosphere, which is implicated in global warming.

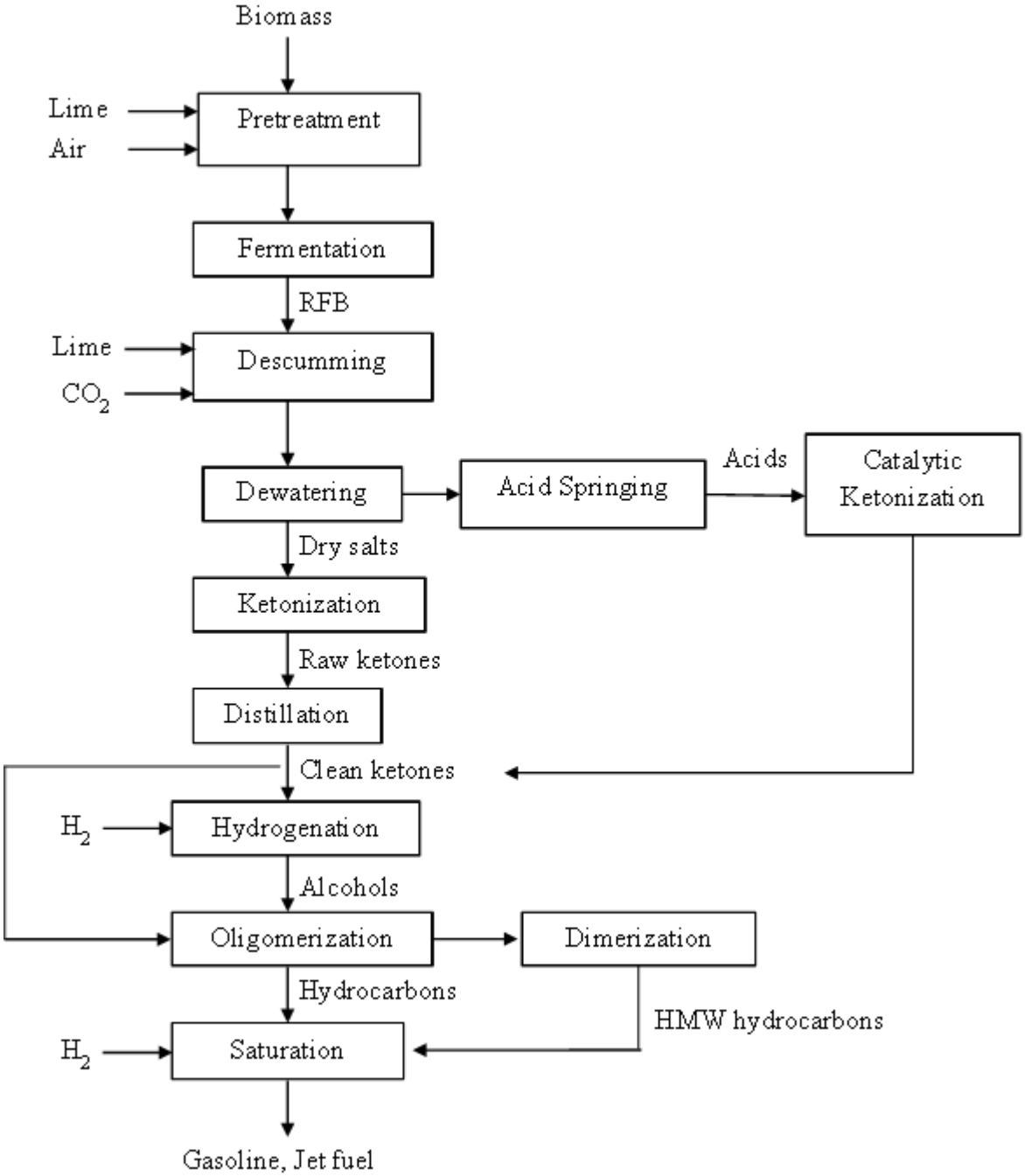

Figure 1-1. Simplified process block diagram of the MixAlco™ process. (RFB = raw fermentation broth.)

The production of liquid transportation fuels from biomass is an attractive alternative because its combustion does not contribute net carbon dioxide to the environment. Currently, at a commercial scale, sugarcane (Brazil) and corn (United States) are converted to ethanol. As a stop-gap measure, this is acceptable; however, it is not a viable long-term solution. Both these approaches use food as a feedstock, which raises food prices. Per-hectare yields of fuel are relatively low, thus requiring excessive land area to meet the large demand for liquid transportation fuels. Ethanol is a less-than-ideal fuel because it has a low energy content compared to hydrocarbons. Because it is hydroscopic, it cannot be shipped through common-carrier pipelines and thus requires special handling. Common engines are not able to combust fuel that contains more than about 10% ethanol, so there is a limit to the amount that can be incorporated into the fuel supply without major overhaul of the transportation infrastructure.

Rather than using food as feedstock for producing biofuels, lignocellulose is a superior alternative. Examples of lignocellulose are wood and grasses, which typically contain cellulose (38–50%), hemicellulose (23–32%), and lignin (15–30%). Some lignocellulose feedstocks (e.g., poplar, energy cane, miscanthus, sorghum) have very high per-hectare yields. Also, lignocellulose is a common component of waste streams, such as municipal solid waste, sewage sludge, manure, and agriculture residues.

Ideally, rather than converting lignocellulose to ethanol, it would be converted to hydrocarbons that are similar to those currently produced from fossil fuels, which would be completely compatible with our current infrastructure. One option is the MixAlco™ process, which converts lignocellulose into hydrocarbon fuels (e.g., gasoline).

Preliminary economic studies indicate that bio-gasoline can be sold for $2.56/gal ($0.68/L) in a base-case scenario.[1] The selling price can range from $1.25/gal ($0.33/L) to $3.75/gal ($0.99/L), depending upon assumptions.

Gasoline hydrocarbons include paraffins, isoparaffins, naphthenes, and aromatics.[10] The carbon number ranges from C5 to C11 with C8 the most abundant.[11] Gasoline quality depends not only on the additives and octane number; but also, on the carbon distribution and type of hydrocarbon mixture. Figure 1-2 shows the hydrocarbon type distribution of three grades of gasoline: regular, plus and power gasoline. Power gasoline contains 42 wt% isoparaffins; whereas, regular gasoline contains 25 wt%. On the other hand, regular gasoline has more aromatics (54 wt%) than power gasoline (41 wt%). For the different grades of gasolines, the carbon distribution differs slightly (Figure 1-3). The carbon distribution of regular gasoline is centered on C9; whereas power gasoline is centered on C8. Overall, the type of hydrocarbons and carbon distribution are important to determine the quality of the gasoline. Jet fuel hydrocarbons include aromatics (25 wt%), paraffins (38 wt%), isoparaffins (29 wt%), and naphthenes (7 wt%). The carbon number ranges from C8 to C14 with C11 the most abundant.[12]Appendix B has a more detailed analysis of commercial gasolines and jet fuel.

This dissertation focuses on oligomerization of alcohols and ketones to obtain hydrocarbons, dimerization of olefins to obtain high-molecular-weight hydrocarbons, catalytic ketonization, and an integrated approach to obtain fuels using the MixAlco™ process. Figure 1-4 shows the steps in red-colored boxes that were the focus for this

study. The overall objectives are to economically produce hydrocarbons similar to commercial fuel (gasoline, jet fuel) with high yields.

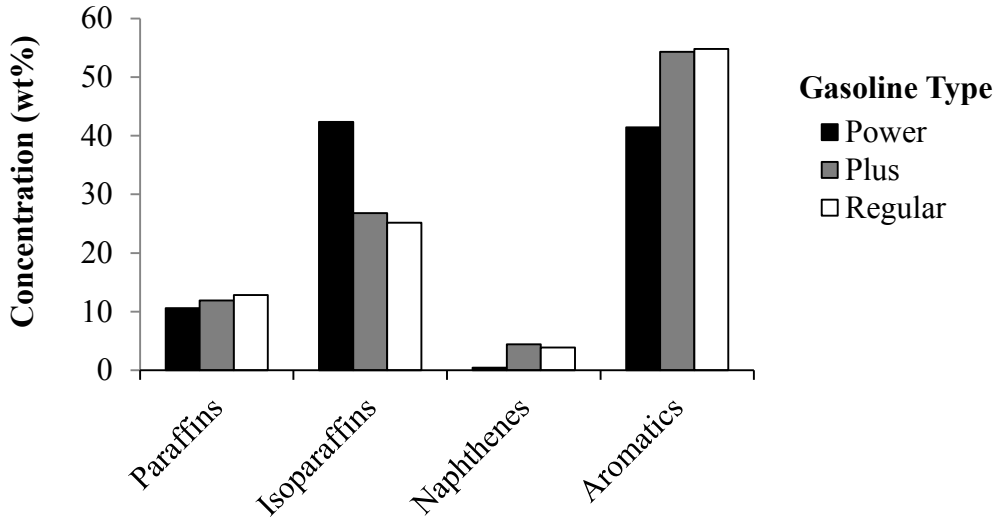

Figure 1-2. Hydrocarbon distribution of commercial gasoline from a Shell gas station taken in February 2009.

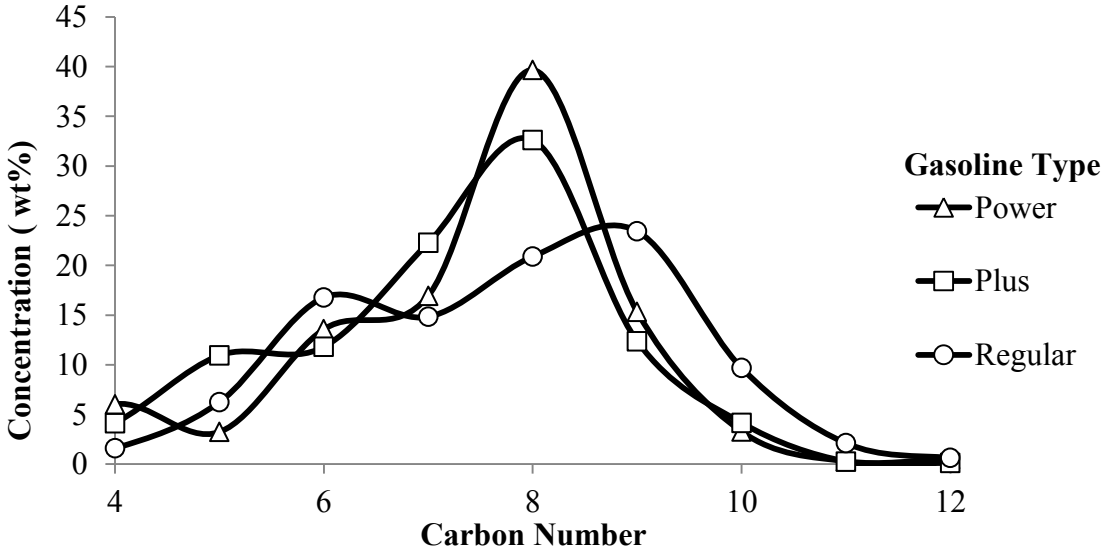

Figure 1-3. Carbon distribution of commercial gasoline from a Shell gas station taken in February 2009.

This dissertation has nine sections:

Section 1 is the introduction and literature review.

Section 2 describes the experimental procedure and focuses on the reaction of isopropanol and mixed alcohols over HZSM-5 (280) catalyst in a packed-bed reactor. It investigates the effects of temperature, weight hourly space velocity (WHSV). Section II also shows the effect of scaling up the reactor.

Section 3 describes the experimental procedure and focuses on the reaction of isopropanol and mixed alcohols over HZSM-5 (280) catalyst in a packed-bed reactor at high pressure. It investigates the effects of temperature, and weight hourly space velocity (WHSV).

Section 4 describes the experimental procedure and focuses on the reaction of acetone and mixed ketones over HZSM-5 catalyst in a packed-bed reactor. It investigates the effects of temperature and WHSV.

Section 5 describes the experimental procedure and focuses on the dimerization reaction of olefins (e.g., 1-hexene, 1-octene, and 1-decene) over Beta (25) catalyst in a batch reactor. It investigates the effects of temperature and time on stream (T.O.S.).

Section 6 describes the pilot plant and reports results from an 11-month production campaign that converted paper and chicken manure into hydrocarbons using the MixAlco™ process.

Section 7 describes the experimental procedure and focuses on the reaction of acetic acid and mixed acids over zircounium oxide catalyst in a packed-bed reactor. It investigates the effects of temperature, and WHSV.

Section 8 shows integrated approaches to obtain gasoline or jet fuel using LINGO optimization software and future studies for this research.

Section 9 presents the conclusions and recommendation for this research.

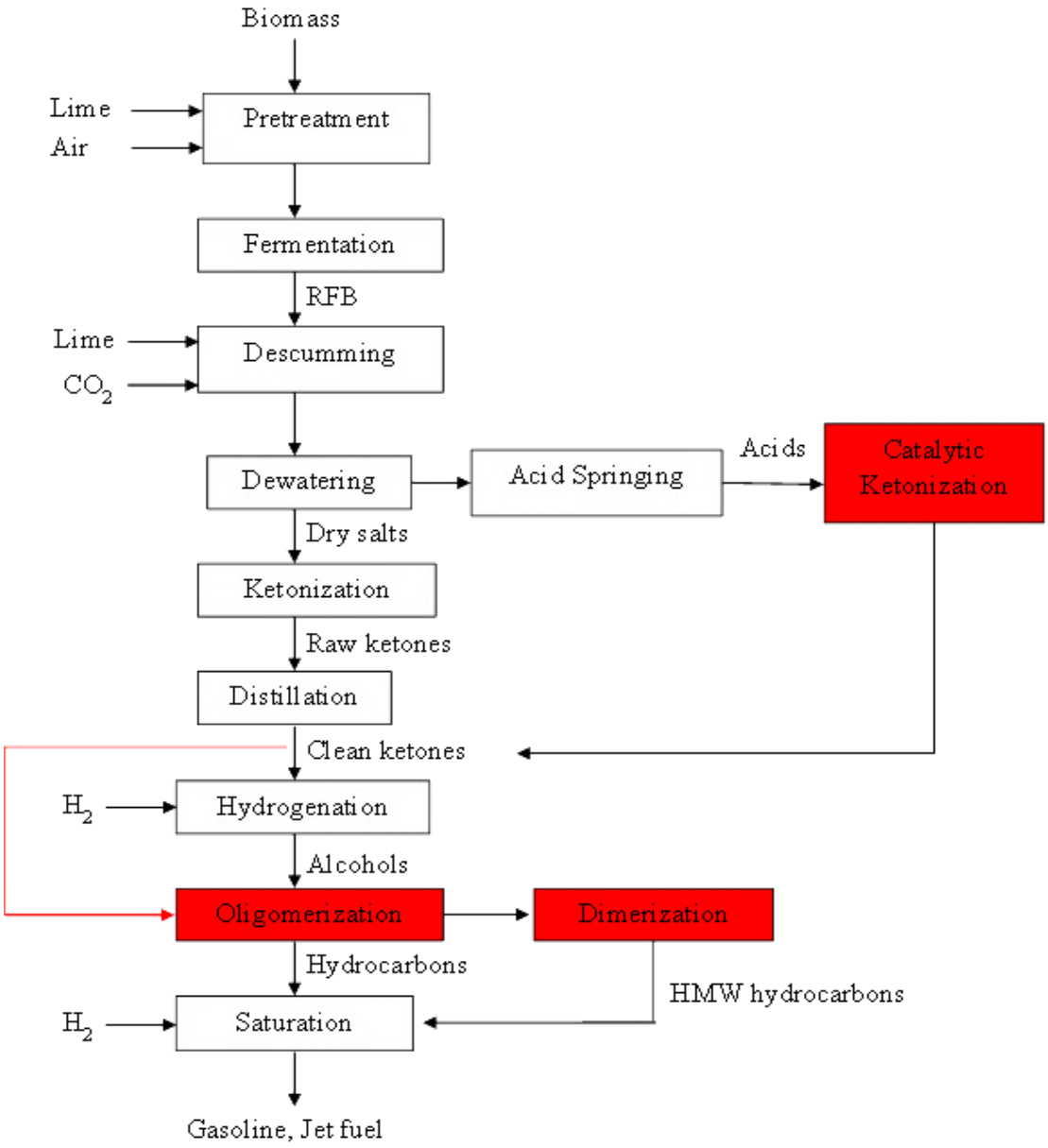

Figure 1-4. Simplified process block diagram of the MixAlco™ process. (Red-colored boxes represent the processes that were the focus for this dissertation.)

2. ALCOHOL OLIGOMERIZATION AT ATMOSPHERIC PRESSURE

The objectives of this section follow:

a) Describe the transformation of isopropanol and mixed alcohol to hydrocarbons at atmospheric pressure.

b) Evaluate the scaling up of the oligomerization reactor.

2.1 Introduction

This section explores oligomerization, the last step of the MixAlco™ process. The objective is to convert alcohols to hydrocarbons similar to commercial fuel (gasoline, jet fuel) using a solid catalyst in a packed-bed reactor.

Beginning with the discovery of the methanol-to-olefin (MTO) process by Mobil in 1977, methanol conversion to hydrocarbons studies employed HZSM-5 catalyst, a medium-pore zeolite with channel size ~0.54 nm.[13–16] Before the discovery of MTO, alcohols could only be dehydrated, but were not oligomerized to produce an olefin mixture. For instance, Komarewsky et al. (1944) dehydrated 1-hexanol and 1-octanol to 1-hexene and 1-octene, respectively, using alumina catalyst. [17]

Chang and Silvestri published the first experimental results showing the effectiveness of HZSM-5 catalyst for converting methanol to gasoline. The reaction products were hydrocarbons (C1–C11) and dimethyl ether.

HZSM-5 is an aluminosilicate zeolite catalyst composed of AlO_4 and SiO_4 tetrahedra interconnected through shared oxygen atoms (Figure 2-1). “H” stands for the cation name, “Z” stands for zeolite, the “SM” stands for Socony-Mobil, and “5” is just a

number assigned to denote a structure.[18] The aluminum ion (charge 3+) and silicon ion (charge 4+) interconnect with oxygen atoms and require the addition of a proton. This additional proton gives the zeolite a high level of acidity, which is responsible for its activity. Figure 2-1a shows ammonium ZSM-5, which is the commercial ZSM-5 catalyst. Above 300°C, NH_4^+ ZSM-5 loses ammonia and forms H^+ZSM-5. ZSM-5 is a powder when synthesized; a binder (γ-Al_2O_3) is added to the powder to create a rigid form that withstands attrition, lowers pressure drop, and improves pelletization. It represents 20 wt% in the final form of the catalyst.

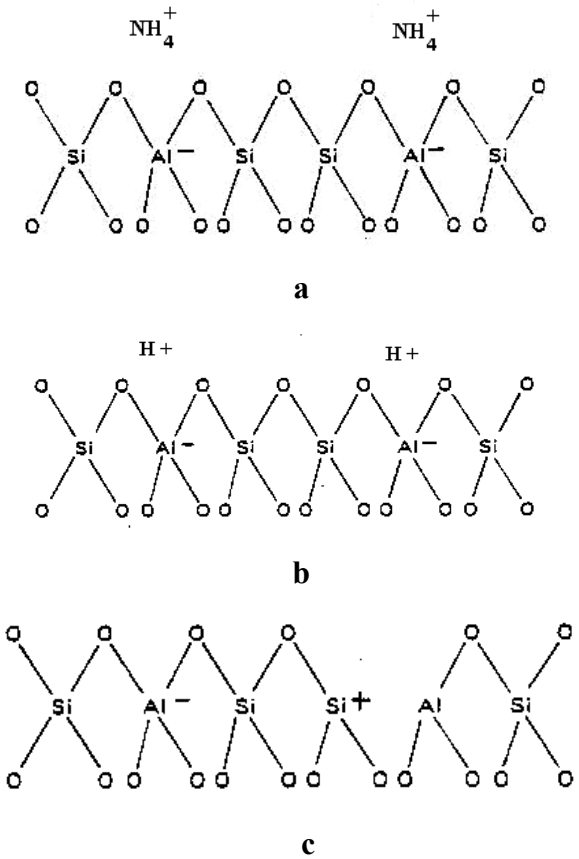

Figure 2-1. Structure of ZSM-5. (a) Structure of NH_4^+ZSM-5. (b) Structure of NH_4^+ZSM-5. (c) Dehydration of HZSM-5 to Lewis Acid.

ZSM-5 has two types of acidity: Bronsted (Figure 2-1b) or Lewis (Figure 2-1c). The dehydration of a Bronsted acid site produces a Lewis acid site. In the production of hydrocarbons, the contribution of the Lewis acidity is considered to be negligible compared to Bronsted acidity. Anderson et al., (1980) showed that the active sites involved in the conversion of methanol on zeolites are Bronsted acids rather than Lewis acids.[18]

The catalyst HZSM-5 is characterized by the silica alumina molar ratio. For example ZSM-5 (80) has 80 moles of silica per mole of alumina. Larger Si/Al ratios are less acidic, and hence less reactive. All of the reactions are catalyzed by acid sites, which are located on the internal surface of the channels of ZSM-5 (acid site density = 0.45 mmol/g-zeolite). About 97% of the acidic sites are inside the channels, and the remaining are on the outside of the zeolite.[19]

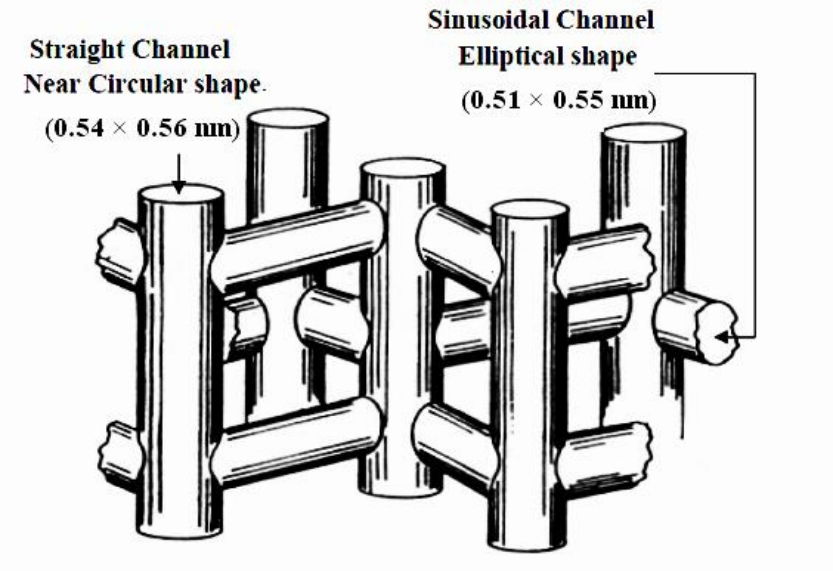

Figure 2-2. Pore structure of HZSM-5 (Figure from Chang, 1983).[16]

Figure 2-2 shows that ZSM-5 zeolite contains two three-dimensional perpendicular intersecting channels with pore openings (10-member ring): (1) sinusoids with cross-sections of approximately 0.51 × 0.55 nm, and (2) straight channels with cross sections of 0.54 × 0.56 nm.[13]

Small-pore zeolites (e.g., erionite, chabazite, zeolite T, ZK-5, sapo-17, and sapo-34) also received attention as catalysts for methanol conversion. The channel size was ~0.34–0.41 nm. The products were mainly light olefins ranging from C1–C4 because the small-pore zeolite was selective to low-molecular-weight hydrocarbon. Large-pore zeolites such as Faujasite-type (e.g., X, Y, modernite ZSM-4) have been applied in the MTO process. Faujasite-type zeolites contain large channel size (~1.3 nm). The reaction products were mainly high-molecular-weight aromatics.[16] For small- and large-pore zeolites, coke formation was rapid; in contrast, medium-pore zeolites have high coke tolerance.[16]

Methanol was not the only oxygenated feedstock studied over zeolite catalyst, but also a number of alcohols, ethers, ketones, aldehydes, carboxylic acids, esters, and cyclic compounds. Chang and Silvestri studied the conversion of 1-butanol, 1-heptanol, acetone, acetic acid, propanal, and *n*-propyl acetate over HZSM-5. Alcohols were easily converted to hydrocarbons and the product distribution was similar to the methanol reaction. Propanal (aldehyde) is efficiently converted to hydrocarbon with high selectivity to aromatics. Acetone undergoes an acid-catalyzed condensation to form mesitylene, a derivative of benzene with three methyl substituents symmetrically placed

on the ring. For acids and esters, dehydration occurs producing ketones and propylene. Then, the ketones react to form mesitylene in an acid-catalyzed condensation.[13]

Fuhse and Bandermann published experimental results of 39 different oxygenated compounds over HZSM-5.[20] The compounds were easily converted to hydrocarbons when the carbon to hydrogen (C/H) ratio of the molecule fragment, remaining after eliminating oxygen as water, is less than 0.62. Figure 2-3 and 2-4 show the product distribution of different alcohols over HZSM-5 (65) at T = 400 °C, WHSV = 0.37 h^{-1}, and P = 101 kPa (abs). For the transformation of alcohols ranging from C2 to C6 to hydrocarbons, the distribution product was the same; therefore, the product depends on the reaction conditions rather than the alcohol feed.

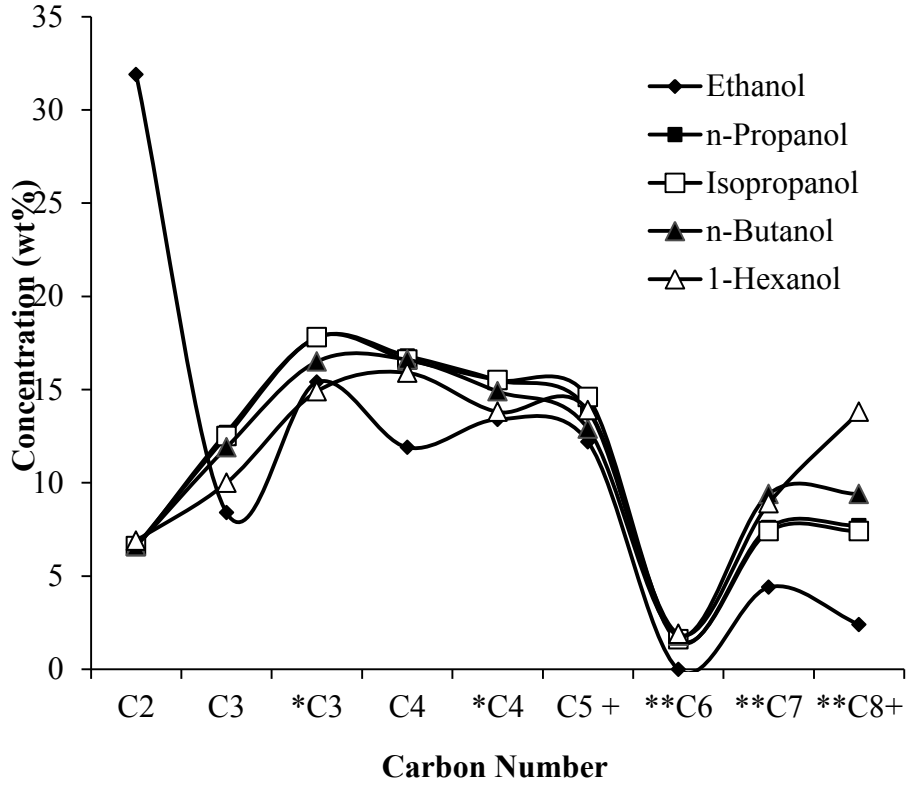

Figure 2-3. Carbon product distribution for different alcohols over HZSM-5 (65) at T = 400 °C, WHSV = 0.37 h^{-1}, and P = 101 kPa (absolute). (* = olefins; ** = aromatics; figure adapted from Fuhse and Friedhelm, 1987).[20]

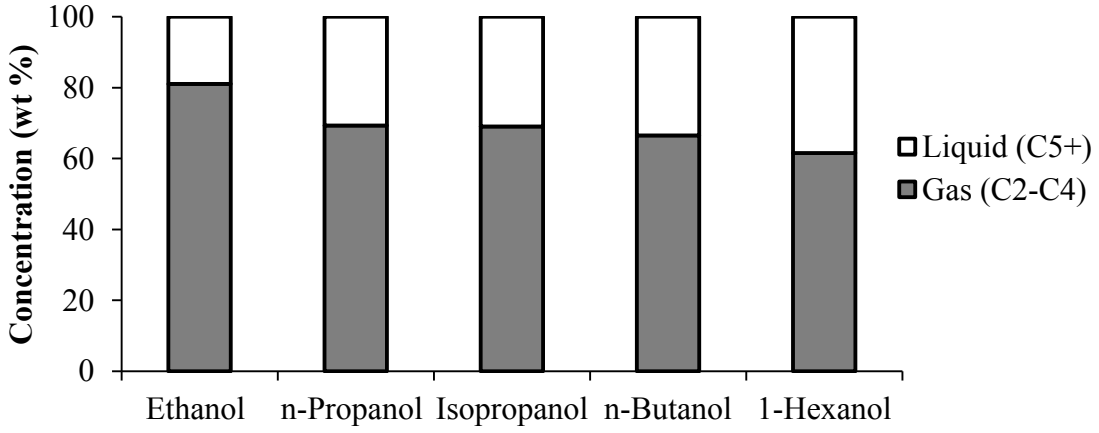

Figure 2-4. Product distribution of gases and liquids for different alcohols over HZSM-5 (65) at WHSV = 0.37 h^{-1}, T = 400 °C, and P = 101 kPa (abs).[20]

Oxygenated compounds derived from biomass were also studied over zeolites. The catalytic transformation of bioethanol to ethene (BETE) and bioethanol to gasoline (BETG) has been studied because sugarcane and bioethanol production has increased since 1950, especially in Brazil and India. Ethanol reaction over zeolites produces mainly ethene with small quantities of other olefins. Gayubo et al. studied the conversion of ethanol over HZSM-5 at different conditions. They studied the effects of temperature, space time, and catalyst activity.[21] At very low space time, ethene was the only product (85%); however, at high space times, ethene dropped drastically (15%) and C5+ olefins increased (50%). Also, they found that temperatures lower than 450 °C resulted in less coking.

Although there is a vast amount of literature about hydrocarbon production from methanol and other alcohols, very few show a detailed compositional analysis of the product. In contrast, this study provides detailed information about the types of liquid-phase hydrocarbons from reagent-grade isopropanol, and also mixed alcohols produced from biomass. The liquid product is characterized by carbon number (C5–C13) and types of products (i.e., paraffins, alcohol, linear and branched olefins, isoparaffins, naphthenes, and aromatics). Also, this dissertation is the first to describe hydrocarbon products resulting from the oligomerization of mixed alcohols made by the MixAlco™ process. HZSM-5 (280) catalyst is selected because it is stable and forms less coke.

2.2 Experimental

For atmospheric pressure, the experiments were conducted in two sets: (1) vary temperature (300–*X* °C) at weight hourly space velocity (WHSV) = 1.31 h^{-1}, and (2)

vary WHSV (0.5–11.5 h^{-1}) at T = 370 °C. For isopropanol, T_{max} = 450 °C and for mixed alcohols T_{max} = 520 °C. Table 2-1 and 2-2 show all the experiments for the isopropanol and mixed alcohol reaction over HZSM-5 (280) at atmospheric pressure, respectively.

Table 2-1. Experiments for the isopropanol reaction over HZSM-5 (280) at atmospheric pressure.

	Catalyst: HZSM-5 (280)					
	WHSV (h^{-1})					
T (°C)	0.5	1.3	1.9	3.7	7.9	11.5
300		I1				
320		I2				
370	I5	I3	I6	I7	I8	I9
410		I4				

Table 2-2. Experiments for the mixed-alcohol reaction over HZSM-5 (280) at atmospheric pressure.

	Catalyst: HZSM-5 (280)					
	WHSV (h^{-1})					
T (°C)	0.5	1.3	1.9	3.7	7.9	11.5
300		MA1				
320		MA2				
370	MA8	MA3	MA9	MA10	MA11	MA12
410		MA4				
450		MA5				
490		MA6				
520		MA7				

2.2.1 Reactor Unit 1

The packed-bed reactor was a stainless steel tube with dimensions 10 mm (i.d.) × 357 mm (long). Commercial HZSM-5 (280) was purchased from Zeolyst International in Malvern, PA (product CBV 28014, SiO_2/Al_2O_3 = 280 mol/mol, surface area = 400 m^2/g 20% alumina binder). The manufacturer supplied cylindrical extruded pellets (diameter = 1.6 mm, length = 3.5 mm), which were packed near the middle section of the reactor. The top and bottom sections of the reactor were filled with α-Al_2O_3 or glass beds as an inert packing before and after the catalytic bed (Figure 2-5). As received, the catalyst had a total acidity (determined by NH_3-TPD) of 0.79 mmol/g in which weak and strong acids were 0.42 and 0.37 mmol/g, respectively.[22] To obtain an acid structure, the catalyst was activated with a N_2 stream at 550 °C for 1 h, which drove off the ammonia.[23]

The reactor unit (Figure 2-6) consists of a packed-bed reactor, a pre-heater, an HPLC pump, mass flow meters, and gas lines for nitrogen and air. The reactor and the pipes are constructed of type-316 stainless steel. Figure 2-7 shows a photograph of the reaction unit.

To vaporize the alcohol feed, the pump injects liquid into the preheater, which operates around 420 °C. Then, the alcohol vapor enters the reactor where it contacts the HZSM-5 catalyst and reacts. Later, the reaction products are heated by heating tape (T = ~200 °C), which ensures that all the products are in the gas phase for the gas chromatograph. Finally, an ice-cooled condenser separates liquid from gas. The gas goes to a vent whereas the liquid is collected for analysis by a gas chromatograph-mass spectrograph.

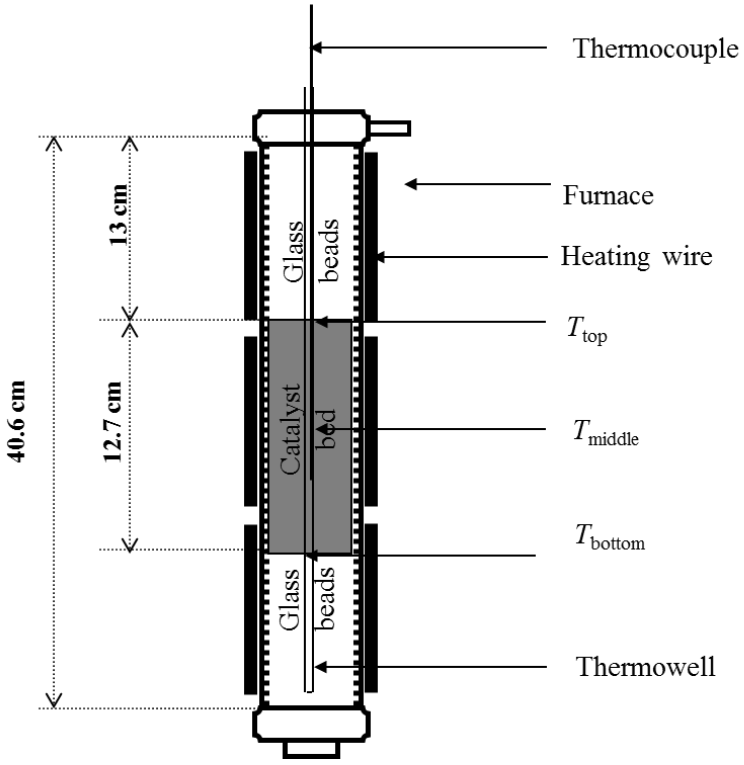

Figure 2-5. Schematic diagram of the reactor bed.

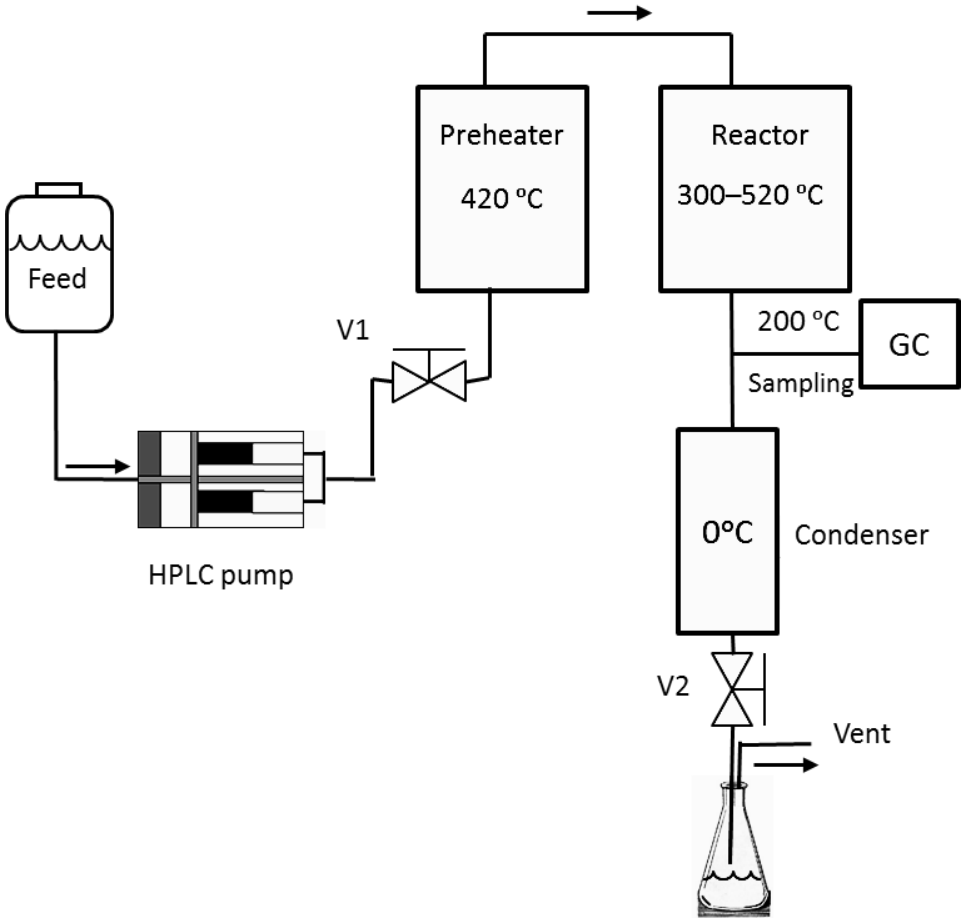

Figure 2-6. Schematic diagram of the Reactor Unit 1.

Figure 2-7. Photograph of the Reactor Unit 1**.**

2.2.2 Product analysis

The reaction products were analyzed by two gas chromatographs: a gas chromatograph (GC) Agilent Technology Model 6890N and gas chromatograph-mass spectrograph (GC-MS) HP Model G1800C. The GC was connected on-line with the reactor. This GC had two detectors: (1) flame ionization detector (FID) and (2) thermal conductivity detector (TCD). The TCD analyzed light hydrocarbon products (C1–C4),

CO, CO_2, and water. The FID analyzed heavier hydrocarbons (C5–C13). Appendix A shows more detailed explanation about the GC analysis.

All the reaction products were analyzed with this chromatograph; however, heavier hydrocarbons (C5–C13) were lumped by carbon number. To identify all the isomers in the liquid phase, the GC-MS analyzed the liquid product samples. Before the analysis, all reaction products were cooled to 0 °C to ensure that all C5+ hydrocarbons were in the liquid phase. A GC-MS analysis of the liquid phase typically determined that the liquid samples had over 100 compounds.

2.2.3 Isopropanol

Reagent-grade isopropanol (99% pure) was obtained from Mallinckrodt Chemicals (Phillipsburg, NJ).

2.2.4 Mixed alcohol

Mixed alcohols were made in the pilot-scale MixAlco™ process located at Texas A&M University (Figure 1-1). Section 6 has a more detailed procedure of the steps followed to obtain mixed alcohol. Mixed alcohols are transparent with odor similar to isopropanol.

2.3 Results

The reaction of isopropanol and mixed alcohols over HZSM-5 is exothermic. Compared to the inlet temperature, the reactor temperature increased about 40 °C.

The alcohols react to form hydrocarbons and water

$$R\text{-}OH \rightarrow [CH_2]_n + H_2O$$

where [CH_2] represents hydrocarbons, such as olefins, paraffins, naphthenes, and aromatics. The product distribution ranged from C3 hydrocarbons (e.g., propene) to C13 hydrocarbons (e.g., 6-tridecene).

The alcohol feed rate is characterized by the weight hourly space velocity (WHSV), which is defined as the weight of feed per hour per unit weight of catalyst loaded in the reactor.

$$\text{WHSV} \equiv \frac{\dot{m}_{feed}}{m_{catalyst}}$$

where

$\dot{m}_{feed}$ = mass flow rate to the reactor (g/h)

$m_{catalyst}$ = mass of catalyst (g)

For example, if the feed rate is 10 g per hour to the reactor and 10 g of catalyst is loaded in the reactor, the WHSV is 1.0 h^{-1}.

2.3.1 Isopropanol at atmospheric pressure

2.3.1.1 Catalyst stability

For the isopropanol reaction, Figure 2-8 shows gas and liquid product distribution over HZSM-5 during T.O.S. During the first 360 min, the product concentration was always constant; therefore, the catalyst did not deactivate during this time. The C4 olefins include 1-butene and isobutylene, whereas C4 paraffins include butane and isobutane. C5+ products were lumped together as liquids. For all experiments of varying temperatures and WHSV, the reported concentrations were the average of all values recorded during T.O.S = 6 h. Approximately eight samples were

measured for each temperature and WHSV; therefore, the average of those eight samples are represented in the figures varying temperatures and WHSV. For instance, the amounts of C5+ over T.O.S. (Figure 2-8) are: 59.73% (T.O.S.= 5 min), 56.65% (T.O.S.= 44 min), 55.48% (T.O.S.= 85 min), 57.01% (T.O.S.= 123 min), 58.54% (T.O.S.= 160 min), 56.92% (T.O.S.= 210 min), 58.38% (T.O.S.= 285 min), and 57.65%(T.O.S.= 338 min); then, calculating the average is 57.55% with a standard deviation of 1.32. The standard deviation was calculated with the excel function. Figure 2-9 shows this data point at T = 370 °C, WHSV = 1.3 h^{-1} , and P = 101 kPa (abs) (C5+ = 57.55%, with standard deviation ±1.32.

2.3.1.2 Effect of varying temperature

Approximately 300 °C was the lower temperature bound. Below this, the temperatures were not stable because of the heat of reaction. For example, when the reaction temperature was set between 250 and 300 °C, the only product was propene but the temperature always increased until it reached 300 °C. On the other hand, if the temperature was lower than 250 °C, the isopropanol did not react.

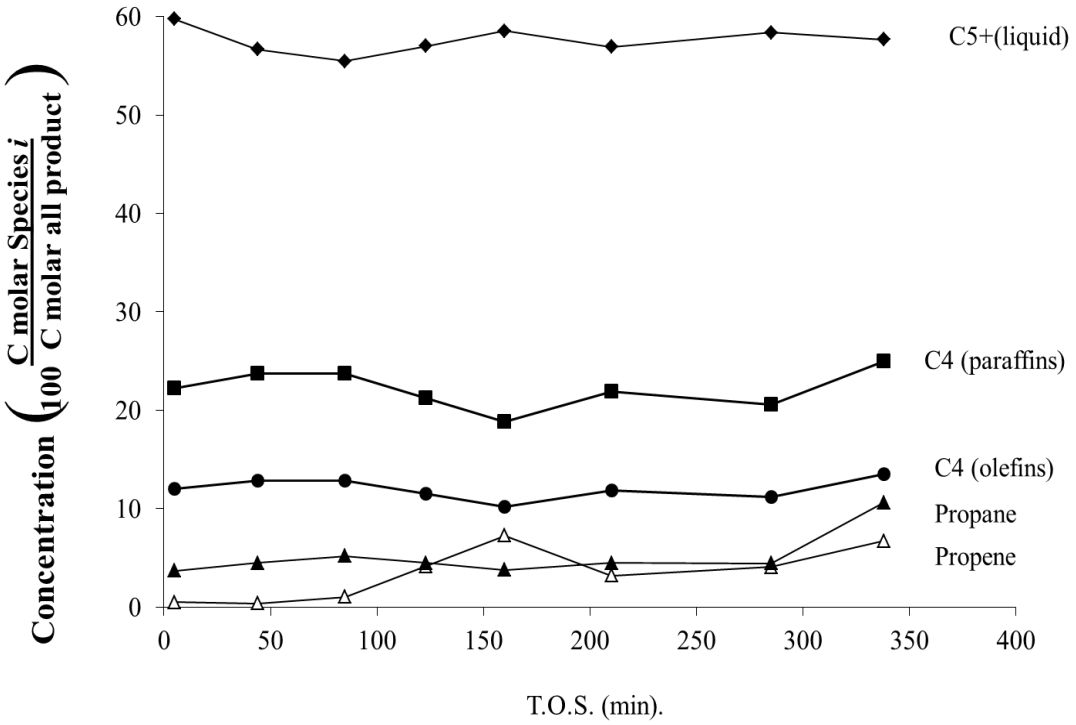

Figure 2-8. Product distribution for isopropanol reaction over HZSM-5 (280), WHSV = 1.31 h^{-1}, P = 101 kPa (abs), and T = 370 °C.

Figure 2-9 shows the gas and liquid product distribution, which is affected by temperature. As the temperature increases, the amount of liquid (C5+) decreased from 70% (300 °C) to 10% (450 °C) and the gaseous products increased from 30% (300 °C) to 90% (450 °C). At high temperatures, gaseous products increase from cracking C5+ olefins.[24] For instance, the amount of propane increases from 2% (300 °C) to 22% (450 °C). Because of the dehydration reaction, the amount of olefinic gaseous products is larger than the paraffinic products.

Temperature affects the type of liquid reaction products obtained (Figure 2-10). At higher temperatures, the concentration of aromatics increases from 5% (300 °C) to more than 48% (450 °C).[21] Because aromatics and gaseous products form, the amount of branched olefins decreases from 48% (300 °C) to 10% (450 °C). At all temperatures, the concentration of isoparaffins, linear olefins, and naphthenes are constant. The concentration of isoparaffinic compounds is always below 10% and the paraffin concentration is negligible.

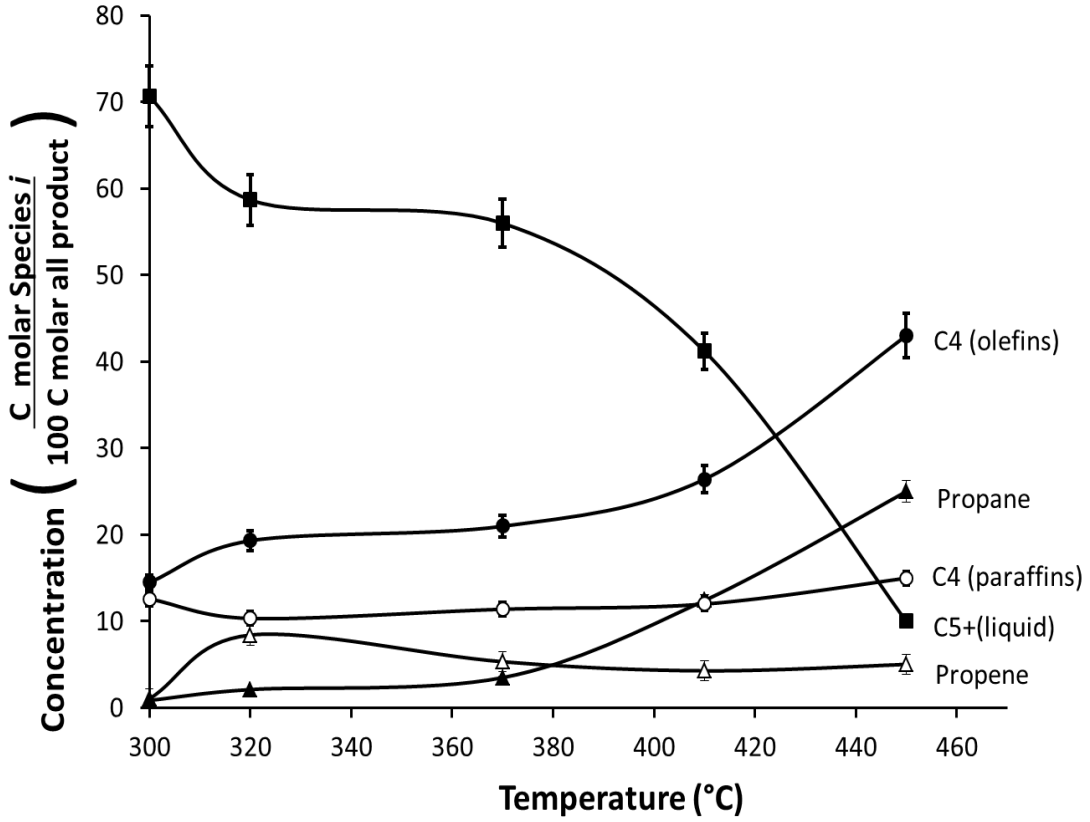

Figure 2-9. Product distribution of gases and liquids for isopropanol reaction over HZSM-5 (280), WHSV = 1.31 h^{-1}, and P = 101 kPa (abs). (Error bars are ± 1σ.)

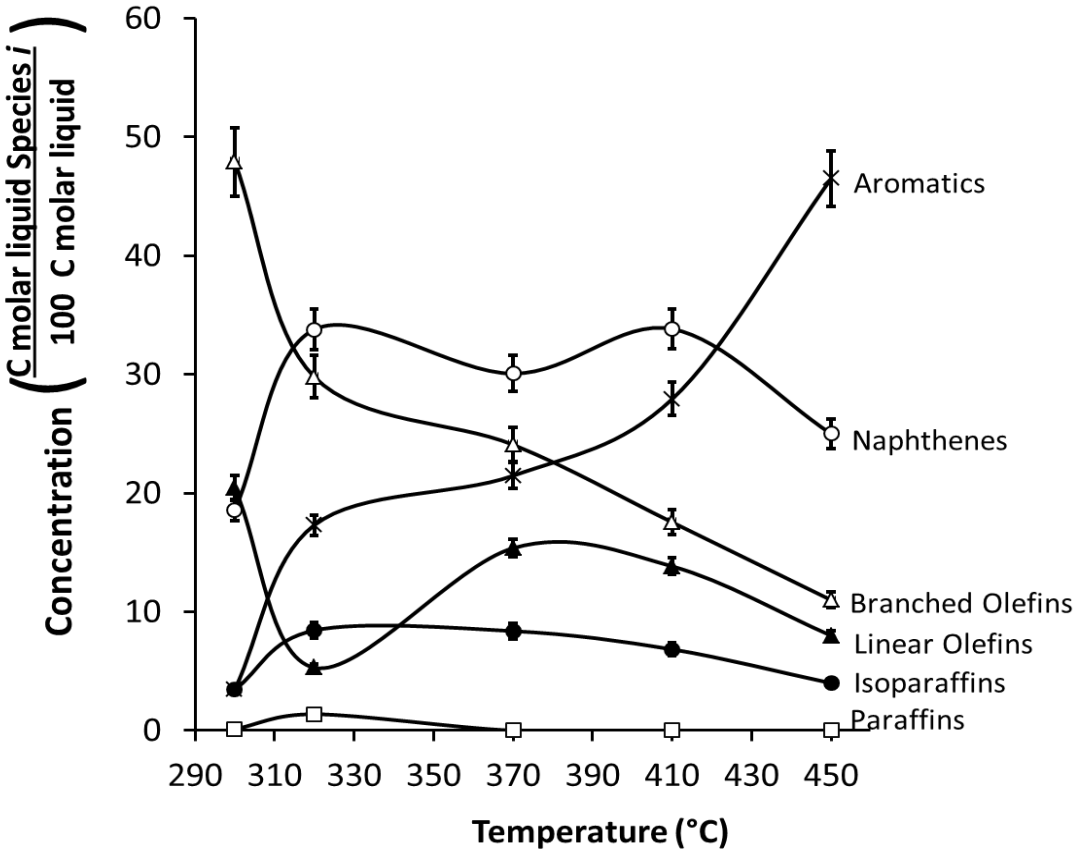

Figure 2-10. Liquid product distribution for isopropanol reaction over HZSM-5 (280), WHSV = 1.31 h^{-1}, and P = 101 kPa (abs). (Error bars are ± 1σ.)

2.3.1.3 Effect of varying WHSV

At T = 370 °C and WHSV = 0.52–11.53 h^{-1}, Figure 2-11 shows the distribution of gas and liquid is not affected by the change of WHSV. At all WHSV, the amount of liquid is constant (~60%). The amount of propene increases from 1% (0.52 h^{-1}) to 15.5% (11.2 h^{-1}); at high WHSV (low residence time), propene forms first and does not have time to continue reacting.

Figure 2-12 illustrates the types of liquid-phase products at different WHSV. At very low WHSV, aromatics are high (60% at 0.52 h^{-1}); however, at high WHSV, aromatics are much less (8% at 11.2 h^{-1}). On the other hand, when the WHSV increases, branched olefins also increase, from 5% (0.52 h^{-1}) to 40% (11.2 h^{-1}). At all WHSV, naphthenes are constant, and the amount of paraffins always stayed below 5%.

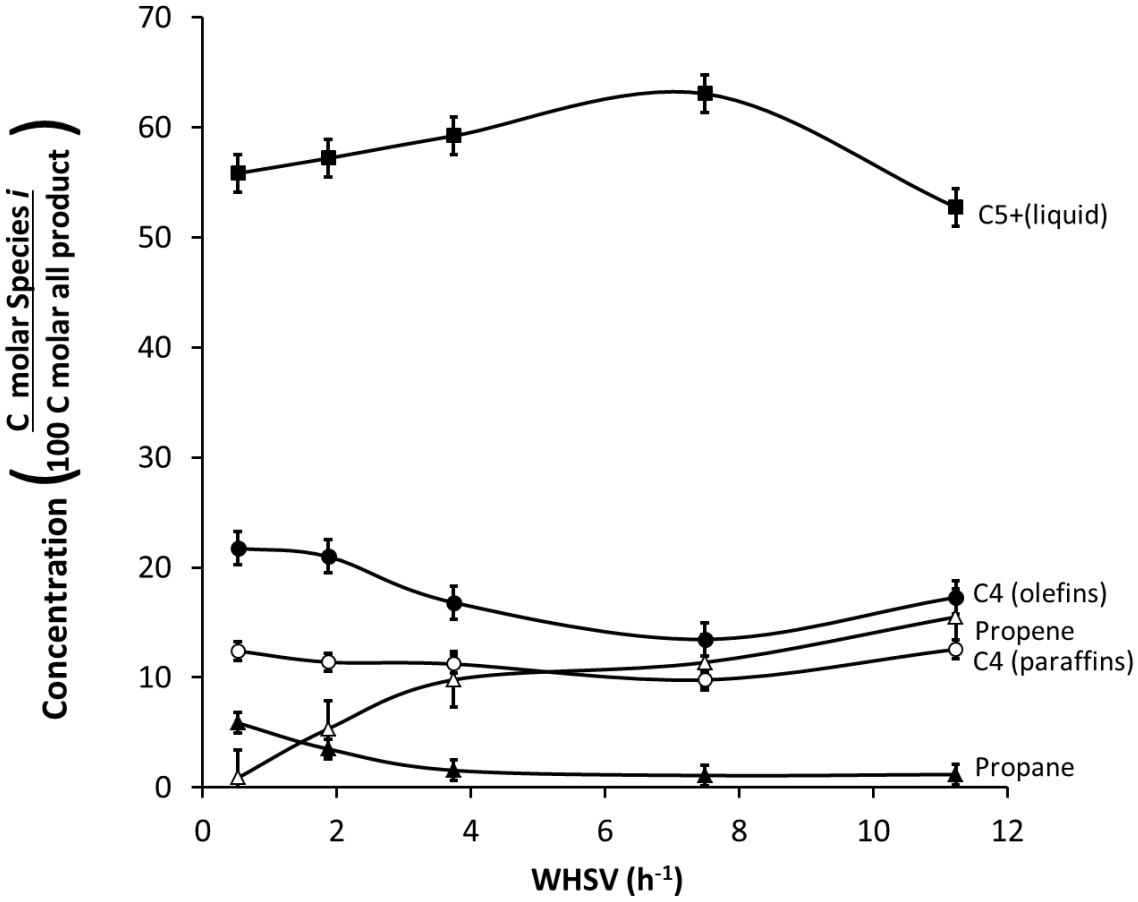

Figure 2-11. Product distribution of gases and liquids for isopropanol reaction over HZSM-5 (280), T = 370 °C, and P = 101 kPa (abs). (Error bars are ± 1σ.)

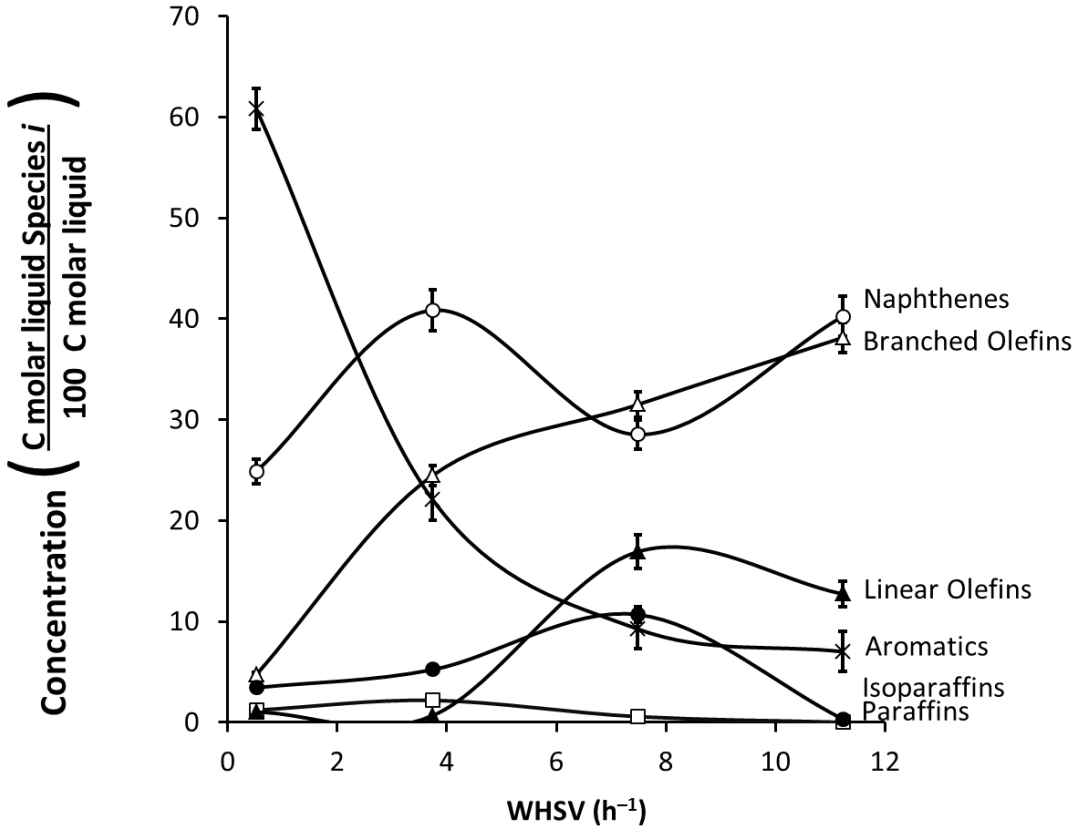

Figure 2-12. Liquid product distribution for isopropanol reaction over HZSM-5 (280), T = 370 °C, and P = 101 kPa (abs). (Error bars are ± 1σ.)

Figure 2-13 illustrates the carbon distribution of the liquid products at different WHSV. At lower WHSV, the most abundant component is C9 whereas at higher WHSV, the most abundant component is C6. At low WHSV, the olefins undergo more oligomerization reactions to produce larger molecules, whereas at high WHSV, the molecules do not have time to form larger molecules. It is noteworthy that the carbon number in the liquid can be changed by WHSV but not temperature.

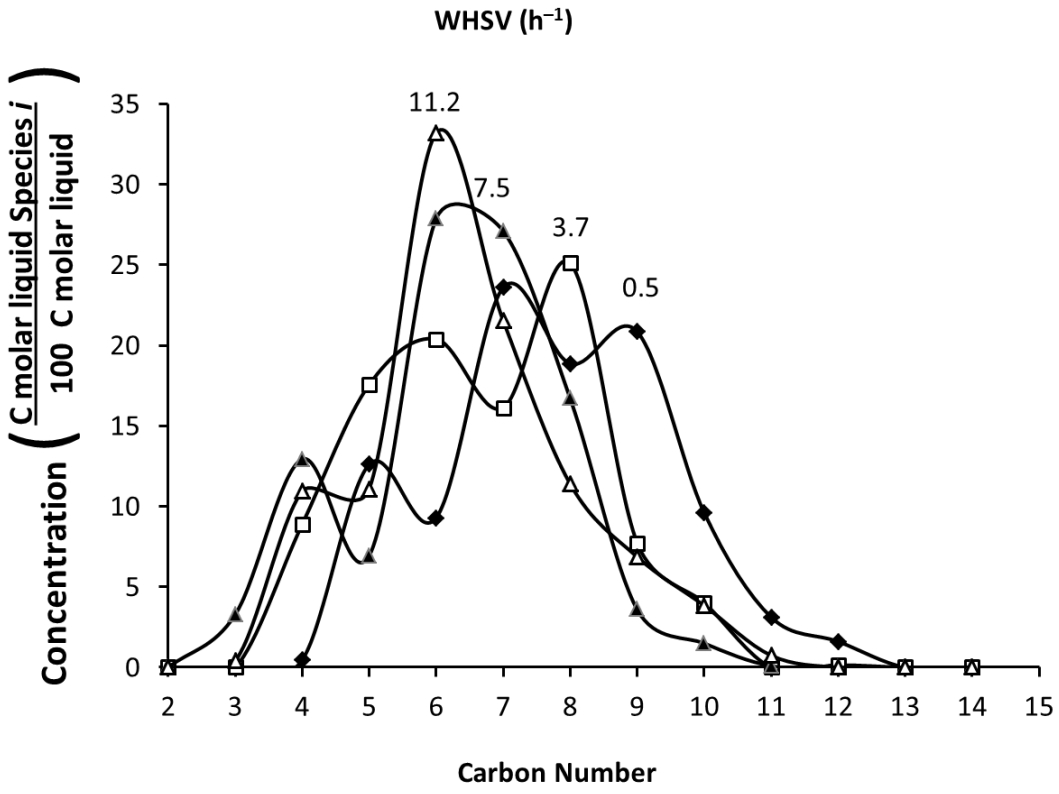

Figure 2-13. Liquid product distribution of isopropanol reaction over HZSM-5 (280), T = 370 °C, and P = 101 kPa (abs).

For Figures 2-8 to 2-13, the isopropanol undergoes only oligomerization reaction. The dehydration region is between 250 and 300 °C, but is very unstable. It may be assumed that the dehydration is very fast, and propene oligomerizes as soon it appears.

2.3.1.4 Liquid product distribution

Table 2-3 shows the most abundant compounds in the liquid-phase product at 370

°C for the different WHSV studied. Branched olefins are more abundant than linear olefins; during oligomerization, the reactive double bond is on a secondary carbon, which forms branched molecules. C6 olefins are the most abundant because of the dimerization of propene. Also present are branched naphthenes that are unsaturated (e.g., cyclohexene, 1,3-dimethyl) or saturated (e.g, cyclopentane, 1,3-dimethyl). For aromatics, branched meta and ortho substitutions are very common. For all the liquids analyzed, approximately 80 to 150 compounds were found by the GC-MS. Usually, ~20 compounds comprised 80% of the molar distribution. The remaining compounds had a concentration less than 1%.

Table 2-3. Most abundant liquid compounds for the isopropanol reaction over HZSM-5, T = 370 °C, WHSV = 0.5–11 h^{-1}, and P = 101 kPa (abs).

Olefins and naphthene olefinics	Concentration (mol%)	Naphthenes	Concentration (mol%)
2,3-dimethyl-1-butene	2.4–6.8	1,2-dimethyl cyclopropane	2.7–7.5
3 methyl-2-pentene	3.7–9.5	1-methylethenyl cyclopropane	1.4–2.7
1,3-dimethyl cyclohexene	2.0–2.9	1,3-dimethyl cyclopentane	1.8–2.7
2-methyl-2-hexene	1.2–7.8	1,2-dimethyl-3-methylene cyclopentane	1.3–2.7
1,3-dimethyl cyclohexene	1.4–2.9		
1-methyl cyclohexene	1.8–2.3		
Aromatics	Concentration (mol%)	Isoparaffins	Concentration (mol%)
methyl benzene	1.8–10	2-methyl pentane	4.2–4.4
1,3-dimethyl benzene	2.9–5.5	2-methyl hexane	2.4–2.8
1-ethyl-2-methyl benzene	2.2–4.4		

2.3.2 Mixed alcohol at atmospheric pressure

For the mixed alcohols, there are two reactions types: dehydration and oligomerization. For all figures, the reaction-type region is specified.

2.3.2.1 Catalyst stability

For the mixed alcohols, Figure 2-14 shows the distribution of gas and liquid products during time on stream. During the first 360 minutes, the product distribution is stable, similar to isopropanol reaction (Figure 2-8). The most abundant fraction (C5+) has a constant concentration over time. Figure 2-14 shows that mixed alcohols produce more hydrocarbon liquids (~90%) than isopropanol (~60%). Propene is about 12% which is the product of the dehydration of isopropanol. C4 olefins are constant over T.O.S. (8%). The gases are 20% which is the amount of isopropanol and 2-butanol in the mixed alcohols feed; therefore, dehydration is the only reaction occurring.

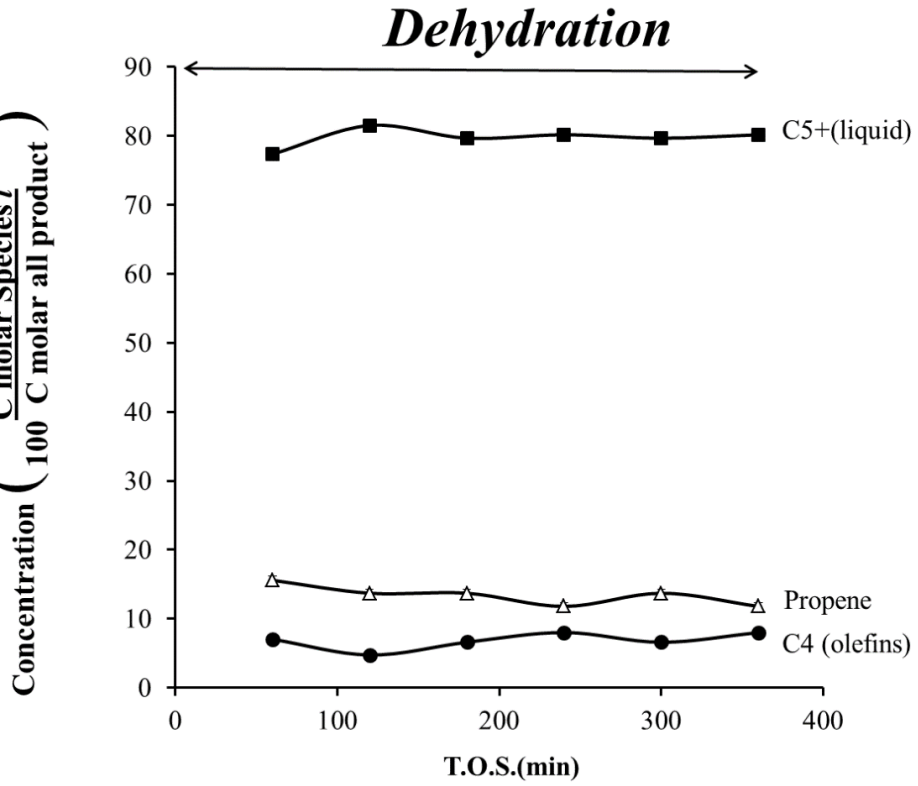

Figure 2-14. Product distribution of gases and liquids for the mixed alcohol reaction over HZSM-5 (280), T = 370 °C, WHSV = 1.31 h^{-1}, and P = 101 kPa (abs).

2.3.2.2 Effect of varying temperature

Figure 2-15 shows that temperature affects the selectivity of gas and liquid products. As temperature increases, the amount of liquid (C5+) decreased from 80% (300 °C) to 40% (520 °C). The gaseous products increased from <10% (370 °C) to 30% (520 °C); the increase results from cracking C5+ olefins at high temperatures. This also occurred with isopropanol; however, isopropanol cracked at lower temperatures (300 °C) compared to mixed alcohols (370 °C). For instance, the amount of C4 olefins increases

from 2% (300 °C) to 30% (520 °C). It is notable that there are more olefinic gaseous products than paraffinic products, which is similar to the isopropanol reaction.

Figure 2-16 shows the effect of temperature on product distribution at WHSV = 1.31 h^{-1}. The unreacted alcohol decreases from 12% at 300 °C to 0% at 320 °C. Between 300 and 410 °C, branched and linear olefins are the only reaction products. Above 410 °C, aromatics and naphthenes appear as reaction products. At higher temperatures, aromatics increase from 3% (410 °C) to 55% (520 °C), which is similar to the isopropanol reaction.

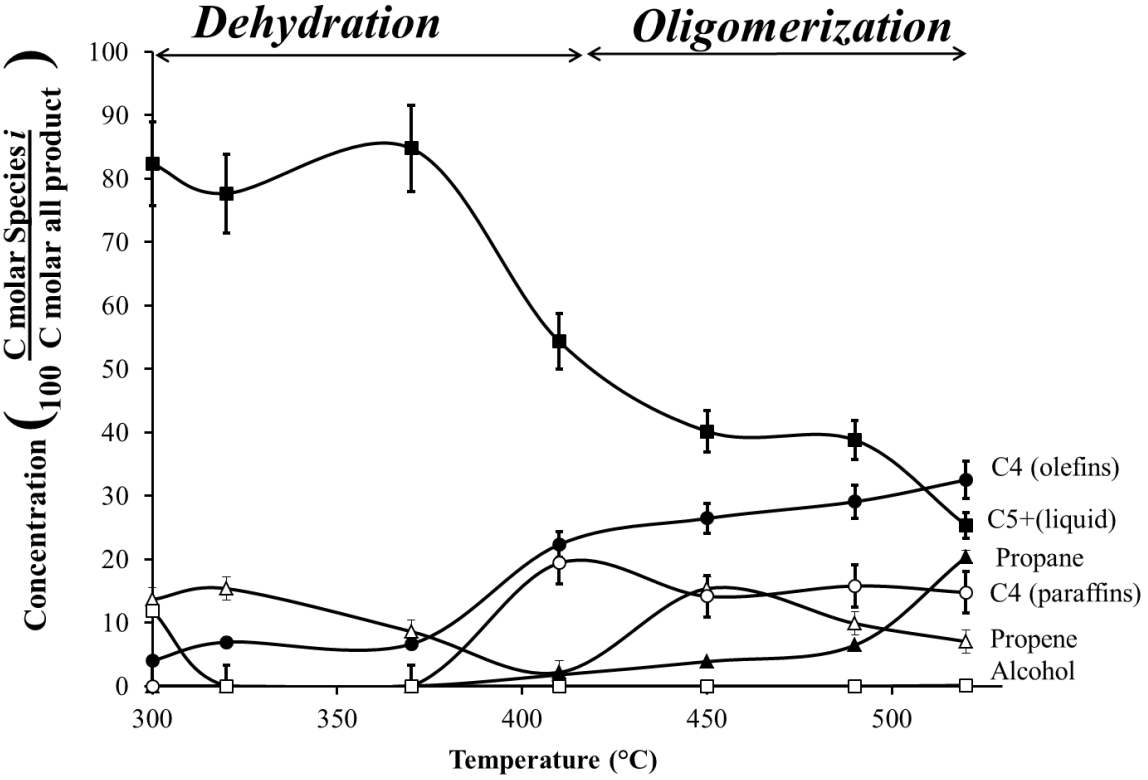

Figure 2-15. Product distribution of gases and liquids for mixed alcohol reaction over HZSM-5 (280), WHSV = 1.31 h^{-1}, and P = 101 kPa (abs). (Error bars are ± 1σ.)

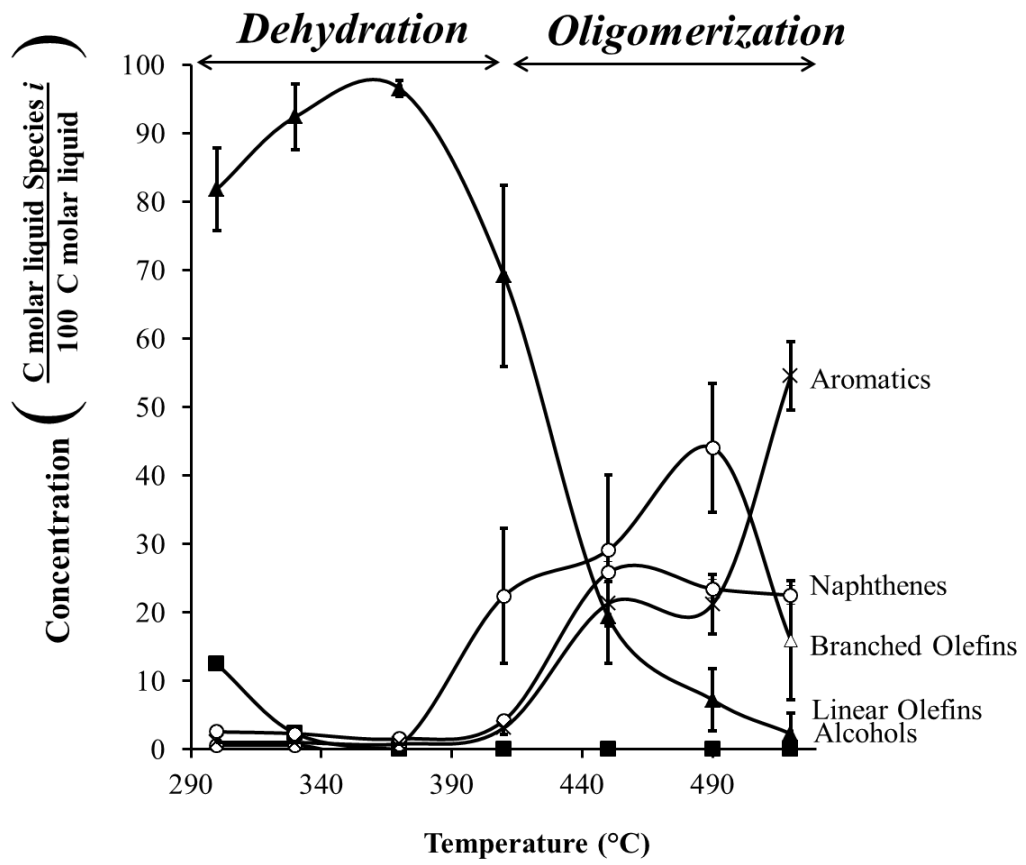

Figure 2-16. Liquid product distribution of mixed alcohol reaction over HZSM-5 (280), WHSV = 1.31 h^{-1}, and P = 101 kPa (abs). (Error bars are ± 1σ.)

2.3.2.3 Effect of varying WHSV

Figure 2-17 illustrates the gas product distribution at different WHSV at T = 370 °C. Between 0.5 and 11.23 h^{-1}, dehydration is the dominant reaction because linear olefins are the most abundant species (~95%). The product distribution is not affected by changing WHSV. In this WHSV range, the amount of gases (C3–C4) is negligible.

Figure 2-18 illustrates the types of liquid-phase products at different WHSV. At very low WHSV, aromatics are high (60% at 0.52 h^{-1}); however, at high WHSV,

aromatics are much less (8% at 11.2 h^{-1}). On the other hand, when the WHSV increases, branched olefins also increase, from 5% (0.52 h^{-1}) to 40% (11.2 h^{-1}). At all WHSV, naphthenes are constant, and the amount of paraffins always stayed below 5%.

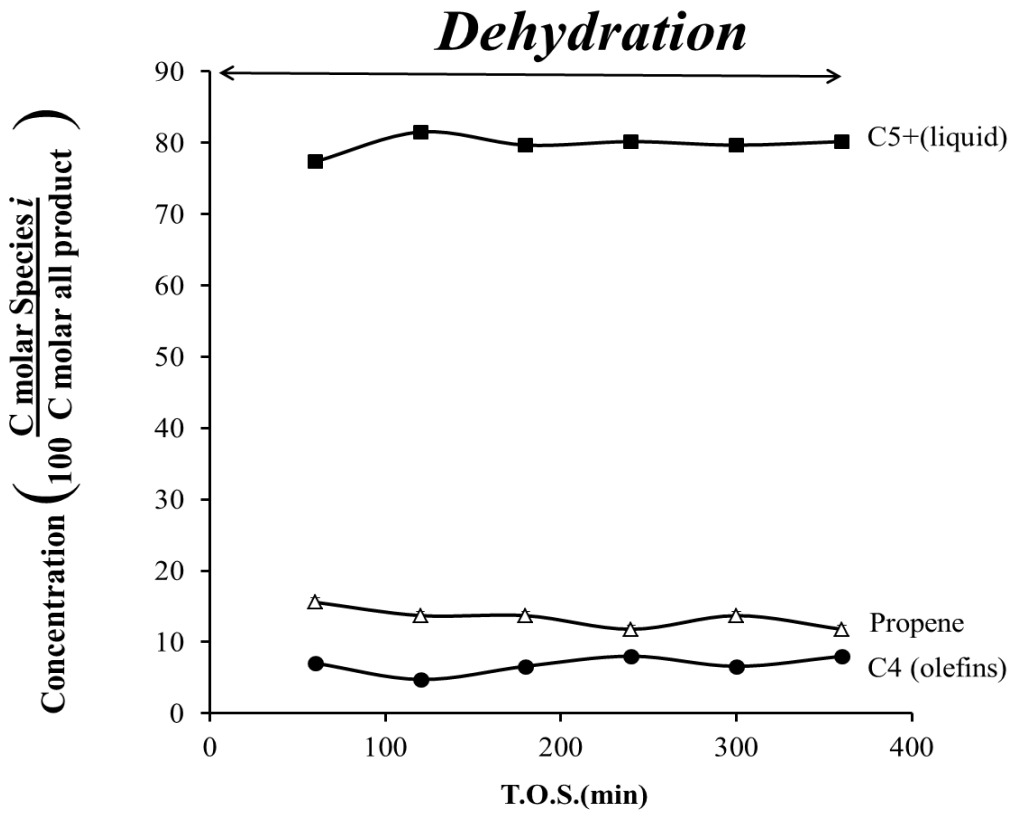

Figure 2-17. Product distribution of gases and liquids for mixed alcohol reaction over HZSM-5 (280), T = 370 °C, and P = 101 kPa (abs). (Error bars are ± 1σ.)

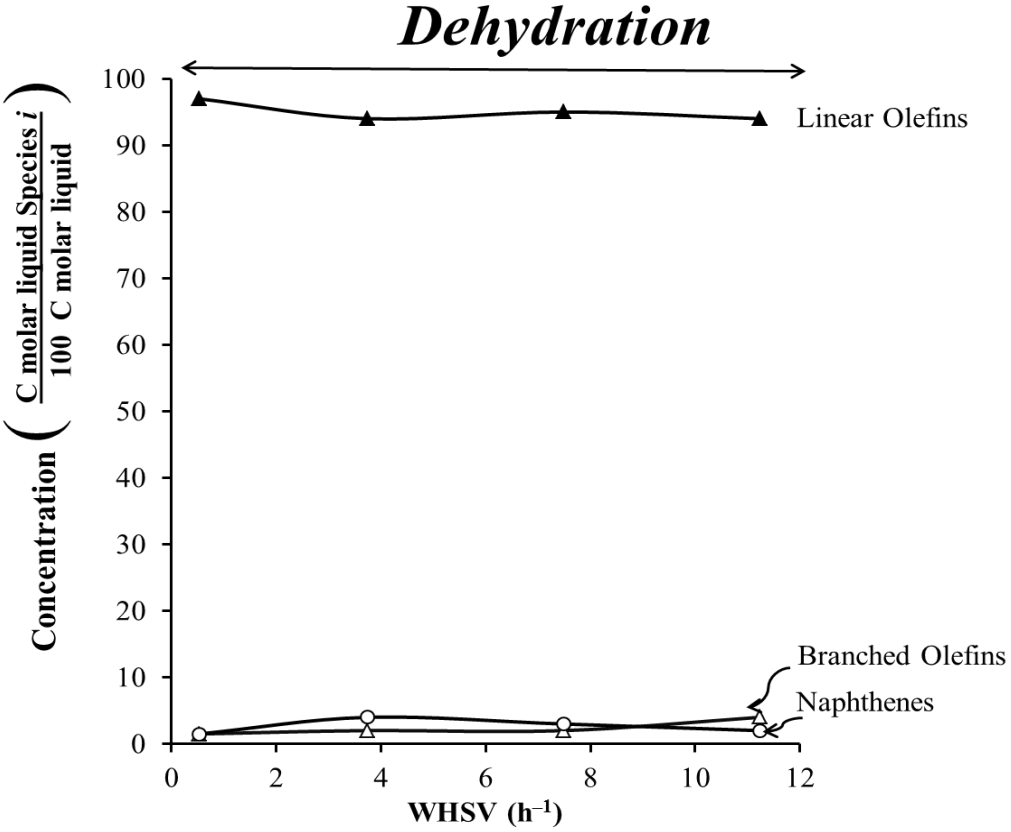

Figure 2-18. Liquid product distribution of mixed alcohol reaction over HZSM-5 (280), T = 370 °C, and P = 101 kPa (abs). (Error bars are ± 1σ.)

Figure 2-19 illustrates the liquid carbon distribution of the liquid products at different WHSV. In this WHSV, the most abundant components are C7 to C9. The product carbon distribution is not affected by changing WHSV.

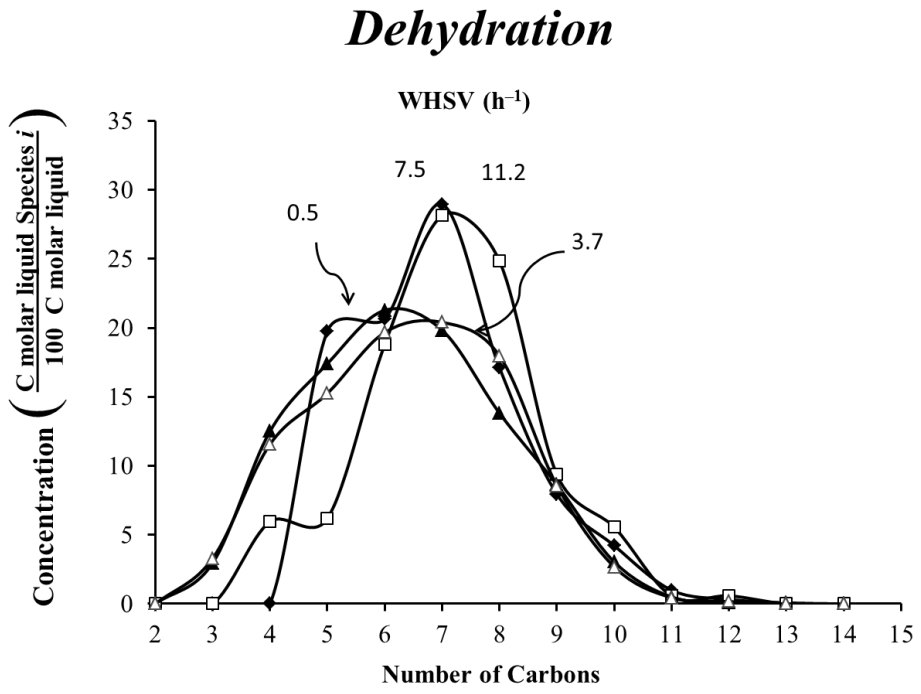

Figure 2-19. Liquid product distribution of mixed alcohol reaction over HZSM-5 (280), T = 370 °C, and P = 101 kPa (abs).

2.3.2.4 Liquid product distribution

Table 2-4 shows the most abundant compounds in the liquid-phase product at 300–410 °C and WHSV = 1.31 h^{-1}. Linear olefins are abundant because dehydration in these variable ranges is the only reaction that occurred. For higher temperatures (450–520 °C), oligomerization occurs and the compounds are similar to isopropanol products shown in Table 2-3.

Table 2-4. Most abundant liquid compounds for the isopropanol reaction over HZSM-5, T = 300–420 °C, WHSV = 1.31 h^{-1}, and P = 101 kPa (abs).

Olefins	Concentration range (mol%)
2-Pentene	6.0–17.0
1-Hexene	1.5–1.7
2-Hexene	2.0–11.3
2-Heptene	3.8–29.7
3-Heptene	2.5–12.8
2-Octene	2.8–4.2
3-Octene	7.6–9.1
4-Octene	1.4–2.3
4-Nonene	9.1–19.3
3-Decene	1.5–1.6
4-Decene	3.5
4-Undecene	4.6–8.4
5-Undecene	1.5
4-Dodecene	1.5–1.9

2.3.3 Coke deposition

Transformation of alcohols to hydrocarbons can be limited by catalyst deactivation. Catalyst activity is affected by the stability of the product distribution during time on stream and the amount of coke produced. During all the experiments with isopropanol and mixed alcohol, the product distribution did not vary during the 360-min time on stream; however, the catalyst coked. The coke is characterized by the coke

yield, which is defined as the weight of coke produced per total weight of feed injected in the reactor.

$$\text{Coke Yield (wt\%)} \equiv \frac{\text{Coke}_{\text{produced}}}{\text{Feed}_{\text{total}}} \times 100$$

where

$\text{Coke}_{\text{produced}}$ = coke produced (g)

$\text{Feed}_{\text{total}}$ = Total feed mass (g)

For example, if the coke weight is 0.6 g and 100 g of alcohol was injected during a period of time, the coke yield is 0.6 wt%.

Table 2-5 shows the amount of coke deposited in the catalyst. For isopropanol, the coke yield at low temperature (320°C) is low (0.31 wt%); whereas, at high temperature (410°C), the coke content doubled to 0.65 wt%. For mixed alcohol, the coke content increased with temperature as well. For example, the coke yield at low temperature (320°C) is low (0.59 wt%); whereas, at high temperature (410°C), the coke content increased to 0.63 wt%.

According to Guisnet et al. (1989), deactivation occurs through the three following modes: (i) limitation of the access of feed (isopropanol or mixed alcohol) to the active sites, (ii) blockage of the access to the sites of the cavities (or channel intersections) in which the coke molecules are situated, and (iii) blockage of the access to the sites of the pores in which there are no coke molecules. The pore structure of zeolites determines for a large part the deactivating effect of coke.[25]

Zeolite HZSM-5 pore system consists of interconnecting channels without cavities. Figure 2-20 shows that HZSM-5 deactivation occurs initially through limitation of the access to the active sites (Mode 1), then blockage of the access to the sites of the channel intersection in which the coke molecules are situated (Mode 2). Lastly, at high coke content, coke molecules located on the outer surface of the crystallites can block the access to the sites of channel intersections in which there are no coke molecules (Mode 3). HZSM-5 coking has a moderate deactivating effect.

To regenerate the catalyst, it is burned in an oven at 550 °C for 24 hours, or it is kept inside the reactor with air flowing (100 mL/min) at 550 °C for 24 hours. To ensure the catalyst has the same activity before and after regeneration, Figure 2-21 shows two experiments at the same conditions with fresh and regenerated catalyst. The concentration products were similar; therefore, the catalyst was successfully regenerated and there is no difference between them.

Table 2-5. Coke yield for different reactants and temperatures.

T (°C)	Feed	Time on stream (h)	Coke yield (wt%)
320	Isopropanol	6	0.31
370	Isopropanol	6	0.58
410	Isopropanol	6	0.65
320	Mixed alcohol	6	0.59
370	Mixed alcohol	6	0.55
410	Mixed alcohol	6	0.63

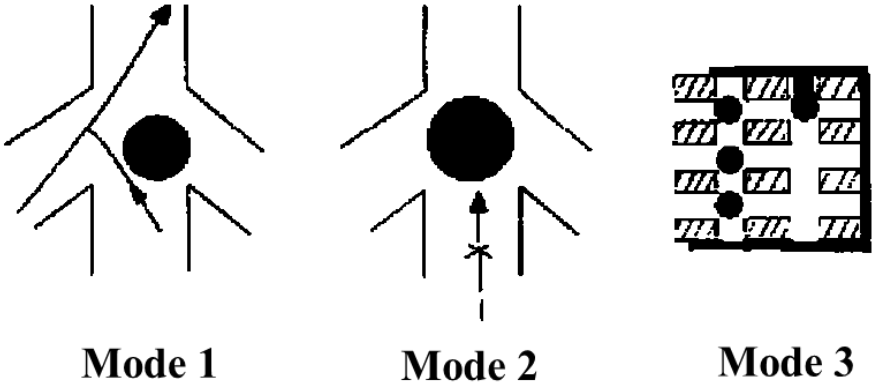

Figure 2-20. Modes of HZSM-5 zeolite deactivation (Figure adapted from Guisnet et al., 1989).[25]

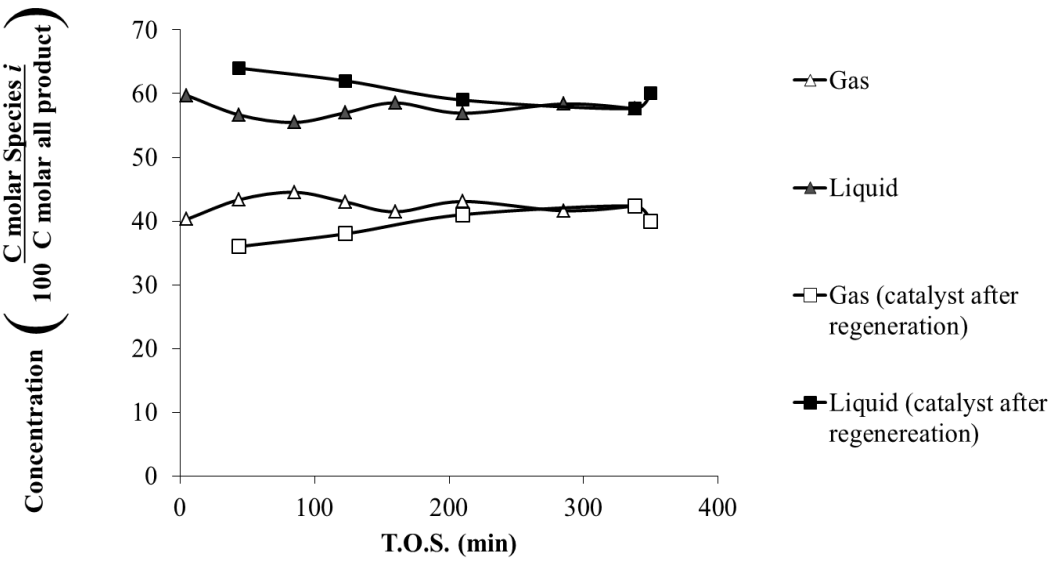

Figure 2-21. Product distribution of gases and liquids for the isopropanol reaction over HZSM-5 (280), T = 370 °C, WHSV = 1.31 h^{-1}, and P = 101 kPa (abs).

2.3.4 Scale-up oligomerization reactor

The gasoline unit was constructed in summer 2010. The unit was designed to process up to 10 times the small reactor unit. The unit consisted of a preheater, four reactors, a HPLC piston pump, and a cooler. The pump injects liquid into the preheater to gasify it. The preheater temperature is around 410 °C. Then, after the liquid becomes gas, it splits and goes through the four reactors where it contacts the HZSM-5 catalyst and reacts. Later, a cooler condenses and separates liquid from gas. The gas goes to a vent whereas the liquid is collected for a gas chromatograph-mass spectrograph analysis. This first gasoline unit configuration gave poor results. Because the alcohol did not distribute evenly in the four reactors, the dehydration and oligomerization occurred simultaneously, and the conversion never reached 100%. Therefore, another type of configuration was implemented, with the objective to obtain total conversion and minimize gas production.

The objective was achieved with the second configuration of the gasoline unit. Figure 2-22 shows the process flow diagram of the gasoline unit (Reactor Unit 2). Conversion was 100%, and the amount of gas produced was minimized. As shown in Figure 2-21, the pump injects liquid into the preheater (400°C) to vaporize it. After the liquid becomes a vapor, it goes through Reactor A, where it contacts the HZSM-5 catalyst and reacts (dehydration reaction). The reaction products go through a condenser (0°C), which separates the liquid and gas. The liquid is collected, and the gases are further oligomerized in Reactor B (the gases are mainly C3 and C4). Every hour, the liquid from Condenser 1 is collected by opening Valve 2 for approximately 3 minutes

until all the liquid is collected. A back pressure regulator (set point = 374 kPa (abs)) is connected to the end of Condenser 2. Reactor A contains 50 grams of catalyst HZSM-5 (280). Reactor B contains 60 grams of the same catalyst. The mixed-alcohol feed flow ranges between 120–360 mL/h. Dehydration reaction occurred on Reactor A whereas oligomerization on Reactor B.

The gasoline unit had two products: A and B. Product A exits from Condenser 1, and Product B exits from Condenser 2. Figure 2-23 and 2-24 show a photograph from Condenser 1 (same as Condenser 2). The condenser is an ice-cooled type with an inlet in the middle section and exit on the top.

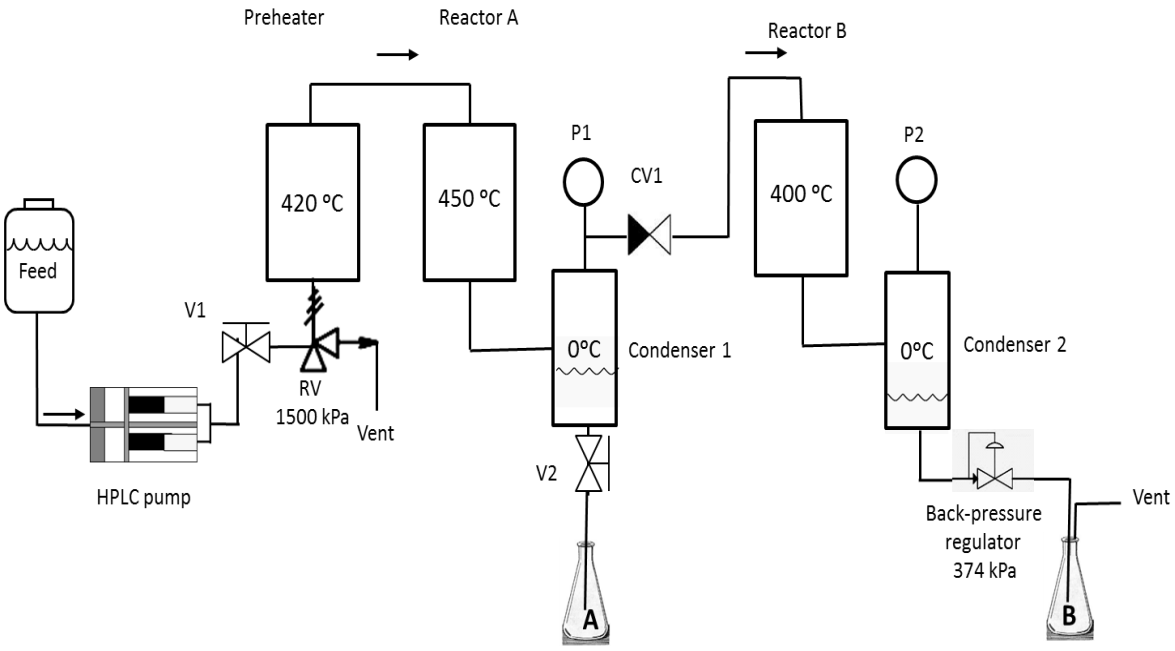

Figure 2-22. Schematic diagram of Reactor Unit 2.

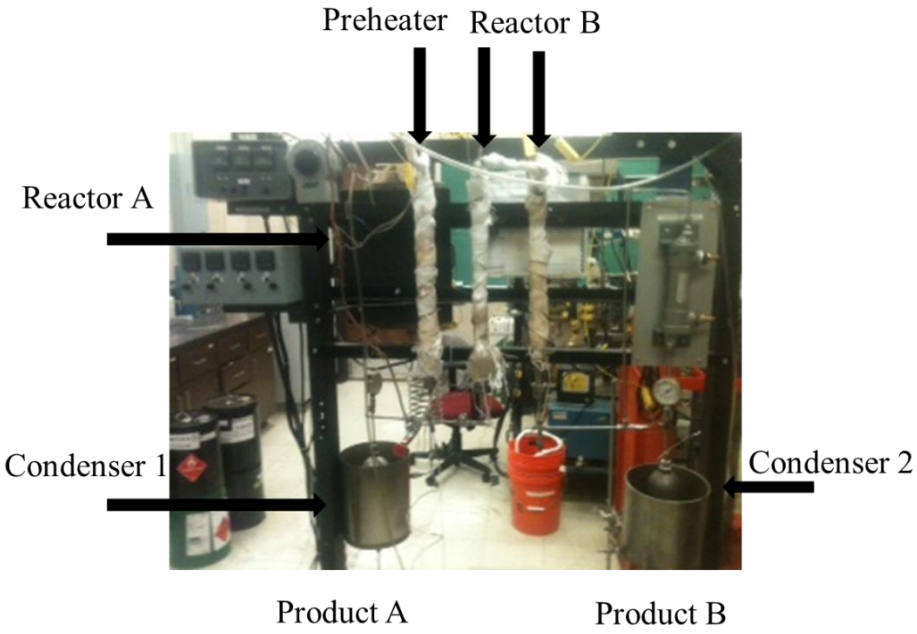

Figure 2-23. Photograph of of Reactor Unit 2.

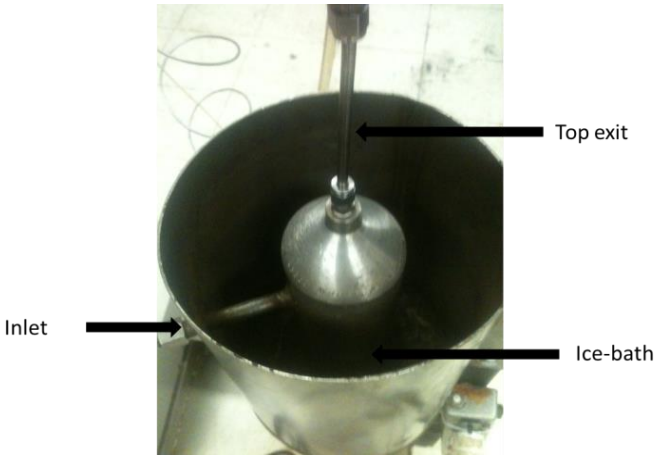

Figure 2-24. Photograph of the condenser**.**

Figure 2-25 shows the mass balance with 100 g of mixed alcohol as the basis. Table 2-6 shows the composition of Product A. The most abundant products are linear olefins (70%) and branched olefins (12%). It is noteworthy that dehydration occurred on Reactor A because olefins are the most abundant in Product A. The average carbon number is 7.84. Table 2-7 shows the product distribution for Product B. The most abundant products are aromatics (72%) and branched olefins (16%). These results illustrates that oligomerization is predominant on Reactor B. The average carbon number is 8.57, which is slightly higher than Product A.

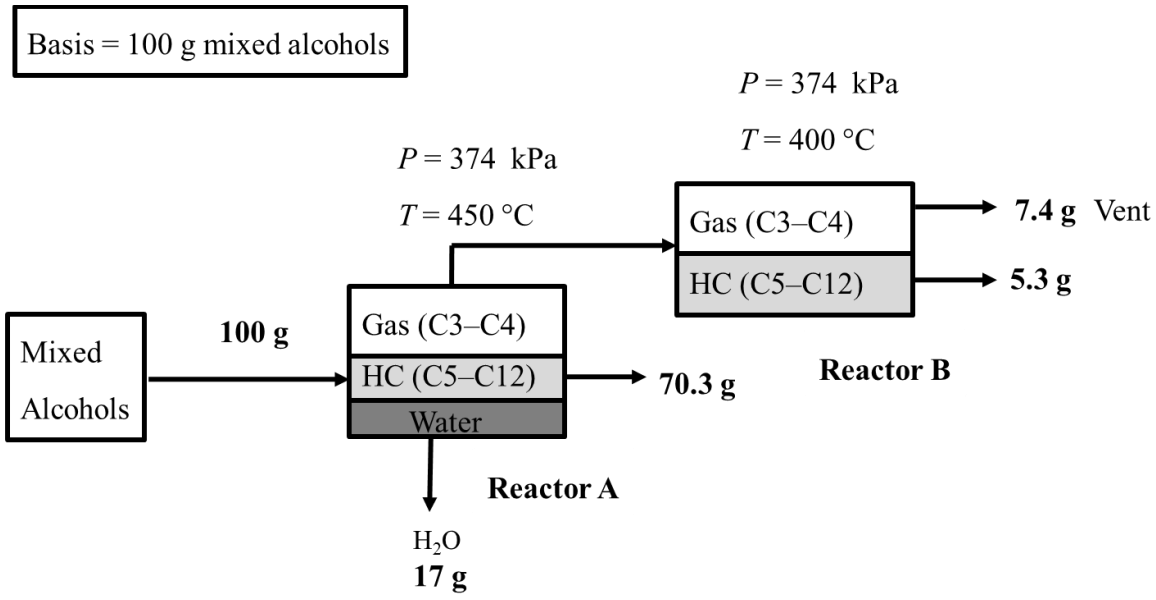

Figure 2-25. Mass balance for mixed alcohol oligomerization reaction before optimization. (*Note*: Pressures are absolute.)

Table 2-6. Product A liquid carbon distribution of mixed alcohol reaction using HZSM-5 (280), WHSV = 6 h^{-1}, and P = 374 kPa (abs).

C#	Paraffins	Linear Olefins	Isoparaffins	Naphthenes	Branched Olefins	Aromatics	Total
5	0	4.3	0	0	0	0	4.3
6	0	0	0	0	9.7	0	9.7
7	0	37.2	1.7	0	0	0.5	40.4
8	0	14.3	0	0	0.3	1.4	16.0
9	0.3	8.6	0	0	2.8	1.2	14.4
10	0	1.4	0.9	0.4	0	2.3	5.9
11	1.8	3.0	0	1.8	0	0.7	7.3
12	0.7	0.5	0	0	0	0.9	2.1
Total	2.8	69.2	2.6	2.3	12.8	7.0	100.0

Table 2-7. Product B liquid carbon distribution of mixed-alcohol reaction using HZSM-5 (280), WHSV = 1.33 h^{-1}, and P = 374 kPa (abs).

C#	Paraffins	Linear Olefins	Isoparaffins	Naphthenes	Branched Olefins	Aromatics	Total
5	0	0	0	0	5	0	5
6	0	0	0	0.6	3.2	0	3.8
7	0	0	0	1.5	0.5	6.2	8.2
8	0	0	0	8	0.7	29.2	37.9
9	0	0	0	1.1	5.6	15.3	22
10	0	0	0	0.4	0	7.8	8.2
11	0	0	0	0.5	1.1	7.9	9.6
12	0	0	0	0	0	4.1	4.1
13	0	0	0	0	0	1	1
Total	0	0	0	12.2	16.2	71.5	100

2.4 Conclusions

This study investigated the conversion of isopropanol and mixed alcohols to hydrocarbons using HZSM-5 at 101 kPa (abs). For both isopropanol and mixed alcohols during the first 360 min, there was no catalyst deactivation during the oligomerization reaction.

For isopropanol, higher temperatures (410 to 450 °C) produced more gaseous products and aromatics whereas the olefins decreased. High WHSV gives high concentrations of C6+ olefins whereas low WHSV gives high concentrations of C9 aromatics.

For mixed alcohols, the amount of liquid produced was much greater than isopropanol. Between 300 and 410 °C, dehydration occurs producing only linear olefins.

Above 410 °C, the linear olefins are transformed into branched olefins, naphthenes, and aromatics. Isoparaffins were not observed as reaction products from mixed alcohols. Varying WHSV did not affect product distribution; only dehydration products were observed.

Although the catalyst formed coke, it did not affect the product distribution during the isopropanol and mixed alcohol experiments. Higher temperatures produced more coke for both feeds. For isopropanol and mixed alcohol, the amount of coke produced was very similar.

For scaling up the reactor, configuring reactors in parallel, where the dehydration and oligomerization occurs at the same time, is not effective. To transform alcohols into hydrocarbons, a dehydration rector followed by an oligomerization reactor is a better approach. The amount of waste gaseous products are lower (7.4 wt%).

3. ALCOHOL OLIGOMERIZATION AT HIGH PRESSURE

The objectives of this section follow:

a) Describe the transformation of isopropanol and mixed alcohol to hydrocarbons at high pressure.

3.1 Introduction

Chang et al., (1979) were the first to show the effect of pressure on the transformation of methanol reaction to hydrocarbons over ZSM-5.[26] Figure 3-1 shows the product distribution of methanol reaction at WHSV = 1 h^{-1}, T = 370 °C, P = 4, 101, and 5063 kPa (abs). At low pressure, C3–C5 olefins are high (77 wt% at 4 kPa); however, at high pressure, C3–C5 olefins disappear (0 wt% at 5063 kPa). On the other hand, when the pressure increases, paraffins also increase from 20% (4 kPa) to 63% (5063 kPa). From this study, it is clear that the pressure has a great effect on the product distribution of methanol over HZSM-5.

Transformation of other alcohols over HZSM-5 has been studied over HZSM-5 at atmospheric or mild-pressure conditions. Chang and Silvestri (1979) showed successfully the transformation of 1-butanol and 1-heptanol over HZSM-5 to gasoline at atmospheric pressure. Fuhse and Bandermann (1987) published results for transformation of C2 to C6 alcohols over HZSM-5. The product distribution ranged from C2 to C12, which is similar to the finding of Chang and Silvestri. For the transformation of 1-propanol, isopropanol, 1-butanol, and 2-butanol over HZSM-5, Gayubo et al. (2004) showed systematically the effect of varying *T,* WHSV, and T.O.S on the product

distribution. The conclusions for this study are that alcohols first dehydrate before they oligomerize; then, if the temperature is above 400 °C, the products start to crack. For these alcohols, the reaction scheme is very different than methanol over HZSM-5 (in which dimethyl ether is an intermediate). Mentzel et al., (2009) studied the conversion of isopropanol, methanol, and ethanol over HZSM-5 at P = 101 and 2025 kPa (abs).[27] For isopropanol, the lifetime and conversion capacity of HZSM-5 catalyst are higher than methanol or ethanol. The amount of aromatics increases at high pressure.

For isopropanol and mixed alcohol (C3–C13) reaction over HZSM-5, oligomerization occurs after dehydration (Section 1). Alcohols dehydrate to produce olefins and depending on the reaction temperature, olefins oligomerize to hydrocarbon ranging from C3 to C12. Theoretically, olefins can be injected in the reactor to skip the dehydration step. Tabak et al., (1986) shows the conversion of C2–C10 olefins to higher olefins over ZSM-5.[28] According to Tabak et al., the product distribution depends only on the reaction conditions (T, P, and T.O.S.) not on the catalyst or the feedstock. Table 3-1 shows the carbon average number (ACN) for different propylene partial pressures over HZSM-5 at 277 °C. At very low pressure, the ACN is low (7.3 at 100 kPa); however, at high pressure, the ACN is higher (17.6 at 10,000 kPa).

Table 3-1. Average Carbon Number (ACN) for propylene reaction over HZSM-5, T = 277 °C at different partial pressures. (Data adapted from Tabak et al., (1986)).[28]

Average Carbon Number	Propylene Partial Pressure (kPa (abs))
6.1	10
7.3	100
9.3	350
12	2300
13.3	3500
17.6	10,000

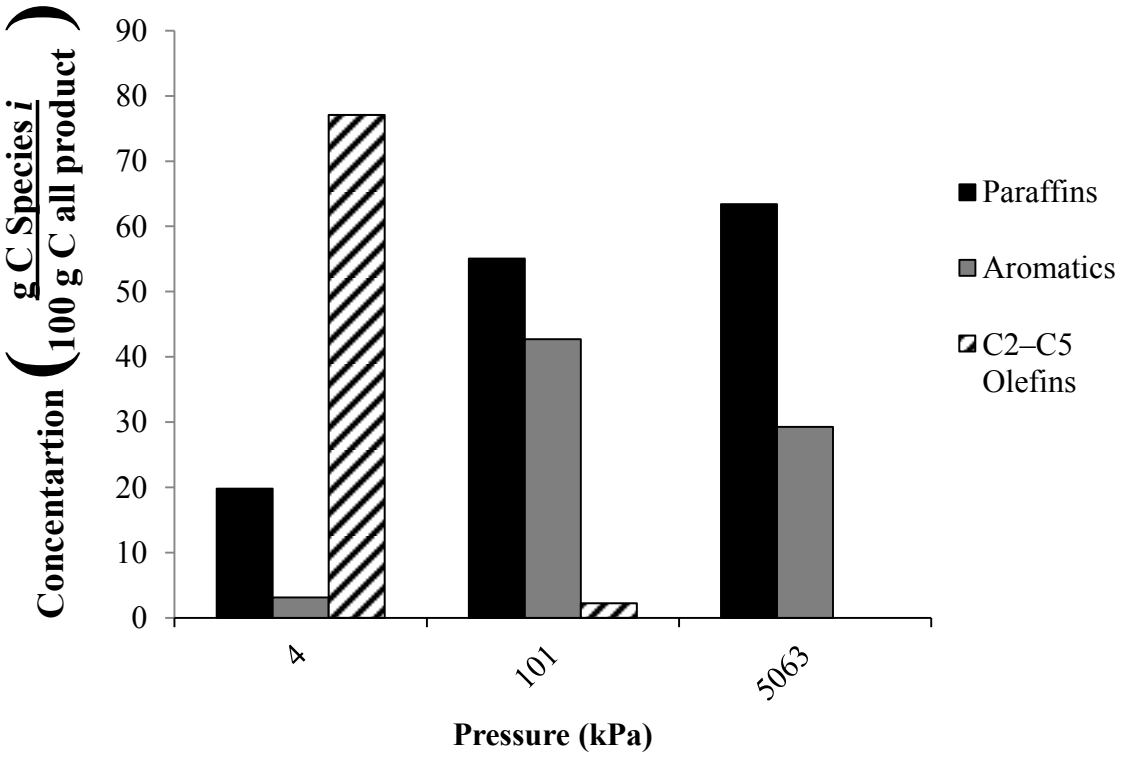

Figure 3-1. Carbon product distribution for methanol over ZSM-5 at WHSV = 1 h^{-1}, and T = 370 °C. (Figure adapted from Chang et al.,1979.)[26]

There is a vast amount of literature about the conversion of olefins over zeolite catalyst. MOGD (Mobile olefin to gasoline and distillate) uses ZSM-5 to convert light olefins to higher molecular weight gasoline and diesel fuel (Tabak et al., 1986).[28] Figure 3-2 shows the carbon distribution resulting from the oligomerization of propene over HZSM-5 at T = 550 K**.** The carbon distributions are predictions using thermodynamic properties of the products at equilibrium. The carbon distribution of low pressure (100 kPa) ranges from C3 to C12; whereas the carbon distribution at high pressure (2000 kPa) ranges from C3 to C40. Although the simulation at high pressure predicted high-molecular-weight products (up to C40), Tabak et al., did not experimentally validate the high molecular weight products at high pressure. Olefins (C14) were the largest molecules at WHSV = 1 h^{-1}, T = 315 °C, P = 5063 kPa (abs).

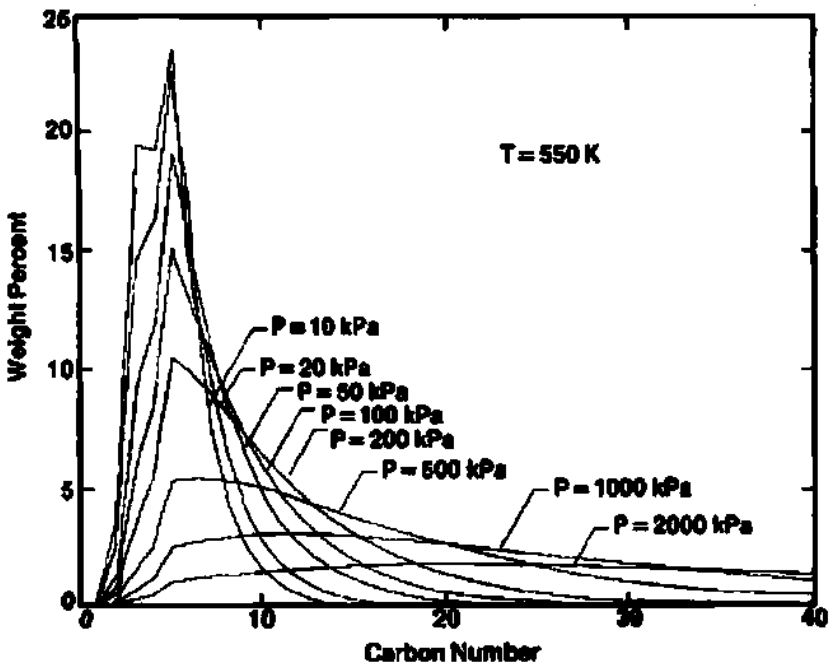

Figure 3-2. Carbon product distribution for methanol over ZSM-5 at WHSV = 1 h^{-1}, and T = 370 °C. (Figure from Tabak et al., 1986.)[28]

3.2 Experimental

At high pressures, the experiments were conducted in two sets: (1) vary temperature (T_{min} to 450 °C) at weight hourly space velocity (WHSV) = 1.92 h^{-1}, and (2) vary WHSV (1.92–11.5 h^{-1}) at T = 370 °C. For isopropanol, T_{min} = 260 °C and for mixed alcohols T_{min} = 320 °C. Tables 3-2 and 3-3 show all the experiments for the isopropanol and mixed alcohol reactions over HZSM-5 (280) at high pressure, respectively.

Table 3-2. Experiments for isopropanol reaction over HZSM-5 (280) at 5000 kPa (abs).

	Catalyst: HZSM-5 (280)			
	WHSV (h^{-1})			
T (°C)	1.92	3.84	7.68	11.52
260	HPI-1			
300	HPI-2			
320	HPI-3			
370	HPI-4	HPI-7	HPI-8	HPI-9
410	HPI-5			
450	HPI-6			

Table 3-3. Experiments for mixed-alcohol reaction over HZSM-5 (280) at 5000 kPa (abs).

	Catalyst: HZSM-5 (280)			
	WHSV (h^{-1})			
T (°C)	1.92	3.84	7.68	11.52
320	HPMA-1			
370	HPMA-2	HPMA-5	HPMA-6	HPMA-7
410	HPMA-3			
450	HPMA-4			

3.2.1 Reactor Unit 1(modified)

A dome-loaded back-pressure regulator (Model: S-91KW, P_{range} = 3000 psi, T_{range} = –65 to 200°C, REDQ Regulator, Salt Lake City, UT) was installed at the reactor exit before the condenser in the Reactor Unit 1. Figure 3-3 shows a schematic diagram of the modified unit. Flexible electric heating tape (Model: AWH-051-020D-MP, Series Miniature Autotune; Hts/Amptek Co) was wrapped around the regulator to keep the products as vapor. A variable autotransformer (input = 120 V, 10 A; Model: 3PN1010B

Staco Energy Products Co.) controlled the heating tape temperature. The back-pressure regulator (Figure 3-4) was connected to a N_2 tank at the desired set point pressure. The gas was injected into the dome of the regulator. This pressure seals off the fluid or gas flow from the process. Once the process pressure into the regulator exceeds the dome pressure, the diaphragm flexes and allows the fluids and gas to pass, thus maintaining the process pressure. When the pressure of the process drops below the dome pressure, the diaphragm again seals off the process and maintains the pressure. The set point pressure is usually 690 kPa lower than the one reached in the system.

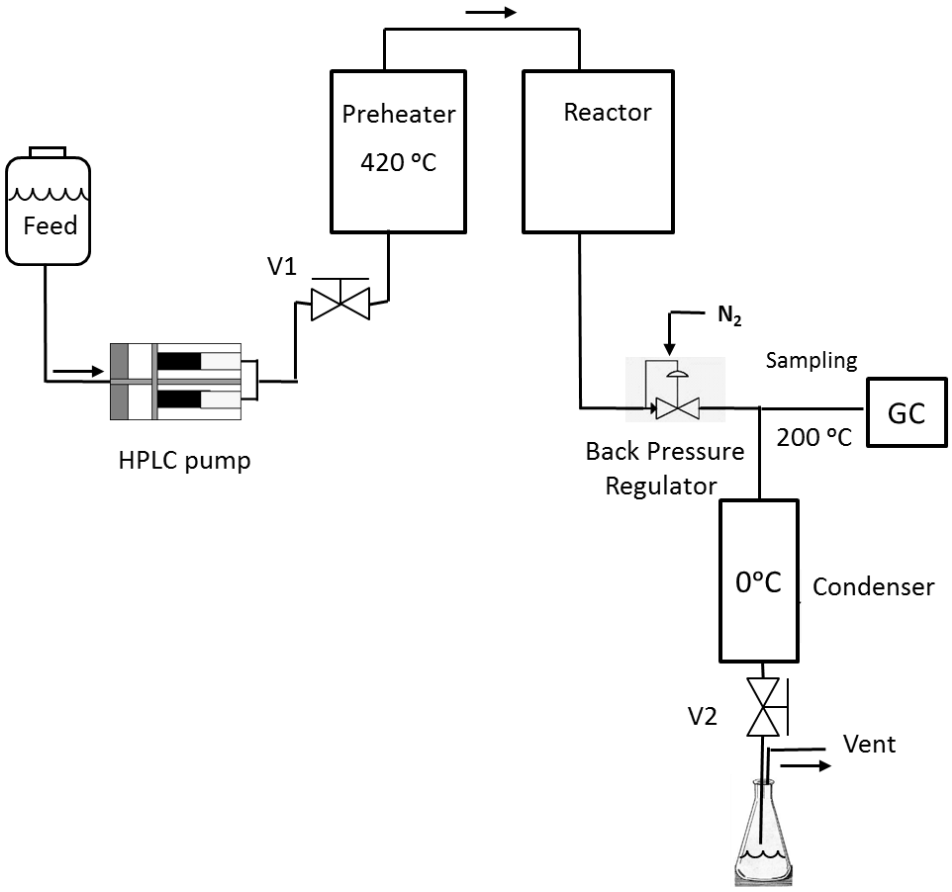

Figure 3-3. Schematic diagram of the Reactor Unit 1 modified with back-pressure regulator.

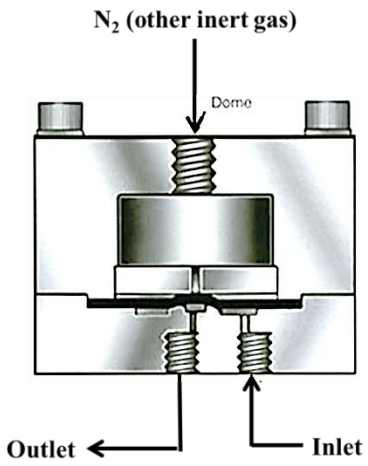

Figure 3-4. Schematic diagram of the dome-loaded back-pressure regulator.

3.3 Results

3.3.1 Isopropanol at high pressure

3.3.1.1 Catalyst stability

For the isopropanol reaction, Figure 3-5 shows the liquid product distribution over HZSM-5 during T.O.S. During the first 430 min, the product concentration was always constant; therefore, the catalyst did not deactivate during this time. For all experiments of varying temperature and WHSV, the reported concentrations were the average of all values recorded during the first 480 min. Approximately, six to eight samples were measured for each temperature and WHSV.

3.3.1.2 Effect of varying temperature

Approximately 300 °C was the lower temperature bound. Below this, the temperatures were not stable because of the heat of reaction. For example, when the reaction temperature was set between 250 and 300 °C, the only product was propene but

the temperature always increased until it reached 300 °C. On the other hand, if the temperature was lower than 250 °C, the isopropanol did not react.

Figure 3-6 shows the gas and liquid product distribution, which is affected by temperature. As the temperature increases, the amount of liquid (C5+) decreased from 55% (300 °C) to 22% (450 °C) and the gaseous products increased from 45% (300 °C) to 78% (450 °C). At high temperatures, gaseous products increase from cracking C5+ olefins.[24] For instance, the amount of propane increases from 0% (300 °C) to 45% (450 °C). Because of the dehydration reaction, the amount of olefinic gaseous products is larger than the paraffinic products.

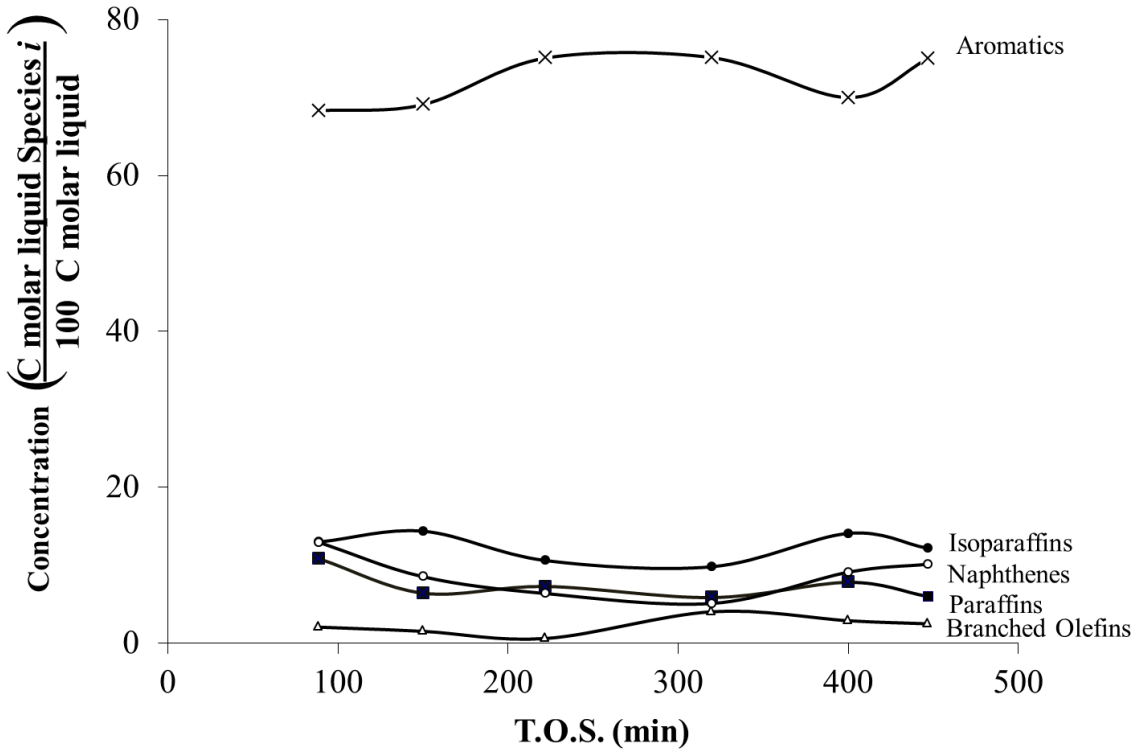

Figure 3-5. Liquid product distribution for isopropanol reaction over HZSM-5 (280), WHSV = 1.31 h^{-1}, P = 5000 kPa (abs), and T = 370 °C.

Temperature affects the type of liquid reaction products obtained (Figure 3-7). At higher temperatures, the concentration of aromatics increases from 5% (300 °C) to more than 90% (450 °C).[21] Because aromatics and gaseous products form, the amount of branched olefins decreases from 65% (300 °C) to 2% (450 °C). Also, the amount of naphthenes decreases from 20% (300 °C) to 2% (450 °C). Isoparaffins and paraffins reached the maximum of 18% (320 °C) and 5% (320 °C), respectively. The concentration of isoparaffinic and paraffinic compounds are always below 2% at all temperatures except 320°C.

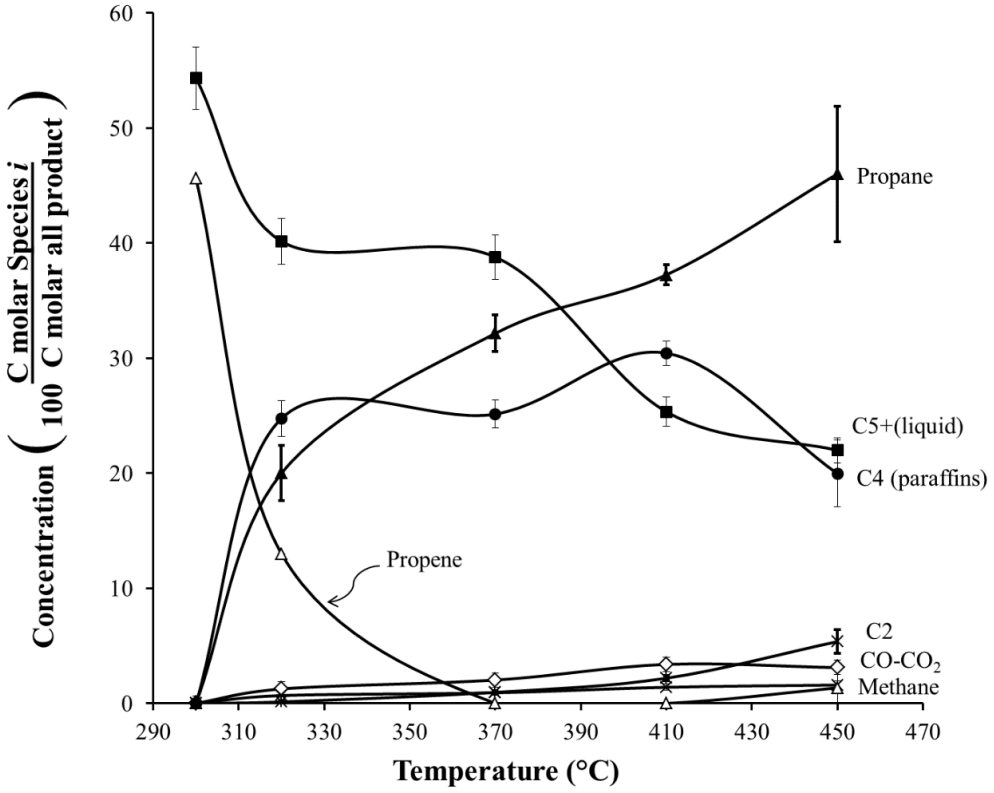

Figure 3-6. Product distribution of gases and liquids for isopropanol reaction over HZSM-5 (280), WHSV = 1.31 h^{-1}, and P = 5000 kPa (abs). (Error bars are ± 1σ.)

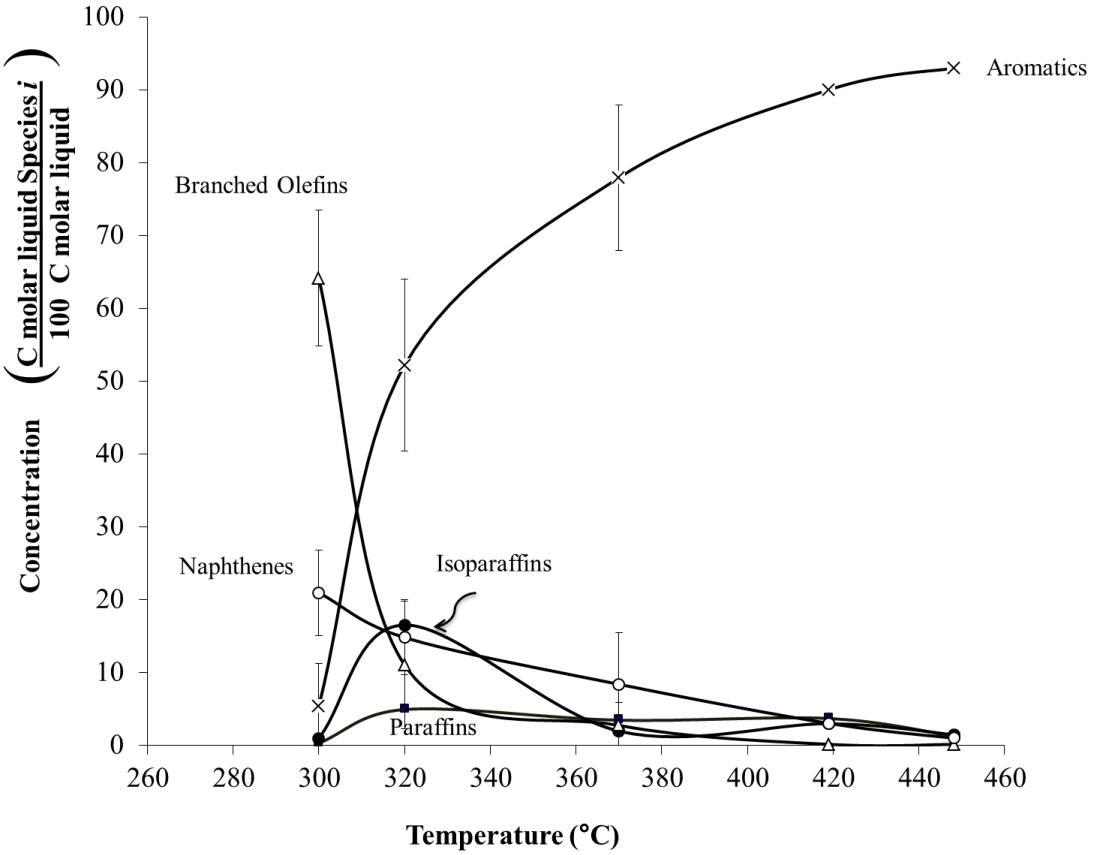

Figure 3-7. Liquid product distribution for isopropanol reaction over HZSM-5 (280), WHSV = 1.31 h^{-1}, and P = 5000 kPa (abs). (Error bars are ± 1σ.)

Figure 3-8 illustrates the carbon distribution of the liquid products at different temperatures. At lower temperatures, the most abundant component is C9 whereas at higher temperature, the most abundant component is C7–C8. At high temperatures, the olefins undergo more cracking reactions to produce smaller molecules, whereas at low temperatures, the molecules have less energy to avoid cracking and form larger molecules. At T = 300 °C, the carbon distribution is bimodal at C9 and C12. Propene

was the only gas produced at 300 °C (Figure 3-6), which explains that cracking did not occur yet and destroy high-molecular-weight molecules. Additionally, oligomerization occurs but the active energy to produce isoparaffins, paraffins, and aromatics is not sufficient. At 300 °C, propene trimerization and tetramerization occurs producing C9 and C12, respectively (Figure 3-8).

Figure 3-9 shows the liquid product distribution for isopropanol reaction over HZSM-5 (280) at different T.O.S. and P = 5000 kPa (abs). As the T.O.S. increases, the carbon distribution increases from centered on C8 (T.O.S. = 125 min) to C9 (T.O.S. = 125 min). Tetramerization does not occur until after T.O.S. = 190 min. For instance, the amount of C12 increases from 2% (T.O.S. = 125 min) to 17% (T.O.S. = 683 min).

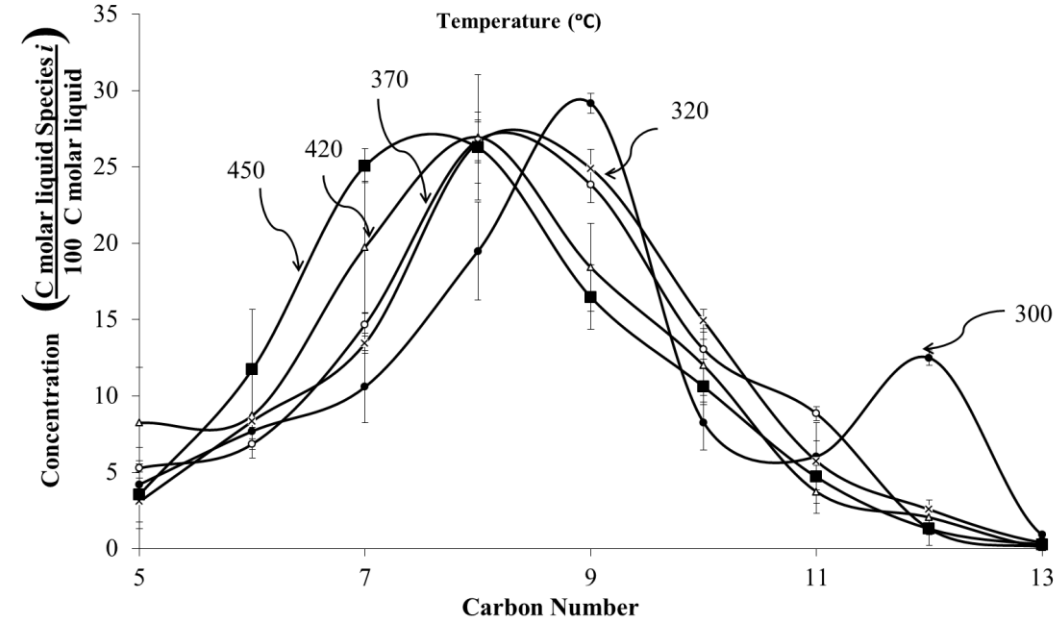

Figure 3-8. Liquid product distribution for isopropanol reaction over HZSM-5 (280), WHSV = 1.31 h^{-1}, and P = 5000 kPa (abs). (Error bars are ± 1σ.)

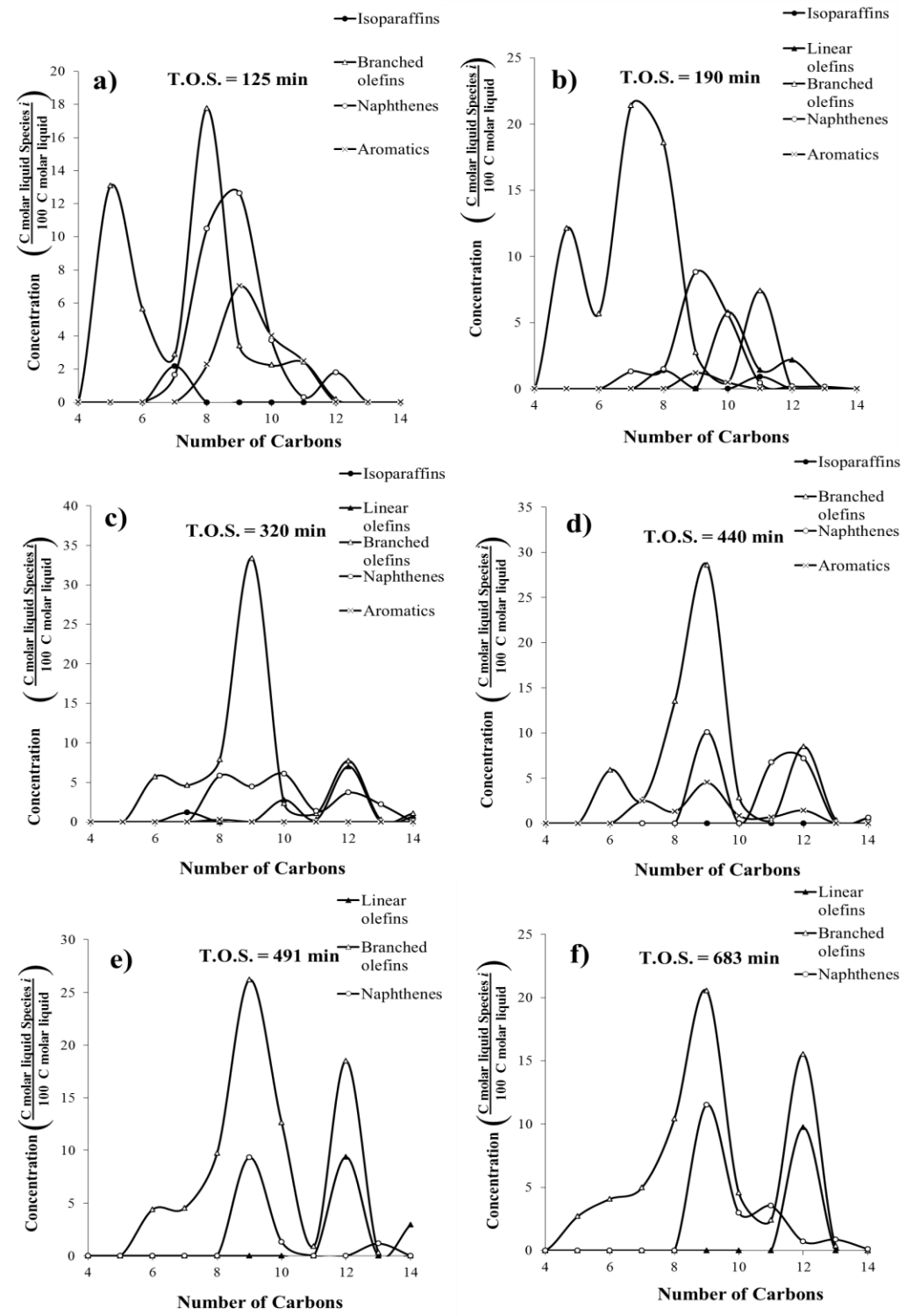

Figure 3-9. Liquid product distribution for isopropanol reaction over HZSM-5 (280) at different T.O.S., WHSV = 1.31 h^{-1}, and P = 5000 kPa (abs). (Error bars are ± 1σ.)

At first, it was assumed that the change of concentration products occurred because of catalyst deactivation. However, a temperature analysis through the catalyst bed revealed that there was a temperature increase that caused the different concentrations over time. Figure 3-10 show the temperature profile of the catalyst bed. Temperatures at the top, medium, and bottom were recorded over time. Before 300 min, the system is not stable. At WHSV = 1.92 h^{-1}, the time to fill the system and reach P = 5000 kPa (abs) is about 120 min. The reaction already started before 120 min, but the temperature along the catalyst bed was not stable because of a very high reactivity of the catalyst at 190 min (T_{middle} = 315 °C). Later, the temperature stabilized at 305 °C. This temperature increase explains the different carbon distributions at T.O.S. < 190 min, when aromatics and isoparaffins are present.

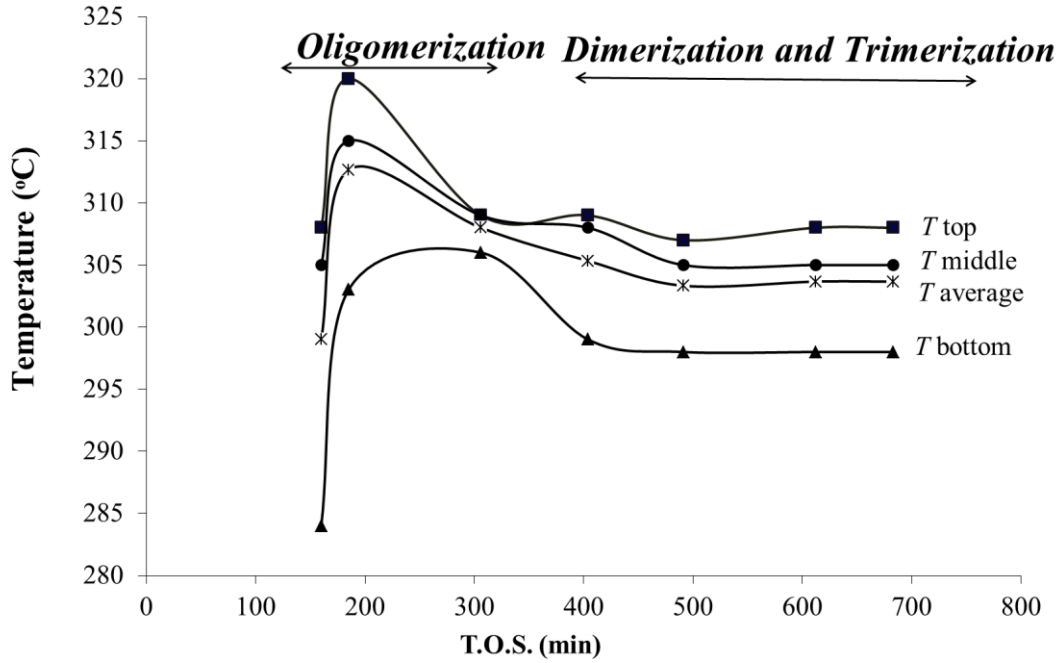

Figure 3-10. Temperature profile for the top, medium, bottom and average temperature for isopropanol reaction over HZSM-5 (280), WHSV = 1.9 h^{-1}, P = 5000 kPa (abs), and T = 300 °C.

3.3.1.3 Effect of varying WHSV

At T = 370 °C and WHSV = 1.92–11.5 h^{-1}, Figure 3-11 shows the distribution of gas and liquid is not greatly affected by the change of WHSV. At all WHSV, the amount of liquid slightly increases from 38% (1.92 h^{-1}) to 45% (11.5 h^{-1}). The amount of propene is low (~3%) and constant, which results because high pressure decreases the WHSV and allows enough time for the propene to react and form other compounds. The amount of C4 paraffins increases from 25% (1.92 h^{-1}) to 32% (11.5 h^{-1}). On the other hand, when the WHSV increases, propane decreases, from 32% (1.92 h^{-1}) to 22% (11.5 h^{-1}). The gas products are mostly saturated, which makes it difficult for them to be recycled and further oligomerized.

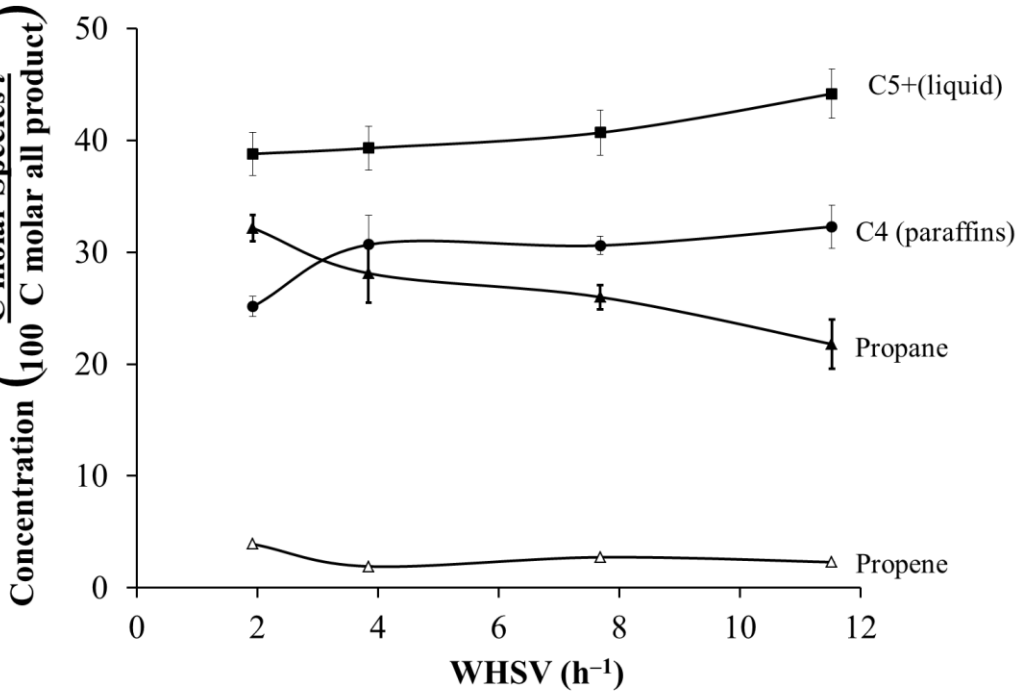

Figure 3-11. Product distribution of gases and liquids for isopropanol reaction over HZSM-5 (280), T = 370 °C, and P = 5000 kPa (abs). (Error bars are ± 1σ.)

Figure 3-12 illustrates the types of liquid-phase products at different WHSV. At very low WHSV, aromatics are high (79% at 1.92 h^{-1}); however, at high WHSV, aromatics are low (45% at 11.5 h^{-1}). On the other hand, when WHSV increases, isoparaffins also increase from 2% (0.52 h^{-1}) to 39% (11.5 h^{-1}). At all WHSV, naphthenes are constant (~10%) and the amount of branched olefins always stayed below 5%. Paraffins slightly increase from 3% (1.92 h^{-1}) to 10% (11.5 h^{-1}). At atmospheric pressure (Figure 2-12) and high pressure (Figure 3-12) when the WHSV increases, the amount of aromatics decreases. In contrast, when WHSV increases, branched olefins increase at atmospheric pressure but they are negligible at high

pressure. There is a new region formed, which has not previously been reported in the literature.

Figure 3-13 illustrates the carbon distribution of the liquid products at different WHSV. In this WHSV, the most abundant components are C8, C9, and C7, in that order. The product carbon distribution is not affected by changing WHSV.

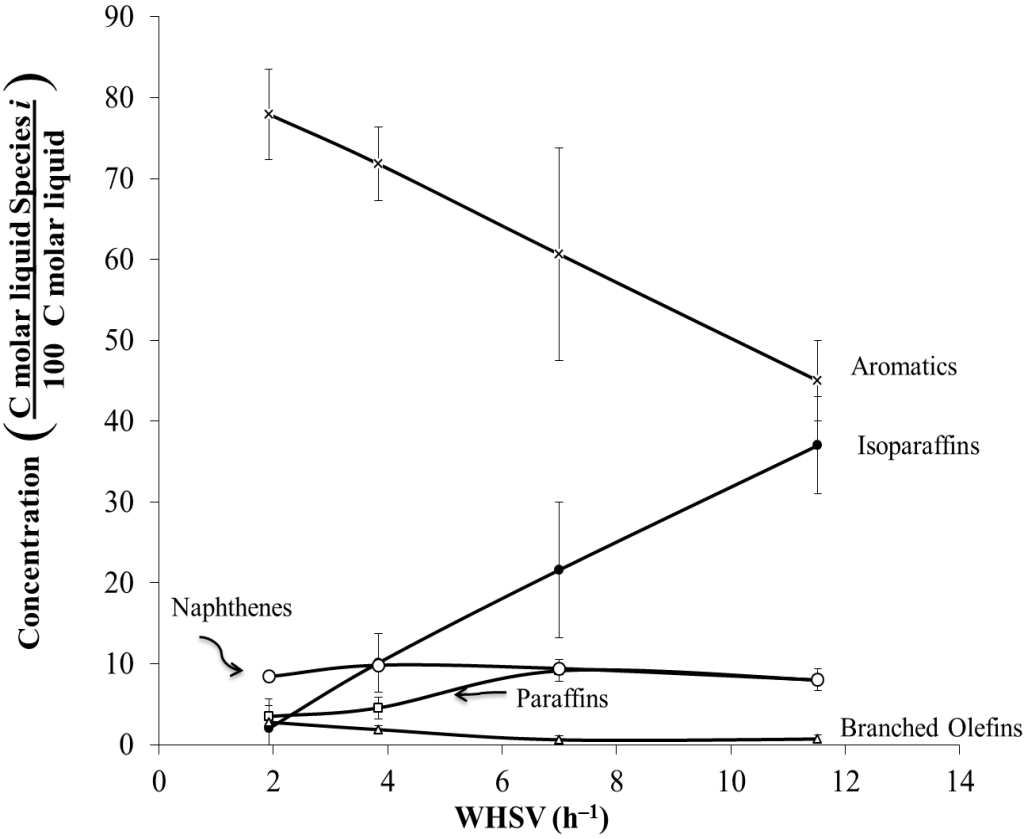

Figure 3-12. Liquid product distribution for isopropanol reaction over HZSM-5 (280), *T* = 370 °C, and *P* = 5000 kPa (abs). (Error bars are ± 1σ.)

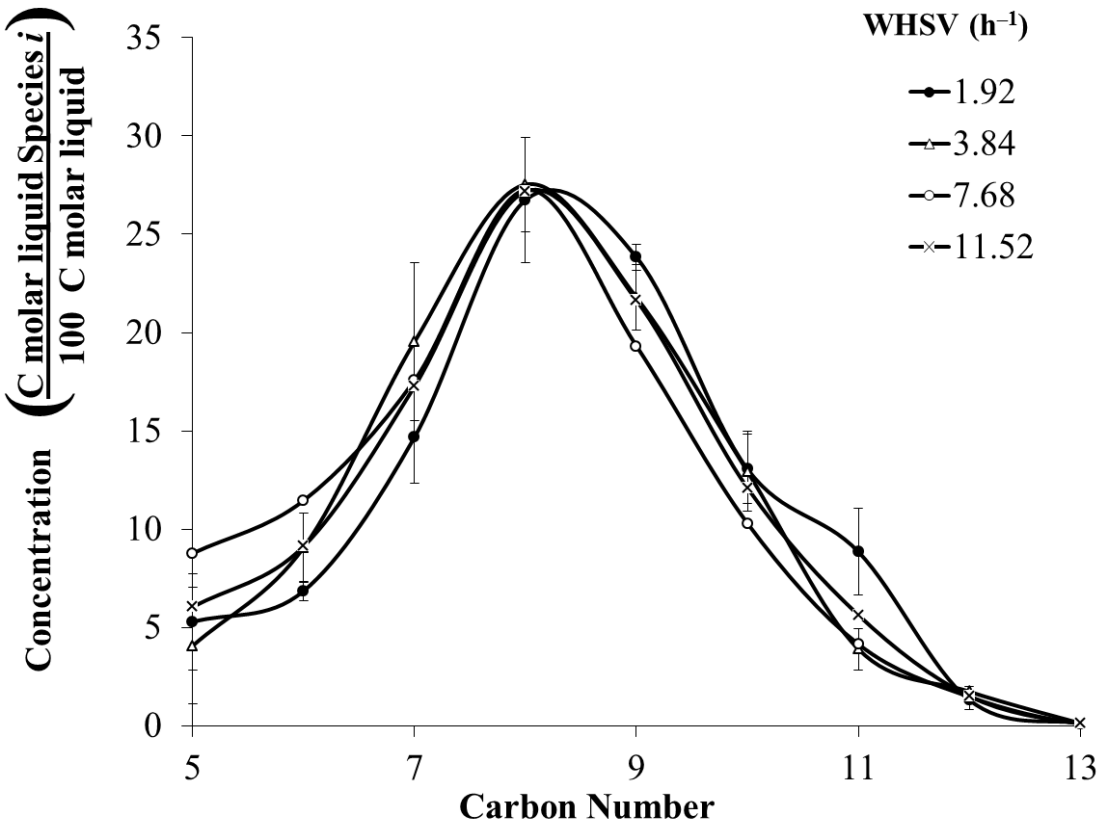

Figure 3-13. Liquid product distribution of isopropanol reaction over HZSM-5 (280), T = 370 °C, and P = 5000 kPa (abs).

The dehydration region is still between 250 and 300 °C (similar to atmospheric pressure), but only produces propene. It may be assumed, that the dehydration is very fast, and propene oligomerizes as soon it appears.

3.3.2 Mixed alcohol at high pressure

For mixed alcohols, there are two reactions types: dehydration and oligomerization. For all figures, the reaction-type region is specified.

3.3.2.1 Catalyst stability and effect of varying the temperature

For mixed alcohols at high pressure, the product concentration changes during T.O.S. Depending on temperature and WHSV, the catalyst deactivates faster or slow. For instance, Figure 3-14 shows the liquid product distribution during T.O.S. at T = 370 °C, WHSV = 1.9 h^{-1}, P = 5000 kPa (abs). The temperature and WHSV are low. During the first 470 min, the product distribution is not stable; however, the product concentration does not vary greatly. At very low T.O.S., branched olefins are high (60% at 280 min); however, at high T.O.S., branched olefins are less (40% at 480 min). On the other hand, when the T.O.S. increases, naphthenes also increase from 10% (280 min) to 30% (480 min). Linear olefins, isoparaffins, and aromatics concentrations are relatively constant. Overall, at low temperature and low WHSV, two types of reactions coexist: dehydration and oligomerization. This region is characterized by large amounts of branched and liner olefins

However, the product concentration varies more at high temperatures than low temperatures. For instance, Figure 3-15 shows the liquid product distribution during T.O.S. at T = 450 °C, WHSV = 1.9 h^{-1}, P = 5000 kPa (abs). The temperature is high and WHSV is low. During the first 680 min, the product distribution is not stable and varies greatly. At very low T.O.S., aromatics are high (85% at 150 min); however, at high T.O.S., aromatics are less (10% at 680 min). In contrast, when the T.O.S. increases,

linear olefins also increases from 0% (280 min) to 60% (680 min). Overall, at high temperature and low WHSV, two types of reactions occur consecutively: oligomerization and then dehydration. This region is characterized by aromatics and isoparaffins during oligomerization and liner olefins during dehydration.

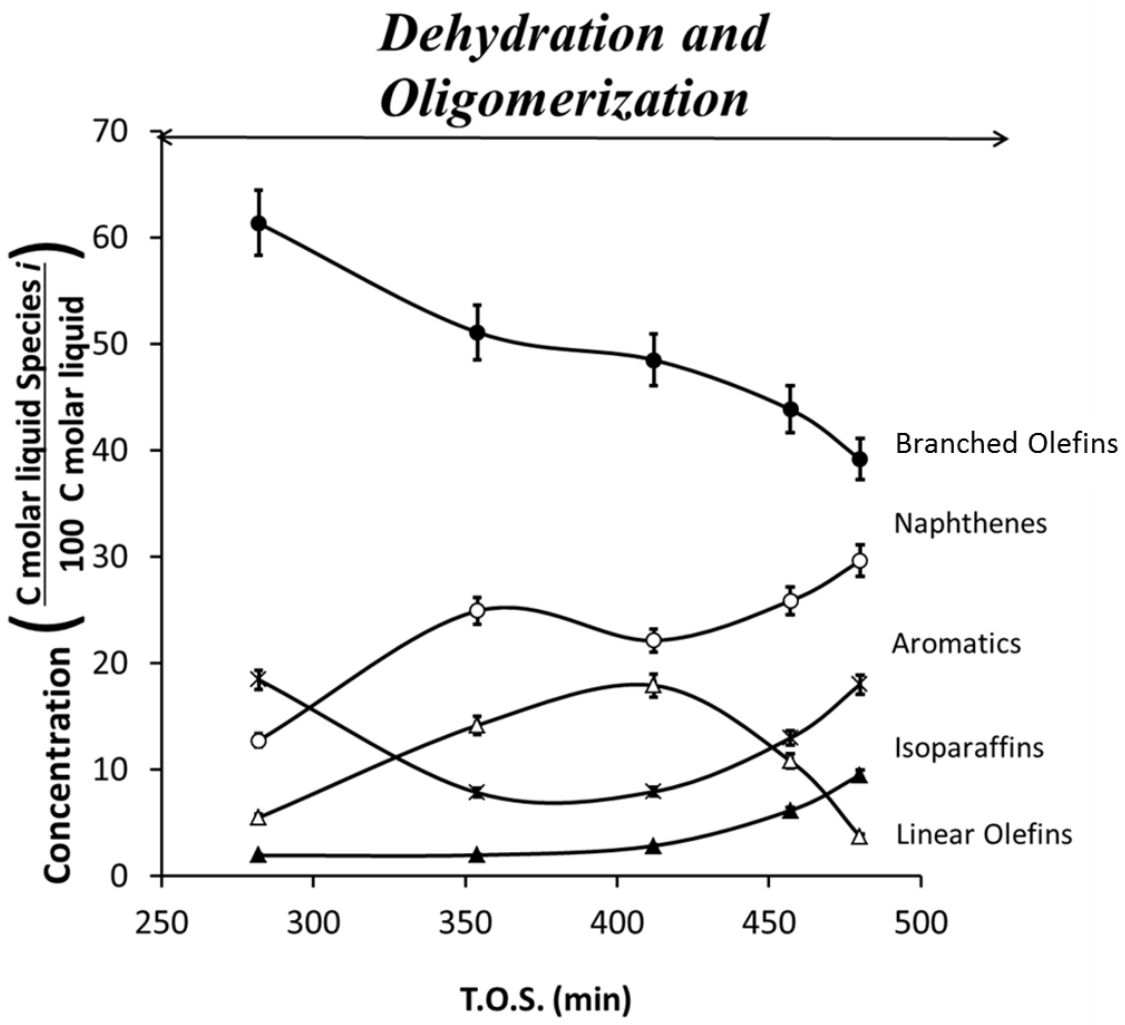

Figure 3-14. Liquid product distribution for the mixed alcohol reaction over HZSM-5 (280), T = 370 °C, WHSV = 1.9 h^{-1}, and P = 5000 kPa (abs).

Finally, the product concentration varies less at low temperatures and high WHSV. For instance, Figure 3-16 shows the liquid product distribution during T.O.S. at T = 370 °C, WHSV = 3.84 h^{-1}, P = 5000 kPa (abs). The temperature is low and WHSV is high. During the first 450 min, the product distribution is stable and does not vary. At all T.O.S., the amount of linear olefins always stayed above 85%. The amount of branched olefins, naphthenes, and isoparaffins stayed below 10%. Overall, at low temperature and low WHSV, only the dehydration reaction occurs. This region is characterized by high amounts of linear olefins.

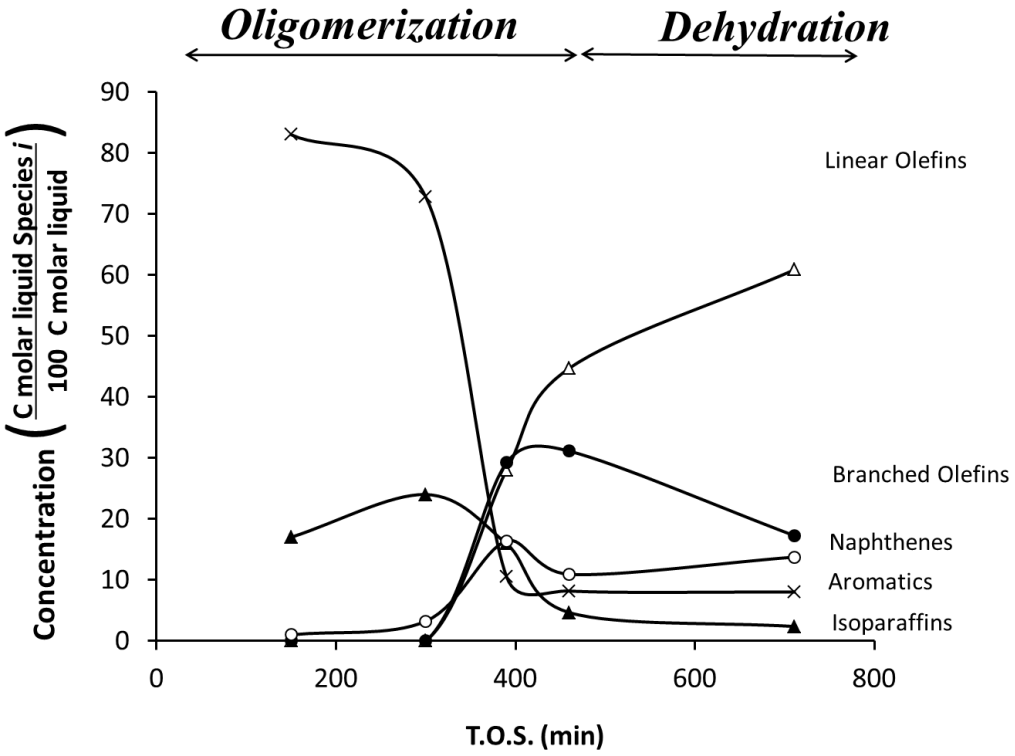

Figure 3-15. Liquid product distribution for the mixed alcohol reaction over HZSM-5 (280), T = 450 °C, WHSV = 1.9 h^{-1}, and P = 5000 kPa (abs).

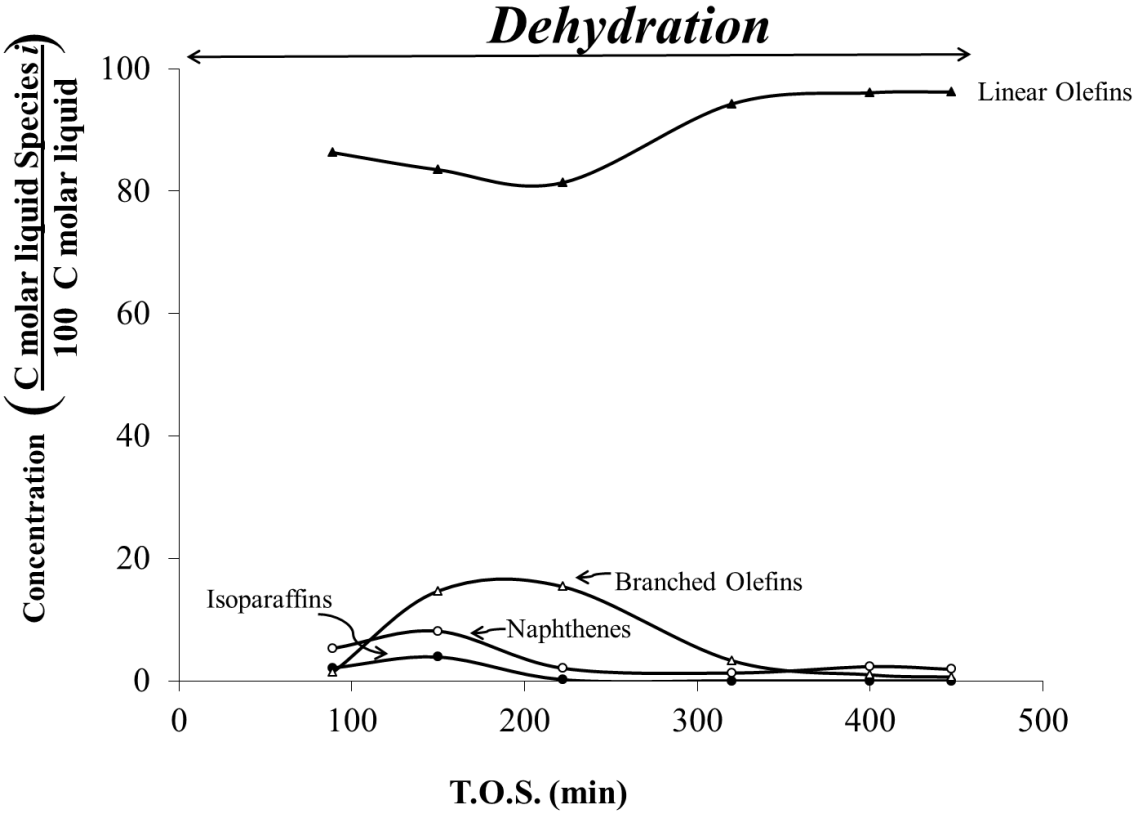

Figure 3-16. Product distribution of gases and liquids for mixed alcohol reaction over HZSM-5 (280), T = 370 °C, WHSV = 3.84 h^{-1}, and P = 5000 kPa (abs).

3.3.2.2 Effect of varying WHSV

Figure 3-17 illustrates the gas product distribution at different WHSV at T = 370 °C. Between 1.9 and 11.53 h^{-1}, dehydration is the dominant reaction because C5+ are the most abundant species (~95%). The product distribution is affected by changing WHSV. In this WHSV range, the amount of gases (C3–C4) decreases from 50% at 1.9 h^{-1} to less than 10% at 11.53 h^{-1}. On the other hand, the amount of C5+ increases from 50% at 1.9

h^{-1} to a maximum of 90% at 3.8 h^{-1}, then decreases to 72 % at 11.53 h^{-1}. This is attributed to unreacted alcohols in the concentration product.

Figure 3-18 illustrates the liquid product distribution of the liquid products at different WHSV. In this WHSV range, the most abundant components are linear olefins. The liquid product carbon distribution is affected by changing WHSV. As WHSV increases, the amount of linear olefins increases from 0% (1.9 h^{-1}) to a maximum of 90% (3.8 h^{-1}), and then decreases to 72% (11.53 h^{-1}), which is also attributed to unreacted alcohols in the concentration product. The unreacted alcohols increased from 0% (1.9 h^{-1}) to 17% (11.53 h^{-1}). On the other hand, the amount of aromatics decreased from 45% (1.9 h^{-1}) to 1% (11.53 h^{-1}). Also, the amount of branched olefins decreased from 35% (1.9 h^{-1}) to 3% (11.53 h^{-1}).

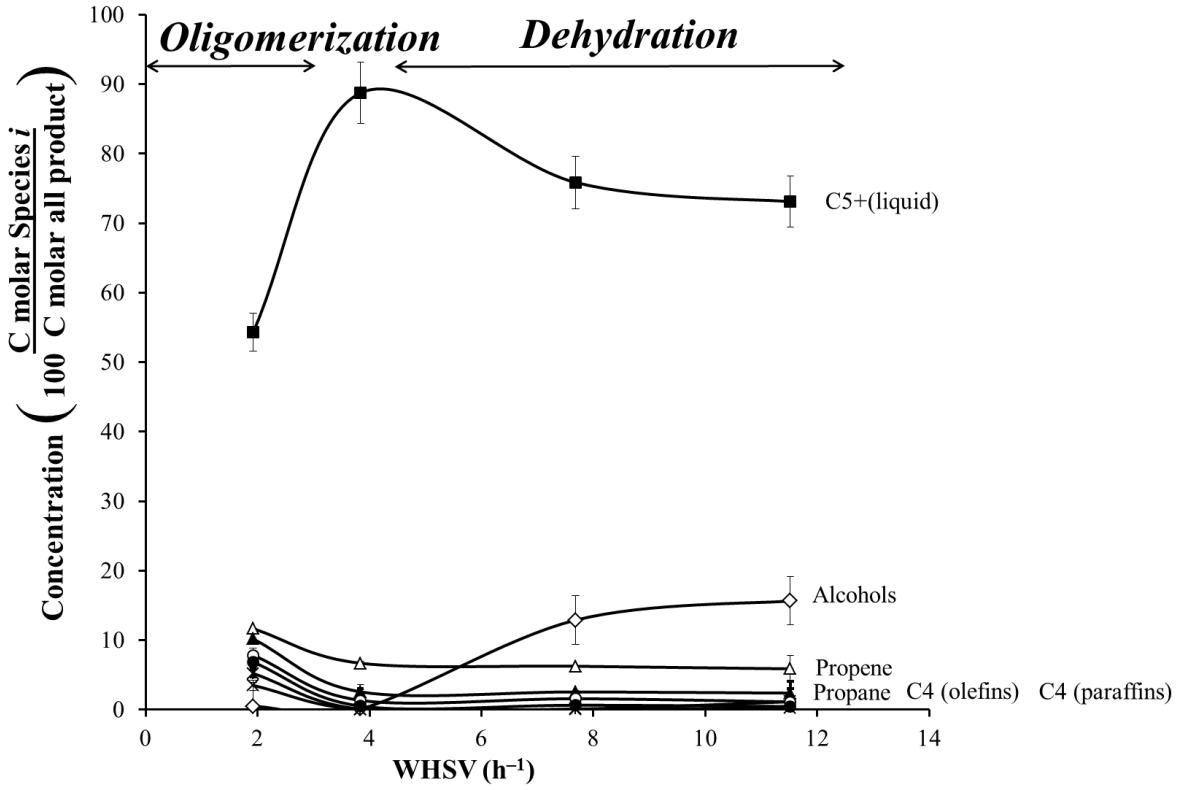

Figure 3-17. Product distribution of gases and liquids for mixed alcohol reaction over HZSM-5 (280), T = 370 °C, and P = 5000 kPa (abs). (Error bars are ± 1σ.)

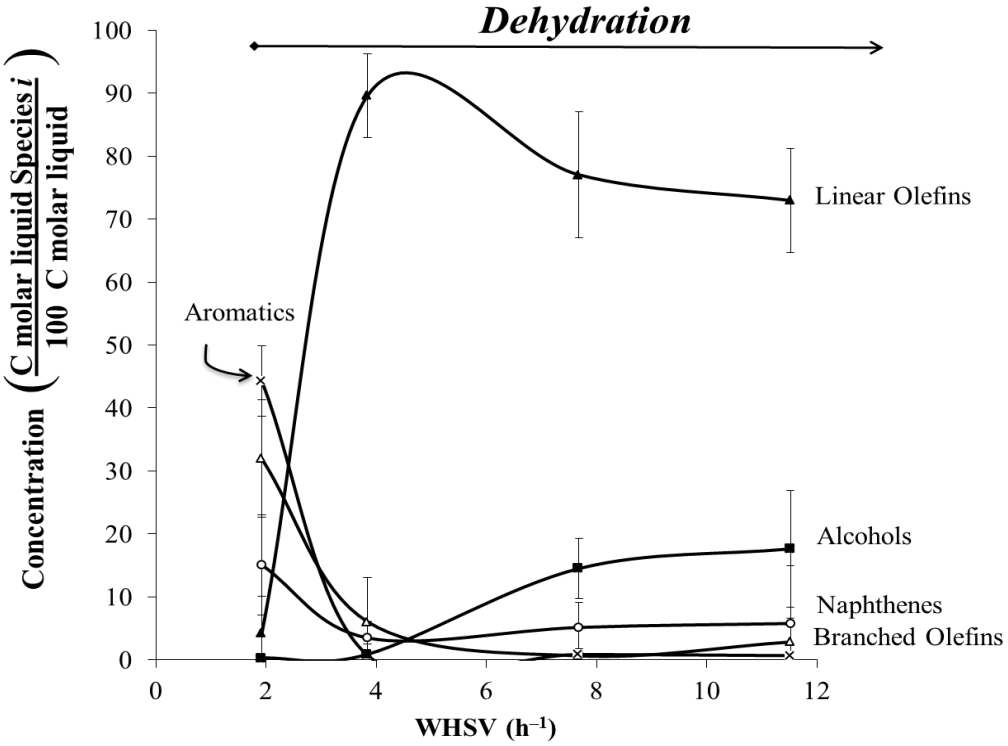

Figure 3-18. Liquid product distribution of mixed alcohol reaction over HZSM-5 (280), T = 370 °C, and P = 5000 kPa (abs).

For WHSV 7.68 and 11.52 h^{-1}, the amount of unreacted alcohols is significant (~17%). Figure 3-19 compares the unreacted alcohol distribution of mixed alcohol with the alcohol feed at these WHSV. Low-molecular-weight alcohol (C3–C7) had better conversion than high-molecular-weight alcohols (C9–C12). For instance, when the isopropanol feed concentration is 7%; the unreacted isopropanol in the liquid product is 0% (7.68 h^{-1} and 11.2 h^{-1}). Therefore, the conversion of isopropanol is 100%. As well, when 2-heptanol feed concentration is 29%, the unreacted alcohol concentration is about 5%. The conversion of 2-heptanol is about 32%. On the other hand, high-molecular-weight alcohol has less conversion.

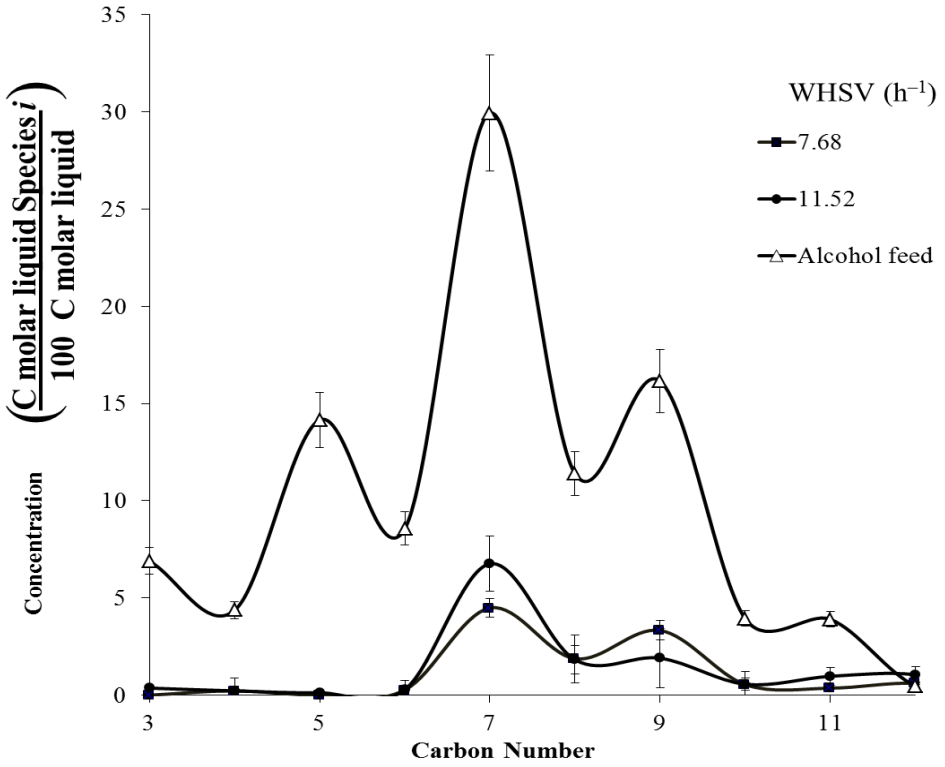

Figure 3-19. Liquid unreacted alcohol and alcohol feed distribution of mixed alcohol reaction over HZSM-5 (280), WHSV = 1.9 h^{-1}, and P = 5000 kPa (abs).

3.3.2.3 Effect of varying the pressure

Figure 2-15 shows the pressure effect on the liquid product distribution of mixed alcohol reaction over HZSM-5 (280). In a pressure range from 101 to 8500 kPa, the liquid product distribution does not vary drastically. Increased pressure slightly changes the reaction from dehydration to oligomerization. For mixed alcohol, the effect of temperature on the product distribution is higher than pressure. As pressure increases, the amount of linear olefins decreased from 95% (101 kPa (abs)) to 82% (8400 kPa

(abs)). On the other hand, the amount of other hydrocarbon increased from 5% (101 kPa (abs)) to 18% (8400 kPa (abs)). The most abundant hydrocarbon type is branched olefins. The presence of branched olefins indicates that higher pressure promotes oligomerization.

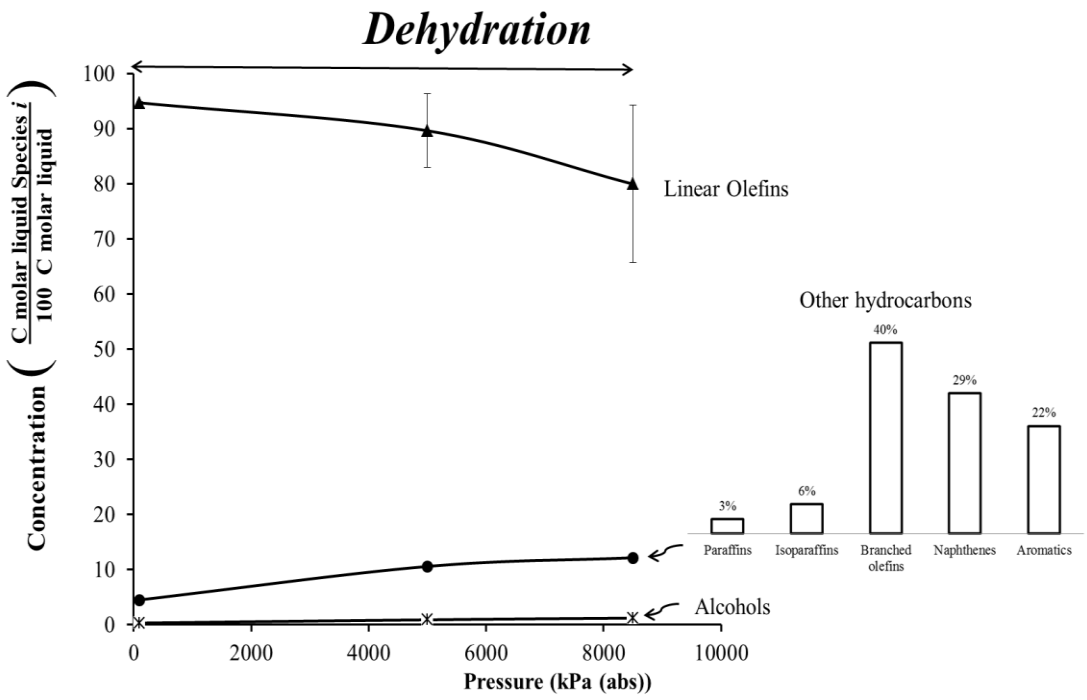

Figure 3-20. Liquid product distribution of mixed alcohol reaction over HZSM-5 (280), T = 370 °C, and WHSV = 1.31 h^{-1}.

3.4 Conclusions

For isopropanol reaction over HZSM-5 at high pressure, the catalyst does not deactivate. The products are stable and do not vary over time. On the other hand, reacting mixed alcohol at high pressure causes catalyst deactivation at three speeds (slow, medium and fast) depending on the reaction conditions. At low temperature and high WHSV, catalyst deactivation is less. On the other hand, deactivation has a medium rate when the temperature is low and the WHSV is lower. If both temperature and WHSV are low, the deactivation rate is fast. In this region, the concentration product changes during T.O.S..

At high pressure, the transformation of alcohols is governed by two types of reactions (dehydration and oligomerization) and occurs in the same order as well. Inside the oligomerization reaction, the possibilities are in the following order: *n*-merization or organized oligomerization (e.g., dimerization, trimerization, and tetramerization); disproportionation (formation of branched olefins); and cracking (production of aromatics, paraffins, and gas products). When the temperature increases, first dehydration occurs and then oligomerization, in that order. For isopropanol at high pressure, all types of reaction occur between 300 and 370 °C. In contrast, for mixed alcohols all type of reactions occur between 300 and 450 °C, except for the *n*-merization or organized oligomerization.

4. KETONE OLIGOMERIZATION

The objectives of this section follow:

a) Describe the transformation of acetone to hydrocarbons.

b) Describe the transformation of mixed ketones to hydrocarbons.

4.1 Introduction

Although isopropanol and acetone differ by only two hydrogen atoms in their molecules, their reaction mechanisms are very different.

According to Chang (1977), with HZSM-5, acetone undergoes classic acid-catalyzed condensation to mesitylene (also called aldol condensation), which occurs when acetone contacts any acid. For example, when acetone contacts sulfuric acid for a long time, it forms an aldol. If the temperature is high enough, the aldol forms mesitylene.[13]

Because zeolites have catalytic acid sites in their structure, the reaction of acetone with sulfuric acid is similar to the reaction of acetone with zeolite. Both the zeolite (HZSM-5) and the acid catalyze the reaction. However, according to Salvapatini et al. (1989), the catalytic self-condensation of acetone is very complex and has numerous products, including diacetone alcohol, mesityl oxide, phorone, mesitylene, isophorone, and 3,5-xilenol (Figure 3.1). The product spectrum depends on the experimental conditions. Experimental conditions (e.g., temperature, pressure, and catalyst) also determine the reaction products obtained from acetone (Salvapati et al. 1989). [29]

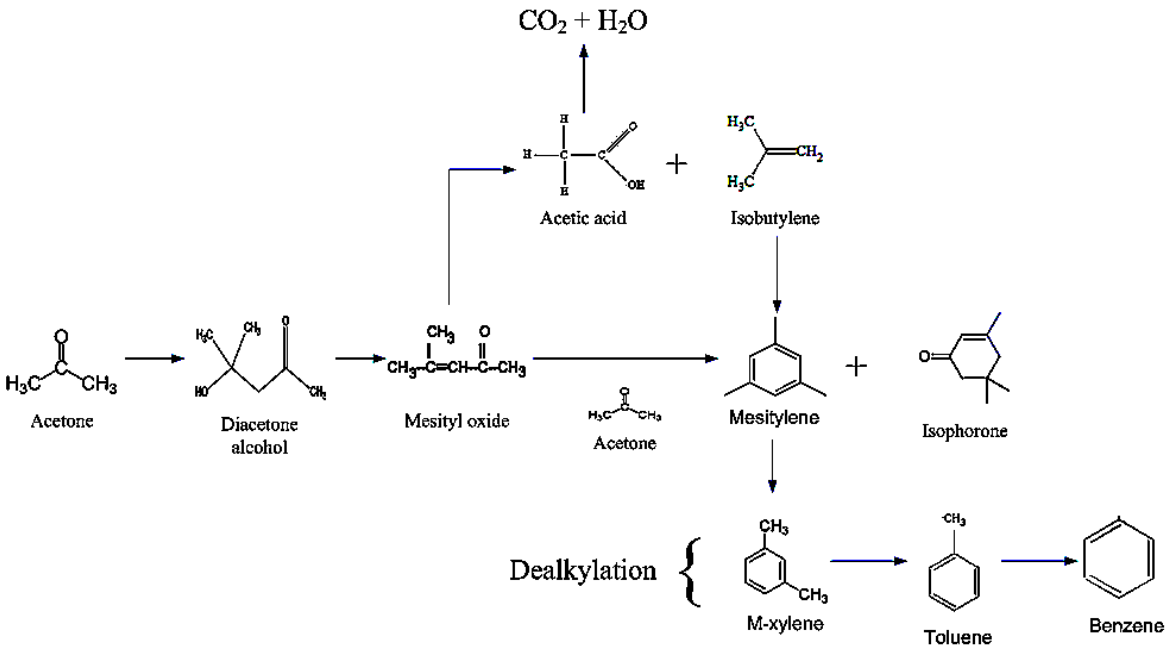

Figure 4-1. Formation of reaction products in the autocondensation of acetone (Salvapati et al. 1989).[29]

Chang and Silvestri (1977) pioneered the oligomerization of acetone on HZSM-5 catalyst using a packed-bed reactor for their experiments. They studied temperatures from 250 to 400 °C using WHSV = 8 h^{-1} at 101 kPa (abs)

Table 4-1 shows the product distribution of acetone reaction presented by Chang and Silvestri (1977). The conversion increased from 3.9% (250 °C) to 95.3% (400 °C). The amount of isobutene decreased significantly with increased temperature from 83.3% (329 °C) to 3.6% (399°C). This may be attributed to the oligomerization of isobutene into aromatics according to the study by Salvapati et al. (1989). It is noteworthy that the most abundant hydrocarbon at high temperatures (399°C) is xylene. It is also notable, that among all the reaction liquid products ($C6^{+}$), most are aromatics.

Table 4-1. Product distribution of acetone reaction over HZSM-5 catalyst (Chang and Silvestri, 1977).[13]

Reaction Conditions				
T (°C)	250	288	329	399
WHSV (h^{-1})	8.0	8.0	8.0	8.0
Conversion (%)	3.9	6.0	24.5	95.3
Carbon Selectivity, (%)				
Diacetone alcohol	3.5	2.9	0.1	–
Mesityl oxide	27.3	19.7	1.2	–
Isophorone	–	<0.1	5.3	–
Other O-compounds	6.0	15.0	<0.1	–
$CO + CO_2$	–	0.7	10.0	6.1
Hydrocarbons	63.2	61.2	83.4	93.9
Hydrocarbon Distribution (wt%)				
Methane	–	–	0.2	0.1
Ethane	–	–	0.4	0.2
Ethylene	<0.1	<0.1	1.2	2.4
Propane		0.3	1.9	4.2
Propylene	2.5	3.8	4.2	5.2
i-Butane	–	–	0.1	3.9
n-Butane	–	–	–	1.7
i-Butene	19.1	31.3	83.3	3.6
n-Butene	–	–	<0.1	2.3
i-Pentane	–	–	–	1.5
n-Pentane	–	–	–	0.6
Pentenes	–	–	–	2.5
C6+ Aliphatics	19.1	3.8	1.6	8.2
Benzene	–	–	–	2.6
Toluene	–	–	0.1	13.0
Ethylbenzene	–	–	–	2.7
Xylenes	–	1.3	2.1	22.3
1,2,3-Trimethylbenzene	–	<0.1	<0.1	1.1
1,2,4-Trimethylbenzene	–	7.0	2.0	8.8
1,3,5-Trimethylbenzene	59.3	52.5	2.6	0.6
Other C9 Aromatics	–	–	0.3	9.7

Gayubo (2004) also reported the oligomerization of acetone on HZSM-5.[30]

Acetone and water (50% mol) were used in their experiment in a fixed-bed reactor with

temperatures ranging from 250 to 450 °C with a temperature ramp of 0.5 °C/min. For WHSV = 1.2 h^{-1} and P = 101 kPa (abs), they studied the effect of temperature on the product distribution. Their results are more detailed than the results presented by Chang and Silvestri (1977). Profiles of aromatics, $C5^+$ olefins, $C4^+$ paraffins, ethenes, propenes, *n*-butenes, CO, CO_2, and water were recorded with changing temperature.

At low temperatures (250 to 300 °C), aromatic compounds are the most abundant. However, at higher temperatures the aromatic concentration decreases and the concentration of $C5^+$ olefins and isobutene increases.[30]

Gayubo (2004) showed the effect of co-feeding the acetone/water mixtures with nitrogen, which inhibited the production of aromatics and $C4^+$ paraffins. Nitrogen increased the selectivity of propene and $C5^+$ olefins. Also, nitrogen reduced catalyst deactivation because it attenuates coke formation.[30]

Salvapati et al. (1989) explained the mechanism of acetone condensation (see Figure 2.6). Over an acid catalyst, the first reaction product of acetone is diacetone alcohol. Then, this ketone alcohol is transformed to mesityl oxide ($CH_3C(O)CH=C(CH_3)_2$) and water. Next, the mesityl oxide reacts with acetone, forming most of the reaction products of the condensation of acetone, e.g., phorone, isophorone, isobutene, acetic acid, mesytilene, and others.[29]

Figure 4-1 (Salvapati et al. 1989) shows the transformation of mesytil oxide to acetic acid and isobutene. This reaction is important because isobutene is oligomerized to mesitylene. According to Silvestri et al. (1989), all the aromatic compounds are

formed from mesytilene. The dealkylation reaction of mesytilene produces xylenes, toluene, and benzene, in that order.

Acetone was not the only ketone feedstock oligomerized by zeolite catalyst, but also a number of ketones. Fuhse and Bandermann (1987) published experimental results of 10 different ketones (ranging from C3 to C8) compounds over HZSM-5. The compounds were easily converted to hydrocarbons when the carbon to hydrogen (C/H) ratio of the molecule fragment, remaining after eliminating oxygen as water, is less than 0.62. For example, acetone (C/H ratio = 0.75) conversion was ~50%; whereas, 3-heptanone (C/H ratio = 0.75) conversion was 100% at T.O.S = 500 min.

According to Fuhse and Bandermann, the ketone reaction products were mainly aromatic hydrocarbons, predominantly xylene. The hydrocarbons produced are in the gasoline fraction (C5–C11).[18] Table 4-2 shows the C/H ratio of the mixed ketone produced from paper and chicken manure ranged from C3 (acetone) to C13 (6-tridecanone). According to Fuhse and Bandermann, it is expected that acetone, 2-butanone, and 2-pentanone with C/H ratio > 0.6 had less conversion than the remaining ketones (C/H ratio < 0.6).

Table 4-2. C/H ratio of the mixed ketone obtained from paper and chicken manure.

Mixed Ketones	C/H (mol/mol)
Acetone	0.75
2-Butanone	0.67
2-Pentanone	0.63
2-Hexanone	0.60
2-Heptanone	0.58
2-Octanone	0.57
4-Nonanone	0.56
5-Decanone	0.56
6-Undecanone	0.55
6-Dodecanone	0.55
6-Tridecanone	0.54

For the MixAlco™ process, the transformation of mixed ketones into hydrocarbon skips the hydrogenation process which reduces the number of steps to obtain hydrocarbons (e.g., jet fuel or gasoline). Although mixed alcohols and mixed ketones have the same carbon distribution, their reaction mechanisms are very different.

4.2 Experimental

For the acetone reaction over HZSM-5 (80), 12 experiments were performed. Reactor Unit 1 was used (Figure 2-6) and temperatures ranged from 305 to 415 °C. The weight hourly space velocities (WHSV) studied were: 1.32, 2.63, 3.95, 5.27, 6.58, and 7.9 h^{-1}.The reaction pressure evaluated was 101 kPa (abs). Table 4-3 summarizes

experiments for the acetone reaction over HZSM-5 (80) and the conditions for each experiment.

For the transformation of mixed ketones to hydrocarbons, five experiments were performed with temperatures ranging from 430 to 590 °C. The WHSV studied was 1.92 h^{-1}, and the catalyst was HZSM-5 (280). For mixed ketones, HZSM-5 (280) was chosen because it deactivates slower than HZSM-5 (80). Table 4-4 shows all the experiments for the mixed-ketone reaction.

Table 4-3. Experiments for acetone reaction over HZSM-5 (80).

	Catalyst: HZSM-5 (80)					
	WHSV (h^{-1})					
T (°C)	1.3	2.6	3.9	5.2	6.5	7.9
305	A1					
350	A2	A3	A4	A5	A6	
415	A7	A8	A9	A10	A11	A12

Table 4-4. Experiments for the mixed-ketone reaction over HZSM-5 (280).

	WHSV (h^{-1})
T (°C)	1.92
430	MK-1
460	MK-2
510	MK-3
560	MK-4
590	MK-5

4.2.1 Acetone

Reagent-grade acetone (99% pure) was obtained from Mallinckrodt Chemicals (Phillipsburg, NJ).

4.2.2 Mixed ketone

Mixed ketones were made in the pilot-scale MixAlco™ process located at Texas A&M University (Figure 1-1). Section 6 has a more detailed procedure of the steps followed to obtain mixed alcohol. Mixed ketones are yellow with a very strong odor. The mixed ketones turn black over time when oxygen is present. To avoid color changes, the bottle must be well sealed and previously purged with nitrogen to displace the air.

4.3 Results

The reaction of acetone and mixed ketones over HZSM-5 is exothermic. The ketones react to form hydrocarbons (aromatics), other oxygenated compounds, and water.

4.3.1 Acetone

The following section describes results for acetone.

4.3.1.1 Catalyst stability

Figure 4-2 shows the percentage of liquid and gas with respect to T.O.S. for acetone over HZSM-5 (80) at T = 410 °C, WHSV = 1.3 h^{-1}, and P = 101 kPa (abs). The conversion was 100% at all times.

The gas phase contains hydrocarbons from C1 to C4, CO_2, and CO, and the liquid phase contains hydrocarbon $C5^+$ (mainly aromatics). Figure 4-2 shows that with time, the yield for gaseous products decreases and the yield for liquid products increases. Therefore, the product selectivity changes with time, which is attributed to catalyst deactivation.

Figure 4-3 shows the product distribution of the gas phase with respect to T.O.S. for acetone over HZSM-5 (80) at T = 415 °C, P = 101 kPa (abs), and WHSV = 1.3 h^{-1}. Only gases with concentrations over 5 mol% are reported. The most abundant gases are propane and isobutane. For all the gaseous products, the tendency is to decrease with time.

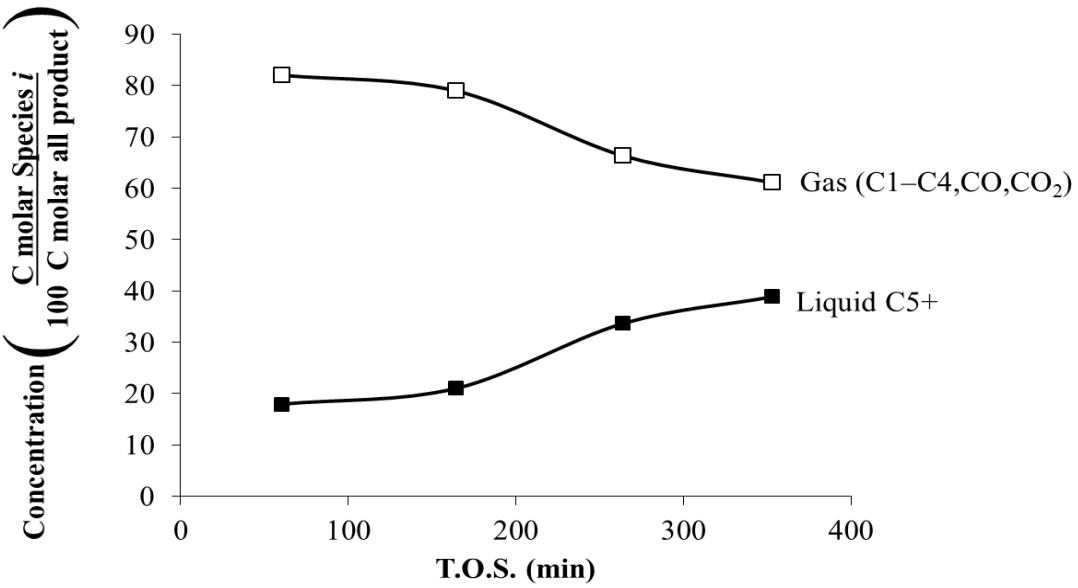

Figure 4-2. Product distribution of gases and liquids for the acetone reaction over HZSM-5 (80), T = 415 °C, WHSV = 1.3 h^{-1}, and P = 101 kPa (abs).

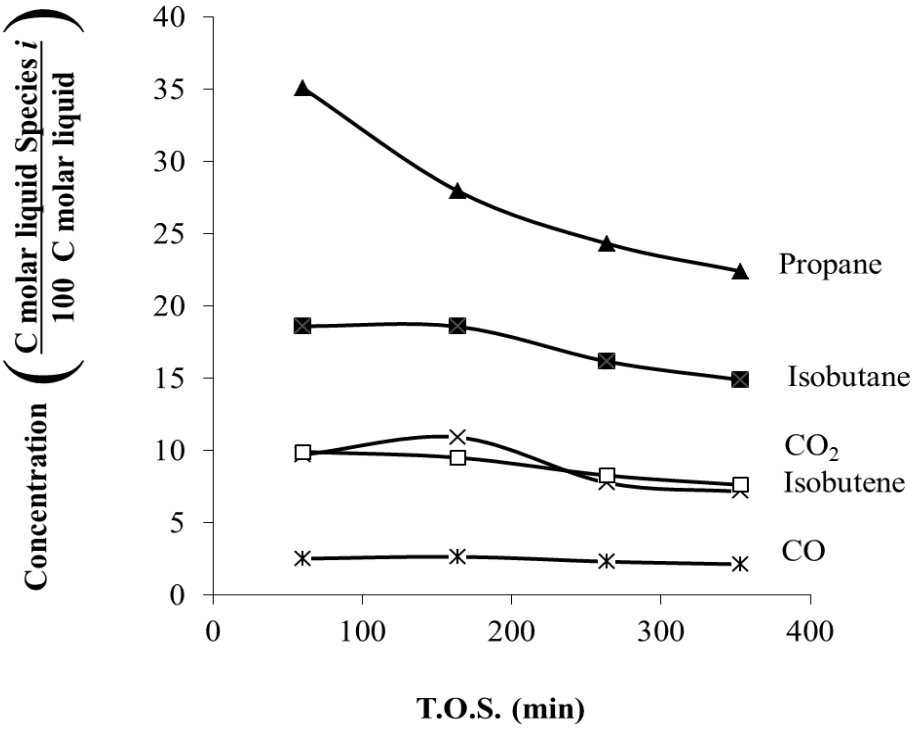

Figure 4-3. Product distribution of gases for the acetone reaction over HZSM-5 (80), T = 415 °C, WHSV = 1.3 h^{-1}, and P = 101 kPa (abs).

4.3.1.2 Effect of varying temperature

Using catalyst HZSM-5 (80), Figure 4-4 shows the distribution of gases and liquid, and the conversion of acetone for T = 305 to 415°C and WHSV = 1.3 h^{-1}. The amount of gases increased from 20% (305°C) to 72% (415°C); whereas, the amount of liquids decreased from 80% (305°C) to 28% at (415°C). The conversion slightly increased from 90% to 100%.

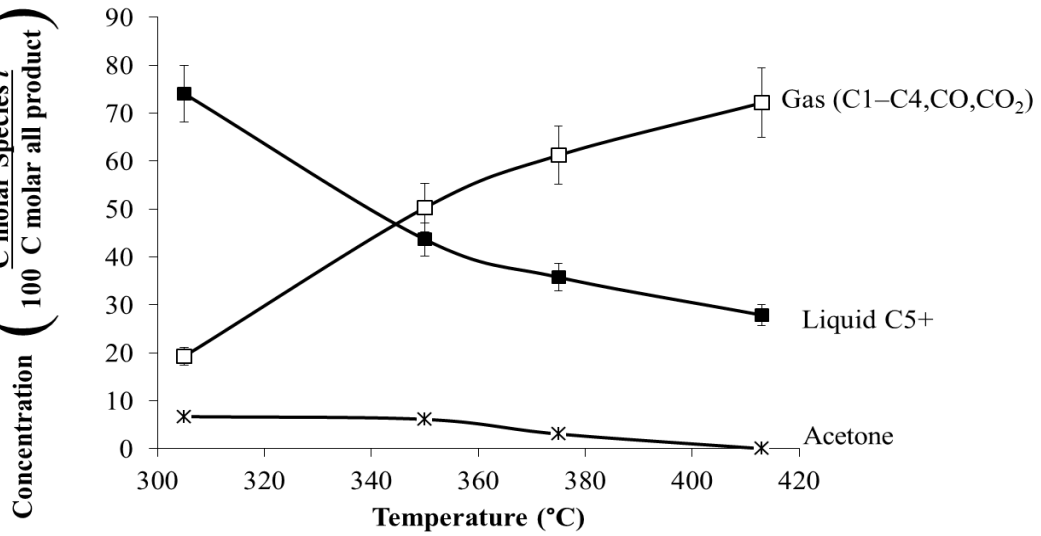

Figure 4-4. Product distribution of gases and liquids for the acetone reaction over HZSM-5 (80), WHSV = 1.3 h^{-1}, and P = 101 kPa (abs).

Figure 4-5 shows the type of liquid-phase products at T = 305, 350, and 415°C. Aromatics, naphthenes, and oxygenated compounds were the only types of products in the liquid phase. At T = 305°C, the most abundant component in the liquid phase was C9, mainly mesytilene (1,3,5-trimethylbenzene C_9H_{12}) and isophorone (1,1,3-trimethyl-3-cyclohexene-5-one $C_9H_{14}O$). The concentration of isophorone decreased from 15 to

0% when *T* increased from 305 to 415 °C and the concentration of C9 aromatics decreased from 25% (305°C) to 20% (415°C).

On the other hand, the concentration of C8 aromatics increases from 15% (305°C) to 40% (415°C), which is attributed to cracking of mesitylene (C9) into xylene. Kunyuan et al. (2007) reported the cracking of mesitylene over HZSM-5 at 480 °C, and showed that the most abundant reaction product is xylene. According to Kunyuan et al. (2007), cracking benefits from increased temperature. For the three experiments at different temperatures, the amount of benzene is less than 5% of the liquid.

Furthermore, it is noteworthy that there is a Gaussian normal distribution of compounds centered on C9 (305°C) and C8 (415°C). This Gaussian distribution of products was not observed in the isopropanol and mixed alcohol reactions. Figure 4-5 also shows the most abundant compound for each carbon number. For example, at 305 °C and C9 fraction, the most abundant aromatic component is mesitylene; on the other hand at 415 °C and C8 fraction, the most abundant aromatic compound is *p*-xylene.

At *T* = 305°C, the amount of naphthenes is less than 5% and ranges from C5 to C9. However, at high temperatures, the amount of naphthenes is 0%. Tables 4-5, 4-6, and 4-7 show the liquid composition at three temperatures: 305, 350, and 415°C, respectively. There were about 100 components for each sample; however, Tables 4-5, 4-6, and 4-7 show only the most abundant compounds. The total amount of all components for each table represents about 80% (mol) of the total amount of liquid products. The other components that represent 20% (mol) are not shown in the tables because they are numerous, and the concentration is less than 1% (mol).

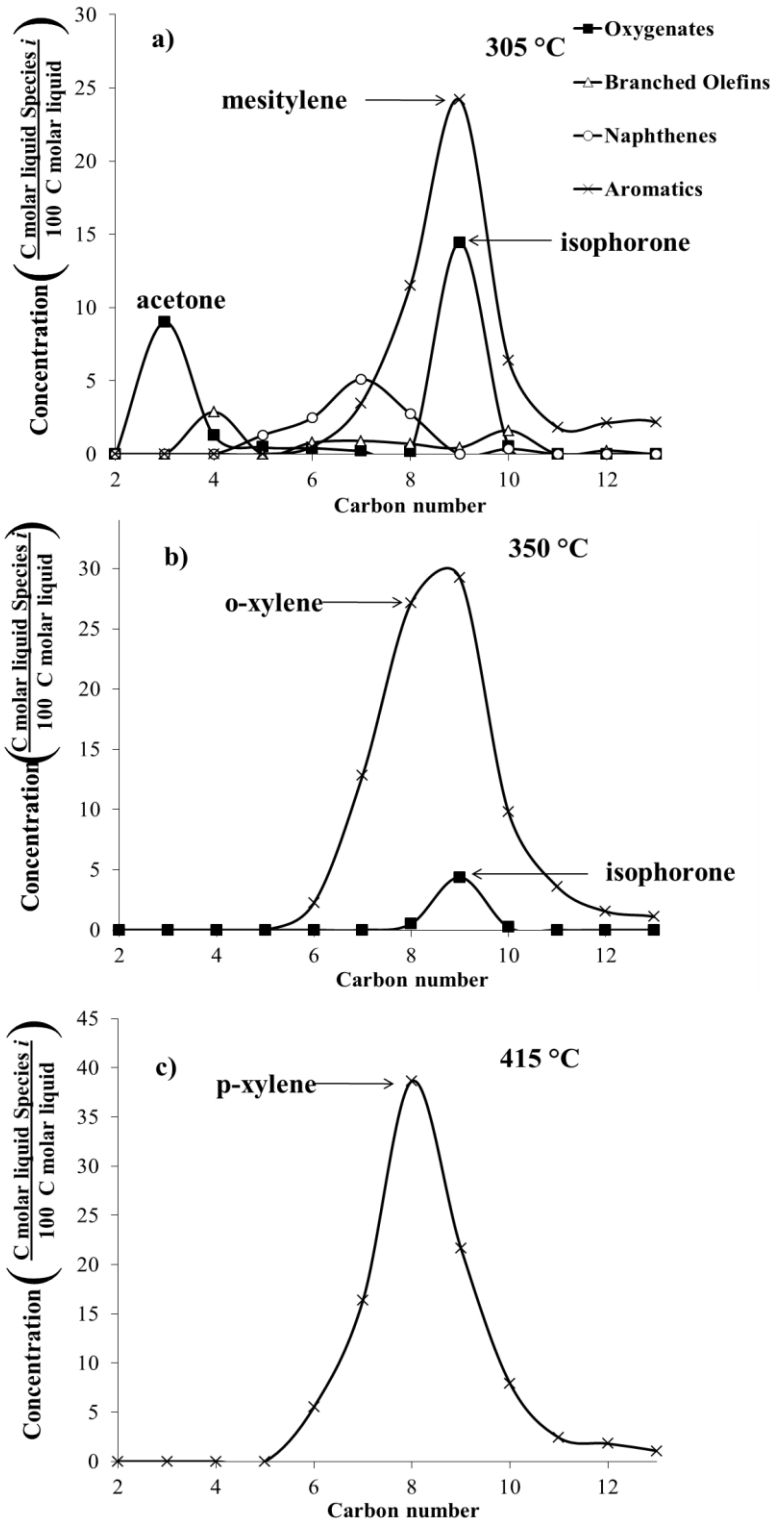

Figure 4-5. Liquid type product distribution of acetone reaction over HZSM-5 (80), WHSV = 1.3 h^{-1}, and P = 101 kPa (abs).

Table 4-5. Most abundant compound distribution for the acetone reaction over HZSM-5 (80), T = 305°C, WHSV = 1.3 h^{-1}, and P = 101 kPa (abs).

Aromatics (C molar liquid Species *i* /100 C molar liquid)		Oxygenated (C molar liquid Species *i* /100 C molar liquid)		Others (C molar liquid Species *i* /100 C molar liquid)	
benzene, 1,3-dimethyl	10.5	isophorone	14.1	cyclopropane, (1-methylethenyl)	2.4
Mesitylene	8.3	2-propanone	9.0	cyclobutane, isopropylidene	2.2
benzene, 1-ethyl-2-methyl	8.2	2-butanone	1.2	cyclopropane, 1,2-dimethyl	1.3
benzene, 1,2,3-trimethyl	6.7			cyclopentene, 1,5-dimethyl	2.1
benzene, methyl	3.4			1-propene, 2-methyl	2.8
benzene, 1-methyl-3-propyl	1.6				
benzene, 1,2-diethyl	1.5				
benzene, 1,2,3,5-tetramethyl	2.1				
benzene, ethyl	0.9				
naphthalene, 1,2,3,4-tetrahydro-2	0.8				

Table 4-6. Most abundant compound distribution for the acetone reaction over HZSM-5 (80), T = 415°C, WHSV = 1.3 h^{-1}, and P = 101 kPa (abs).

Aromatics (C molar liquid Species *i* /100 C molar liquid)	
benzene, 1,4-dimethyl	30.3
benzene, methyl	16.3
benzene, 1,2,4-trimethyl	9.5
benzene, 1,3,5-trimethyl	8.6
benzene, 1,3-dimethyl	8.3
benzene	5.5
naphthalene, 2-methyl	1.5

Table 4-7. Most abundant compound distribution for the acetone reaction over HZSM-5 (80), T = 350 °C, WHSV = 1.3 h^{-1}, and P = 101 kPa (abs).

Aromatics (C molar liquid Species *i* /100 C molar liquid)		Oxygenated (C molar liquid Species *i* /100 C molar liquid)		Others (C molar liquid Species *i* /100 C molar liquid)	
benzene, 1,3-dimethyl	18.0	isophorone	10.5	propane, 2-methyl	1.5
benzene, methyl	12.3				
benzene, 1-ethyl-4-methyl	12.1				
benzene, 1,2,3-trimethyl	10.8				
benzene, 1,4-diethyl	6.6				
benzene, 1,2,3-trimethyl	4.0				
benzene, ethyl	3.0				
benzene, 2-ethyl-1,3-dimethyl	2.8				
Benzene	1.7				
naphthalene, 1,5-dimethyl	1.5				
1H-indene, 2,3-dihydro-4-methyl	1.2				
benzene, 1,2,3,4-tetramethyl	1.1				
naphthalene, 1-methyl	1.0				

4.3.1.3 Effect of varying WHSV

For HZSM-5 (80), T = 415 °C, and P = 101 kPa (abs), Figure 4-6 shows the acetone conversion at different WHSV (1.32, 2.63, 3.95, 5.27, 6.58 and 7.9 h^{-1}). As expected, acetone conversion is lower at high WHSV, dropping from 100% to 87%. The amount of gas decreases because there is not enough residence time for oligomerization at high WHSV. The tendency is for all gaseous products to decrease at high WHSV.

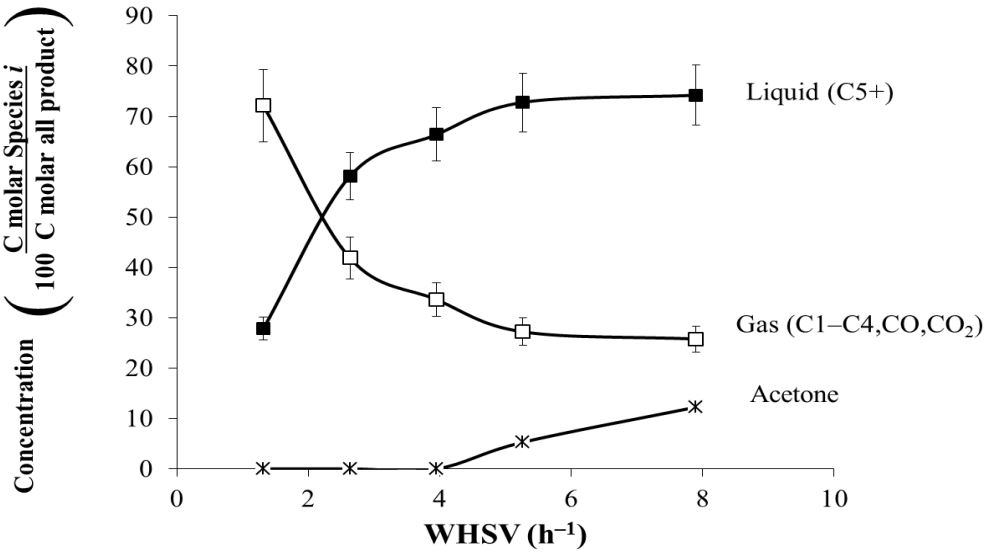

Figure 4-6. Product distribution of gases and liquids for the acetone reaction over HZSM-5 (80), T = 415 °C, and P = 101 kPa (abs).

At T = 415 °C, Figure 4-7 shows the type of liquid-phase products for WHSV = 1.32, 2.63, 3.95, 5.27, 6.58 and 7.9 h^{-1}. At WHSV = 1.32 h^{-1}, the most abundant component in the liquid phase was C8, mainly *p*-xylene. The concentration of isophorone increases from 0% to 7% when WHSV increased from 1.32 to 7.90 $h^{-1}$and the concentration of unreacted acetone increases from 0% (1.32 h^{-1}) to 10% (7.90 h^{-1}).

On the other hand, the concentration of C8 aromatics decreases from 40% (1.32 h^{-1}) to 23% (7.90 h^{-1}), which is attributed to cracking of mesitylene (C9) into xylene. At WHSV = 1.32 h^{-1}, the carbon product distribution is centered on C8; whereas at WHSV = 7.90 h⁻1, the carbon distribution product is centered on C9. For these experiments at different temperatures, the amount of benzene is less than 5% of the liquid. Naphthenes

increases from 0% to 5% when WHSV increased from 1.32 to 7.90 h^{-1}. Overall, WHSV determines the carbon distribution.

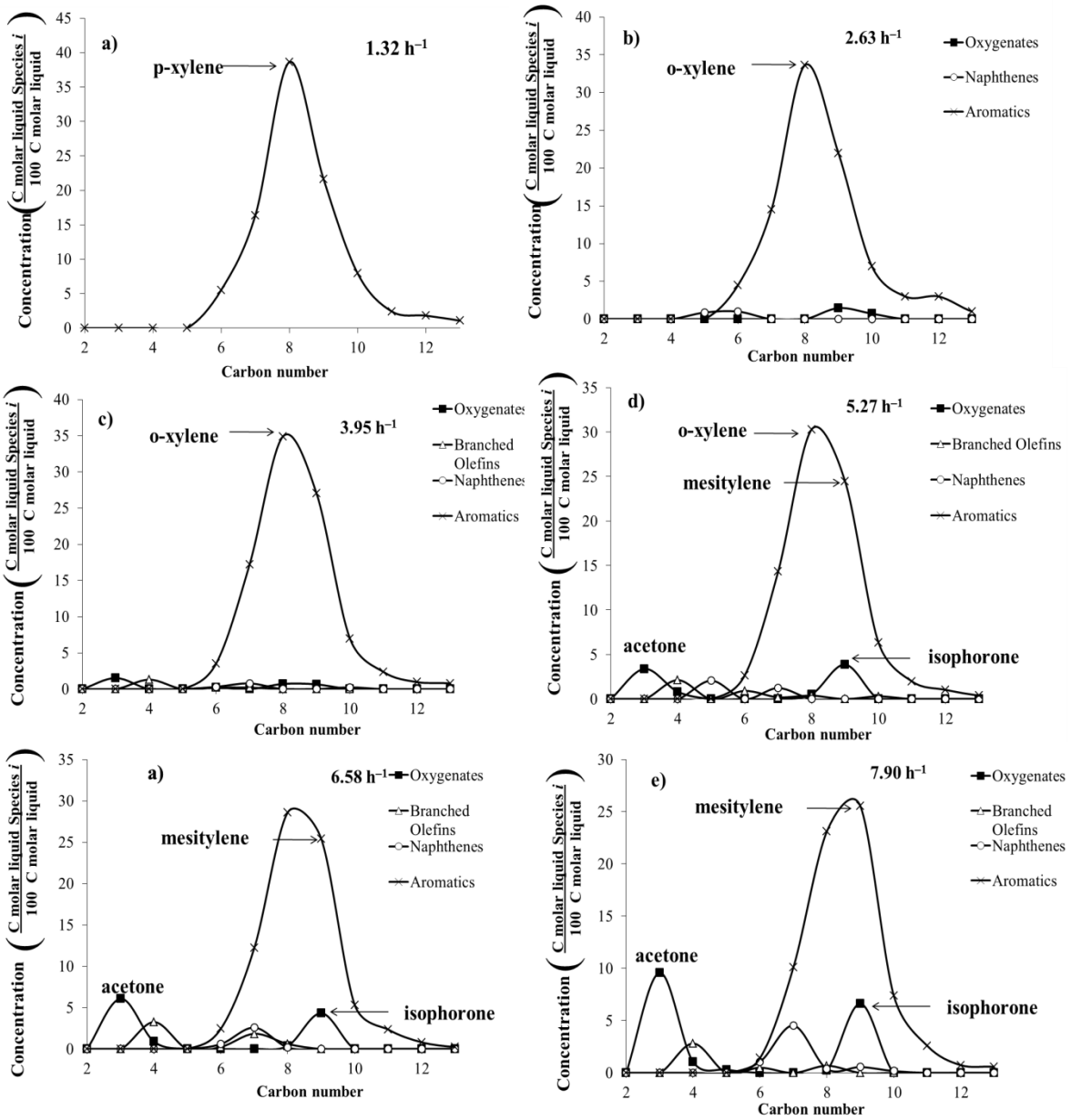

Figure 4-7. Liquid carbon product distribution of acetone reaction over HZSM-5 (80), T = 415 °C, and P = 101 kPa (abs).

Figure 4-8 shows the distribution of gases and liquid and the conversion of acetone at T = 350 °C for 1.32, 2.63, 3.95, 5.27, and 6.58 h^{-1} using catalyst HZSM-5 (80). The amount of gases decreased from 55% (1.32 h^{-1}) to 0% (6.58 h^{-1}); whereas, the amount of liquids increased from 10% (1.32 h^{-1}) to 80% at (6.58 h^{-1}). The unreacted acetone slightly increased from 5% to 23%.

Figure 4-7 shows the type of liquid-phase products at T = 350 °C for WHSV = 1.32, 2.63, 3.95, and 5.27 h^{-1}. At WHSV = 1.32 h^{-1}, the most abundant component in the liquid phase was C9 and C8, mainly mesitylene and *p*-xylene, respectively. The concentration of isophorone is constant (5%). Unreacted acetone increased from 0% (1.32 h^{-1}) to 14% (5.2 h^{-1}). Overall, at a lower temperature (350°C), the WHSV still determines the carbon distribution.

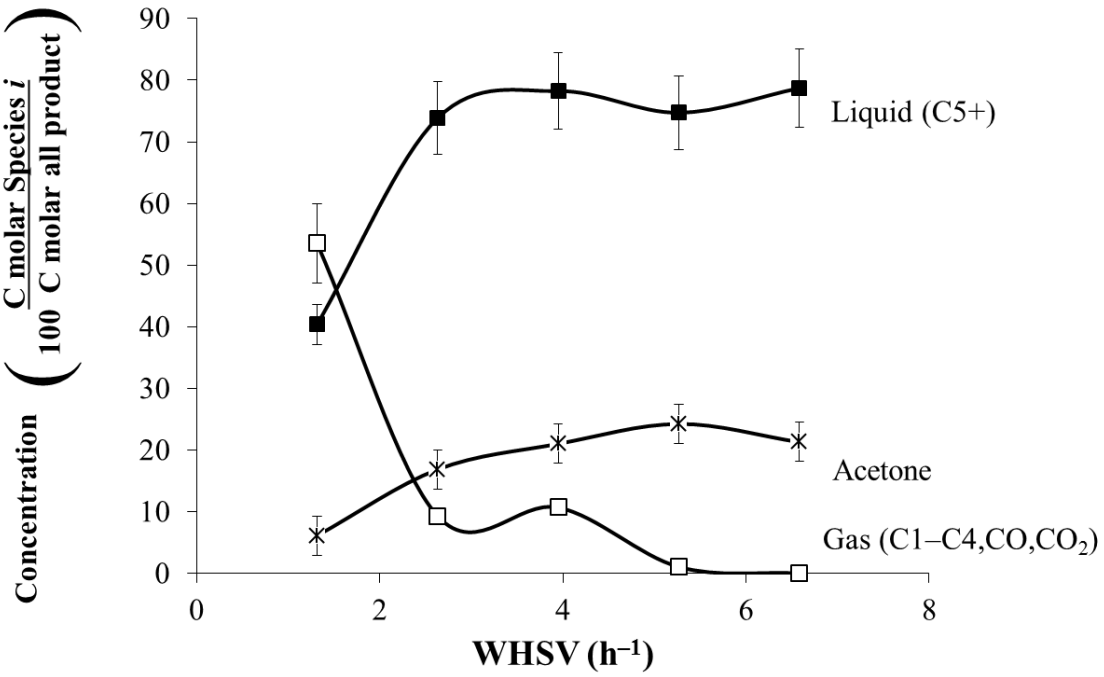

Figure 4-8. Product distribution of gases and liquids for the acetone reaction over HZSM-5 (80), T = 350 °C, P = 101 kPa (abs).

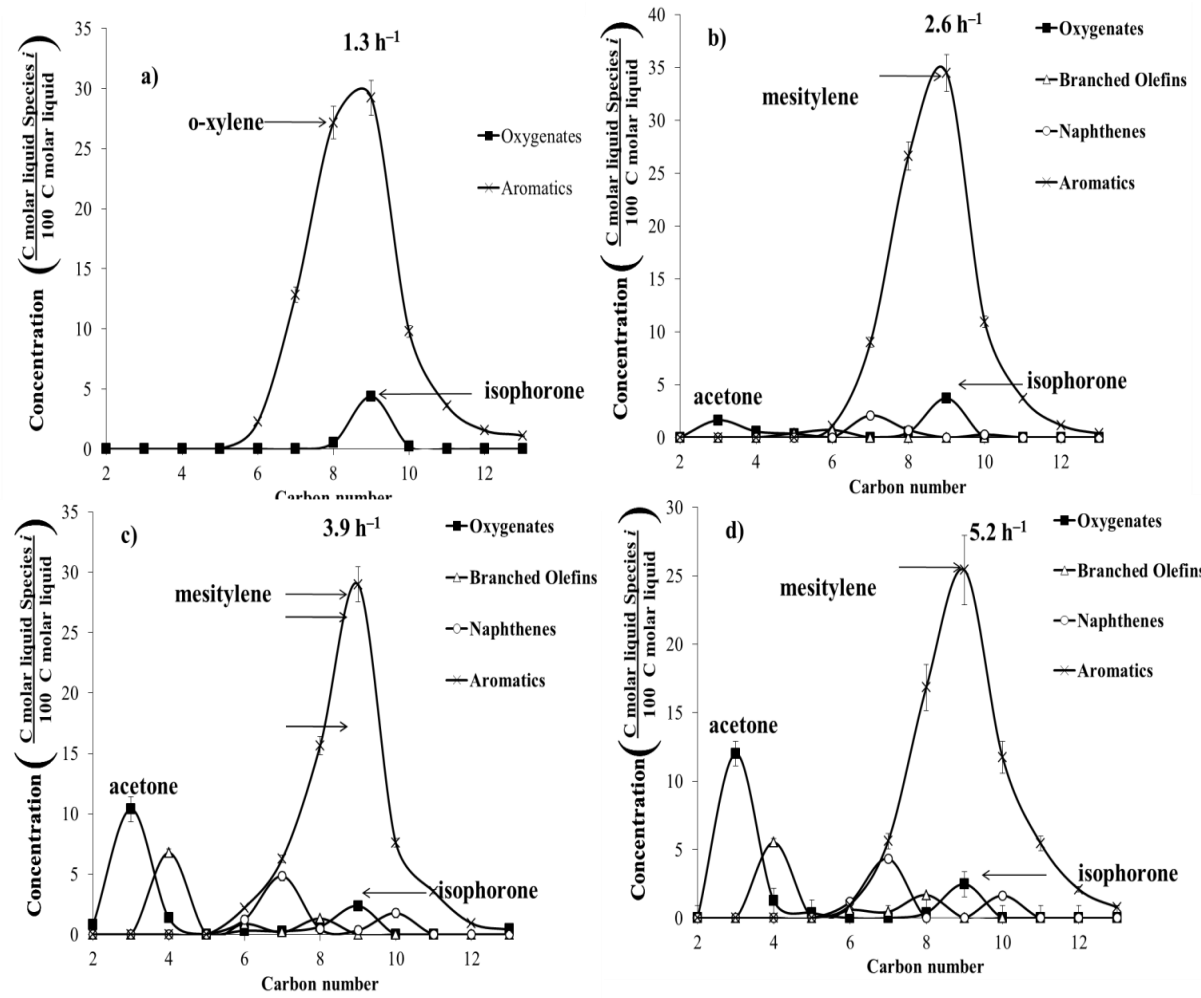

Figure 4-9. Liquid product distribution of acetone reaction over HZSM-5 (80), T = 350 °C, P = 101 kPa (abs).

4.3.2 Mixed ketones

The following section describes results for mixed ketones.

4.3.2.1 Catalyst stability

Figure 4-9 shows liquid product distribution for the mixed-ketone reaction over HZSM-5 during T.O.S. at 430 °C. During the first 410 min, the product concentration was not constant; therefore, catalyst deactivated during this time. The product distribution was affected by changing T.O.S. At very low T.O.S., the amount of unreacted ketones was 70% (120 min); however, at high T.O.S., the unreacted ketones increased to 95% (420 min). After 420 min, the unreacted ketones stabilized at 95%. The amount of aromatics was about 16% (120 min); but it decreased to less than 5% after 200 min. Also, the amount of branched olefins was about 10% (120 min); but it decreased to less than 5% after 200 min. Other hydrocarbon products are naphthenes and linear olefins.

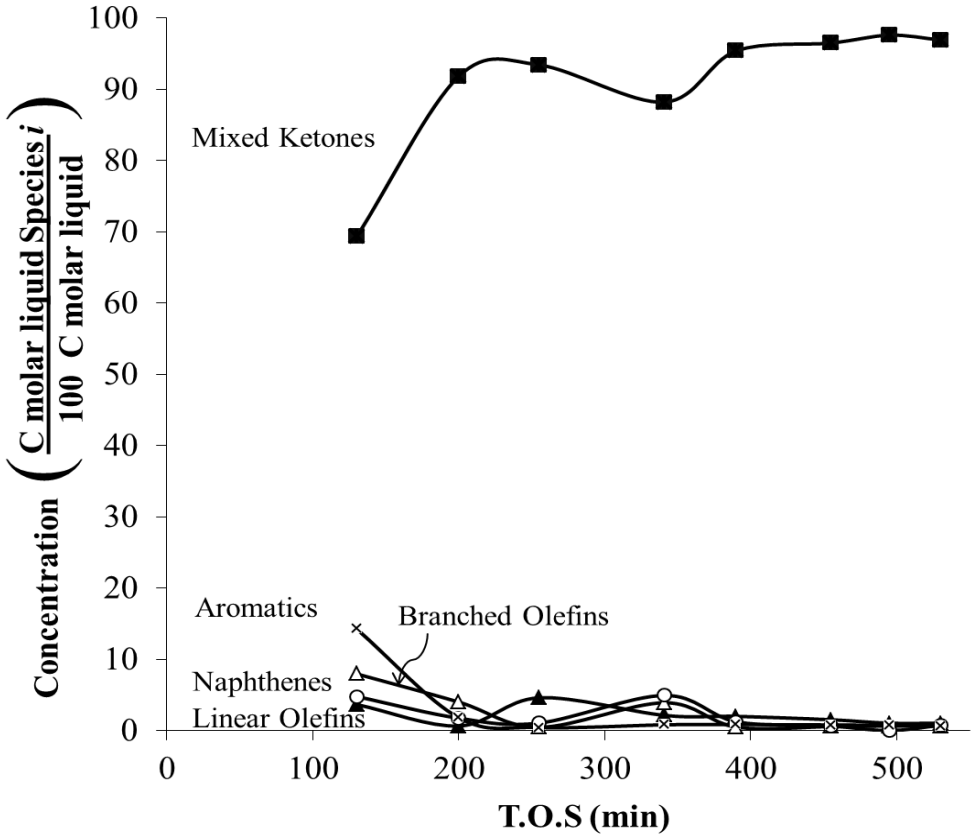

Figure 4-10. Liquid product distribution for mixed ketone reaction over HZSM-5 (280), WHSV = 1.92 h^{-1}, T = 430 °C, and P = 101 kPa (abs).

Figure 4-11 shows the liquid product distribution over HZSM-5 during T.O.S. at 510 °C (600 °C was highest temperature allowed by the system). The conversion increased by 20% when the temperature increased from 420 °C (Figure 4-10) to 510 °C (Figure 4-11). During this time, the catalyst also deactivated because the product distribution was affected by changing T.O.S. At very low T.O.S., the amount of unreacted ketones was 42% (70 min); however, at high T.O.S., the unreacted ketones increased to 75% (410 min). On the other hand, the amount of aromatics decreased from

30% (70 min) to 16% (410 min). According to Fuhse and Bandermann, aromatics are the most abundant products for the ketone reaction. Figure 4-11 shows the amount of aromatics is always higher than the other hydrocarbons. Furthermore, the amount of saturated hydrocarbons (paraffins and isoparaffins) was 0%. According to Chang (1977), the most abundant product for the ketone reaction is aromatics; however, over time branched olefins, and naphthenes are produced (Figure 4-11).

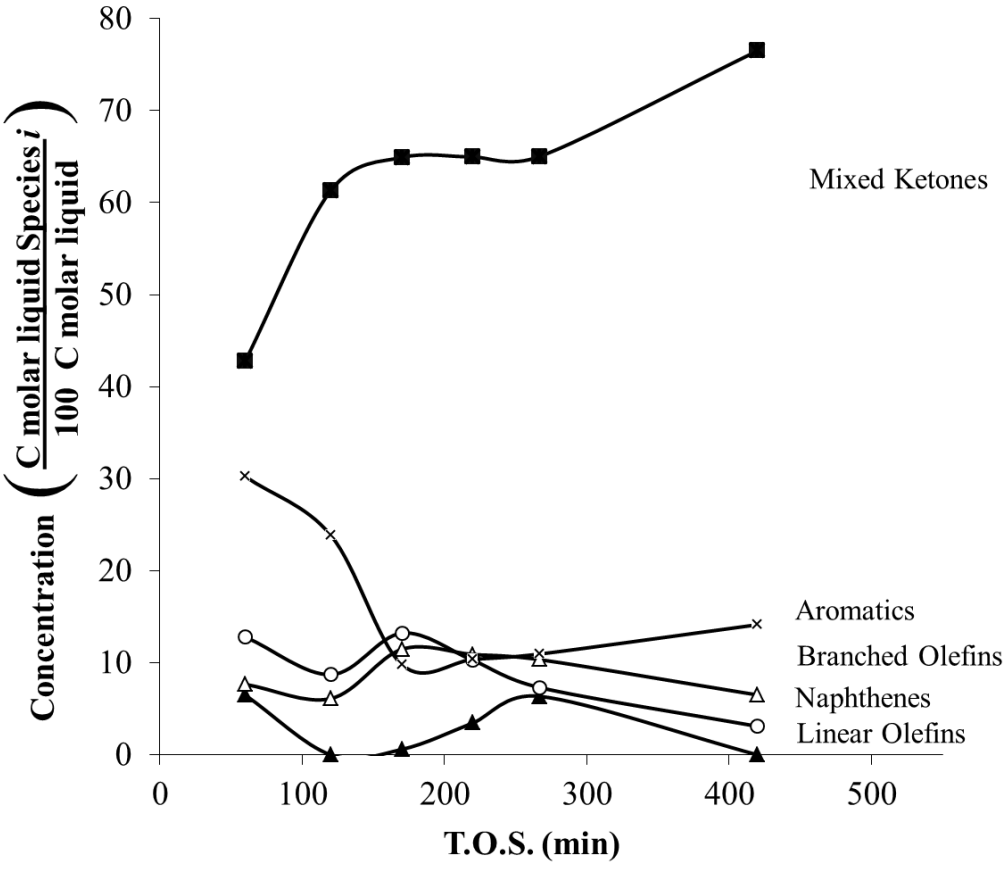

Figure 4-11. Liquid product distribution for mixed-ketone reaction over HZSM-5 (280), WHSV = 1.92 h^{-1}, T = 510 °C, and P = 101 kPa (abs).

4.3.2.2 Effect of varying temperature

Figure 4-12 illustrates the types of liquid-phase products at different temperatures. At lower temperatures, unconverted ketones are about 90% (420–460 °C); however, at higher temperatures, unconverted ketones decrease to 62% (510–590 °C). Aromatics are also the most abundant hydrocarbon product (20%). It is noteworthy that the conversion is about the same from 510 to 590 °C (~40%), meaning there is no benefit to increasing the temperature more than 510 °C. The maximum amount of hydrocarbon product obtained was 40% at 510 °C.

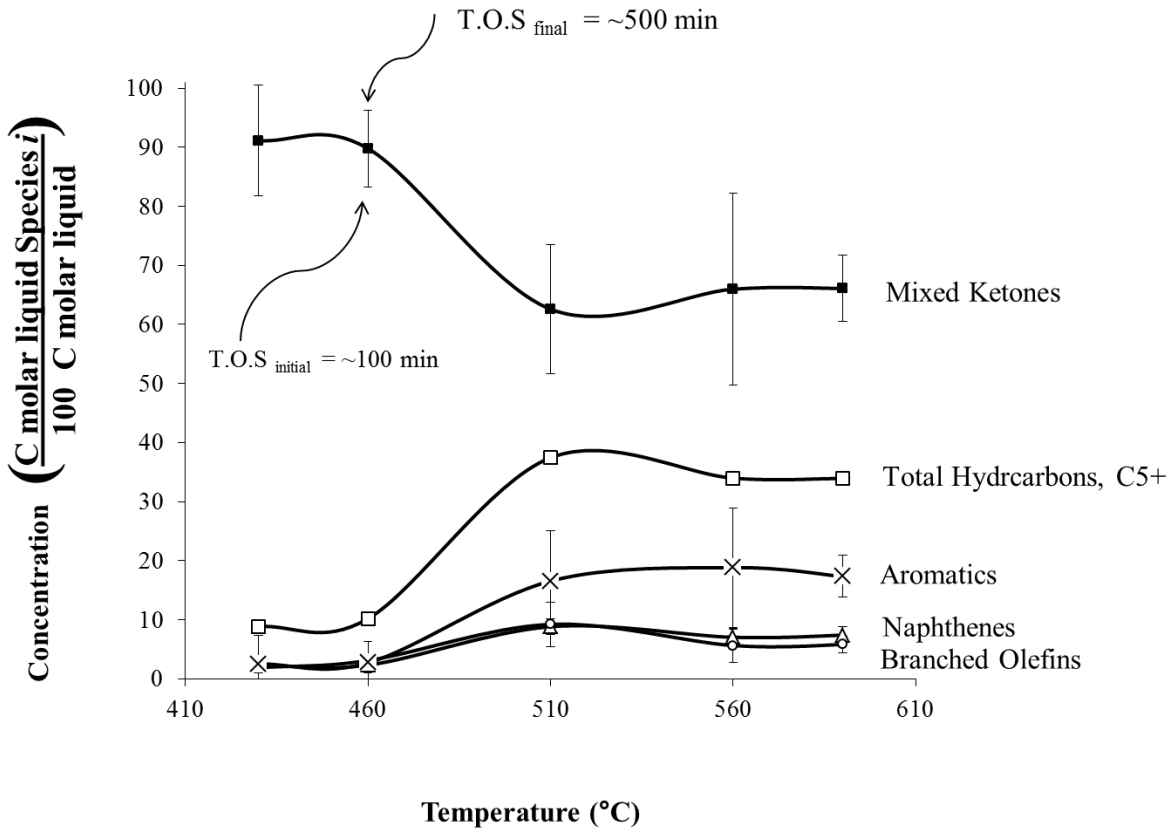

Figure 4-12. Liquid product distribution for mixed-ketone reaction over HZSM-5 (280), WHSV = 1.9 h^{-1}, and P = 101 kPa (abs). (Error bars are ± 1σ.)

Figure 4-13 shows the average carbon number (ACN) at different temperatures. At very low temperatures, ACN was 8.7; however, at high WHSV, ACN decreased to 8.3. At high temperatures, the ACN decreases because mesitylene dealkylates to xylene. Cracking reaction usually causes the lower ACN.

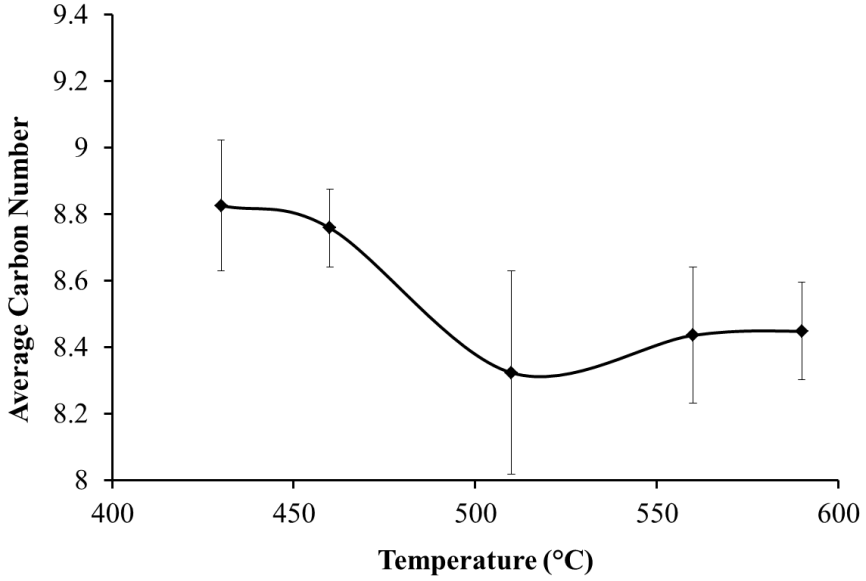

Figure 4-13. Average carbon number for mixed-ketone reaction over HZSM-5 (280), WHSV = 1.9 h^{-1}, and P = 101 kPa (abs). (Error bars are ± 1σ.)

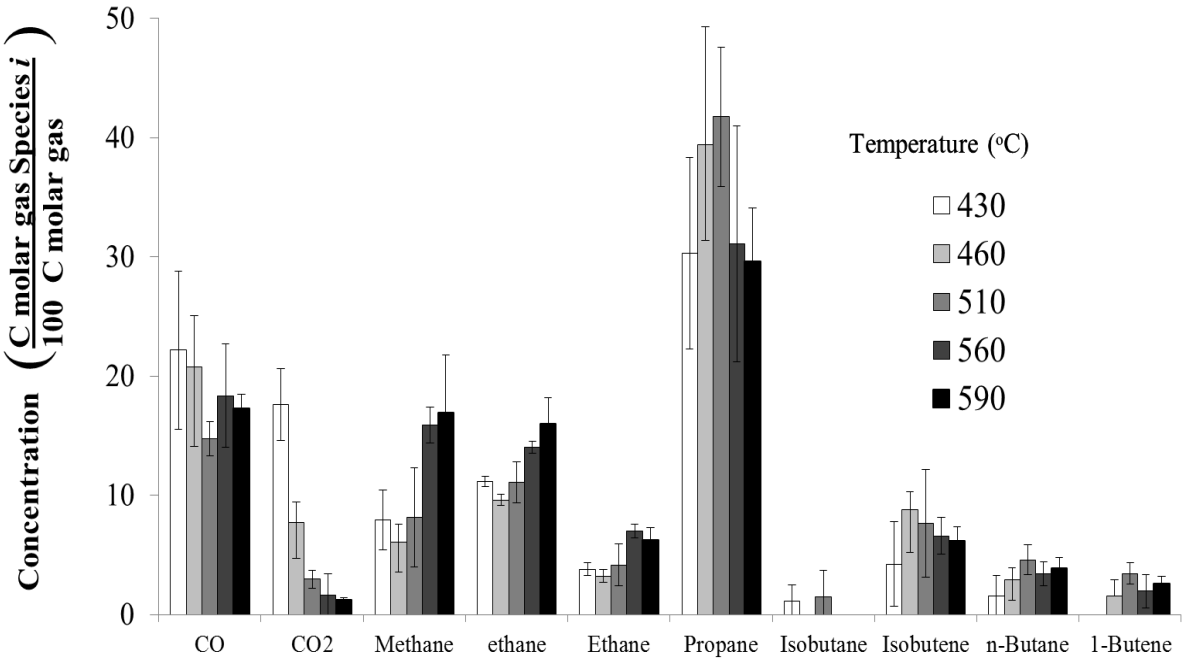

Figure 4-14. Gaseous product distribution of mixed-ketone reaction over HZSM-5 (280), WHSV = 1.9 h^{-1}, and P = 101 kPa (abs).

For temperatures 510, 560, and 590 °C, the conversion is significant (~40%). For the mixed-ketone reaction, Figure 4-15 compares the unreacted ketone distribution with the ketone feed at these temperatures. According to Fuhse and Bandermann, it is expected that acetone, 2-butanone, and 2-pentanone with C/H ratio > 0.6 had less conversion than the remaining ketones (C/H ratio < 0.6). However, Figure 4-15 illustrates that low-molecular-weight ketones (C3–C7) had better conversion than high-molecular-weight ketones (C9–C12). For instance, the acetone feed concentration is 7%; however, the unreacted acetone in the liquid product is 0% (510, 560, and 590 °C); therefore, the acetone conversion is 100%. As well, 2-heptanone feed concentration is 29%; however, the unreacted ketone concentration is about 10%; therefore, the

conversion of 2-heptanone is about 65%. On the other hand, high-molecular-weight ketone has less conversion. For instance, 2-noonanone feed concentration is 16%; however, the unreacted 2-nonenone concentration is 14%; therefore, the conversion of 2-nonenone is about 12%. Also, 2-decanone does not react at this temperature range; the conversion is 0%.

In conclusion, low-molecular-weight ketones have better conversion over HZSM-5 than high-molecular-weight ketones, which might result because small molecules can enter easily into the channels of HZSM-5. For instance, acetone size is 0.31 nm and HZSM-5 channel size is 0.51 nm; therefore, acetone not only can react on the surface but also in the internal surface of HZSM-5. On the other hand, larger molecules such as 9-nonene (kinetic diameter >0.5 nm) can only react at the catalyst surface.

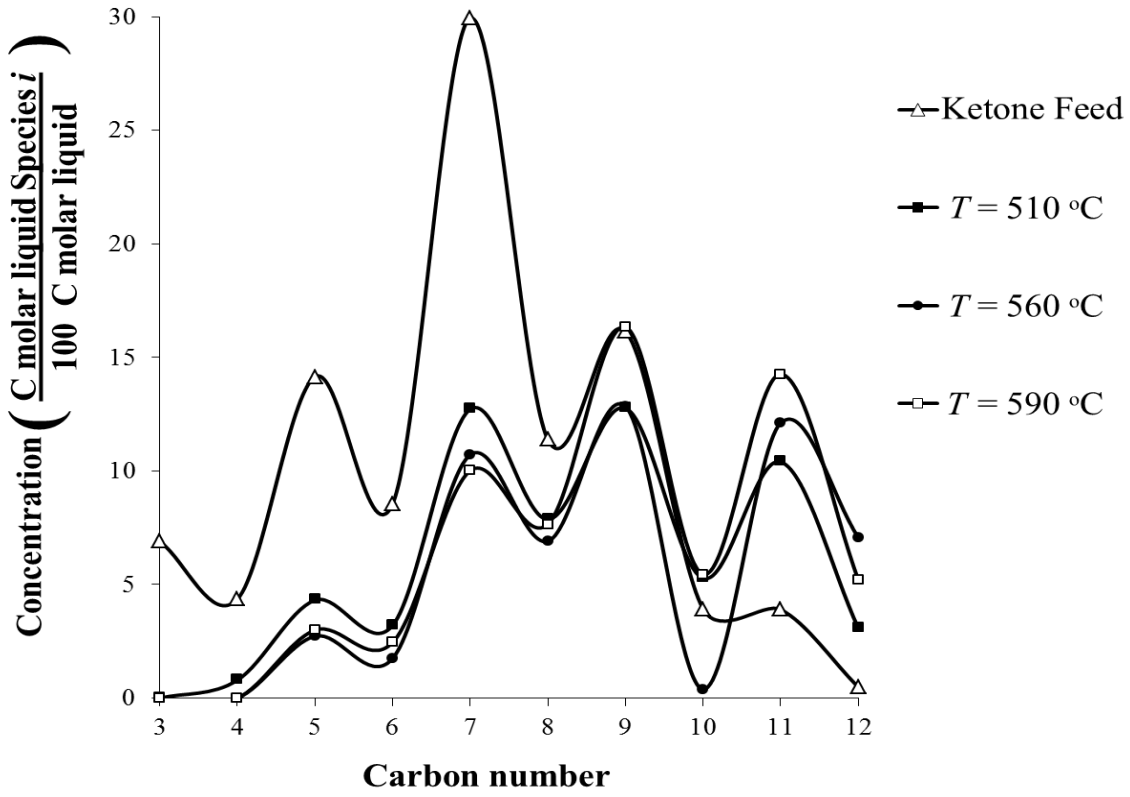

Figure 4-15. Liquid unreacted product ketone distribution of mixed-ketone reaction over HZSM-5 (280), WHSV = 1.9 h^{-1}, and P = 101 kPa (abs).

According to Wang et al. (2008), for proper catalyst performance, the catalyst pore size catalyst relate to the molecule size is very important. The reaction they studied was cracking of 1,3,5-trimethyl benzene (TMB) and 1,2,4-TMB over nanoscale HZM-5 and microscale HZSM-5. The kinetic diameter of 1,3,5-TMB and 1,2,4-TMB is 0.75 and 0.67 nm, respectively, and the catalyst pore opening is 0.5 nm. They concluded that both molecules do not enter the channel of ZSM-5 and only react on the surface.

Figure 4-16 illustrates the carbon product distribution of mixed ketone over HZSM-5 at different T.O.S., WHSV = 1.9 h^{-1}, T = 590 °C, and P = 101 kPa (abs). As T.O.S. increases, conversion and hydrocarbon product decreases. For instance, C9 aromatics decrease from 12% (T.O.S. = 60 min) to 3% (T.O.S. = 367 min). On the other hand, unreacted ketones increases with longer T.O.S.. For instance, C7 ketone increases from 6% (T.O.S. = 60 min) to 17 % (T.O.S. = 367 min).

Figure 4-16a illustrates an example of the liquid product of mixed ketone over HZSM-5. Aromatics are centered on C8, ranging from C6 to C12. Naphthenes and branched olefins are centered on C7 and C6, respectively. Naphthenes distribution ranges from C6 to C9, and branched olefins ranges from C5 to C9.

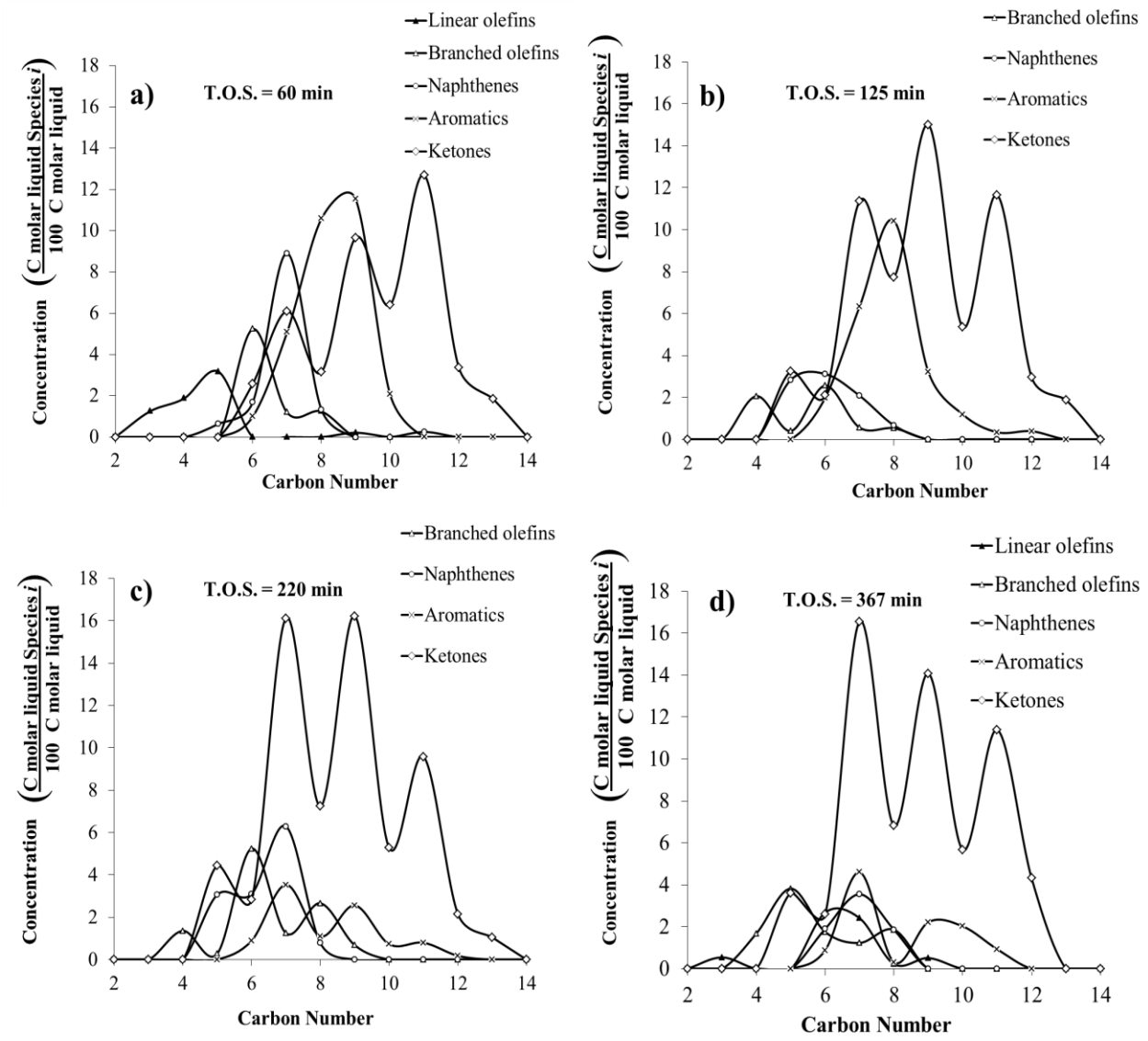

Figure 4-16. Liquid carbon product distribution of mixed-ketone reaction over HZSM-5 (280), WHSV = 1.9 h^{-1}, T = 590 °C, and P = 101 kPa (abs).

4.3.3. Temperature profile of the catalyst bed

For the mixed-ketones reaction, Figure 4-17 shows the temperature profile during T.O.S. for HZSM-5. The temperatures recorded were at the top (T_{top}), middle (T_{middle}), and bottom (T_{bottom}) of the catalyst bed. For Figures 4-1 to 4-16, the reported temperature is the average temperature of the catalyst bed during T.O.S. The temperatures are constant over time. T_{top} is the highest of the temperature, whereas T_{bottom} was the lowest temperature of the catalyst bed. The difference between T_{top} and T_{bottom} was between 20 and 30 °C. T_{top} and $T_{midddle}$ are very close temperatures.

The highest temperatures are T_{top} and $T_{midddle}$ because the dehydration reaction occurs mainly on this section. The heat of reaction raises the temperature on the top and the middle. The bottom section occurs other side reaction (e.g., alkylation, oligomerization, and aromatization).

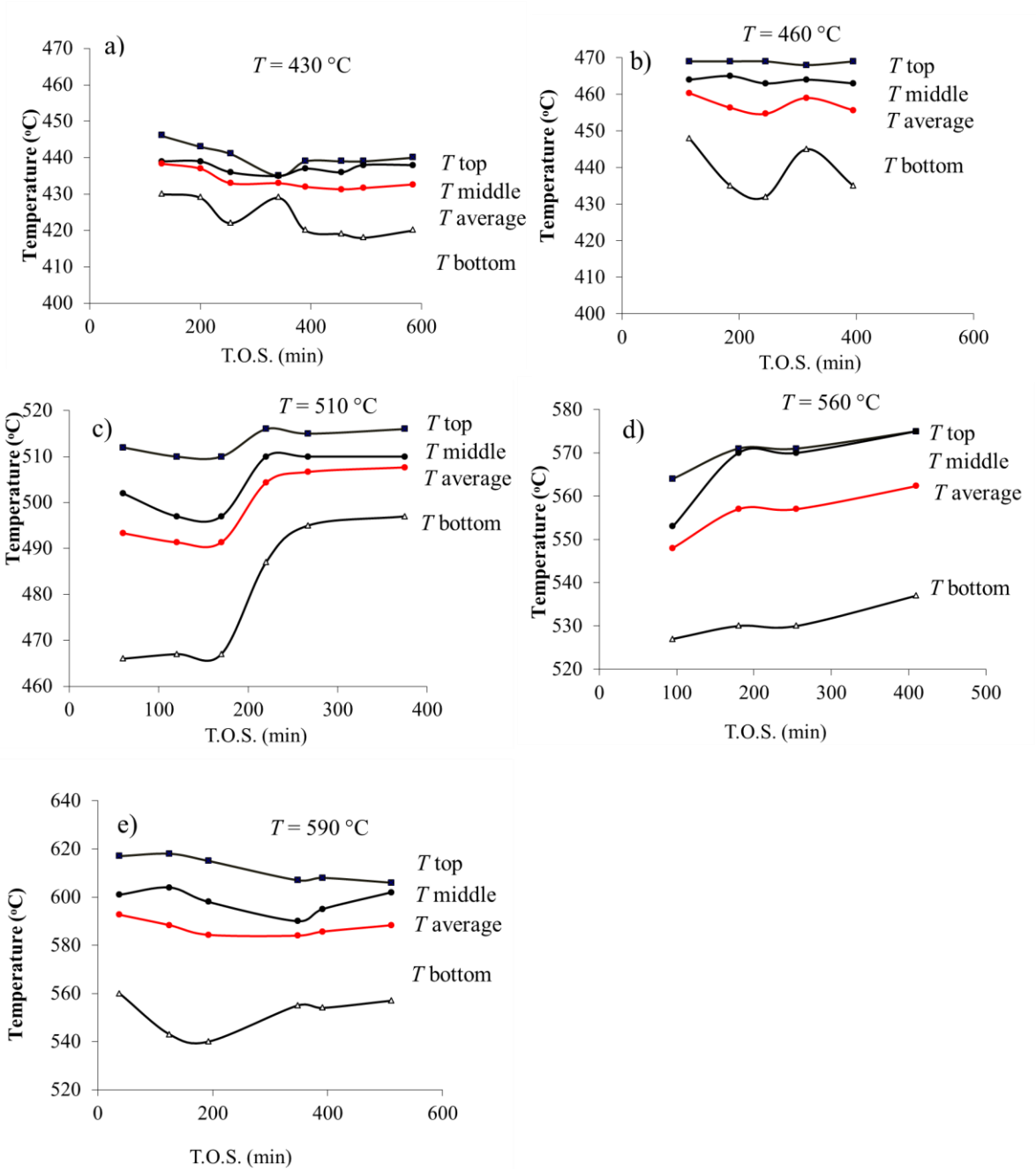

Figure 4-17. Temperature profile for top, medium, bottom and average temperature for mixed- ketone reaction over HZSM-5 (280), WHSV = 1.9 h^{-1}, and P = 101 kPa (abs), T = 430–590 °C.

4.4 Conclusion

For the acetone reaction, temperatures above 400 °C are needed to get 100% conversion. Gaseous products are more abundant at high temperatures.

Mixed ketone transformation to hydrocarbon is favored at high temperatures. At very low temperatures, the mixed ketone conversion was 9% (420 °C); however, at $T >$ 510 °C, the conversion increased to 41–45%.

The reaction products were aromatics, naphthenes, and branched olefins. Low-molecular-weight ketones had better conversions than high-molecular-weight. In all runs above 510 °C, acetone and 2-butanone conversion are 100%. The concentration of reaction products changed over time because of catalyst coking.

The gas products are different from mixed alcohol reaction. The gases contain methane, CO, ethane, ethene, and CO_2. The gases are mostly hydrogen saturated which are difficult to be recycled in an oligomerization reactor. Propane is the most abundant product in the gas phase.

5. OLEFIN DIMERIZATION

The objectives of this section follow:

a) Describe the dimerization of 1-hexene, 1-octene and 1-decene using Beta (25) catalyst in a batch reactor.

5.1 Introduction

This section describes the dimerization of olefins to produce higher-molecular-weight olefins using Beta zeolite. Depending on the reaction condition (*T, P*, and WHSV), mixed alcohols, dehydrate and then oligomerize using HZSM-5 as described in Section 2. The alcohol oligomerization is nearly instantaneous and randomly paired. There are thousands of reactions occurring at the same time.

Several mechanisms for the oligomerization reaction have been published, but it is still uncertain which one is the most accurate. Some mechanisms of olefin oligomerization suggested include the following: (1) carbenium ion species intermediate, (2) surface ethoxy structure intermediate, (3) cationic intermediate, (4) cyclic derivatives intermediate, and (5) ionic mechanism. For zeolite HZSM-5, Mechanisms 1 to 3 appear to occur. These mechanisms explain the interaction of the reactant with the zeolite structure and the formation of the product at atomic levels. On the other hand, the reaction scheme of olefin oligomerization is much more clear (Figure 5-1). Oligomerization is accompanied by parallel reactions: (1) isomerization, (2) cracking, (3) disproportionation, and (4) hydrogen transfer. These reactions are identified because of the production of isoparaffins and aromatics.[31]

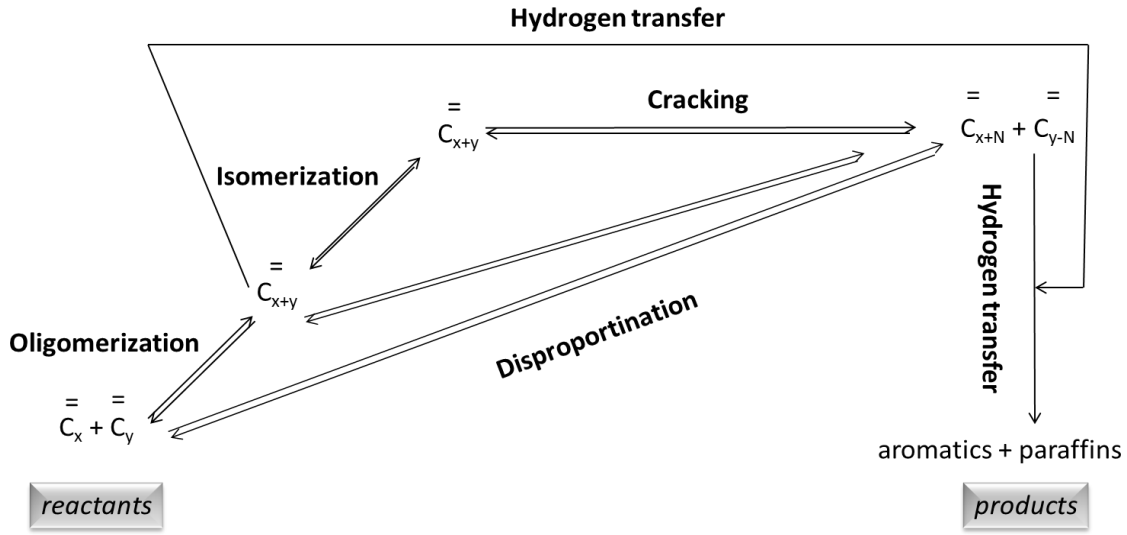

Figure 5-1. Olefin oligomerization reaction scheme. (Figure adapted from Sanati et al. 1999.)

Several type of catalysts are used in dimerization, with the most efficient being Beta zeolite. Yoon et al. (2007) reported the trimerization of isobutylene over zeolites Beta (25), USY, and modernite.[23] Figure 5-3 shows the conversion of isobutylene over time with different zeolites. Beta (25) shows 100% conversion during T.O.S. = 25 h; whereas USY and modernite conversion is about 80 and 20%, respectively. Yoon et al. compared the trimerization selectivity of Beta (25), USY, and modernite. Figure 5-4 shows the type of products obtained from isobutylene reaction with different zeolites. Beta (25) is the most effective catalyst to form trimmers and tetramers.

The dimerization is usually performed in a batch reactor under more gentle conditions than a plug flow reactor (PFR). The conditions are lower temperature and more residence time. The catalyst can be in a powder form to get a better surface contact. This report will show conditions and results obtained using Beta catalyst with several types of olefins.

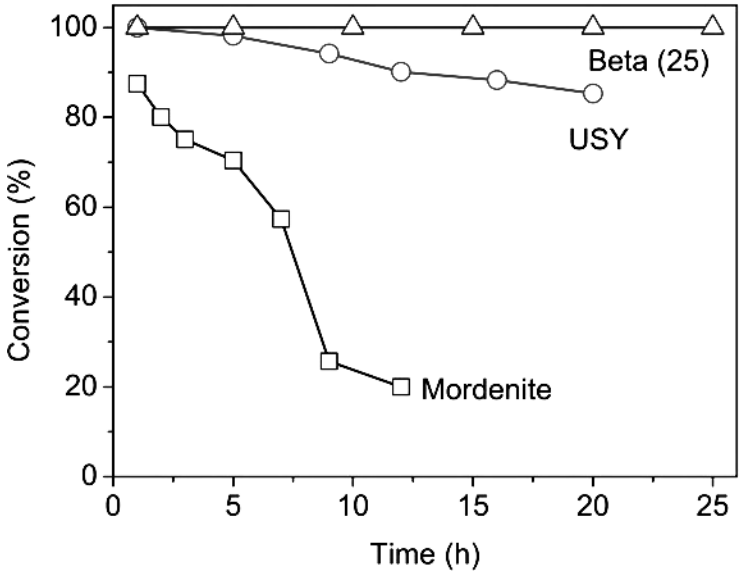

Figure 5-2. Conversion of isobutene at different times over various zeolites. (Figure from Yoon et al., 2007.)[23]

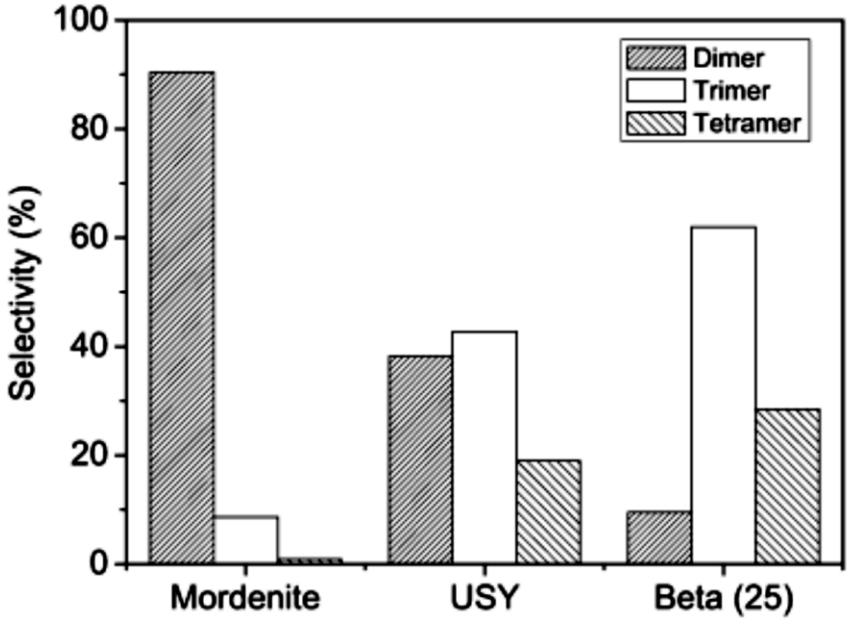

Figure 5-3. Selectivity of isobutene products at different time over various zeolites at T.O.S. = 12 h. (Figure from Yoon et al., 2007.)[23]

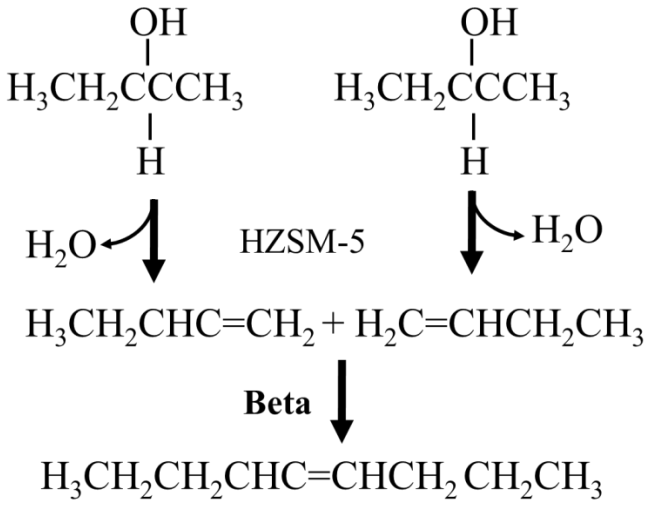

Figure 5-4. Dehydration and dimerization of 2-butanol to produce octane using HZSM-5 and Beta catalysts.

For mixed alcohols, the process can be divided into two processes: (1) dehydration and (2) dimerization of low-molecular-weight olefins. Figure 5-4 shows the dehydration of two molecules of 2-butanol using HZSM-5 and then the dimerization of 2-butene to produce sub-octene using Beta (25).

For instance, isopropanol and 2-heptanol dehydrate to propene and 2-heptene, respectively. Then, the olefins dimerize to produce high-molecular-weight olefins using Beta (25) zeolite. High-molecular-weight liquid olefins hydrogenate to produce jet fuel, kerosene, and diesel; whereas low-molecular-weight liquid olefins produce gasoline. The dimerization of olefins is usually performed in a batch reactor under more gentle conditions than a packed-bed reactor. The conditions employ lower temperatures and longer residence times.

5.2 Experimental

Dimerization was performed in a 1-L stainless steel batch reactor (P_{max} = 34,400 kPa at T = 343 °C, Pressure Products Industry, Co. Warminster, PA) (Figure 5-6). The batch reactor was equipped with a magnetic drive connected to the stirrer (0–1000 rpm) for mixing. The temperature inside the reactor was monitored via a thermocouple and regulated via a controller connected to a heating jacket outside the vessel.

First, 400 mL of distilled ketones and 7 g of Beta (25) catalyst were charged to the reactor. The reactor head was put in place and tightened. Excess air inside the reactor was purged with helium. Helium was added until the reactor pressure reached 2000 kPa (abs). The stirrer rotated at 750 rpm. After the reaction was over, the reactor was cooled, and the liquid filtered to separate the catalyst.

Nine experiments at different conditions were performed in a batch reactor. Three temperatures were analyzed 170, 220, and 270 °C. The olefins studied over Beta (25) catalyst were 1-hexene (99% pure), 1-octene (99% pure), and 1-decene (98% pure). Table 5-1 shows all the experiments for the olefins reaction over Beta (25) zeolite. The maximum time of operation was 360 to 420 min. Samples were taken approximately every 30 min.

Table 5-1. Experiments for the olefins reaction over Beta (25).

	Temperature		
Feed	170 °C	220 °C	270 °C
1-hexene	O1	O2	O3
1-octene		O4	O8
1-decene		O5	O9
1-hexene + 1-decene		O6	
1-hexene + 1-octene		O7	

5.2.1 Beta (25)

In recent years, Beta zeolite has been used for dimerization and trimerization of isobutene.[23–27] HZSM-5 and Beta (25) have a similar channel size (~0.55 nm); therefore, high-molecular-weight olefins (4 > C > 12) can potentially be dimerized using Beta.

The catalyst used was obtained from Zeolyst; Beta zeolites are denoted as Beta (*n*) for the sample, with *n* representing the SiO_2/Al_2O_3 mol ratio. Beta (25) (CP 814E, surface area = 680 m^2/g) was calcinated at 550 °C for t = 24 h in a muffle furnace to convert the ammonium form into a proton form. Figure 5-5 shows the Beta zeolite pore structure.

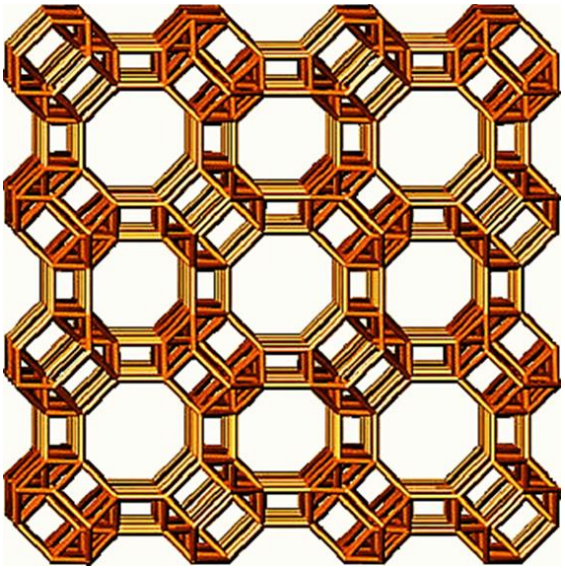

Figure 5-5. Pore structure of Beta zeolite (Figure from Chang 1983.)[16]

5.2.2 Batch reactor (1 L)

The 1-L batch reactor (Figure 5-6) was equipped with a stirrer (B) and a pressure gauge (G) to see the reaction progress. The temperature inside the reactor was monitored via a thermocouple and regulated via regulator connected to the heating jacket. The liquid olefin and the catalyst were weighed and placed inside the reactor vessel. Then, the reactor was assembled and flushed three times with helium to remove traces of oxygen. Samples were taken at regular intervals by opening Valve E.

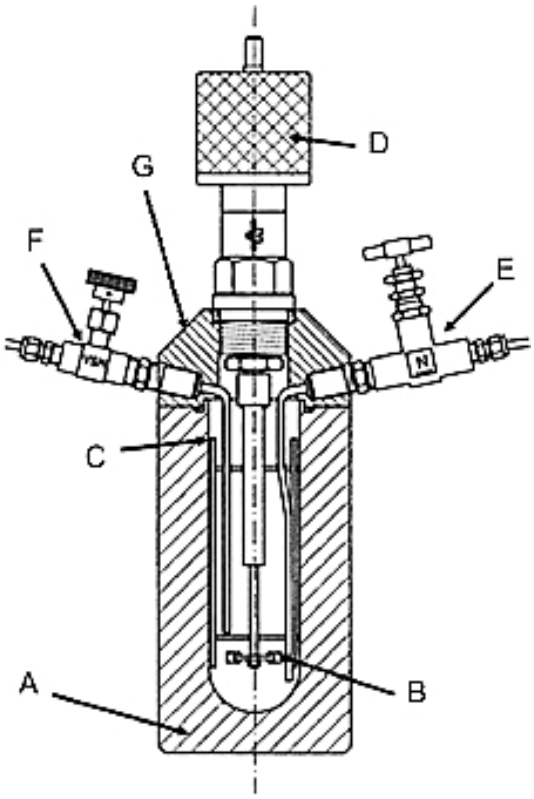

Figure 5-6. Autoclave used in the dimerization experiments. A, heating jacket; B, stirrer; C, stainless steel vessel; D, magnetic coupling; E, needle valve for liquid phase sampling; F, needle valve for inlet; G pressure gauge.

5.2.3 Product analysis

The composition of liquid mixtures was analyzed by using a gas chromatograph-mass spectrograph analysis where samples were injected manually. A batch reactor is characterized by the conversion during reaction time.

5.2.4. Reactants

Reagent-grade 1-hexene (99% pure), 1-octene, 1-decene were obtained from Fischer Scientific (Waltham, MA).

5.3 Results

The variable time (t) starts at 0 min when the reactor has reached the set temperature. For all the experiments, the start-up time varies between 60 and 90 minutes, depending on the final temperature.

5.3.1 Dimerization of pure substances: 1-hexene, 1-octene, and 1-decene

5.3.1.1 Effect of time

Figure 5-7 shows the carbon distribution for 1-hexene at T = 270 °C during time. At t = 100 min, the dimer C12 reaches the maximum concentration (57%) and is the only product. Dimerization is the only type of reaction during this time. After 100 minutes, the dimer starts cracking to produce C7, C8, and others.

Figure 5-8 shows the type of components produced during the reaction. The concentration of linear olefins decreases from 78% (0 min) to ~1% (320 min). The amount of isoparaffins is 0% during the first 110 min, but increases to 90% (320 min). The amount of branched olefins decreases from 20% (0 min) to ~5% (320 min).

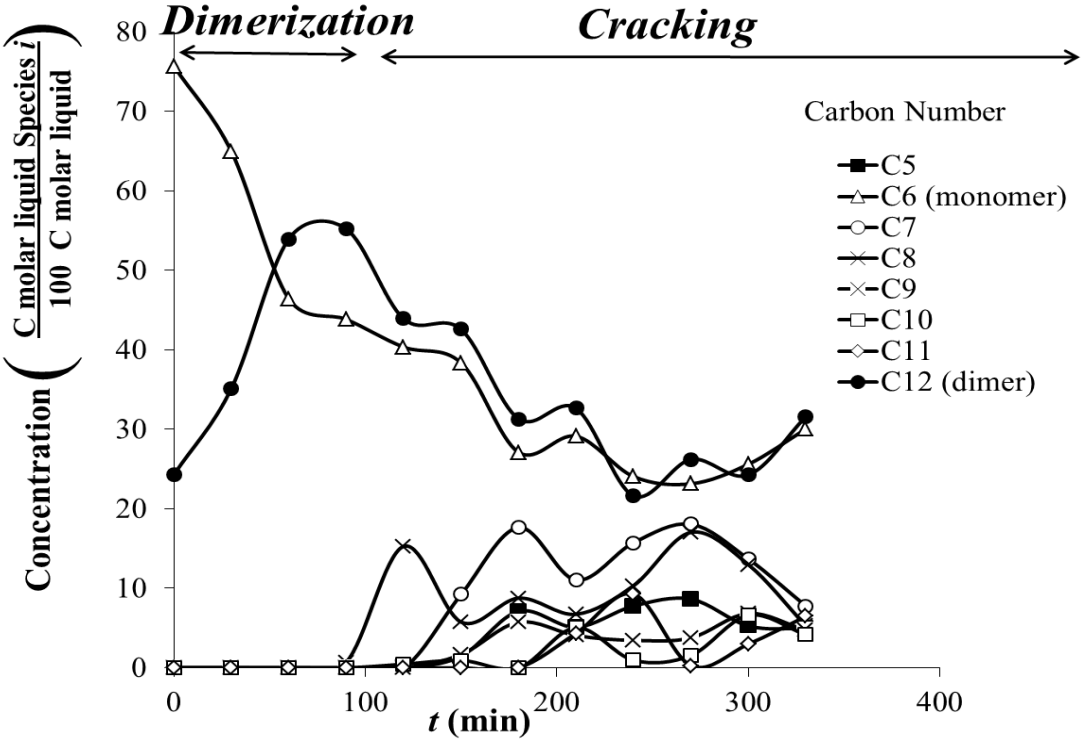

Figure 5-7. Liquid carbon distribution during the reaction of 1-hexene using Beta (25) at T = 270°C.

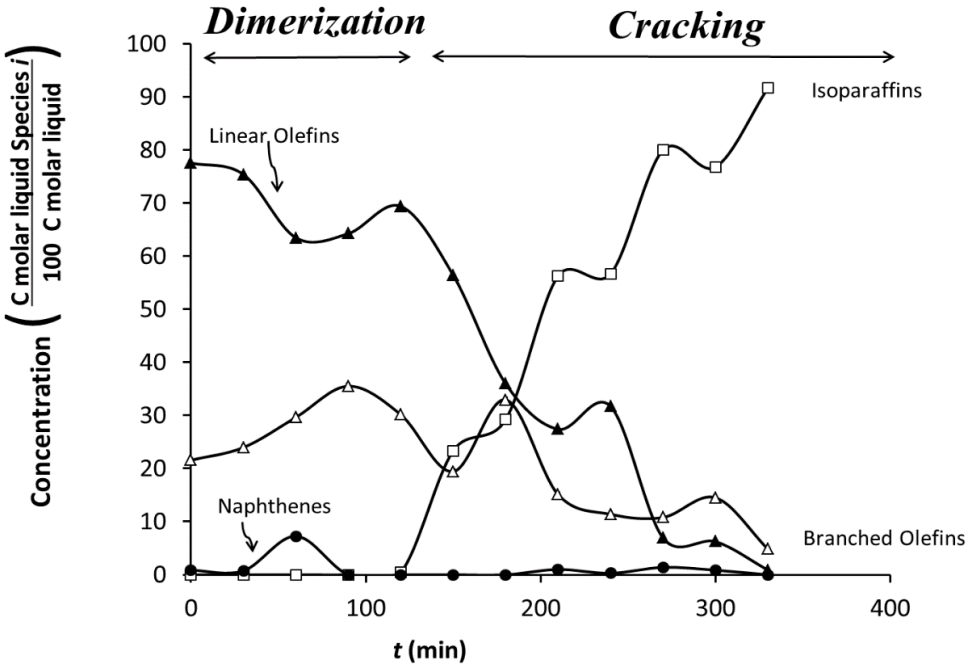

Figure 5-8. Liquid type distribution during the reaction of 1-hexene using Beta (25) at T = 270°C.

Figure 5-9 shows the number of isomers during time. At t = 0 min, there are about 16 types of isomers; whereas, at t = 330 min, there are about 60 types of isomers. Therefore, time affects the carbon distribution. Also, Figure 5-10 shows the GC carbon distribution charts at different reaction times. For instance, at the reaction beginning (t = 0 min, Figure 5-10a), it has only C6 and C12 products; whereas, later (t = 300 min, Figure 5-10d) C7–C11 are produced.

For C6, the isomers follow: 2-hexene, 3-hexene, and 1-methyl 1-pentene. For the dimer C12, the isomers are more diverse: 1-dodecene; 4-octene, 2,3,6,7-tetramethyl; 5-undecene 5-methyl; 3-decene 2,2-dimethyl; 5-undecene, 7-methyl; 2-undecene, 2-methyl; and cyclopentane 1-butyl-2-propyl. C12 has more isomers because it is a large molecule and has multiple ways for C6 to attach.

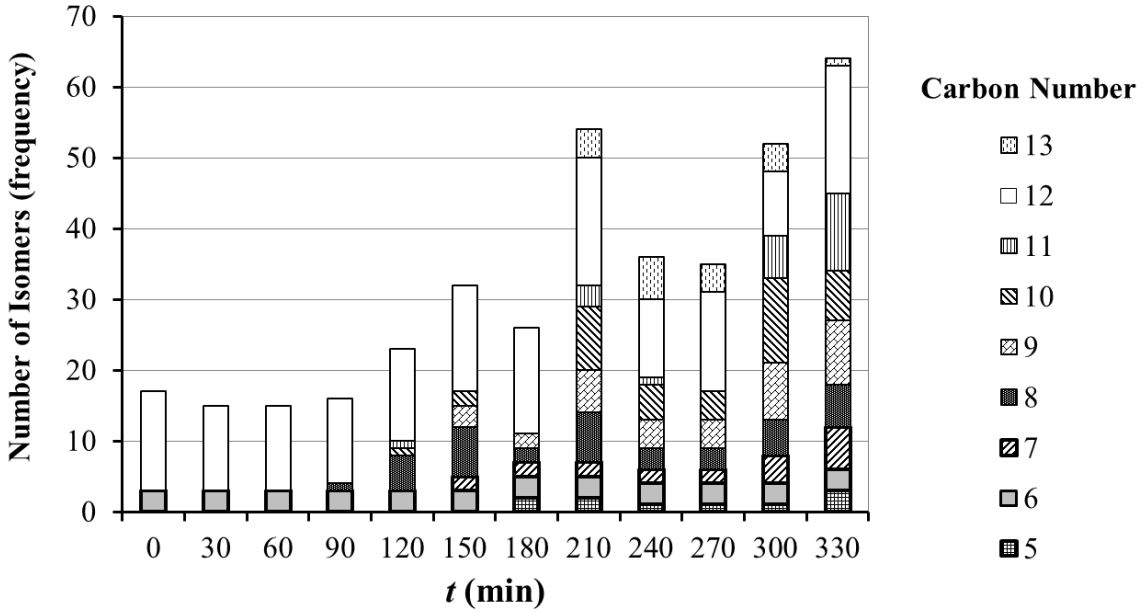

Figure 5-9. Number of isomers during the reaction of 1-hexene using Beta (25) at T = 270°C.

Figure 5-10 illustrates the GC-MS charts of 1-hexene over Beta (25) at T = 270 °C for different times. The number of peaks increases during time, meaning the number of compounds increases as well. There is a tendency to form more isomers.

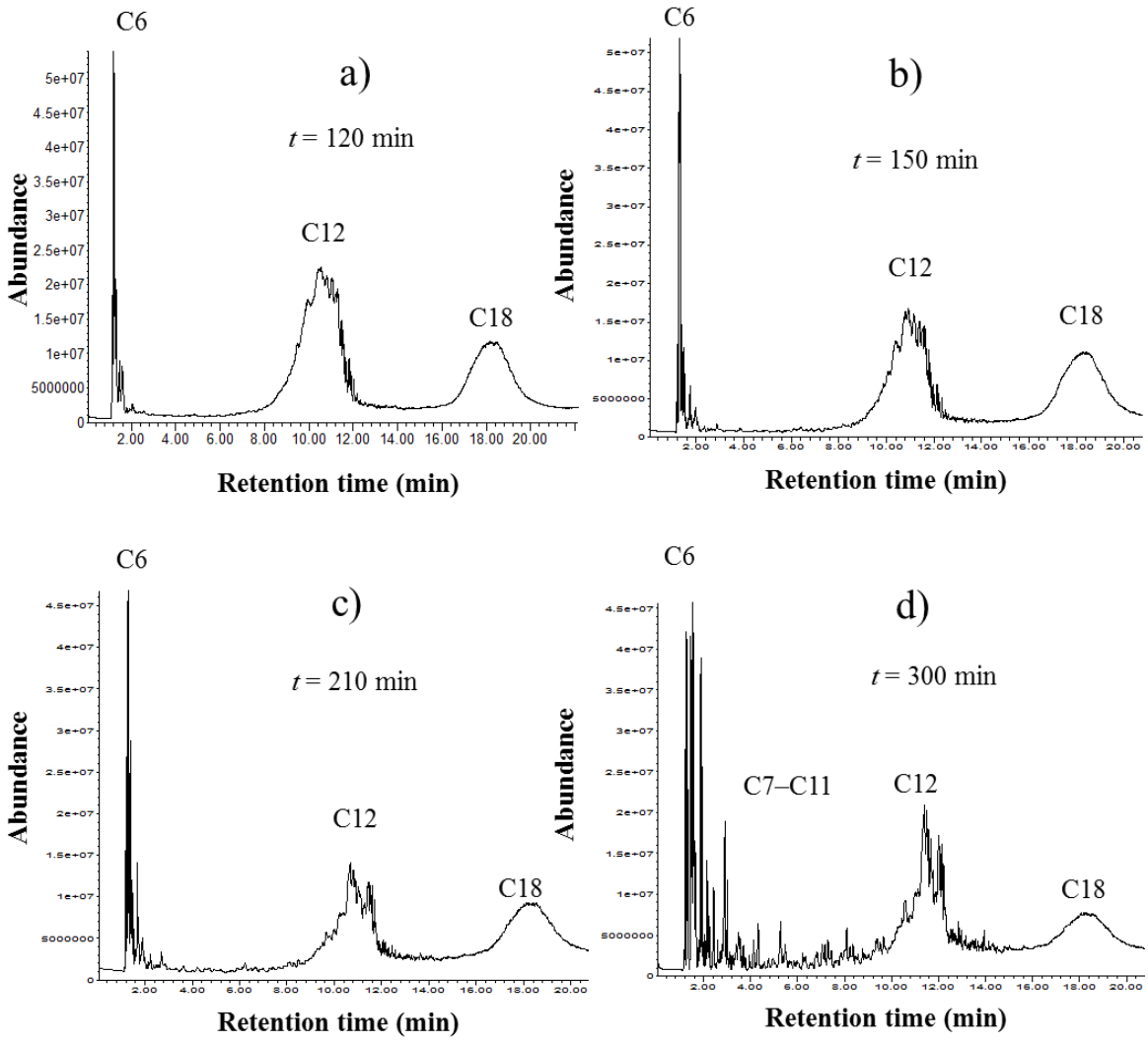

Figure 5-10. Carbon distribution GC-MS charts at different times for the 1-hexene reaction over Beta (25) at T = 270°C.

5.3.1.2 Effect of varying the temperature

Figure 5-11 shows the carbon distribution of 1-hexene reaction using Beta (25) at T = 170°C. After reaching a steady state (t = 160 min), the amount of C6 (~70%) and C12 (~30%) was constant and there were the only products; therefore, cracking reaction did not occur. The temperature was not high enough to form other molecules. The amount of C12 increased from 13% (t = 30 min) to 30% (t = 160 min); whereas, the amount of C6 decreased from 85% (t = 30 min) to 68% (t = 160 min). After t = 160 min, the amount of C6 and C12 are constant during time, which means the reaction is in equilibrium. The dimer never surpasses the amount of reactant C6.

Figure 5-12 shows the carbon distribution for 1-hexene at T = 220 °C during time. At t = 160 min, the dimer C12 reaches the maximum concentration (40%) and is the only product. During t < 160 min, dimerization is the only type of reaction. After 160 minutes, other products appear (C5, C7–C9), and the amount of C12 decreases during time; therefore, cracking reaction occurs. Before 160 min, the dimer C12 is constant and the only compound. After that, C7 and C8 become significant and cracking reactions appear. The dimer never surpasses the amount of reactant C6.

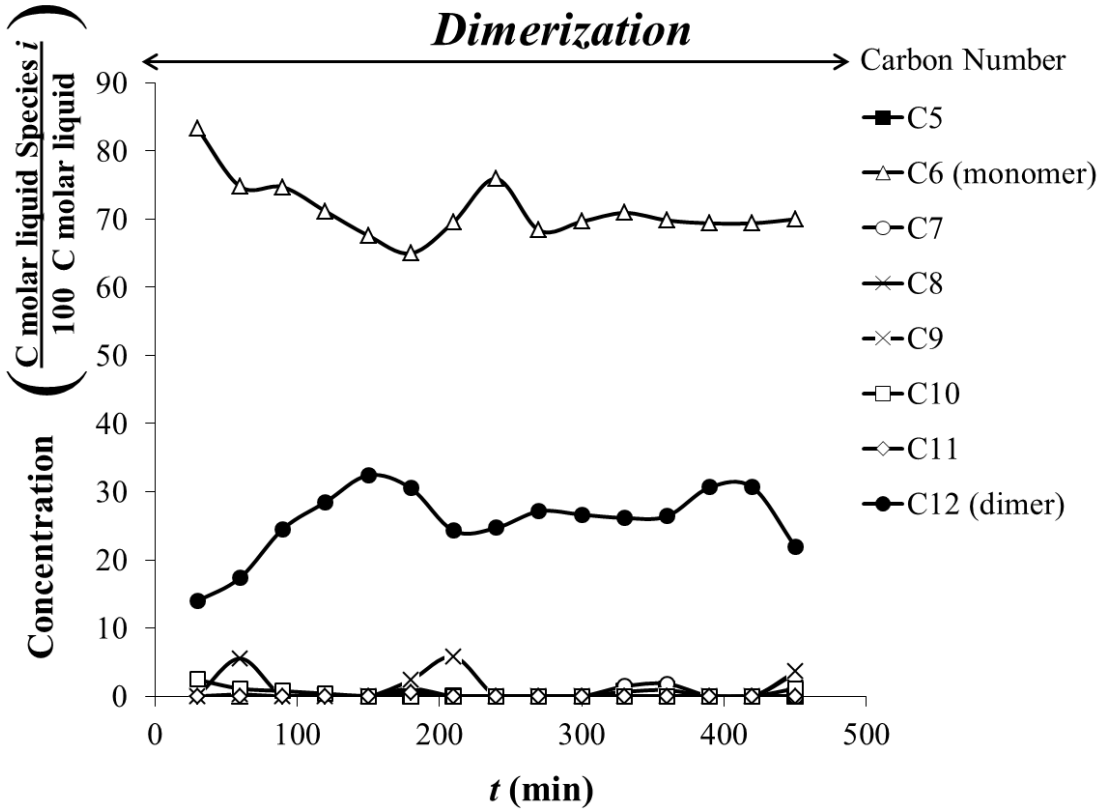

Figure 5-11. Liquid carbon distribution during the reaction of 1-hexene using Beta (25) at T = 170°C.

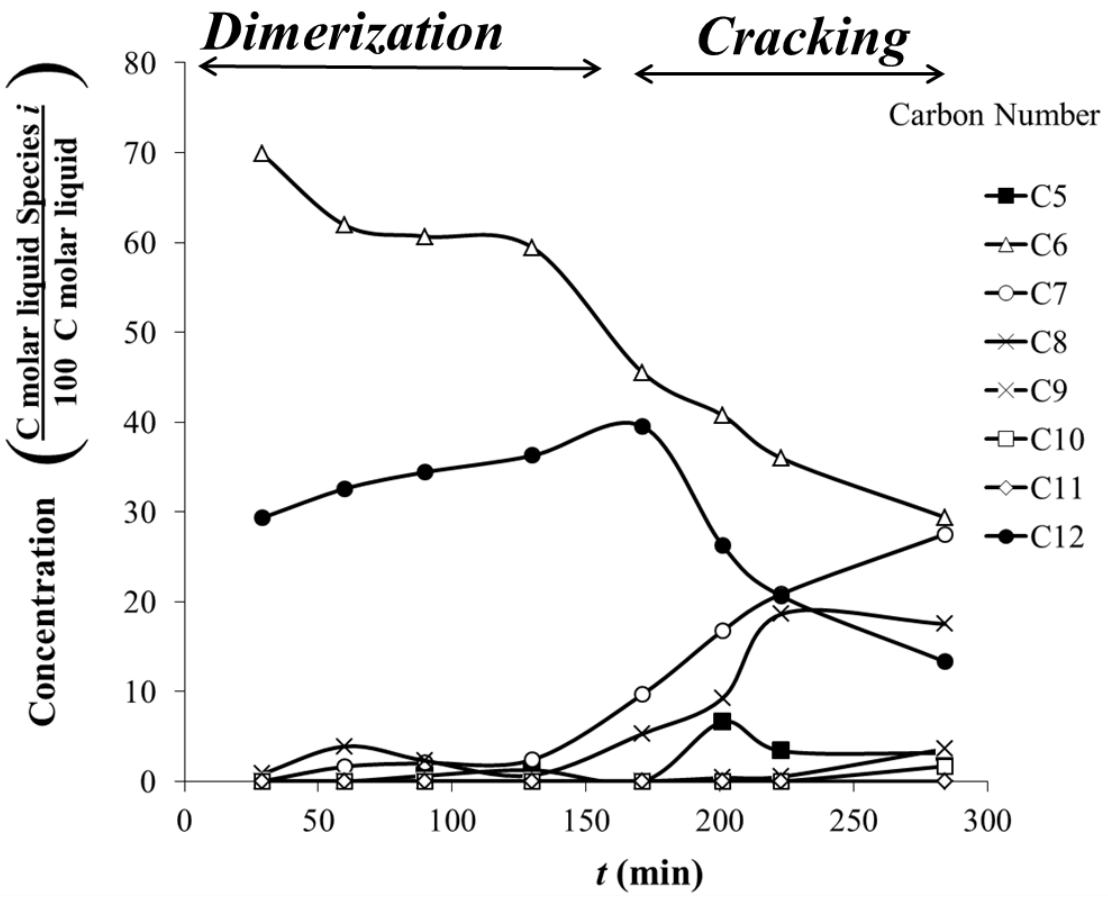

Figure 5-12. Liquid carbon distribution during the reaction of 1-hexene reaction using Beta (25) at T = 220°C.

Figure 5-13 shows the number of isomers for the 1-hexene reaction using Beta (25) at T = 170, 220, 270 °C, and t = 360 min. At all temperatures, the number of isomers for C6 and C12 are, 4 and 30, respectively. When the temperature increases, the amount of isomers increases, except for C6 (monomer) and C12 (dimer).

Figure 5-14 shows the carbon type distribution for the 1-hexene reaction using Beta (25) at T = 170°C. The amount of branched olefins (~50%) and linear olefins (~50%) were constant after reaching a steady state and were the only product types;

therefore, cracking reactions did not occur. The temperature was not high enough to form other types of hydrocarbons. The amount of branched olefins increased from 30% (t = 30 min) to 50% (t = 160 min); whereas, the amount of linear olefins decreased from 72% (t = 30 min) to 50% (t = 160 min). After t = 160 min, the amount of linear and branched olefins were oscillating over time which means the reaction is in equilibrium. C6 and C12 have similar concentrations during time.

Figure 5-15 shows the carbon type distribution for 1-hexene at T = 220 °C during time. During t < 160 min, linear olefins and branched olefins are constant ~70% and ~30% on average, respectively. The amount of isoparaffins increased from 0% (t = 90 min) to 50% (t = 280 min); whereas, the amount of linear olefins decreased from 85% (t = 90 min) to 5% (t = 280 min). Branched olefins reach the maximum concentration at t = 220 min.

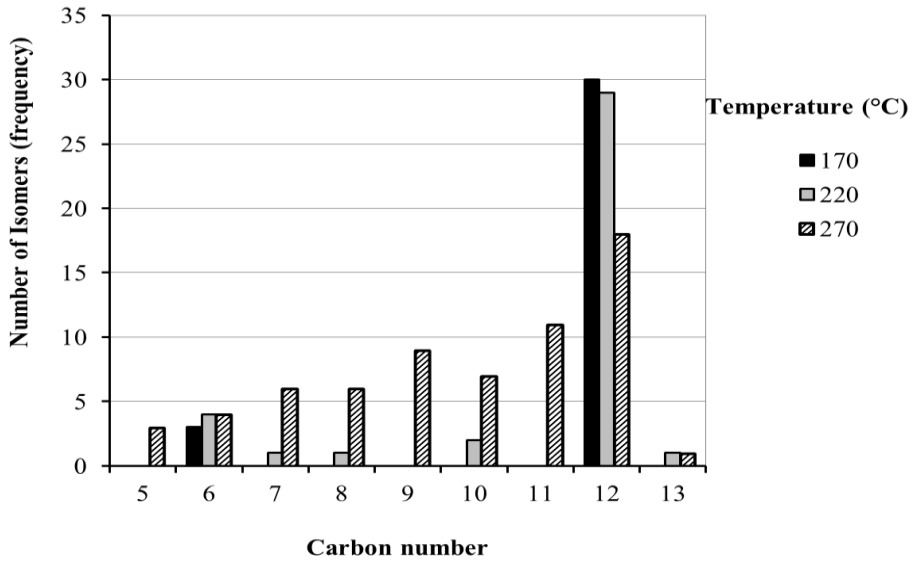

Figure 5-13. Number of isomers at different temperatures of the 1-hexene reaction using Beta (25) at t = 360 min.

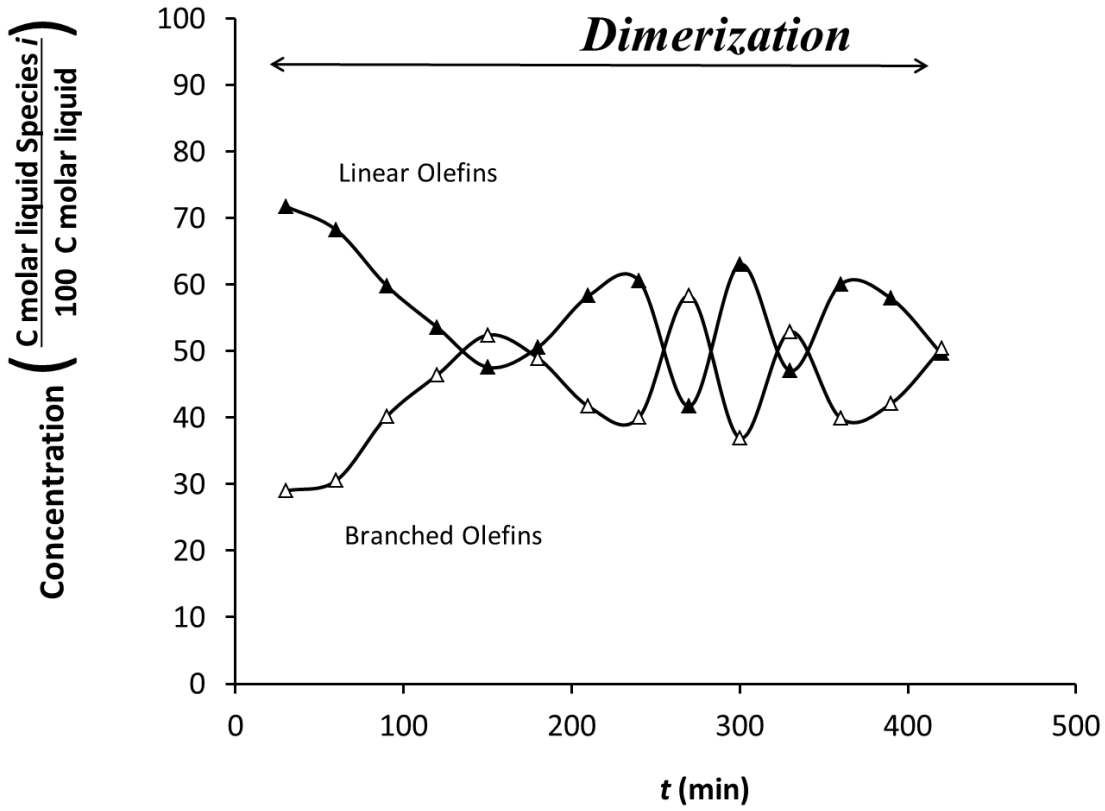

Figure 5-14. Liquid carbon distribution during the reaction of 1-hexene using Beta (25) at T = 170°C.

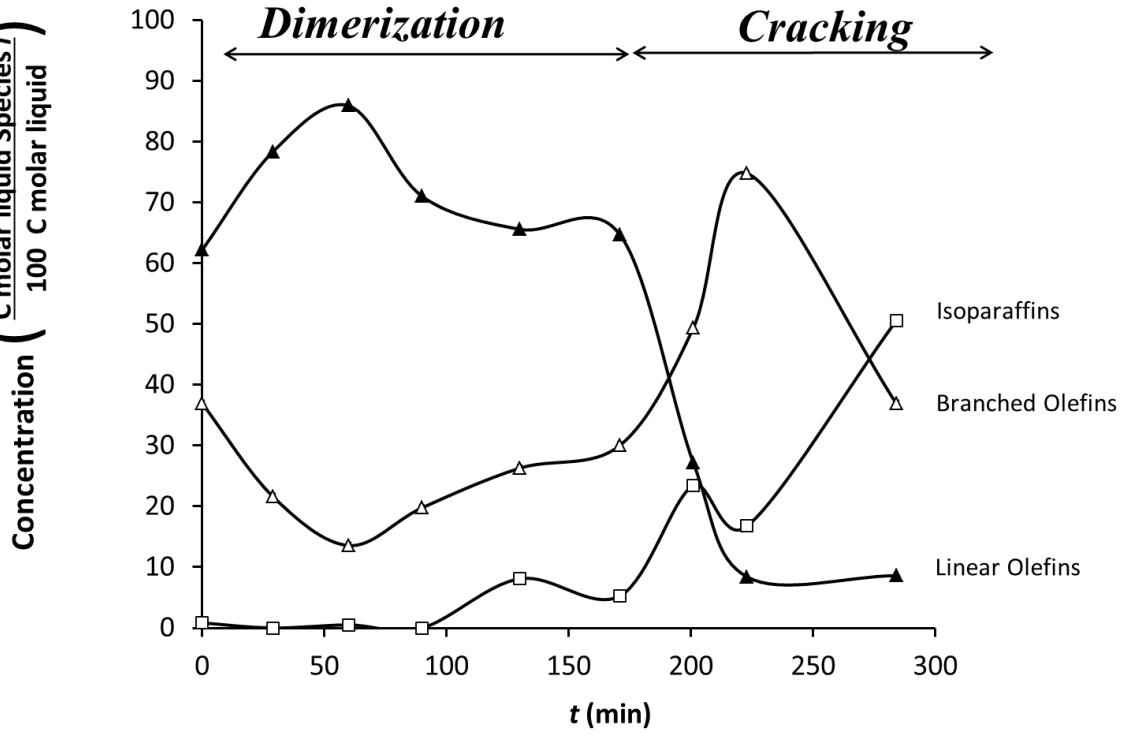

Figure 5-15. Liquid carbon distribution during the reaction of 1-hexene using Beta (25) at T = 220°C.

Figures 5-7 to 5-15 show the effect of time and temperature for the 1-hexene reaction over Beta (25). It is unknown if the results of 1-hexene can be applied to other olefins. To determine the effect of other olefins reactants over Beta (25), 1-octene and 1-decene were studied. Figure 5-16 shows the carbon distribution for 1-octene at T = 220 °C during time. At t = 160 min, the dimer C16 reaches the maximum concentration (21%) and is the only product. During t < 160 min, dimerization is the only type of reaction. After 160 minutes, other products appear (C5, C7–C9), and the amount of C12 decreases during time; therefore, cracking reactions occur. The dimer never surpasses the amount of reactant C8.

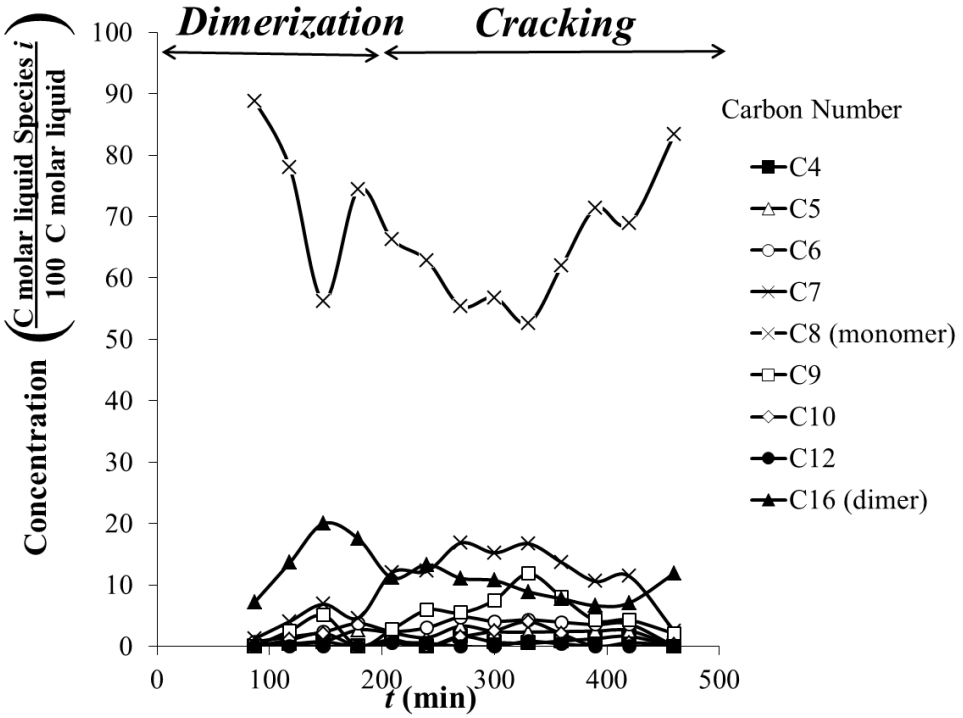

Figure 5-16. Liquid carbon distribution for the reaction of 1-octene reaction using Beta (25) at T = 220°C.

Figure 5-17 shows the carbon type distribution for 1-octene at T = 220 °C during time. During t < 160 min, linear olefins and branched olefins are ~90% and ~10% , respectively. The amount of isoparaffins increased from 0% (t = 90 min) to 17% (t = 450 min); whereas, the amount of linear olefins decreased from 90% (t = 90 min) to 60% (t = 450 min).

For 1-decene dimerization over Beta (25), the reaction performed similar to 1-hexene and 1-octene, but the dimer selectivity was lower than the other olefins. Table 5.2 shows the maximum dimer selectivity for 1-decene dimerization reactions.

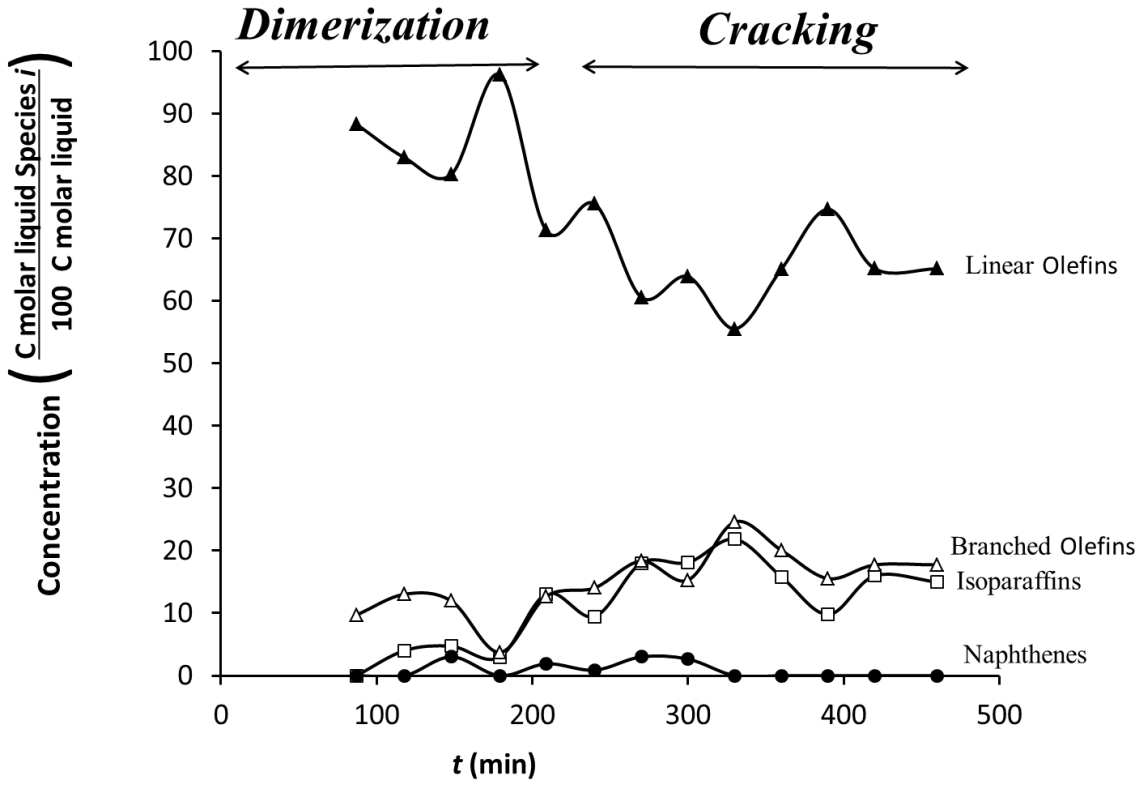

Figure 5-17. Liquid type distribution during the reaction of 1-octene using Beta (25) at T = 220°C.

5.3.2 Dimerization of mixtures

In this section, the effect of mixing two different olefins is studied. Figure 5-18 shows the carbon distribution GC-MS charts at different times of 1-hexene and 1-octene mixture (50/50 wt%) reaction over Beta (25) at T = 220 °C. At longer residence times, more isomer products appear, similar to the single-reactant experiments (Figures 5-7 to 5-17). The most abundant hydrocarbon product is C14, which results from C6 and C8 bonding. Dimers C12 and C16 are also products, but they are less abundant than C14.

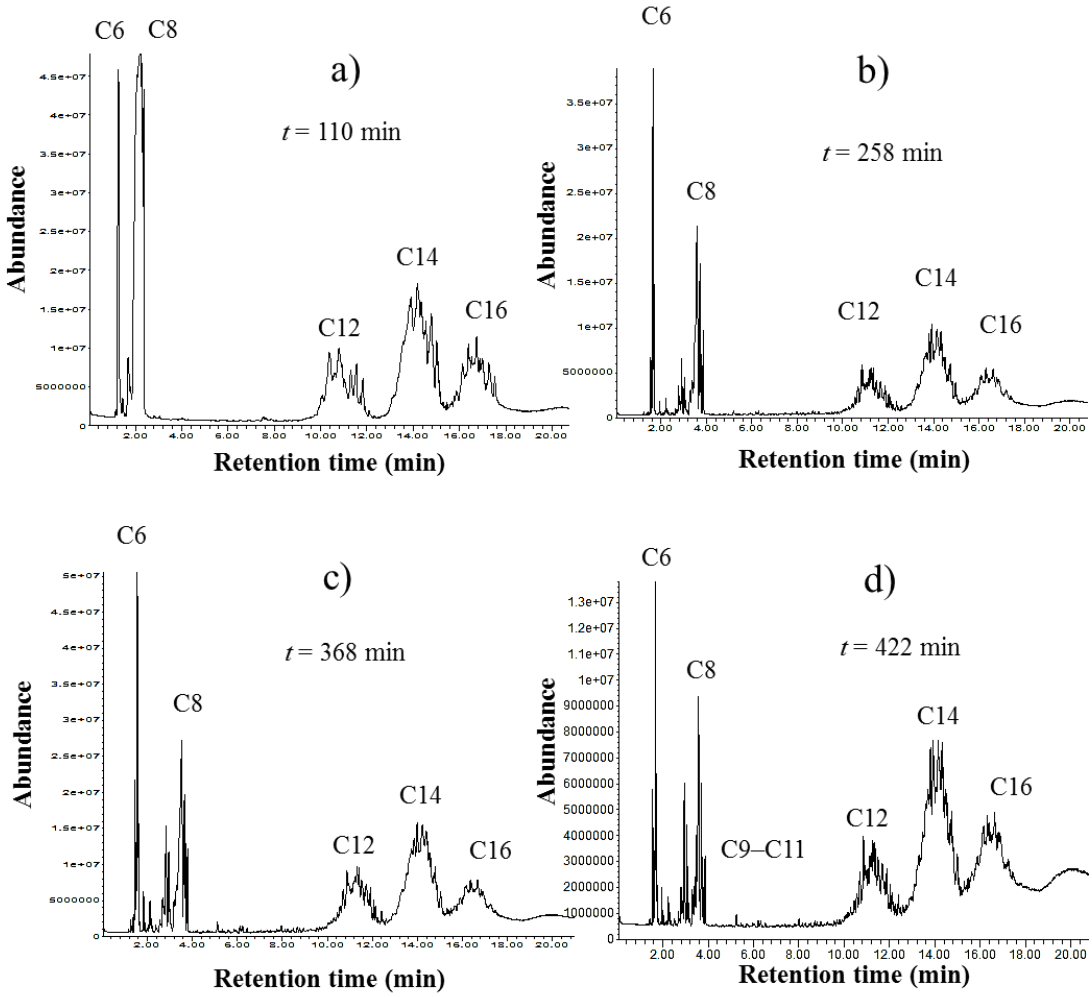

Figure 5-18. Carbon distribution GC-MS charts at different times of 1-hexene and 1-octene mixture (50/50 wt%) reaction using Beta (25) at T = 220 °C.

Figure 5-19 shows the carbon distribution GC-MS charts at different times of 1-hexene and 1-decene mixture (50/50 wt%) reaction using Beta (25) at T = 220 °C. The most abundant hydrocarbon product is dimer C12. Dimer C16 is less abundant than C12 because 1-decene reactivity is lower. This is attributed to the large size of 1-decene,

which affects access inside the porous structure of Beta (25). Dimer product C20 is negligible.

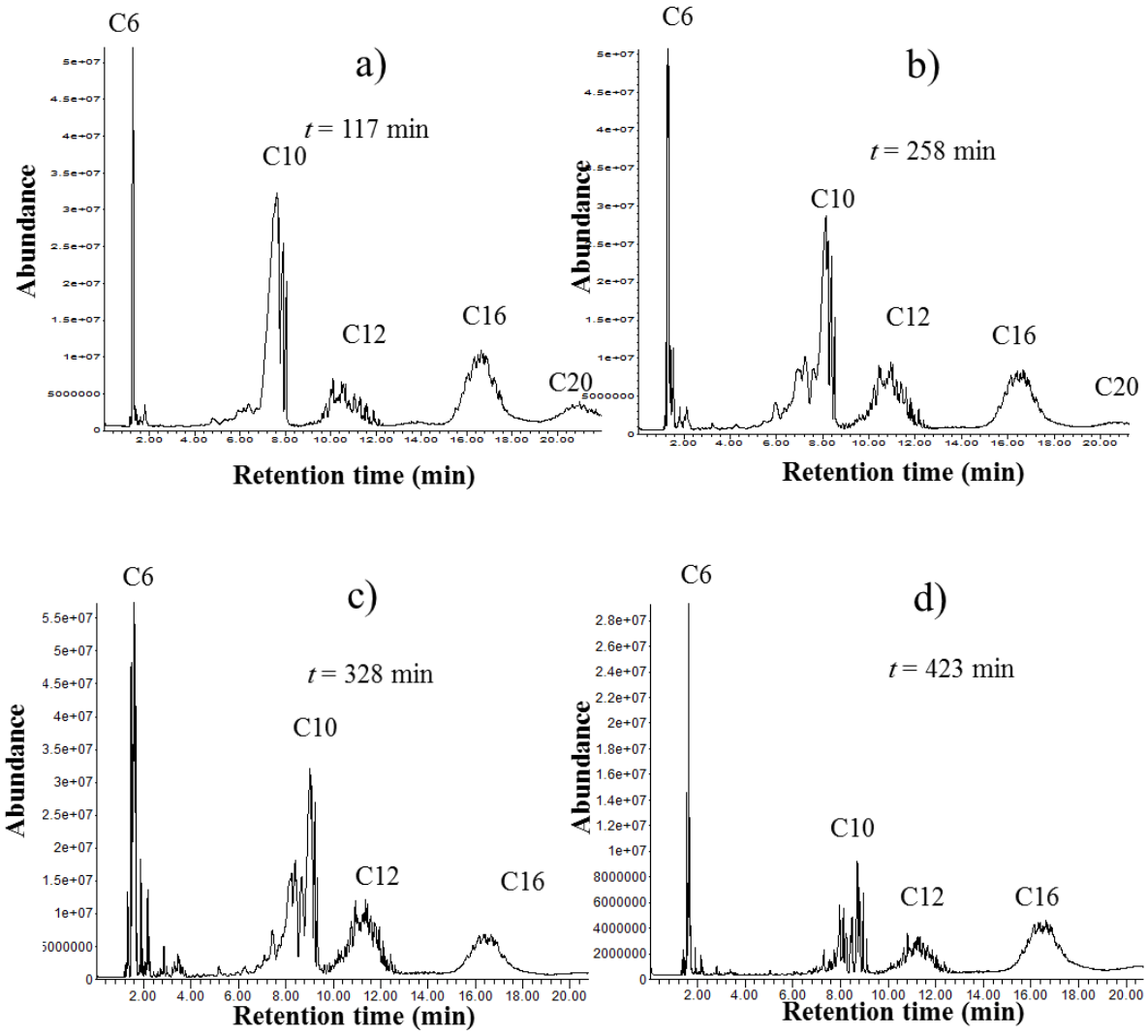

Figure 5-19. Carbon distribution GC-MS charts at different times of 1-hexene and 1-decene mixture (50/50 wt%) reaction using Beta (25) at T = 220°C.

5.4 Conclusions

For the transformation of olefins with Beta (25) at T = 220–270 °C, the first reaction to occur is dimerization and then, as time progresses, cracking and oligomerization occur. On the other hand, at lower temperature (170 °C) only dimerization occurs.

Using Beta (25), olefins transform to isoparaffins, branched olefin, linear olefins, and naphthenes, and are the only types of products obtained. For low temperatures (170 °C), cracking did not occur, so isoparaffins were not present because they result from cracking reactions. Using Beta (25), dimerization reaction over Beta (25) is recommended for olefins with carbon number less than C8 because larger molecules cannot enter the pores. Table 5-2 shows the best conditions to obtain the most amount of dimer product.

Table 5-2. Maximun dimer concentration obtained using Beta (25).

	Dimer Concentration		
	Temperature		
Feed	170 °C	220 °C	270 °C
1-hexene	30% at 160 min	40% at 160 min	57% at 100 min
1-octene		22% at 160 min	30% at 130 min
1-decene		10% at 160 min	12 % at 120 min
1-hexene + 1-decene		18% at 160 min	
1-hexene + 1-octene		35% at 160 min	

6. BIOMASS CONVERSION TO HYDROCARBON FUELS USING THE MIXALCO™ PROCESS

The objectives of this section follow:

a) Describe the pilot plant and reports results from an 11-month production campaign that converted shredded paper and chicken manure into gasoline and jet fuel.
b) Describe the steps performed used to convert the biomass into fuel.
c) Determine the concentration and yield results.

6.1 Introduction

The MixAlco™ pilot plant converts biomass to hydrocarbons (i.e., jet fuel, gasoline) using the following steps: fermentation, descumming, dewatering, thermal ketonization, distillation, hydrogenation, and oligomerization. This study describes the pilot plant and reports results from an 11-month production campaign. The focus was to produce sufficient jet fuel to be tested by the U.S. military. Because the scale was relatively small, energy-saving features were not included in the pilot plant. Further, the equipment was operated in a manner to maximize productivity even if yields were low. During the production campaign, a total of 6,015 kg of shredded paper and 120 kg of chicken manure (dry basis) were fermented to produce 126,500 L of fermentation broth with an average mixed acid concentration of 12.5 g/L. A total of 1582 kg of carboxylate salts were converted to 587 L of raw ketones, which were distilled and hydrogenated to 470 L of mixed alcohols ranging from C3 to C12. These alcohols, plus 300 L of alcohols made by an industrial partner (Terrabon, Inc.), were shipped to an independent

contractor (General Electric) and transformed to jet fuel (~100 L) and gasoline (~100 L) by-product.

The carboxylate platform produces liquid hydrocarbons from carboxylate intermediates.[1-4] The MixAlco™ process is a version of the carboxylate platform that does not require sterilization to obtain fuels. First, during the fermentation, the biomass is converted to raw fermentation broth (RFB), an aqueous mixture of carboxylate salts (C2–C7), nutrients, microorganisms, and impurities. In the descumming step, RFB is treated with lime followed by CO_2, which precipitates calcium carbonate and eliminates many of the impurities. The descummed RFB is concentrated by evaporation, and the carboxylate salts are crystallized. In a batch reactor, [5] the salts are thermochemically transformed into raw ketones, which are distilled and then hydrogenated to mixed alcohols.[6] In a plug-flow reactor, the mixed alcohols are dehydrated and oligomerized using a zeolite catalyst.

This section presents results from pilot-scale production of hydrocarbons using the MixAlco™ process. The pilot plant operated from February to December 2010. The emphasis was to produce 100 L of jet fuel for military testing; yield and efficiency were secondary considerations.

6.2 Experimental

6.2.1 Fermentation

In each batch, shredded office paper (98%) and chicken manure (2%) were the biomass feedstocks. These were selected because they are inexpensive and require no pretreatment to render them digestible. Four fermentors (3780 L each) operated in

parallel. Figure 6-1 shows the schematic flow diagram of each fermentor. Every 7–10 days, about 80 to 100 kg of dry shredded paper, dechlorinated water (1700–1900 L), and 1.5–2 kg (dry basis) chicken manure were added manually to the top of each fermentor (Figure 6-2). About 80 to 85% of fermentor volume was used. From the top, the fermentor was mixed manually using a mixing tool. To facilitate microbial metabolic activity, fertilizer-grade urea was added to the fermentor to maintaining a C/N ratio of 30 (g C/g N). The fermentation reaction was performed anaerobically at 40 ^{o}C by circulating warm water through coiled tubing surrounding the fermentor. The pH ranged from 5.5–7.0. The fermentor was operated using non-sterile conditions. The inoculum was marine soil from Galveston, TX. No buffer was required; the minerals naturally present in the feedstock provided sufficient buffering.

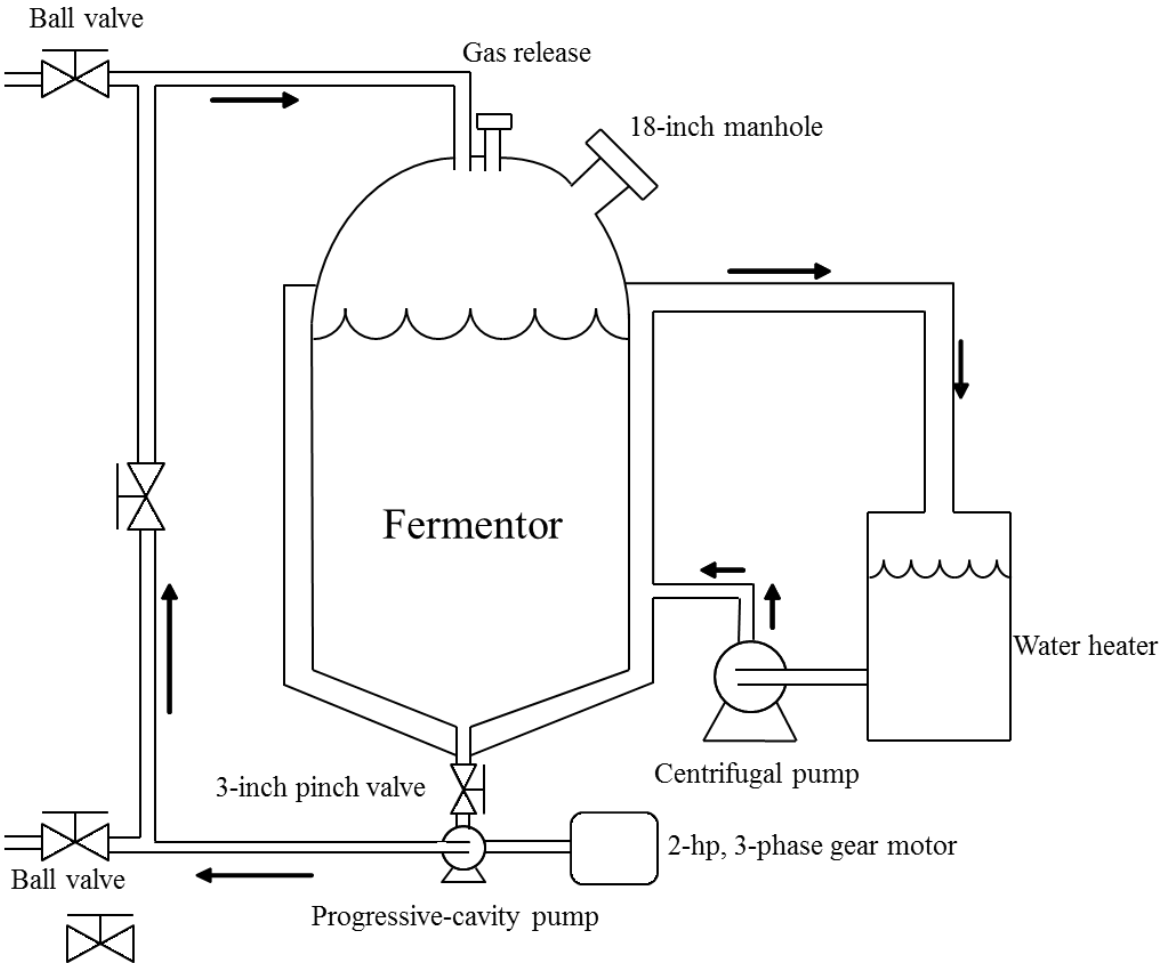

Figure 6-1. Schematic process flow diagram of a fermentor.

Figure 6-2. Top section of the four pilot-plant fermentors including the cat-walk.

To suppress methanogens, iodoform (20 mg/L ethanol)[3] was added to each fermentor (200–800 mL per day). This iodoform solution was mixed into the fermentation broth using a progressive-cavity sludge pump (Moyno 1000 series, Model B1E-CDQ-AAA, Figure 6-1) which ran almost every day for one hour.

The fermentors were operated in a fed-batch mode. Every 7–10 days, when the mixed carboxylic acids concentration in the fermentation broth reached the desired level (10–15 g/L), the broth was harvested from the top of the fermentor using a submersible pump. The undigested paper sludge was collected by opening the ball valve (Figure 6-1) and pumping using the progressive-cavity pump. Before disposing the undigested solids, the liquid was extracted from the solids using a screw press (Vincent Compact Screw Press; Model: CP-6; Vincent Corporation, Florida), which allowed recovery of carboxylate salts from the liquid. Then, the solids were washed with water and pressed

again to remove the remaining salts. This washed water was recycled to the fermentor with fresh water required for the next fermentation.

After harvesting the fermentation broth, about 760 ± 190 L of semi-digested fermentation sludge from the previous batch was left in the fermentor as inocula. Table 6-1 shows typical values of feedstock properties used for the batch fermentation.

Table 6-1. Characteristics of fermentation feedstocks.

Properties	**Shredded waste office paper**	**Fresh chicken manure**	**Urea**
Moisture content, *M* (g /100 g of wet sample)	3.75 ± 0.75	80.67 ± 3. 45	0.0
Ash content, *I* (g/100 g of dry sample)	16.92 ± 0.70	47.55 ± 1.25	0.0
Carbon content, *C* (g/100 g dry sample)	40.35 ± 1.56	28.82 ± 3.58	19.97 ± 0.72
Nitrogen content, N (g/100 g dry sample)	0.13 ± 0.05	1.81 ± 0.36	45.26 ± 0.50

6.2.2 Descumming

Raw fermentation broth (RFB), the liquid obtained from fermentation process, contained 3 to 5 g/L organic scum, which included suspended paper particles, microorganisms, and proteins. To purify RFB, >95% of the scum was removed to

improve salt quality, and avoid fouling in the dewatering process. Descumming was a batch process. A positive-displacement pump loaded 1890 L of RFB into a 2270-L stainless steel steam-jacketed mixing tank. The tank was heated to about 80–90 ^{o}C. Then, industrial-grade slaked lime ($Ca(OH)_2$) was added to increase the broth pH from 5.5–7 to 10.5–11.5. During lime addition, the tank was continuously mixed by circulating the broth using a high-temperature centrifugal pump. Thereafter, CO_2 gas was bubbled from a compressed CO_2 cylinder to remove excess $Ca(OH)_2$ as $CaCO_3$.

The formation of $CaCO_3$ particles helped to nucleate and agglomerate scum. When the flocculation was complete, the descummed broth was transferred to a storage tank for cooling, storage, and settling the solids. Then, the 2270-L mixing tank was cleaned for the next cycle.

To remove the precipitated scum, the broth was centrifuged (1700 rpm, 7 gpm, Model MAPX-204 centrifuge, Alfa Laval Inc.). By precipitating $CaCO_3$ from the mother liquor, it was possible to recover more than 95% of salts from the broth. After centrifuging, the clarified liquid broth passed to the dewatering step.

At the beginning, in addition to lime treatment, descumming employed a costly ($75/gallon) industrial flocculent (4 L flocculent/1890 L RFB). Later, flocculent addition was found to be unnecessary.

6.2.3 Dewatering and crystallization

The 2270-L stainless steel steam-jacketed tank was used for both descumming and dewatering. In each batch, about 1890 L of descummed-and-centrifuged broth was fed to the 2270-L tank and boiled with steam generated from a propane-heated boiler

(Model 103, Parker Boiler Co.). When half the liquid broth evaporated, the salts started to precipitate. The concentrated broth from the 2270-L tank was transferred to a 1130-L steam-jacketed tank for further concentration and crystallization.

First, the high-molecular-weight calcium salts precipitated and floated to the top. A fine-mesh stainless steel screen was used to skim the floating salts for collection. Then, the hot high-molecular-weight salts were filtered using a laboratory-scale vacuum filter unit equipped with a 25-µm cloth filter. Meanwhile, the low-molecular-weight salts were collected from the bottom of the tank and filtered while hot. Continuous removal of salts from the top and bottom of the tank and immediate filtration after collection improved salt quality. When the volume of the broth decreased from 1130 to 190 L, it was quickly transferred to a 227-L tank. Then, removal of salts was repeated for the 227-L tank until all the liquid was completely evaporated.

The filtered carboxylate salts were 45 to 50% moisture; they were dried in a bench-scale oven (120 °C, 1.4-kW, Model 17-Y-11, Precision Scientific Co.) that produced up to 130 kg salts per week. The low-molecular-weight crystallized salts were tightly agglomerated and formed 5-cm chunks. A sand-filled lawn roller was used to crush them and form a powder. From each batch of 1000-L centrifuged broth, an average of 13 kg total mixed dry salts was produced from the dewatering and crystallization. The mixed dry salts were stored and passed to the ketonization unit.

6.2.4 Ketonization

Before ketonization, to keep the salts free of excess moisture, the salts were dried in an oven (Figure 6-3) at 104 °C for at least 24 hours. The ketone unit had a reaction

section and a condensing section. The cylindrical reactor vessel (Figure 6-3) had a flanged head and stirrer operated by a motor and seal-less magnetic drive mounted on top. The cylindrical part of the reactor was surrounded by an electric heating jacket (3.8-kW, three-phase, tubular type, Cat 10-1024-2W, HTS Ampetek Co.). The reactor was constructed from 25.4-cm-diameter stainless steel schedule 20 pipe with 0.64-cm-thick wall. The top flange was 25.4-cm 1034-kPa class. The bottom plate was 1.27 cm thick. The reactor internal volume was 20 L. Four sintered metal filters (20-µm pore size, 502-cm^2 surface area, custom-made filters, Applied Porous Technology Inc., Figure 6-3) were installed on the underside of the reactor top flange to prevent solid salt from plugging downstream tubing and blocking the flow of ketone product.

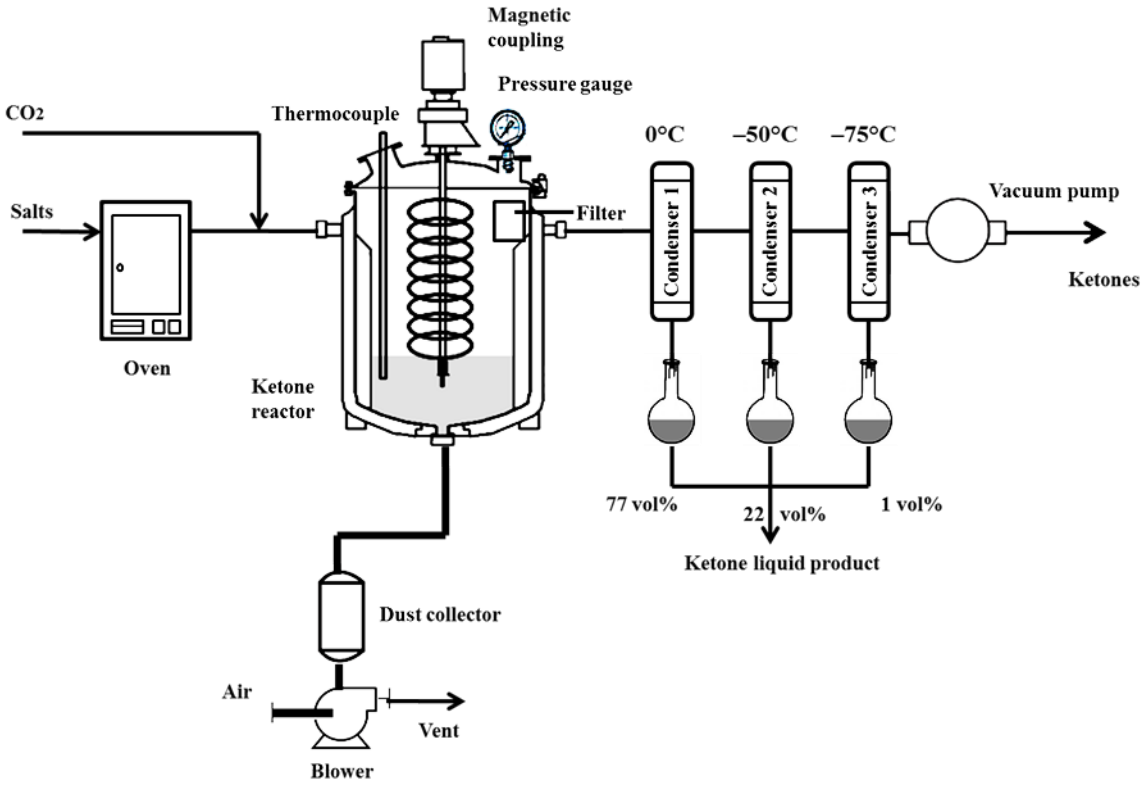

Figure 6-3. Schematic process flow diagram of the ketone reactor.

For each batch, 4 kg of mixed carboxylate salts were charged inside the reactor vessel. The reactor head was put in place and tightened. Excess air inside the reactor was removed with a vacuum pump (Figure 6-3) until the pressure reached 3.12 kPa. The vacuum pump was turned off and sweep gas (CO_2) was run through the system at 1 L/min. The condensation system was turned on and the reactor stirring speed was set to 25 rpm. On occasion, the sweep gas was not employed. In this case, the reactor operated under vacuum to reduce the residence time of the ketone product and thereby reduce degradation.

The reactor temperature was set to 400 °C. As salts heated to 180–290 °C, they went through a plastic state and the stirrer became very hard to turn causing the magnetic drive to slip. Above 290 °C, the stirrer again became functional. Routinely, the stirrer was turned off between 180 and 290 °C. The reaction was completed after 3 h. For each 4-kg salt batch, 1.5 L of raw ketones was collected.

The condensing section was a series of three condensers connected to the reactor exit. These condensers progressively cooled the reactor product effluent to 0 °C (first condenser), –50 °C (second condenser), and –78 °C (last condenser). To collect the raw ketones product during each run, a glass flask was mounted below each condenser.

The three condensers were commercial heat exchangers (Model STS 702-C6-SP, American Industrial Heat Transfer Inc.). The single-pass heat exchangers were 0.57-m-long with 0.68-m^2 internal surface area. Condenser 1 used a pump to circulate water from an iced-filled beer cooler. After each pass, the water returned to the cooler. The cooler was maintained at nearly 0 °C by replenishing ice and draining excess water.

Condenser 2 was cooled by a low-temperature recirculation cooler (Model RC210C0 TLT Recirculating cooler, SP Industries), which was equipped with its own internal refrigeration equipment, coolant (Duratherm XLT-120), and circulation pump. This cooler could circulate refrigerant from 0 to –80 °C. Condenser 3 was cooled by a mixture of dry ice and ethanol. The condensers were made of stainless steel. Most material was collected from Condenser 1. For example, when the system was under vacuum, Condensers 1, 2, and 3 collected 77%, 22%, and 1%, respectively. When the system was under sweep gas (CO_2), Condensers 1, 2, and 3 collected 88, 10, and 2%, respectively.

To remove air from the reaction system, a vacuum pump (Figure 6-3) was provided at the outlet of Condenser 3. If air were present, it could combust the ketone product. It is noteworthy that operating at low pressure caused by the vacuum pump made ketone recovery more difficult because lower temperatures were needed to condense vapors. An alternative operational mode employed an inert sweep gas (CO_2), which resulted in operations at near atmospheric pressure. The use of sweep gas improved yields and helped heat transfer.

After each run, a furnace (550 °C) was used to clean the stainless steel product effluent filters that were removed from the ketone reactor. A spare set of filters allowed the ketone unit to operate while the other set was cleaned.

To provide cooling, an air blower blew room air through a cylindrical loose-fitting metal jacket placed over the reactor. In 15 min, this system cooled the reactor to

below 100 °C when it could be opened to clean-out ash without combusting unreacted residue.

An attempt to prevent the plastic state of the salts from stopping the stirrer between 180 to 290 °C, inert material (0.25- and 0.5-in-diameter-alumina balls) was added to the reactor. Unfortunately, the balls prevented the stirrer from turning, and all four of the sintered metal filters were damaged. The use of inert material was abandoned.

6.2.5 Distillation

Raw ketones had many impurities (e.g., pyrolysis products) and water, so distillation was necessary to purify the mixture. If these impurities were not removed, they would adversely affect the hydrogenation process.

The distillation system included a 20-L distillation flask, an electric-resistance heating mantle (1.5-kW, Cat # TM118, Glas-Col), a 1-m-long packed column, a condenser connected to a chiller, a receiving flask, and a vacuum pump (Figure 6-4). The flasks and the condenser were constructed of Pyrex glass. The column diameter was 10 cm. The column packing was ceramic Raschig rings. The coolant liquid from the chiller was a mixture of water and antifreeze 50/50 (vol%).

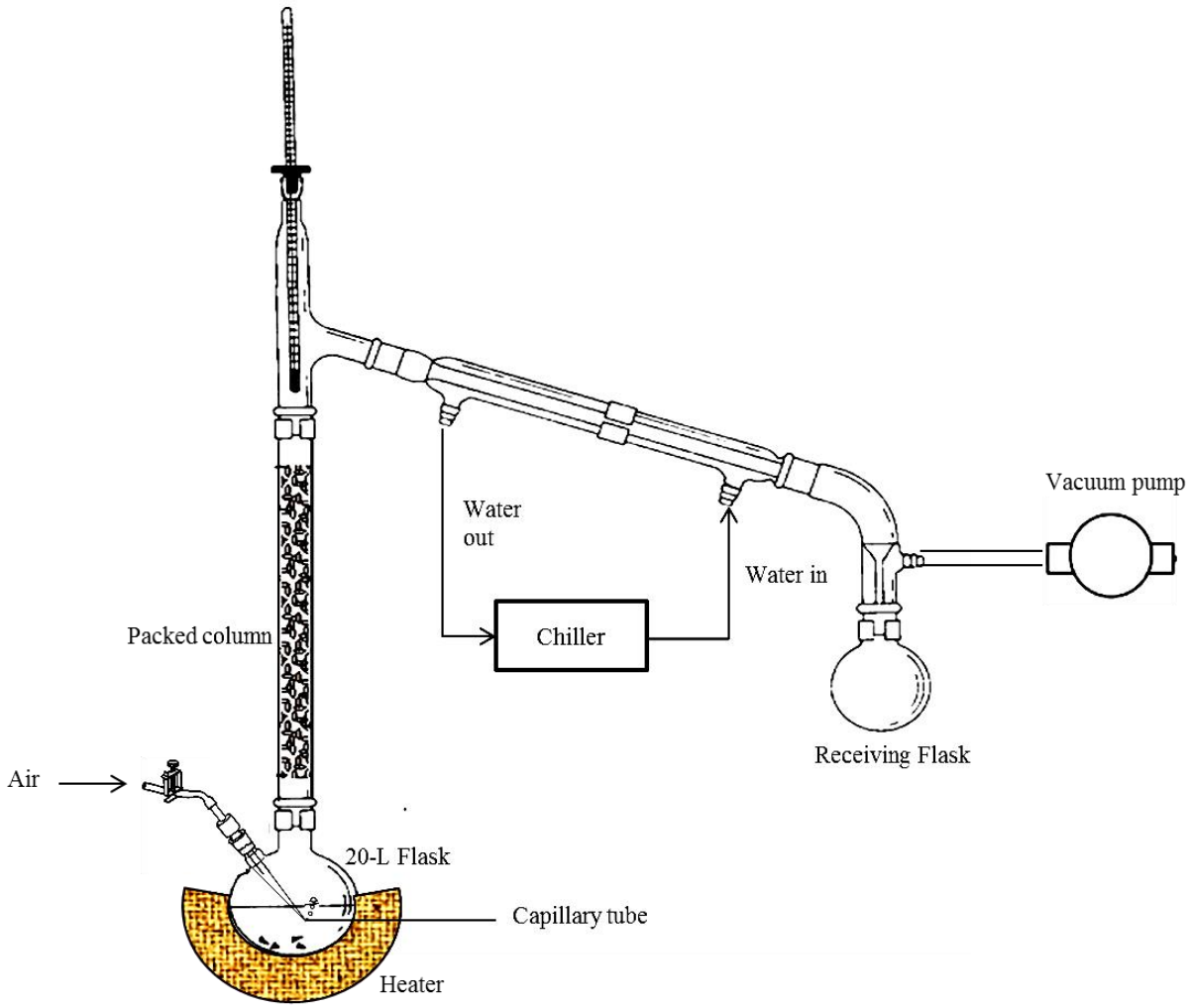

Figure 6-4. Schematic process flow diagram of the distillation unit.

The raw ketones had a dark brown color. The ketone mixture ranged from acetone (BP = 56 °C) to 7-tridecanone (BP = 259 °C). To avoid high-temperature distillation, the distillation was divided into two phases: atmospheric and vacuum. For the atmospheric distillation, 15 L of raw ketones were poured into the distillation flask. The first fraction was obtained at 85 °C, and recovered light ketones (C3–C5). The

second fraction was water obtained between 85–90°C. The vapor from this fraction was white and foggy. The condensed water was disposed as a waste material. The third fraction was collected between 90 and 160°C; most of this fraction was C6–C9. The C6–C13 ketones have a low solubility in water (for example 2-hexanone solubility 14 g/L). If some water remained in the third fraction, the collection flask would have two layers. Water carries too many impurities, and it affects the next catalytic processes, so the water phase was discarded.

For the vacuum distillation fraction, the remaining raw liquid ketones were left in the flask. The vacuum pump was connected to the system, and the system generated a pressure of 23.4 torr. Distillate was collected from 60 °C to 120 °C. To reduce bumping, a capillary tube was placed in the 20-L flask (Figure 6-4), which stirred the liquid with gas bubbles. (Note: For convenience air was used as the gas but an inert gas is a better alternative.) The distillate obtained above 120 °C had a black color, which resulted from oxidation. These oxidized ketones were not collected because they were difficult to hydrogenate. Finally, all the distillate from both the atmospheric and vacuum distillations were mixed and stored with a nitrogen blanket to prevent oxidation.

Table 6-2 shows the typical volumetric distribution from a distillation. The most abundant cut occurred between 80 and 180 °C; 50% of the ketones were obtained between these two temperatures. The total yield was 81.6 L distillate/100 L raw ketones. Although more liquid could have been produced from the vacuum distillation above 120 °C, the liquid product was very dark from impurities. In contrast, below 120 °C the distillate was always light bright yellow.

Table 6-2. Ketone distillation distribution.

	Compounds	Amount (vol%)
Atmospheric distillation 80 °C	C3–C5	15
Atmospheric distillation 90–180 °C	C5–C10	49.9
Vacuum distillation 120 °C	C10–C13	16.7
Water	H_2O	7.3
Residue	C11–C13	10.7
Total		100

For vacuum distillation, to obtain good-quality ketones, the pressure had to reach 23.4 torr. Low pressure ensured minimal air was inside the system and prevented oxidation of the ketones and the formation of black impurities.

6.2.6 Hydrogenation

Hydrogenation was performed in a 7.5-L stainless steel batch reactor (230-V, 2.3-kW Parr Model 4522M Press React APP26 Cart-MA) (Figure 6-5). The catalyst was Raney nickel (Sigma Aldrich, Cat # 221678). The catalyst was in a slurry form with water (50% Raney nickel). The hydrogen was industrial quality from Praxair, Inc. The batch reactor was equipped with a magnetic drive connected to the stirrer (0–1000 rpm) for mixing (Figure 6-6). The temperature inside the reactor was monitored via a thermocouple and regulated via a controller connected to a heating jacket.

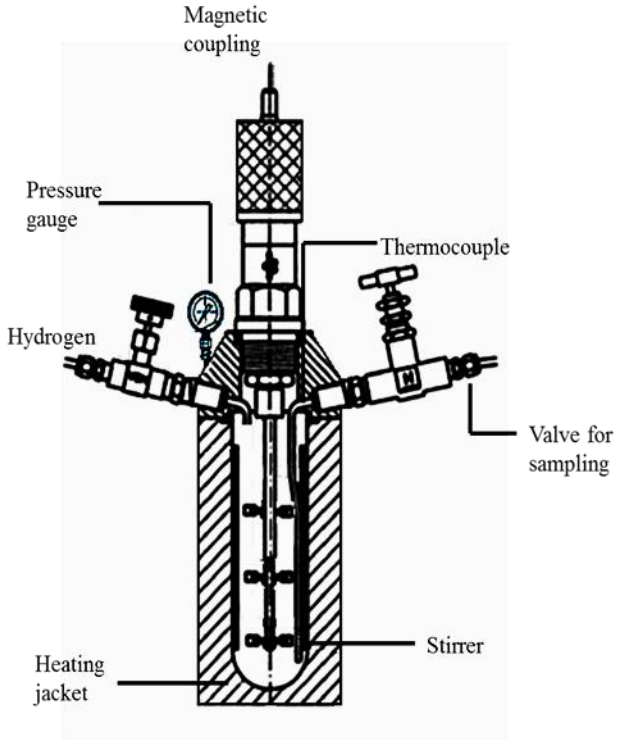

Figure 6-5. Schematic diagram of the batch hydrogenation reactor.

First, 5 L of distilled ketones and 100 L of Raney nickel catalyst were charged to the reactor. The reactor head was put in place and tightened. Excess air inside the reactor was purged with hydrogen. Hydrogen was added until the reactor pressure reached 6900 kPa (abs). The stirrer rotated at 750 rpm. The heating jackets increased the reaction temperature to 155 °C. During heating, fresh hydrogen was added to maintain the reactor pressure at 6900 kPa (abs). After the temperature stabilized to 155 °C, fresh hydrogen was added until the reactor pressure was 8600 kPa (abs). The stabilization time was 1 h, and the reaction was completed after 24 h. All the products were collected and analyzed in a gas chromatograph-mass spectrograph (GC-MS, HP Model G1800C). The alcohol

product was collected and centrifuged to separate the catalyst from the liquid. The used catalyst was placed back into the reactor and used for the next batch. Finally, 100 mL of fresh catalyst was added and the procedure repeated.

Other catalysts besides Raney nickel were tested. For example, copper chromite produced good conversions with reagent-grade ketones with a distribution similar to distilled ketones; however, it deactivated quickly with the distilled ketones obtained from the process. Therefore, an impurity must have deactivated the catalyst.

6.2.7 Analytical methods

The concentration of carboxylic acids in the fermentation broth was analyzed by gas chromatography (GC). To prepare the GC sample, the broth was first centrifuged and then the clean broth was mixed with equal parts of an internal standard (4-methyl-*n*-valeric acid) and 3-M H_3PO_4. The analysis was performed by a Hewlett Packard 5890 GC (Palo Alto, CA) equipped with an FID detector and a Hewlett Packard 7673A autosampler. The column was a 30-m fused-silica capillary column with a 0.32-mm ID 1.0-μm film thickness (Model DB-FFAP Agilent Technologies). The column pressure was 183–197 kPa. A temperature control program heated the GC column from 50 to 240^{o} C at a ramp rate of 20^{o} C/min and held at the upper temperature for 10 min. The carrier gas was helium at a flow rate of 2 mL/min. The analytical procedure converted all the salts to their corresponding acids; therefore, concentrations were reported as g carboxylic acid/L.

The distribution of acids in dry carboxylate salts was also determined by GC. A known amount of dry salt (1.0 – 1.5 g) was dissolved 250 mL dechlorinated water and

then this aqueous solution was processed similar to fermentation broth, as mentioned above.

For the biosolids and liquids, two methods were used to estimate carbon, hydrogen, nitrogen, sulfur (CHNS), and minerals. Various liquid and digested solid samples from the pilot plant fermentors (e.g., fermentation feedstock such as shredded office paper, chicken manure) were analyzed by the Soil, Water, and Forage Testing laboratory located in the Department of Soil and Crop Sciences of Texas A&M University. Analytical procedures and references are available in their website (*http://soiltesting.tamu.edu/webpages/swftlmethods1209.html*). For Method A, the total N and organic carbon were determined by combusting solid samples. The minerals (B, Ca, Cu, Fe, K, Mg, Mn, Na, P, S, and Zn) were determined by Inductively Coupled Plasma (ICP) analysis of HNO_3 digest. For liquid samples, the samples were digested using a H_2SO_4 (modified Kjeldahl). Total N was determined spectrophotometrically and minerals were determined by ICP.

For Method B, a Vario Micro Elemental Analyzer (Elementar Analysen system GmbH; Germany) equipped with a thermal conductivity detector (TCD) was used to determine CHNS in the carboxylate salts. In this analysis, C, H, N, and S combust with oxygen to form gaseous products CO_2, H_2O, N_2, NO_x, SO_2, and SO_3. The helium carrier gas transferred the gaseous combustion products into a reduction tube, where the following processes occurred: nitrogen oxides NO_x were completely reduced to N_2 when contacting copper, SO_3 was reduced to SO_2, and volatile halogens were bound to silver wool. Then, the total N_2, SO_2, CO_2, and H_2O in the sample was analyzed by TCD.

Sulfanilic acid was used for calibration. This is known as 2mgChem80s method, where 2mg indicates the sample size.

A GC-MS (HP Model G1800C) analyzed liquid ketones and alcohols. The compounds were described by carbon number (C3–C12) and types of products.

6.3 Results

6.3.1 Fermentation

After a batch period of 25 to 30 days, about 50 to 60% shredded office paper was digested with a maximum total acid concentration of 27.61 ± 1.34 g/L (Figure 6-6). However, under fed-batch operation, acid production could be maximized if the cycle time was reduced to 7–10 days. From the four fermentors, every 7–10 days about 6820–8330 L broth was harvested with an average total acid concentration of 12.5 g/L (Figure 6-6). In the fed-batch mode, the average digestion of volatile solids was 25–30 wt%. Figure 6-6 shows a typical concentration distribution of carboxylic acids in raw fermentation broth. A total of 126,500 L of raw broth was produced to obtain the required amount of mixed carboxylate salts for the project.

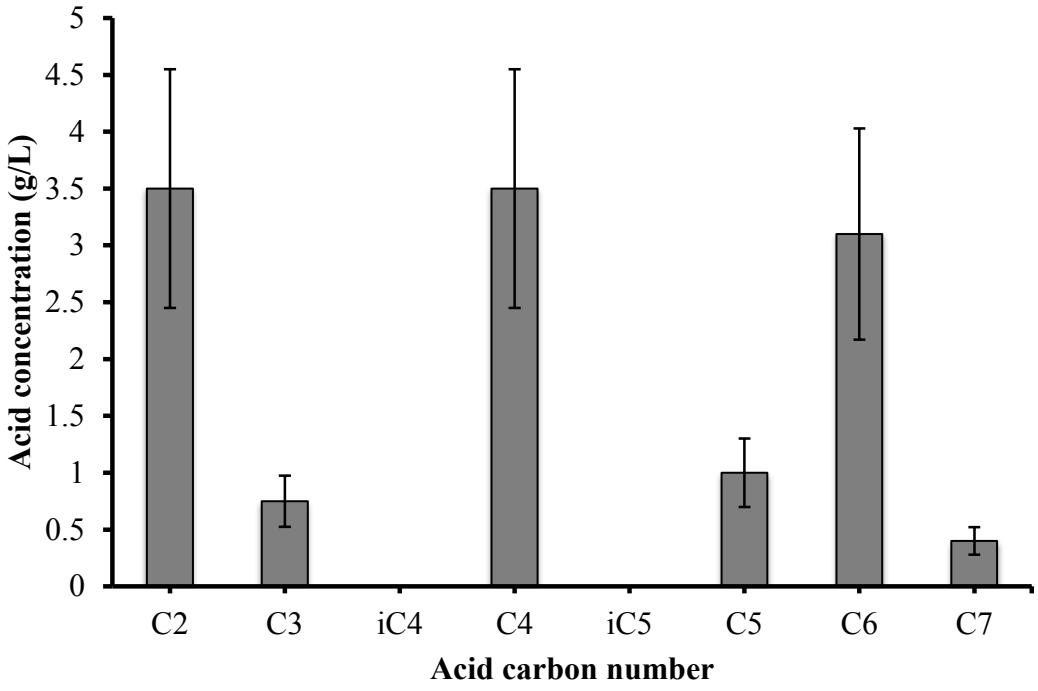

Figure 6-6. Distribution of mixed carboxylic acids in raw broth harvested from fermentor operated in fed-batch mode. (Error bars are ± 2σ.)

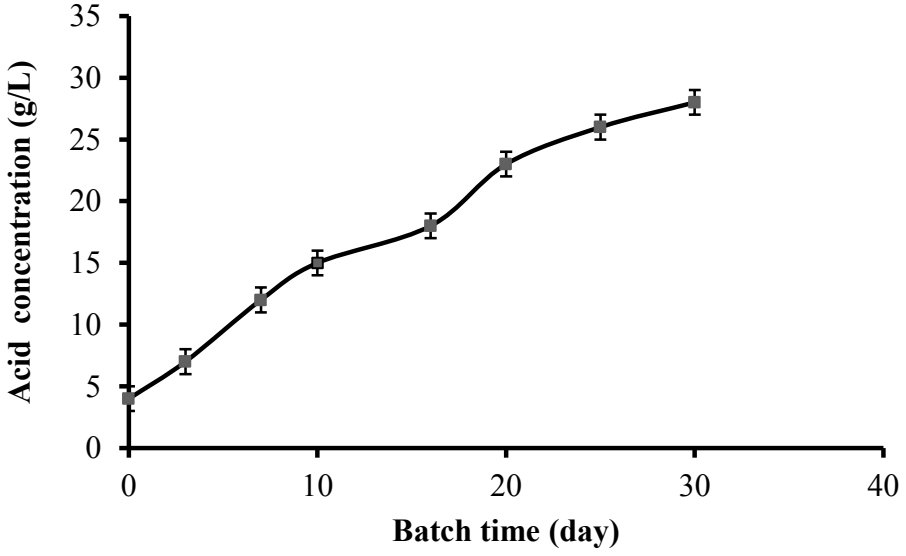

Figure 6-7. Total mixed carboxylic acids concentration in batch fermentation. (Error bars are ± 2 σ.)

6.3.2 Descumming

Even if the descummed broth were not centrifuged, most of the solids would settle by gravity and the liquid supernatant could be used for dewatering. However, these gravity-settled supernatant broths still had significant amounts of fine suspended particles, microorganism, and soluble proteins. When such broth was evaporated to prepare precipitated salts, about 15–25 vol% of the broth turned into a black tarry liquid, so it became extremely difficult to recover salts from such liquors. Also, the salts obtained from uncentrifuged broth had significant amounts of nitrogen, which poisons downstream catalysts. Figure 6-8 shows a typical carboxylic acid composition of this black mother liquor. If it were discarded, about 20–25 wt% of total salt (mostly C2–C4 salts) would be lost.

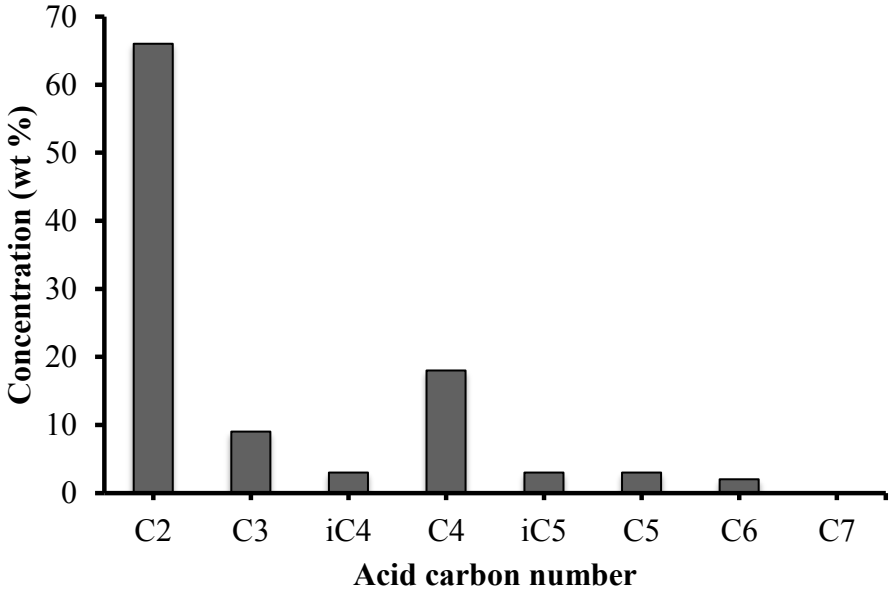

Figure 6-8. Distribution of carboxylic acids in black mother liquor.

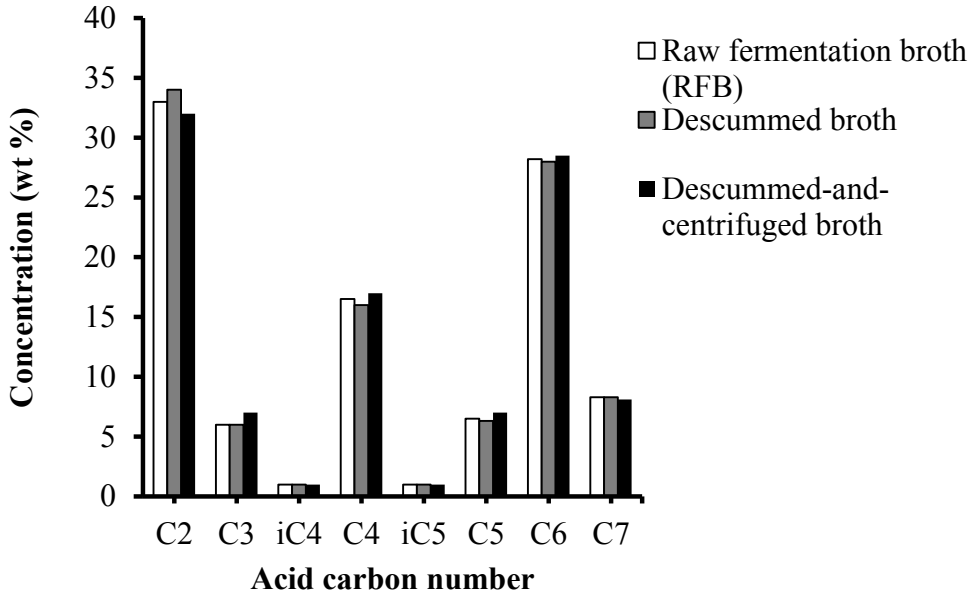

Figure 6-9. Effect of descumming and centrifuging on the distribution of carboxylic acids.

These problems were overcome by centrifuging, which purified the lime-CO_2 treated RFB. These steps had almost no effect on the acid distribution and their concentrations; the concentration remained almost the same as in the original RFB. Figure 6-9 shows the carboxylic acid distribution for RFB, descummed RFB, and descummed-and-centrifuged RFB.

6.3.3 Dewatering and crystallization

In this project, a total of about 1582 kg of dry carboxylate salts were produced in the pilot plant by dewatering lime-treated centrifuged broth in 16 batches. The salts were passed to the ketonization unit. Figure 6-10 shows the typical distribution of acids in the dry mixed carboxylate salts used in the ketonization process. In mixed acid salts, the

average weight ratio of low-molecular-weight acids mostly (C2–C3 acids) to high-molecular-weight acids (C4–C7) was 1:1.

Elemental composition (CHNS) in salts — As described previously, elemental analysis of mixed carboxylic salts was done using Methods A and B. Both methods presented similar data for C, H, N, and S within an acceptable error range (Figure 6-11a-b). Figure 6-11b shows that in the salts, both N and S were in ppm levels. Figs. 6-11c to 6-11e show the elemental composition of C, H, alkali metals, and minerals in the salts, as estimated by Method B.

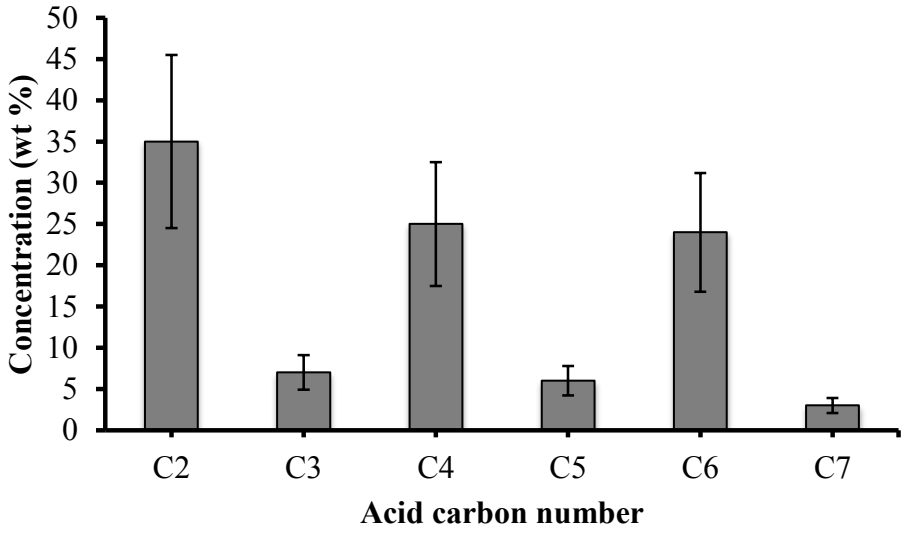

Figure 6-10. Distribution of carboxylic acids in the descummed dry salts. (Error bars are ± 2σ.)

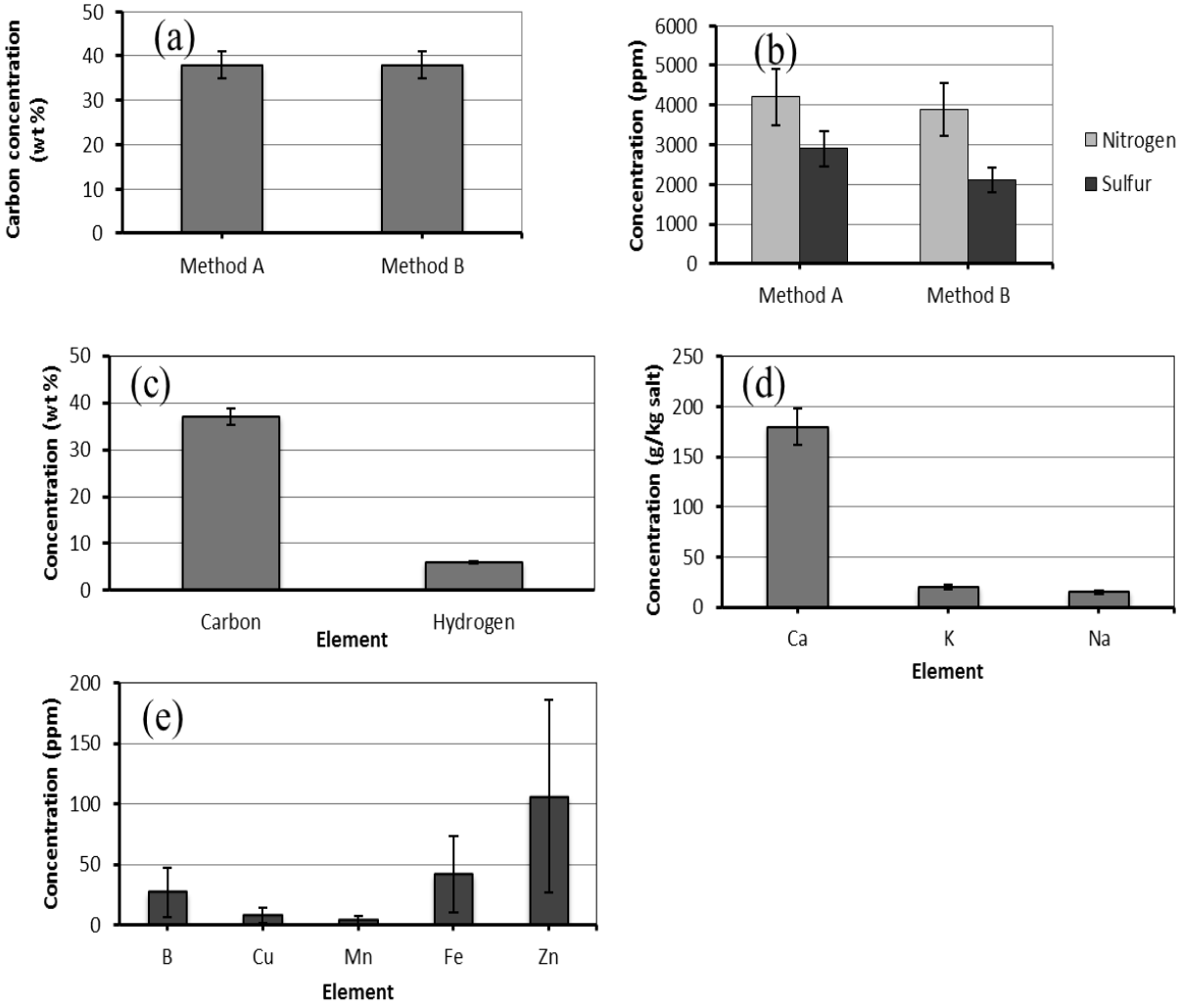

Figure 6-11. CHNS and mineral concentration of carboxylic salts (a) carbon concentration, (b) nitrogen and sulfur concentration, (c) carbon hydrogen concentration, (d) alkali metal, (e) mineral concentration. (Error bars are ± 2σ.)

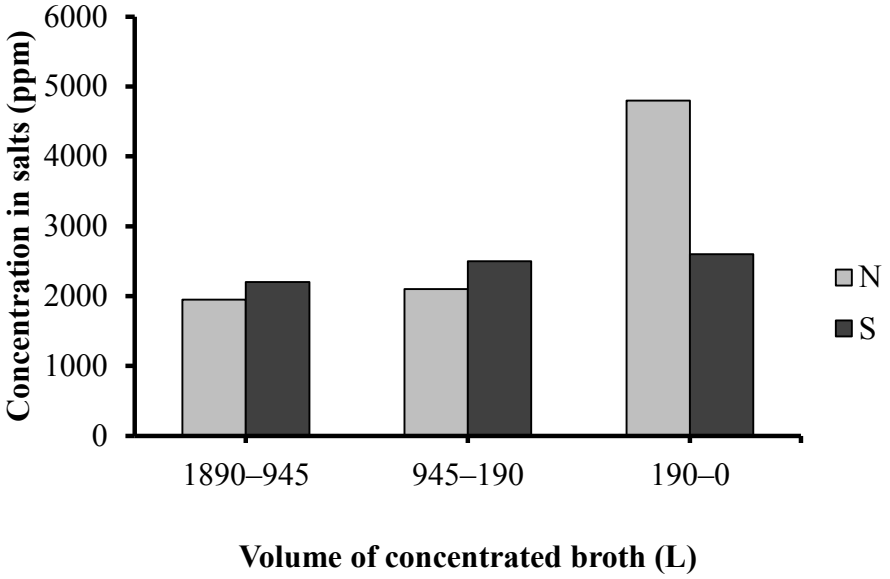

Figure 6-12. Distribution of nitrogen and sulfur in the carboxylate salts obtained from various cuts of broth during dewatering and crystallization.

Figure 6-11b shows that 0.5 wt% nitrogen was found in the dry carboxylate salts. Unfortunately, nitrogen is an unwanted impurity that poisons the catalyst used to produce hydrocarbons (jet fuel and gasoline) from alcohols. During the dewatering and crystallization steps, analysis of nitrogen and sulfur was performed. Figure 6-12 shows that most of the nitrogen was present in the salts in the cut ranging from 190–0 L, which was the last to be obtained in the dewatering process.

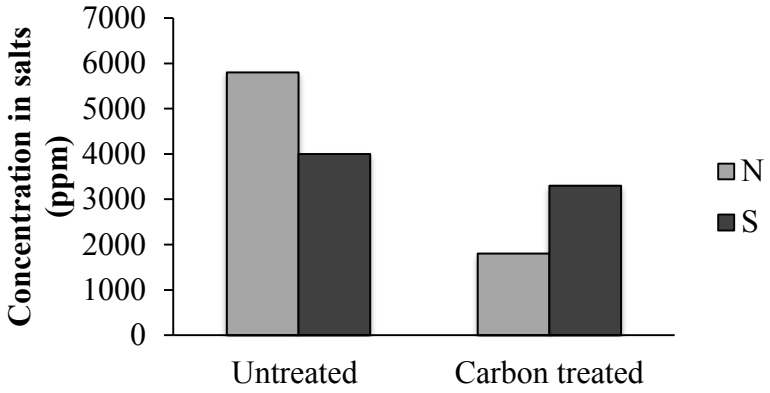

Figure 6-13 Effect of activated carbon treatment on the removal of nitrogen and sulfur from carboxylate salts.

In a preliminary test, activated carbon adsorption was explored as a means to remove N and S from salts. The salts from the 190–0 L cut were dissolved in water and the solution was passed through an activated carbon bed at ambient temperature. The salts obtained from the purified liquid were completely white in color; the nitrogen content in the salts reduced from 5740 ppm to 1790 ppm (Figure 6-13). Also, the sulfur content reduced from 4000 ppm to 3300 ppm. This indicates that purifying mixed carboxylate salts with activated carbon can reduce nitrogen and sulfur.

6.3.4 Ketonization

After performing a total of 396 batch ketonization runs, it was observed that a temperature of 420 °C gave the best yield (0.37 L ketones/kg salts). Sweep gas was found to be an effective method for removing ketones from the reactor. Despite the use of the sweep gas, the crude ketones were still black upon collection, and thus needed distillation.The largest factor influencing the yield of ketones from salts was the salt

composition. Most of the variations observed in the crude ketone yield appear to be linked to the mixing ratio of high- and low-molecular-weight salt. Ketone yields were best when they were mixed in a 1:1 ratio.

Table 6-3 shows the average acid distribution in the salts sent to the ketonization reactor. The distributions were taken from the average mass concentration presented in Figure 6-10, and were transformed to mole fraction using the molecular weight of the salts. The carboxylate salts produced not only ketones, but also calcium carbonate ($CaCO_3$). For example, the ketonization of calcium acetate follows:

$$Ca(CH_3COO)_2 \rightarrow (CH_3)_2CO + CaCO_3$$

If salts obtained from the dewatering process were converted completely, 50 wt% of the products were calcium carbonate and 50 wt% ketones (Table 6-3). The measured density of ketone mixture was 0.82 kg/L; therefore, the maximum yield that can be obtained in the ketonization process is 0.61 L ketones/kg salts (100% conversion). In practice, the actual yield was 0.37 L ketones/kg salts, or 61% of theoretical. By using a longer residence time, the yields could have been higher, but that would have reduced productivity. If proper reaction time is provided, the yields can be as high as 0.53 L ketones/kg salts (88% conversion).[5]

In the salts, one calcium is ionically bonded with two carboxylates, which can have the same or different carbon numbers ranging from C2 to C7. During the ketonization reaction, the salt composition determines the ketone composition. Assuming random pairing, Table 6-4 shows all the acid-pair combinations and the theoretical ketone product. Because the molar concentration of the salt mixture was

known, the probable molar concentration for each ketone product was found (Table 6-4). For example, the calcium acetate molar concentration in the salts was 46.6 mol% (Table 6-3); so the molar probability of obtaining acetone was 21.7 mol% (46.6×46.6/100). Finally, the mass concentration for the ketone mixture was calculated and compared to the experimental values.

Table 6- 3. Average acid distribution of the descummed dry salts**.**

Acid	Concentration (wt%)	Concentration (mol%)	Salt MW	Theoretical $CaCO_3$ (wt%)
C2	35	46.6	158	22.2
C3	7	7.6	186	3.8
C4	25	22.7	214	11.7
C5	6	4.7	242	2.5
C6	24	16.5	270	8.9
C7	3	1.8	298	1.0
Total	100	100.0		50.0

Table 6-4. Experimental and theoretical ketone product distribution.

Acid pair	Probability (mol%)	Ketone product	Theoretical concentration (wt%)	Experimental concentration (wt%)
C2 × C2	21.75	2-propanone	12.9	6.8
C2 × C3	7.05	2-butanone	5.2	3.3
C2 × C4	21.18	2-pentanone	18.6	9.5
C2 × C5	4.39	2-hexanone	4.5	5.2
C2 × C6	15.43	2-heptanone	18.0	21.4
C2 × C7	1.72	2-octanone	2.3	4.6
C3 × C3	0.57	3-pentanone	0.5	---
C3 × C4	3.44	3-hexanone	3.5	2.4
C3 × C5	0.71	3-heptanone	0.8	
C3 × C6	2.50	3-octanone	3.3	3.6
C3 × C7	0.28	3-nonanone	0.4	4.3
C4 × C4	5.16	4-heptanone	6.0	3.0
C4 × C5	2.14	4-octanone	2.8	2.0
C4 × C6	7.51	4-nonanone	10.9	12.4
C4 × C7	0.84	4-decanone	1.3	---
C5 × C5	0.22	5-nonanone	0.3	---
C5 × C6	1.56	5-decanone	2.5	7.0
C5 × C7	0.17	5-undecanone	0.3	0.0
C6 × C6	2.74	6-undecanone	4.8	11.1
C6 × C7	0.61	6-dodecanone	1.1	2.3
C7 × C7	0.03	7-tridecanone	0.1	0.4
Total	100.00		100.0	100.0

6.3.5 Hydrogenation

The objective for hydrogenation was to obtain 100% conversion of ketones to alcohols. First, the low- and high-molecular-weight ketones were hydrogenated separately. Unfortunately, the results were poor because the high-molecular-weight ketones could not be hydrogenated. However, if the low- and high-molecular-weight

were mixed, then the high molecular-weight ketones would hydrogenate. Apparently, the low-molecular-weight ketones acted as a solvent that helped dissolve hydrogen into the liquid phase.

More than 94 batch hydrogenations were performed in the batch reactor. The conversion reached nearly 100% with the following conditions: T = 155 °C, P = 8600 kPa (abs), and 100 mL Raney nickel catalyst for 5 L ketones. Lower hydrogen pressures did not favor high conversions. Hydrogenations are favored at low temperature; however, high temperatures were needed for better mixing. More catalyst always resulted in better conversion, but 100 mL of fresh catalyst was enough to get ~100% conversion after 24 h. If ~100% conversion was not obtained after 24 h, more reaction time did not get higher conversions.

To check conversion, 94 batches were analyzed in a GC-MS. The smaller batches were consolidated into 20-L batches of alcohols and were shipped to General Electric (San Jose, California) to be converted to hydrocarbons. The 20-L batches of alcohols were analyzed; Figure 14 shows the alcohol carbon distribution for 23 samples.

Figure 6.15 shows the carbon distribution for the alcohols (same as distilled ketones), raw ketones, and the theoretical ketones predicted assuming random pairing. The alcohols had lower concentrations of C12 and C13 than the raw ketones because the distillation could not recover all the high-molecular-weight ketones. The raw and theoretical ketones had similar concentrations and distribution. This shows that random pairing is a good, although imperfect, approximation.

Finally, Table 6-5 summarizes the results obtained for each process step. It illustrates the total amount produced and the yield for each step.

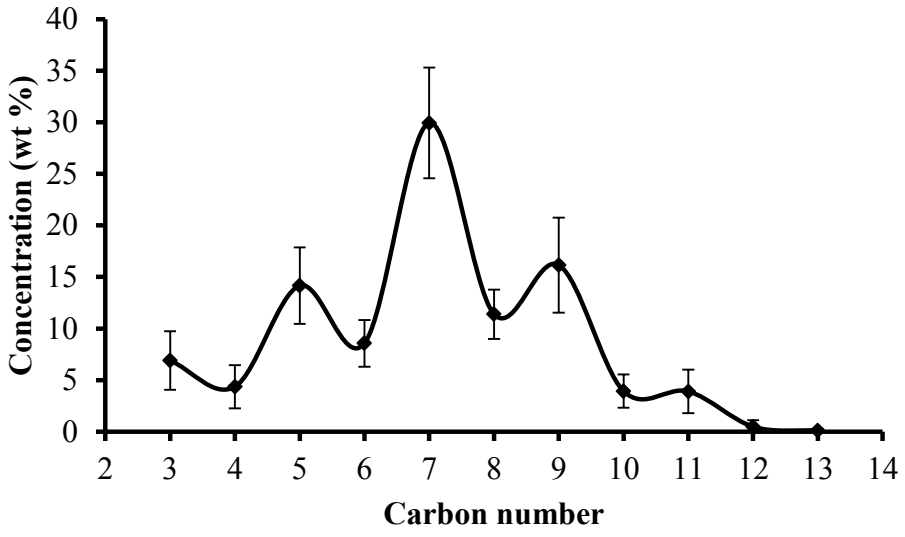

Figure 6-14. Distribution of alcohols obtained from the hydrogenation. (Error bars are ± 1σ.)

Table 6-5. Average parameters obtained in the MixAlco™ process.

Unit	Parameter	Value
Fermentation	Conversion	0.3 g digested/g volatile solids fed
	Concentration	12.5 g acids/L broth
	Reaction Time	7–10 days
	Total broth	126,500 L
Dewatering	Carboxylate recovery	0.013 kg salts/ L broth
	Total salts produced	1582 kg
Ketonization	Conversion	61%
	Yield	0.37 L ketones/kg salt
	Total raw ketones	587 L
Ketone Hydrogenation	Conversion Total hydrogen	100% 7.12 kg
	Total alcohols	470 L

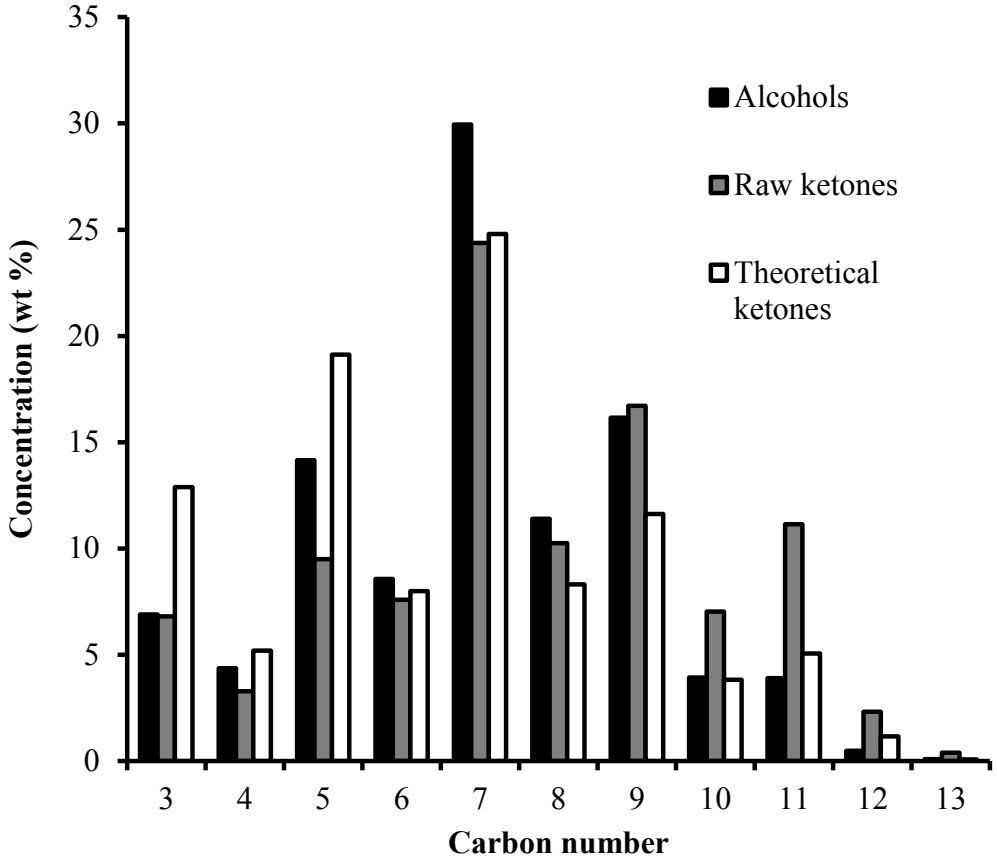

Figure 6-15. Carbon distribution of alcohols, raw ketones, and theoretical ketones.

6.4 Conclusions

The pilot-scale experimental tests performed at Texas A&M and Terrabon, Inc. produced ~100 L of jet fuel and ~100 L of gasoline by-product. The project goals of Phase 1 were met, so the project proceeded to Phase 2, which has the objective of producing 6000 L of jet fuel. The MixAlco™ process proved to be robust and shows the potential to be scaled up to a commercial plant. Waste office paper and chicken manure are promising feedstocks for the MixAlco™ process.

The objective of this project was to produce 100 L of jet fuel within time and resource constraints. As a consequence, each process step was not optimized; high production rates and good product quality were preferred rather than high yields or energy efficiency. To meet the required alcohol production, Figure 6.16 shows the mass balance for the MixAlco™ experimental work with 100 kg dry paper and manure as the mass basis. The liquid hydrocarbon yield was 5.5 kg/100 kg of dry paper and manure fed (8.1 kg/100 kg dry ash-free paper and manure). The yield can be improved tremendously by optimizing each step. Techno-economic studies that employ optimized process steps indicate the yield can be 22.3 kg/100 dry ash-free paper and manure.

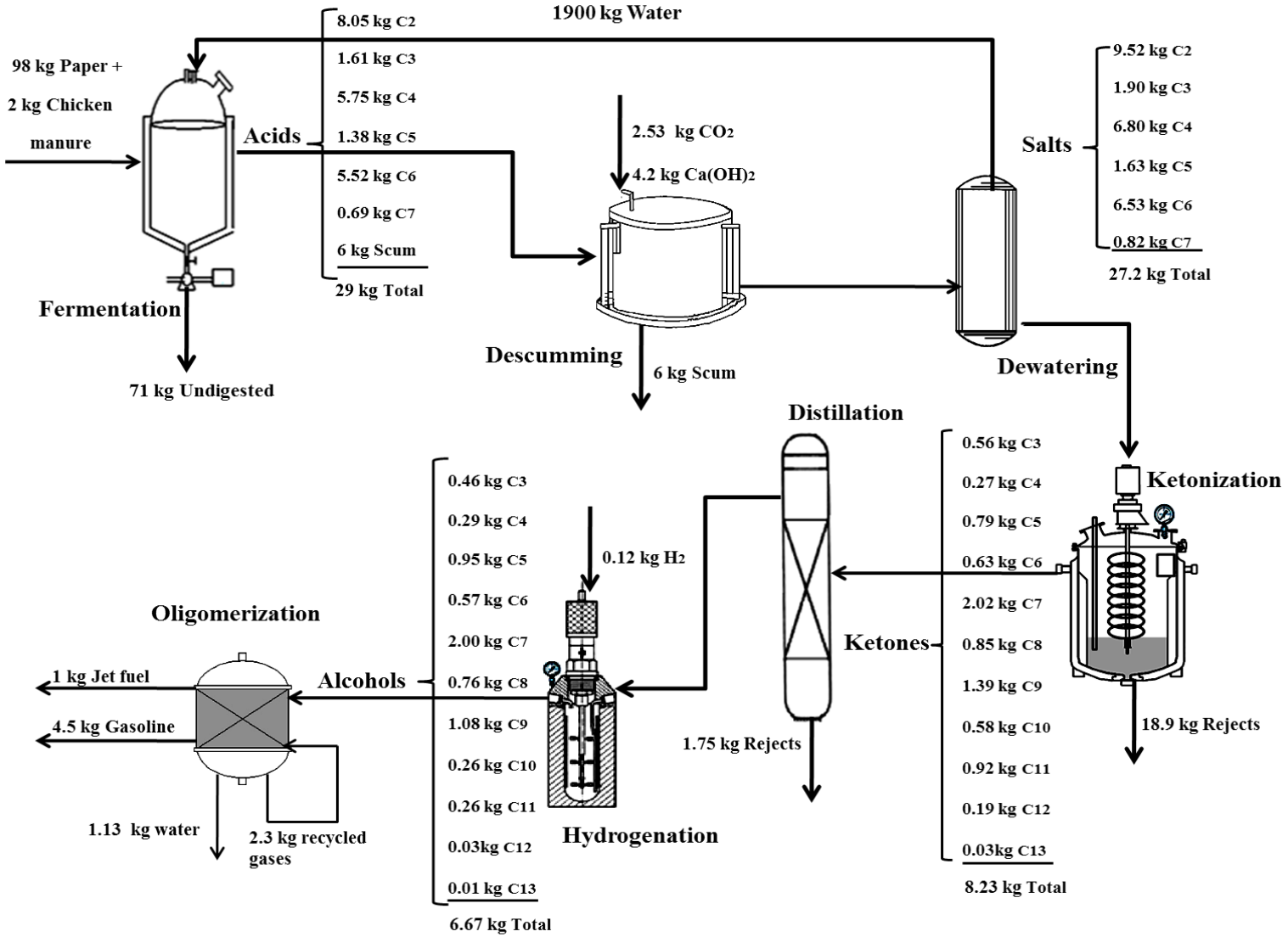

Figure 6-16. Mass balance for the MixAlco™ process with a basis of 100 kg of dry paper and manure fed. (*Note*: The high gasoline yields assume light gases are recycled in the oligomerization reactor.)

7. CATALYTIC KETONIZATION

The objectives of this section follow:

a) Describe the catalytic ketonization of acetic acid and mixed acids over zirconium oxide catalyst.

7.1 Introduction

The transformation of carboxylic acids to ketones has been known for more than 150 years (Glinski et al., 1858).[32] The process was the pyrolytic decomposition of metal carboxylates to ketones, mostly salts of calcium and thorium. Later, catalytic ketonization was a novel process introduced by Winkler et al. (1948). In the gas phase, acids contact a metal oxide catalyst to form ketones in a packed-bed reactor. Thorium, cerium, manganese, and zirconium oxide are usually used as catalysts.

Using zircounim oxide, acetic acid reacts to form ketones, water and carbon dioxide.

$$2RCOOH \rightarrow R-CO-R + H_2O + CO_2$$

For the transformation of acetic, propionic, and heptanoic acid to ketones, Glinski and Kijenski (1995) showed the effect of catalyst (metal oxides) and temperature (275–375 °C) on the reaction products.[32] Figure 7-1 shows the acids conversion to ketones using MnO_2 at LHSV = 2 mL/(g·h), and P = 101 kPa (abs). At all temperatures, acetic acid has a better yield than the other acids. Acetic and propionic acid conversion

is 100% at 375 °C. Overall, low-molecular-weight acids have higher conversion to ketones than high-molecular-weight acids.

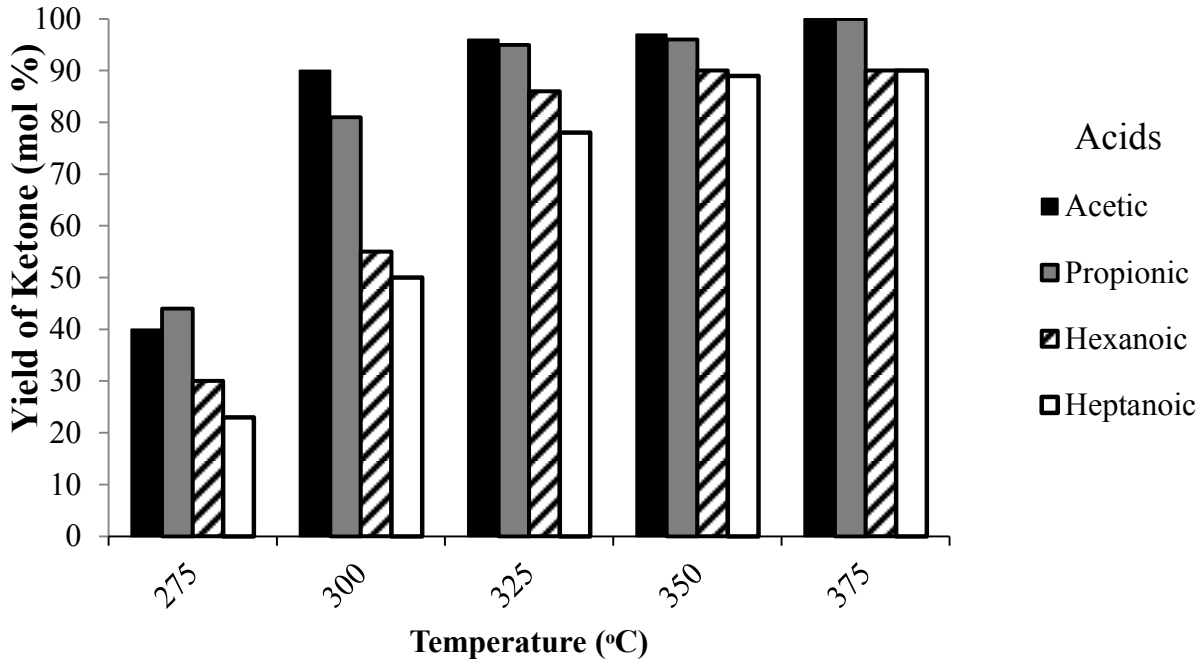

Figure 7-1. Acids conversion to ketones using MnO_2 at LHSV = 2 mL/(g·h) at P = 101 kPa (abs). (Figure adapted from Glinski and Kijenski, 1995.)[32]

7.2 Experimental

Acids were converted to ketones using zirconium oxide catalyst. For acetic acid, 30 experiments were performed with temperatures ranging from 300 to 500 °C. The WHSV studied were 2.4, 3.6, 4.8, 7.2, and 8.4 h^{-1}. The pressure was 101 kPa (abs). Table 7-1 shows all the experiments for the acetic acid reaction over zirconium oxide. For mixed acids, three experiments were performed at 400, 430, and 480 °C. Table 7-2

shows all the experiments for mixed-acid reaction over zirconium oxide. Mixed-acid carbon numbers ranged from C2 to C7.

For reagent-grade mixed acids, the temperature was changed every 8 hours but the flow was constant.

Table 7-1. Experiments for the acetic acid reaction over zirconium oxide.

	Catalyst: ZrO_2; Acetic Acid (90 vol%)					
	WHSV (h^{-1})					
T (°C)	2.4	3.6	4.8	6	7.2	8.4
300	ACC1	ACC2	ACC3	ACC4	ACC5	ACC6
350	ACC7	ACC8	ACC9	ACC10	ACC11	ACC12
400	ACC13	ACC14	ACC15	ACC16	ACC17	ACC18
450	ACC19	ACC20	ACC21	ACC22	ACC23	ACC24
500	ACC25	ACC26	ACC27	ACC28	ACC29	ACC30

Table 7-2. Experiments for mixed-acid reaction over zirconium oxide.

	WHSV (h^{-1})
T (°C)	1.92
400	MAC-1
430	MAC-2
480	MAC-3

7.2.1 Zirconium oxide

The catalyst zirconium oxide consists of a support, precursor of active phase, and the catalyst. The supports were TiO_2 (Aldrich, 99.7%) and silica fumed (Aldrich). The precursor of the active phase was $ZrO(NO_3)_2$ (Fluka, 98%). The catalyst was ZrO_2 (Aldrich, 99.7%) and the catalyst was prepared by impregnating the supports with aqueous solutions of precursors using the incipient wetness technique.[12] TiO_2 (20 wt%), silica fumed (20 wt%), and $ZrO(NO_3)_2$ (20 wt%) were mixed with water until it formed a cake. Later, the catalyst ZrO_2 (40 wt%) was added. Finally, the catalyst was calcined overnight at 500 °C.[12–13] The catalyst powder was pelletized using a hydraulic press (same process described for catalyst Beta (25)).

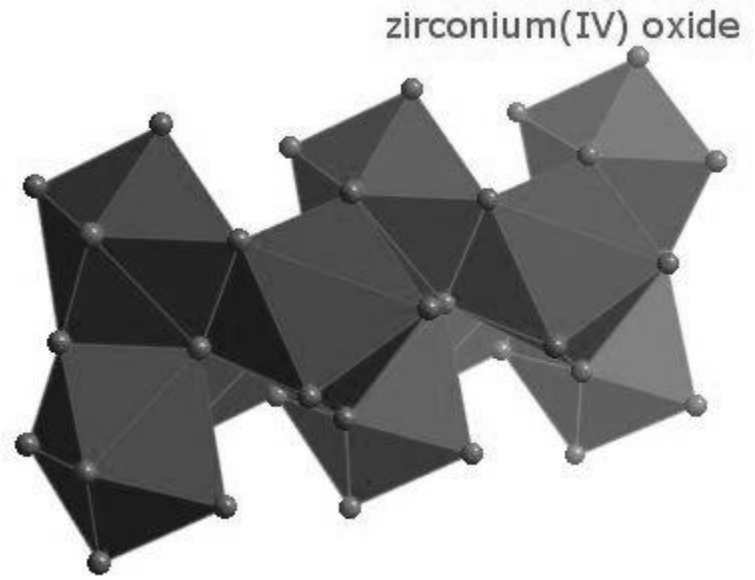

Figure 7-2. Pore structure of zirconium oxide. (Figure from www.webelements.com.)

7.2.2 Product analysis

The reaction products were analyzed using an Agilent 6890 series gas chromatograph, equipped with a flame ionization detector (FID) and a 7683 series injector. A 30-m fused-silica capillary column (J&WScientificModel#123-3232) was used. The column head pressure was maintained at 202 kPa (abs). After each sample injection, the gas chromatograph temperature program raised the temperature from 40 ^{o}C to 200 ^{o}C at 20 ^{o}C min^{-1} rate. The temperature was subsequently held at 200 ^{o}C for 2 min. Helium was used as a carrier gas, and the total run time per sample was 11 min.

7.2.3 Acetic acid

Reagent-grade acetic acid (99% pure) was obtained from Mallinckrodt Chemicals (Phillipsburg, NJ).

7.2.4 Mixed acids

Reagent-grade mixed acids, ranging from C2 to C7, were obtained from Mallinckrodt Chemicals (Phillipsburg, NJ). Figure 7-2 shows the concentration mixture of each reagent-grade acid. The concentration mixture was similar to the concentrations mixture made in the pilot-scale MixAlco™ process located at Texas A&M University (Figure 6-10).

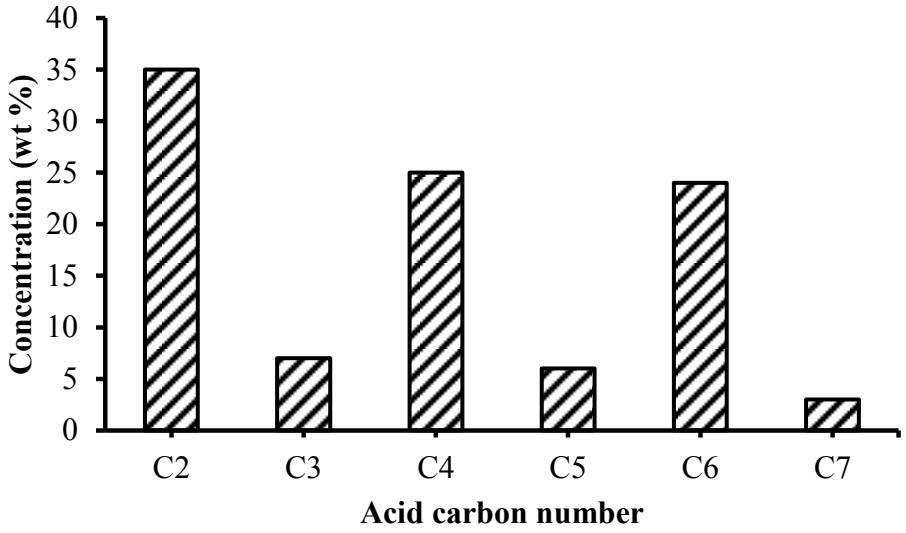

Figure 7-3. Distribution of carboxylic acids in the descummed dry salts. (Error bars are ± 2σ.)

7.3 Results

Figure 7-4 shows the effect of temperature and WHSV on acetic acid conversion to acetone. The conversion increases with temperature. The conversion is 2% at 300 °C; however, the conversion is 100% at 500 °C. For 450 °C, the conversion decreases from 100% (2.4 h^{-1}) to 61% (8.4 h^{-1}). For 400 °C, the conversion decreases from 31% (2.4 h^{-1}) to 2% (8.4 h^{-1}). For temperatures below 400 °C, the conversion is below 10% for all WHSV. The results are consistent with the literature.

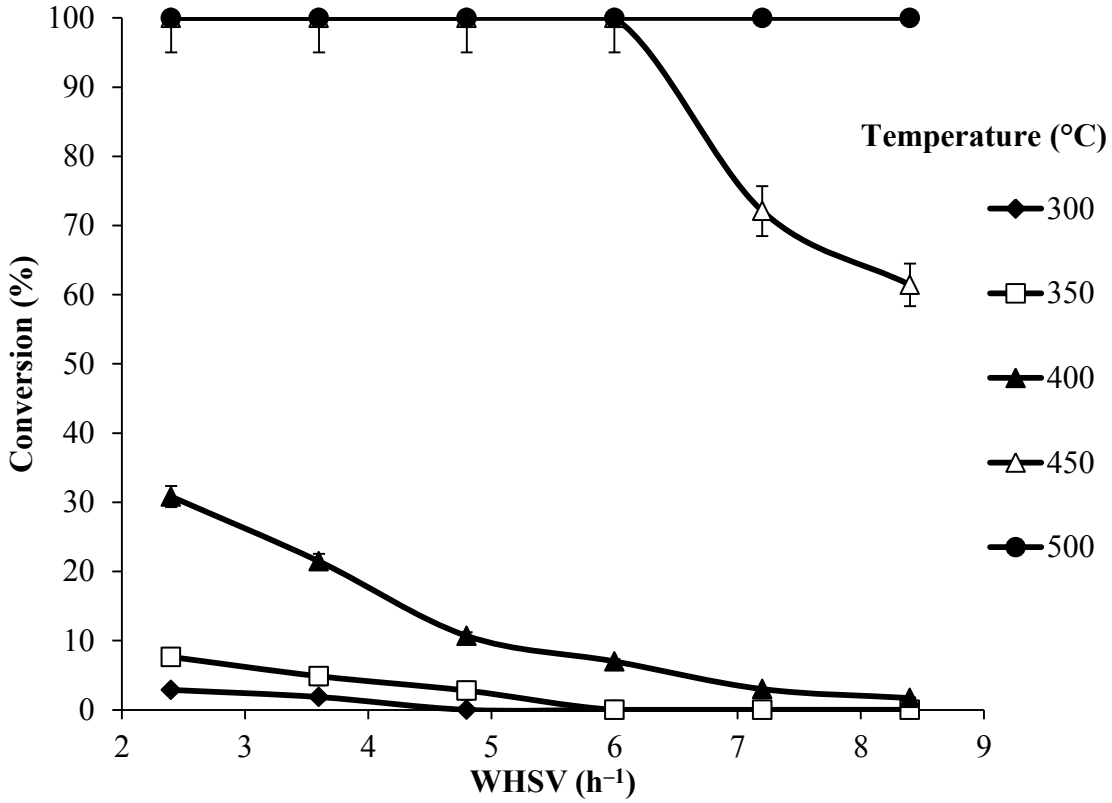

Figure 7-4. Acetic acid conversion using zirconium oxide at P = 101 kPa (abs).

Figure 7-5 shows the effect of temperature on the conversion of mixed acids to ketones. The conversion increases with temperature. The amount of ketones is 60% at 400 °C and t = 3 h; however, the amount of ketones is 82% at 430 °C and t = 9 h. For 400 °C, the amount of ketones increases from 60% (3 h) to 80% (8 h). For 400 °C, the amount of ketones is constant ~ 82%. For T = 480 °C, the amount of ketones is 90% for all times. The results are consistent with the literature. It is noteworthy that branched olefins are products, and they are less than ~3% at all temperatures. Branched olefins were not products of acetic acid catalytic ketonization.

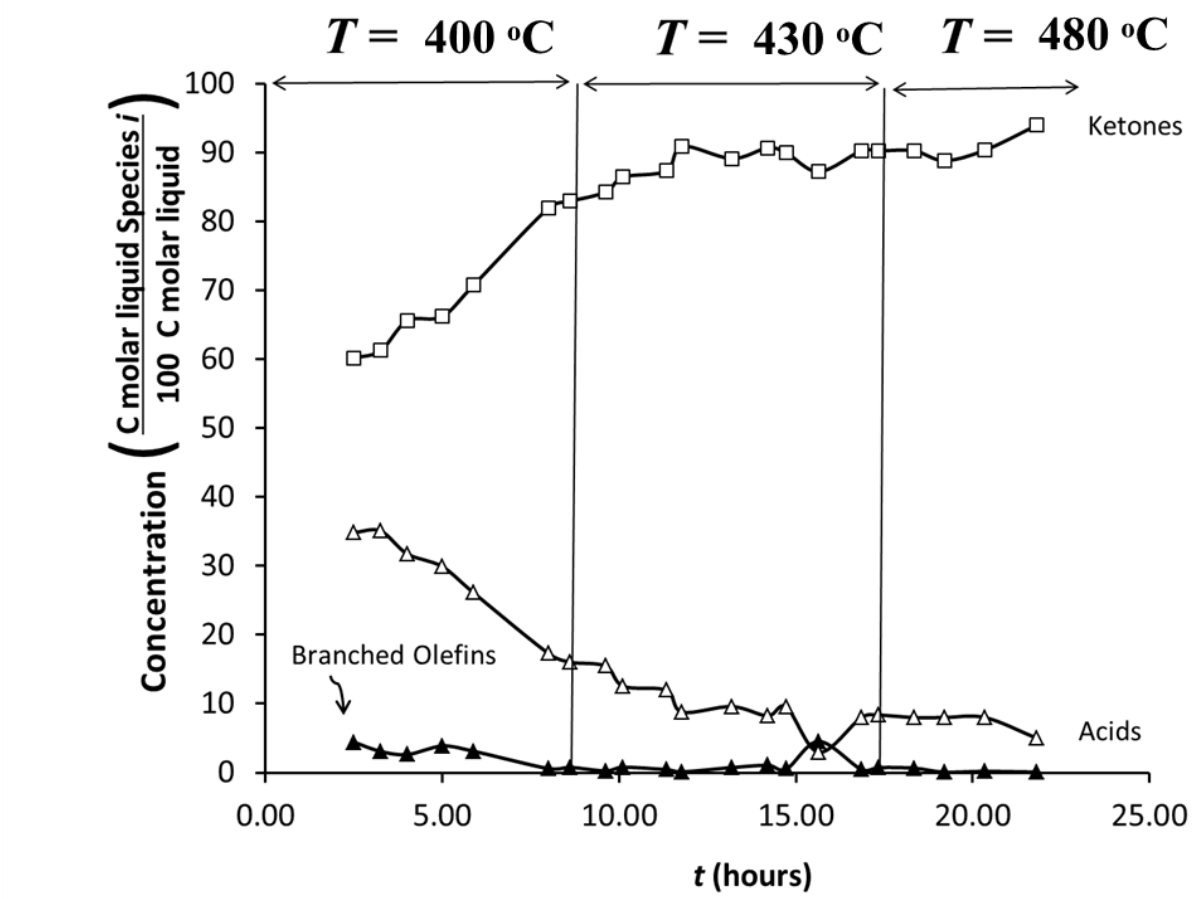

Figure 7-5. Conversion of mixed acids to ketones using zirconium oxide at P = 101 kPa (abs).

Figure 7-6 show the carbon concentration feed and liquid product distribution of the mixed acids reaction using zirconium oxide at WHSV = 1.92 h^{-1}, P = 101 kPa (abs), and T = 400°C. The mixed ketone product distribution is similar to the one obtained in the ketonization reaction in section 6. Branched olefins are less than 1% ranging from C4 to C12.

Figure 7-6 illustrates that low-molecular-weight acids (C2–C4) had better conversion than high-molecular-weight acids (C5–C7). For instance, the acetic acid feed concentration is 35%; however, unreacted acetic acid in the liquid product is 7%. Therefore, the conversion of acetone is 80%. As well, the hexanoic acid feed concentration is 25%; however, the unreacted acid concentration was about 12.5%. The conversion of hexanoic acid is about 50%.

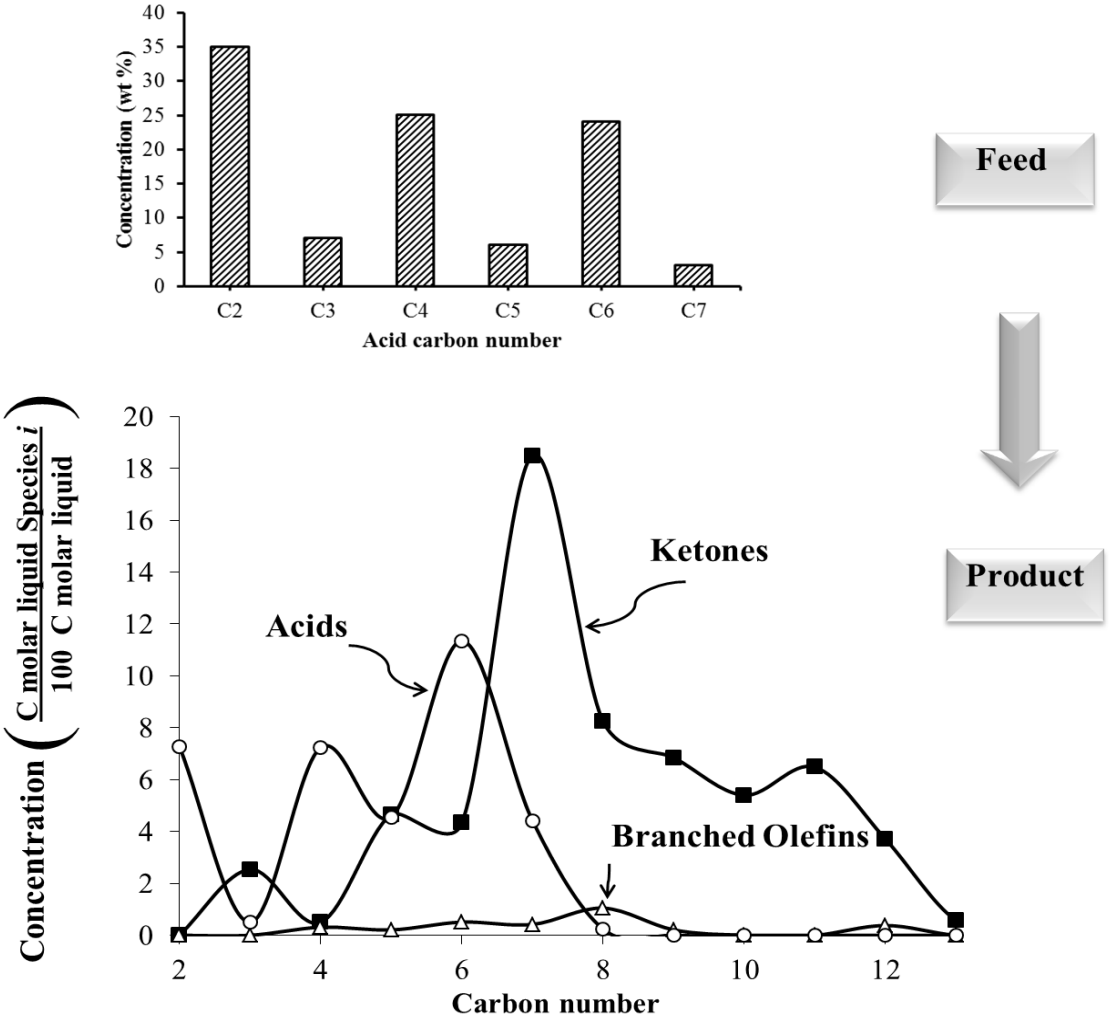

Figure 7-6. Liquid product distribution of mixed acids reacting using zirconium oxide at WHSV = 1.92 h^{-1}, P = 101 kPa (abs), and T = 400 °C.

7.4 Conclusions

Using zirconium oxide, acetic acid reached 100% conversion above 450 °C. Using zirconium oxide, the conversion of mixed acids over zirconium oxide conversion was 95% at T = 480 °C. As predicted, the ketone product distribution is similar to the results from the ketone reactor. The acid composition determines the ketone composition similar results to Table 6-4 where it shows all the acid-pair combinations and the theoretical ketone product. For instance, C7 is the most abundant ketone for the catalytic ketonization and the ketone reactor.

For acetic acid over zirconium oxide catalyst, temperatures higher than 450 °C are preferred to obtain 100% conversion. During T.O.S.= 8 h, the conversion was constant; therefore, the catalyst does not deactivate.

For mixed acids, low-molecular-weight acids have better conversion over zirconium oxide than high-molecular-weight ketones, which might result because small molecules can enter easily into the channels of zirconium catalyst. Also, branched olefins are side products. Also, the conversion was constant over T.O.S.; therefore, the catalyst does not deactivate.

8. OPTIMIZED INTEGRATED APPROACHES TO OBTAIN GASOLINE OR JET FUEL

The objectives of this section follow:

a) Describe different approaches to obtain gasoline or jet fuel

b) Utilize LINGO optimization software for different approaches to obtain gasoline or jet fuel

8.1 Introduction

During the Arab embargo during the 1970's, the methanol to olefins (MTO) process was conceived and developed by Mobil. Before the embargo, about 85% of New Zealand oil consumption was imported. In 1979, the government decided to implement the MTO process as a new route to provide the gasoline needs for the country. The process was to convert natural gas into methanol and then into gasoline. Gas-to-gasoline (GTG) was the process, and was selected because of the great offshores reserves of gas. The plant provided one third of the energy need for the country.

Figure 8-1 shows the block flow diagram of the New Zealand GTG plant.[33] First, methanol is vaporized in the preheater. Then, methanol is transformed into dimethyl ethyl ether in the DME reactor. Later, the product enters a second reactor where it contacts ZSM-5 and reacts. Meanwhile, the catalyst is regenerated constantly. The product mixture contains hydrocarbons and water. Next, the water is extracted by decantation in a separator. Hydrocarbons enter a distillation column where gases and gasoline are separated. The heavy gasoline cut contains durene, a substance with a high

melting point (79°C). Durene produced by the GTG process is more than that permitted by product gasoline specifications; therefore, the durene content is reduced in a HGT (heavy gasoline treatment) reactor. Finally, the light and heavy cuts are blended to the final gasoline product.

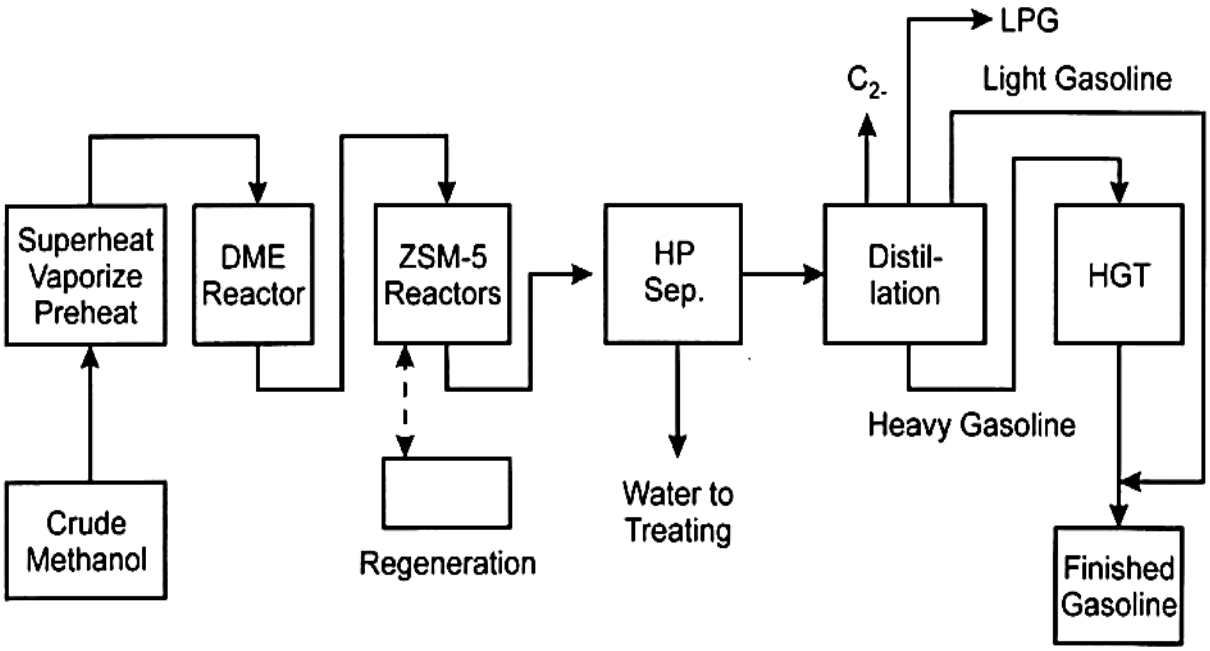

Figure 8-1. Simplified block flow diagram of the New Zealand GTG plant.[33]

8.2 Integrated approaches to obtain jet fuel and gasoline

Depending on the approaches employed in the oligomerization step, the final product in the MixAlco™ process can be gasoline or jet fuel. Several approaches are presented to minimize the waste in gaseous products and obtain the type of hydrocarbon needed. LINGO was used as an optimization tool.

8.2.1 Alcohol approaches

During the dewatering step in the MixAlco™ process, carboxylate salts are collected in two separately batches: (1) low molecular weight, and (2) high molecular weight salts. There are two approaches to transform the carboxylate salts into mixed alcohols. Figure 8-2 shows the one-pot approach to transform salts into alcohols. One-pot approach mixes the low- and high-molecular-weight salts exiting the dewatering process. The salts are converted into ketones and then to alcohols. Later, the alcohols enter a distillation column where they are separated into three alcohol cuts: (1) C3–C5, (2) C6–C7, and (3) C8–C13.

Another method is the two-pot approach, illustrated in Figure 8-3. This approach transforms salts into alcohols. This approach does not mix the salts exiting the dewatering process. The salts are converted to ketones separately. Then the ketones are mixed and transformed into alcohols. Later, the alcohols enter a distillation column where they are separated into three alcohol cuts. To achieve 100% conversion of ketones to alcohols, the low-molecular-weight ketones must be mixed with high-molecular-weight ketones; low-molecular-weight ketones act as a solvent to promote the reaction. However, this approach could potentially skip the distillation process if there is a new method to hydrogenate the high-molecular-weight ketones by themselves.

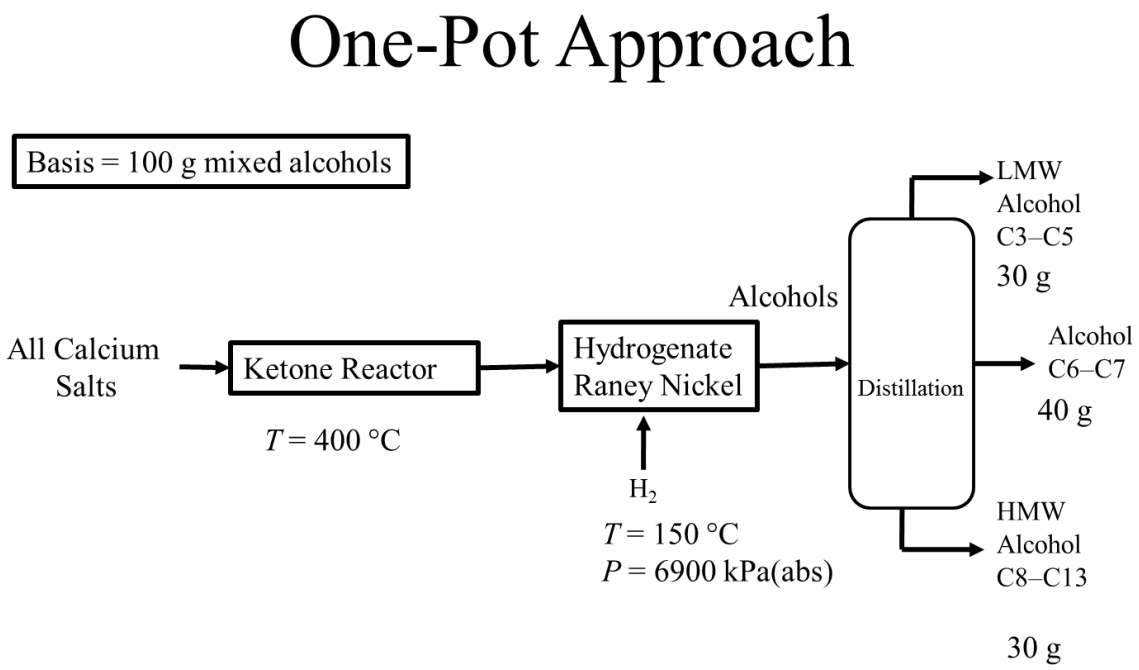

Figure 8-2. Carboxylic salts to mixed alcohols using one-pot approach.

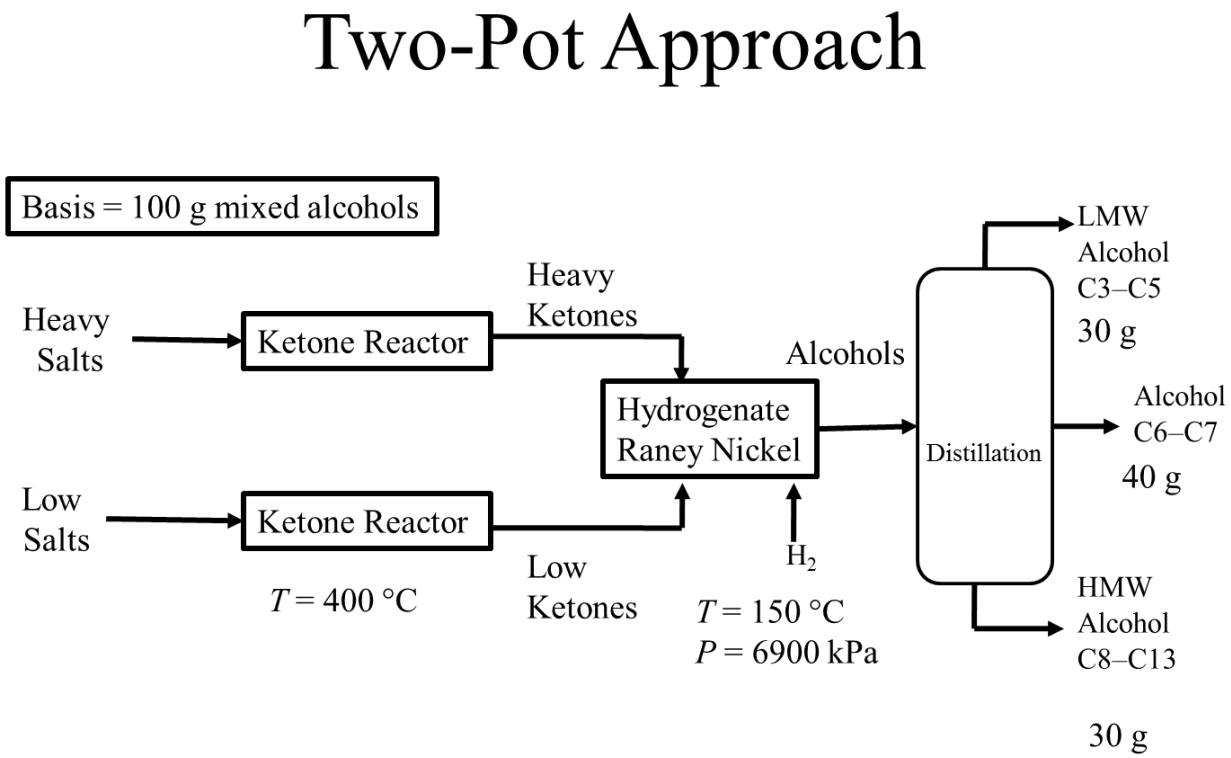

Figure 8-3. Carboxylic salts to mixed alcohols using two-pot approach.

8.2.2 Olefin conversion

After alcohols exit the distillation column into three cuts, they undergo different types of processes. The alcohols can be treated separately to reduce the waste gas products and improve the yield to gasoline and jet fuel. Figure 8-4 shows the transformation C3–C5 alcohols into gasoline. First, the alcohols are dehydrated and oligomerized in a packed-bed reactor. The products enter a condenser where the water is separated by decantation and the gases are recycled in a compressor. Optionally, the hydrocarbon can be distilled in case the aromatic content is high and separation is needed.

Figure 8-5 shows the transformation C6–C7 alcohols into jet fuel. First, the alcohols dehydrate to produce C6–C7 olefins and water. Next, the water is extracted in a condenser. Later, the olefins enter a batch reactor where dimerization occurs using Beta (25). The products are transferred into a distillation column where the unreacted C6 and C7 can be recycled into the batch reactor.

Figure 8-6 shows the transformation C8–C13 alcohols into jet fuel. First, the alcohols dehydrate to produce C8–C13 olefins and water. The water is separated in a condenser and the olefins are hydrogenated to produce paraffins.

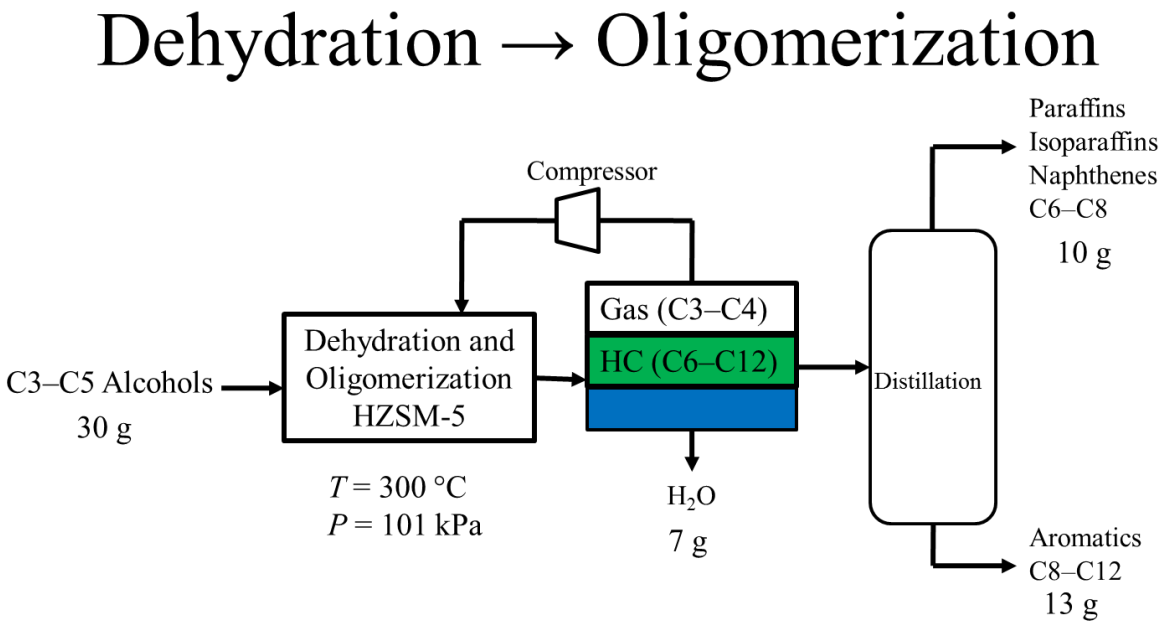

Figure 8-4. Low-molecular-weight alcohols are transformed to gasoline by dehydration followed by oligomerization.

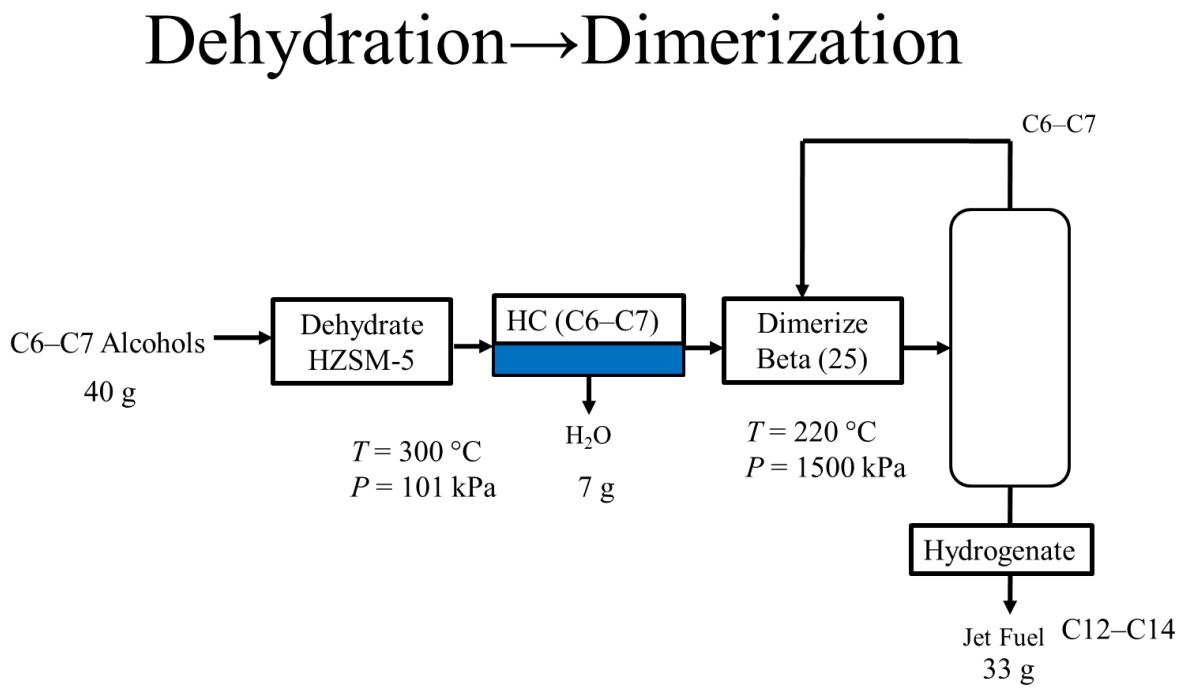

Figure 8-5. Medium-molecular-weight alcohols transform to jet fuel approach using dehydration followed by dimerization.

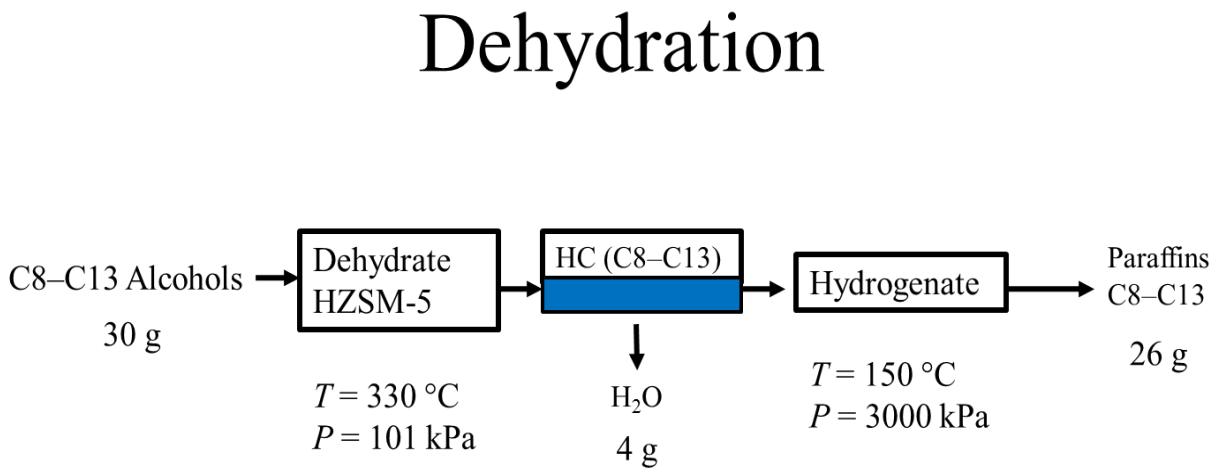

Figure 8-6. High-molecular-weight alcohols transformed to jet fuel using dehydration.

8.3 Simulation results

The results from the scale-up of the oligomerization reactor (Section 2) were used in the optimization software LINGO. Using the two product streams (A and B) from the Reactor Unit 2, the optimization approach is to find the optimum mass flow values of A and B to get a mixture similar to commercial gasoline.

Commercial regular gasoline from a Shell gas station was analyzed in a GC-MS (Appendix B). Table 8-1 shows the weight distribution of the commercial gasoline. After hydrogenation, branched olefins transform to isoparaffins; linear olefins transform to paraffins. Therefore, the names were changed to compare bio-gasoline with commercial gasoline. The bio-gasoline was not hydrogenated yet. These commercial gasoline concentrations will be the objective of the optimization approach.

After running the LINGO optimization software, the mass percentage for Product A needed was 10 wt%; whereas, the percentage for Product B was 90 wt%. These results are consistent with expectations, because Product B has a similar composition to commercial gasoline. Currently, the experimental conditions create 90% Product A and 10% Product B, which is the opposite of the optimal conditions. The results suggest more hydrocarbon must go to the next stage to obtain a mixture of A and B similar to commercial gasoline.

LINGO is a optimization software designed to make building and solving linear, nonlinear (convex & nonconvex/Global), quadratic, quadratically constrained, second order cone, stochastic, and integer optimization. LINGO is free software and can be downloaded at www.lindo.com.

Table 8-1 also shows the compositions between the bio-gasoline (mixture of Product A and B) with respect to commercial gasoline. The blended bio-gasoline is very similar to the commercial gasoline.

Dimerization and oligomerization were studied using a variety of conditions and showed its effectiveness. Depending on the steps and the conditions, the process can be manipulated to obtain a desired product. For instance, Figure 8-7 shows an integrated process to obtain high- molecular-weight hydrocarbons (jet fuel, kerosene, and diesel). Adding a compressor after the oligomerization step, also allows full conversion of the unreacted gases.

Table 8-1. Product distribution for Product A and B from Reactor Unit 2, commercial and bio-gasoline

Type	A (wt%)	B (wt%)	Commercial gasoline (wt%)	Bio-gasoline (wt%)
Linear Olefins	72	0	5.5	5.1
Branched Olefins	15.5	16.1	30.3	16.1
Aromatics	7	71.5	64	67.1
Naphthenes	3.3	0	0	3

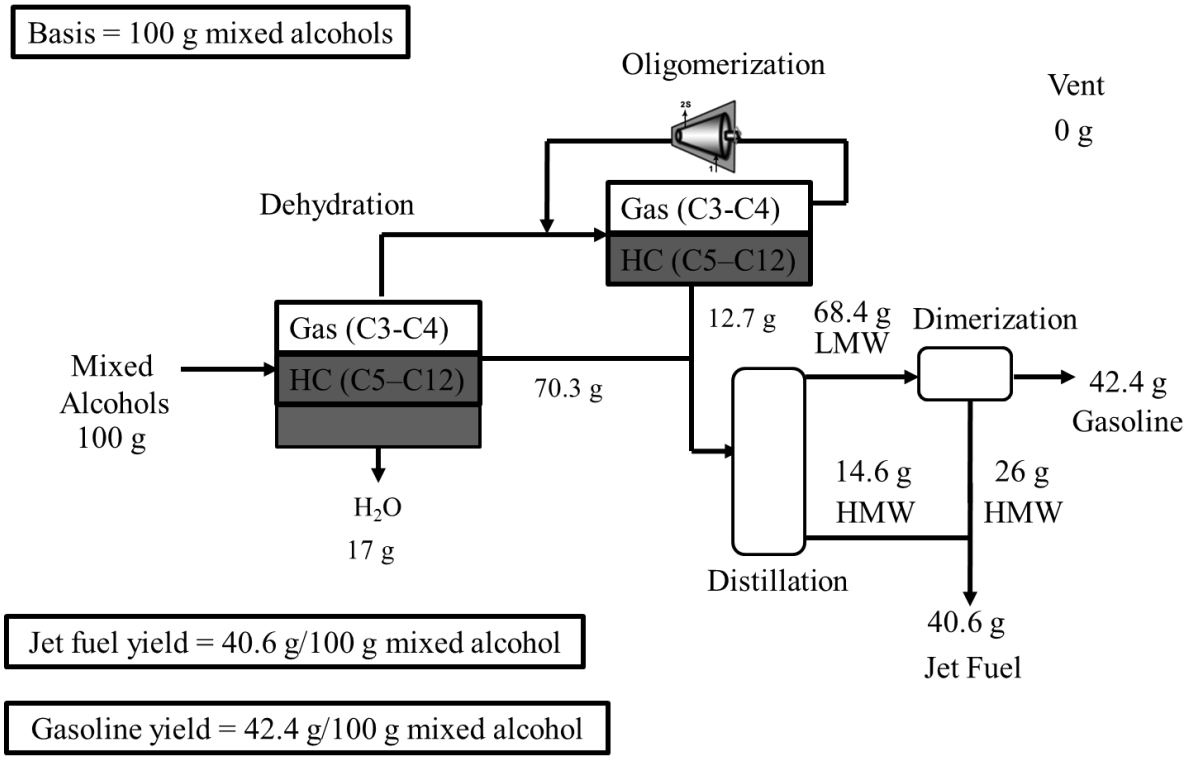

Figure 8-7. Flow diagram to produce high-molecular-weight hydrocarbons.

8.4 Conclusions

LINGO was an important tool to identify the amount of Product A and B needed to create a mixture similar to commercial gasoline. Commercial gasoline and bio-gasoline have similar concentration with a carbon average of 8. If the amount of Product A and B are not at the right ratio to produce a gasoline mixture similar to commercial gasoline, a valve modification solves the problem the system For example, Valve 2 (Figure 2-22) must be closed for longer times and purge only the water phase. Additionally, Product A can be collected and oligomerized using HSZM-5 in a second packed bed reactor.

9. CONCLUSIONS AND RECOMMENDATIONS

For the conversion of isopropanol to hydrocarbons using HZSM-5, to obtain a mixture similar to commercial gasoline or jet fuel, higher carbon number and less waste gas products, the following conditions are recommended: 300 °C < T < 370 °C and WHSV = 0.5–3.7 h^{-1} at atmospheric pressure; and 300 °C < T < 320 °C and WHSV = 1.9 h^{-1} at higher pressure. At these conditions, isopropanol undergoes only oligomerization.

For the conversion of mixed alcohols to hydrocarbons using HZSM-5, temperature determines the reaction type, product type, and carbon distribution. Mixed-alcohol dehydration to linear olefins occurs at 300 °C < T < 420 °C and WHSV = 0.5–11.5 h^{-1} at atmospheric pressure; and 300 °C < T < 370 °C and WHSV = 1.9–3.8 h^{-1} at higher pressure. At WHSV > 3.8 h^{-1} and high pressure, mixed alcohols have lower conversion. On the other hand, mixed alcohol can oligomerize at 420 °C < T < 510 °C and WHSV = 1.3 h^{-1} at atmospheric pressure; and 370 °C < T < 450 °C and WHSV = 1.9 h^{-1} at higher pressure.

For the conversion of acetone to hydrocarbons using HZSM-5, the temperature must be more than 400 °C to obtain 100% conversion. For the conversion of mixed ketones to hydrocarbons using HZSM-5, the highest conversion was 45% at T = 510 °C and WHSV = 1.9 h^{-1}. Higher temperatures do not increase conversion. The products are mainly aromatics. HZSM-5 rapidly deactivated during the ketone reaction.

For the conversion of acetic acid and mixed acids to ketones using zirconium oxide, the conditions to obtain 100% conversion are $T > 450$ °C and WHSV = 1.9 h^{-1}.

For the dimerization of medium-molecular-weight olefins using Beta (25), the following conditions obtain high dimer concentrations: $T = 220–270$ °C and $t = 100–160$ min. The maximum conversion achieved was 57% for 1-hexene.

The MixAlco™ process proved to be robust and shows potential to be scaled up to a commercial plant. It transformed successfully chicken manure to gasoline and jet fuel.

For the isopropanol, mixed alcohol, acetone and mixed ketone transformation to hydrocarbons, Figures 9-1 to 9-4 show the tree diagrams hydrocarbon product that result from different reaction conditions of *P*, WHSV and *T*. Low WHSV is less than 1.92 h^{-1} and high WHSV is more than 7.5 h^{-1}. These tree diagrams were derived from information presented in sections 2, 3, and 4.

For isopropanol, low temperatures and high pressures are preferred to obtain a high liquid yield, and high molecular weight hydrocarbon mixtures. For instance, at $T =$ 300 °C, low WHSV, and $P = 5000$ kPa (Figure 9-1), the liquid yield is 55 % and the hydrocarbon mixture is similar to jet fuel (C9 and C12 centered). On the other hand, to obtain a mixture similar to gasoline and high liquid yield, low temperatures at atmospheric pressure are desired. For instance, at $T = 300–370$ °C, low WHSV, and $P =$ 101 kPa (Figure 9-1), the liquid yield is 55 % and the hydrocarbon similar to commercial gasoline (C8-centered).

For mixed alcohol, low temperature and low WHSV at atmospheric pressure are preferred in order to obtain: (1) high liquid yield (2) C8-centered liquid and (3) 100 % conversion. For instance, at T = 300–370 °C and low WHSV at atmospheric pressure (Figure 9-2), the liquid yield is 80 % and centered on C8; however, the type of hydrocarbons obtained are linear olefins and commercial gasoline contains aromatics. Aromatics can be obtained from linear olefins oligomerization using second reactor using HZSM-5. As well, aromatics can be added from acetone or mixed ketone oligomerization products.

For the transformation of alcohols to hydrocarbons, the reaction conditions can be easily manipulated to produce gasoline or jet fuel. However, hydrogenation of ketones to obtain alcohols is expensive and adds an additional step. Transformation of ketones to hydrocarbons is worth trying.

For acetone, high temperatures and low WHSV are preferred to obtain a 100% conversion and not oxygenates in the liquid fraction. For instance, at T = 400 °C and low WHSV (Figure 9-3), the conversion is 100 % and the hydrocarbon mixture distribution is similar to gasoline (C8-centered); however, the liquid yield is low. To improve the liquid yield, gaseous products can be recycled using HZSM-5 catalyst.

For mixed ketones, high temperatures at low WHSV are desired. For instance, at T = 510–590 °C and WHSV = 1.3 h^{-1} (Figure 9-4), the conversion reached was 40%. The hydrocarbon mixture distribution is similar to gasoline (C8-centered). For acetone and mixed ketone oligomerization the most abundant hydrocarbon products are aromatics.

To obtain a gasoline rich in aromatics using the MixAlco process, mixed ketones can be used as feed. Low molecular weight ketones have 100% conversion to hydrocarbons using HZSM-5. During the fermentation, low molecular acids are produced at T = 55 °C. These acids are neutralized to their corresponding carboxylate salts, which are subsequently transformed into low molecular ketones. These low molecular ketones are converted to aromatics (C8-centered) using HZSM-5 in a packed bed reactor at T > 410 °C and WHSV = 1.9 h^{-1}.

One route to obtain jet fuel or kerosene is to hydrogenate these low molecular weight ketones into alcohols (hydrogenation of low molecular weight ketones is faster than high molecular weight ketones using Raney-Nickel catalyst). The most abundant alcohol is isopropanol. The alcohols are oligomerized in a packed-bed reactor at P = 5000 kPa and T = 300 °C using HZSM-5. The products are high molecular hydrocarbons ranging from C5 to C14 centered on C9 and C12.

Another route to obtain jet fuel using the MixAlco process is to use mixed alcohol as a feed. During the fermentation, low- and high-molecular-weight acids are produced at T = 40 °C. These acids are neutralized to their corresponding carboxylate salts, which are subsequently transformed into mixed ketones. These mixed ketones are hydrogenated to mixed alcohols. Then, mixed alcohols are dehydrated using HSZM-5. The gases are oligomerized in a second packed-bed reactor. Figure 8-7 shows in more detail this oligomerization step. Gasoline and jet fuel are the products of this process.

Future work includes simulation and kinetic studies. First, more complexes optimization approaches can be evaluated. LINGO can be used as optimization tool. For

instance, an economic evaluation of which process can be the optimal, taking into account energy and mass balances systems. For the isopropanol reaction, a kinetic study can be elaborated with the data collected. All the alcohols studied first dehydrate and then oligomerize; therefore, the simulation results are similar for isopropanol and mixed alcohol. The kinetic study will predict the type of products, given the reaction conditions.

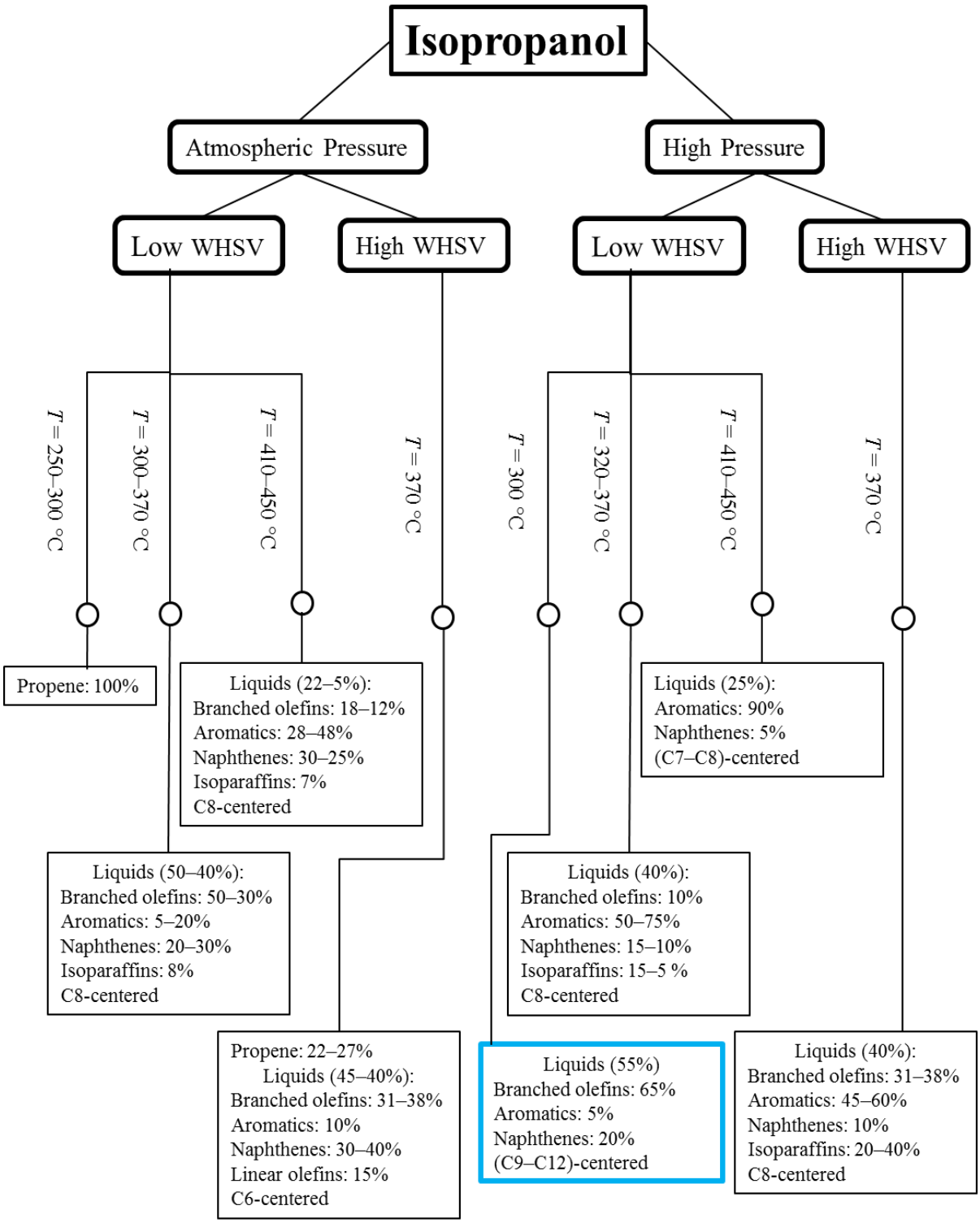

Figure 9-1. Tree diagram of isopropanol transformation to hydrocarbons at different reaction conditions of *P*, WHSV, and *T*.

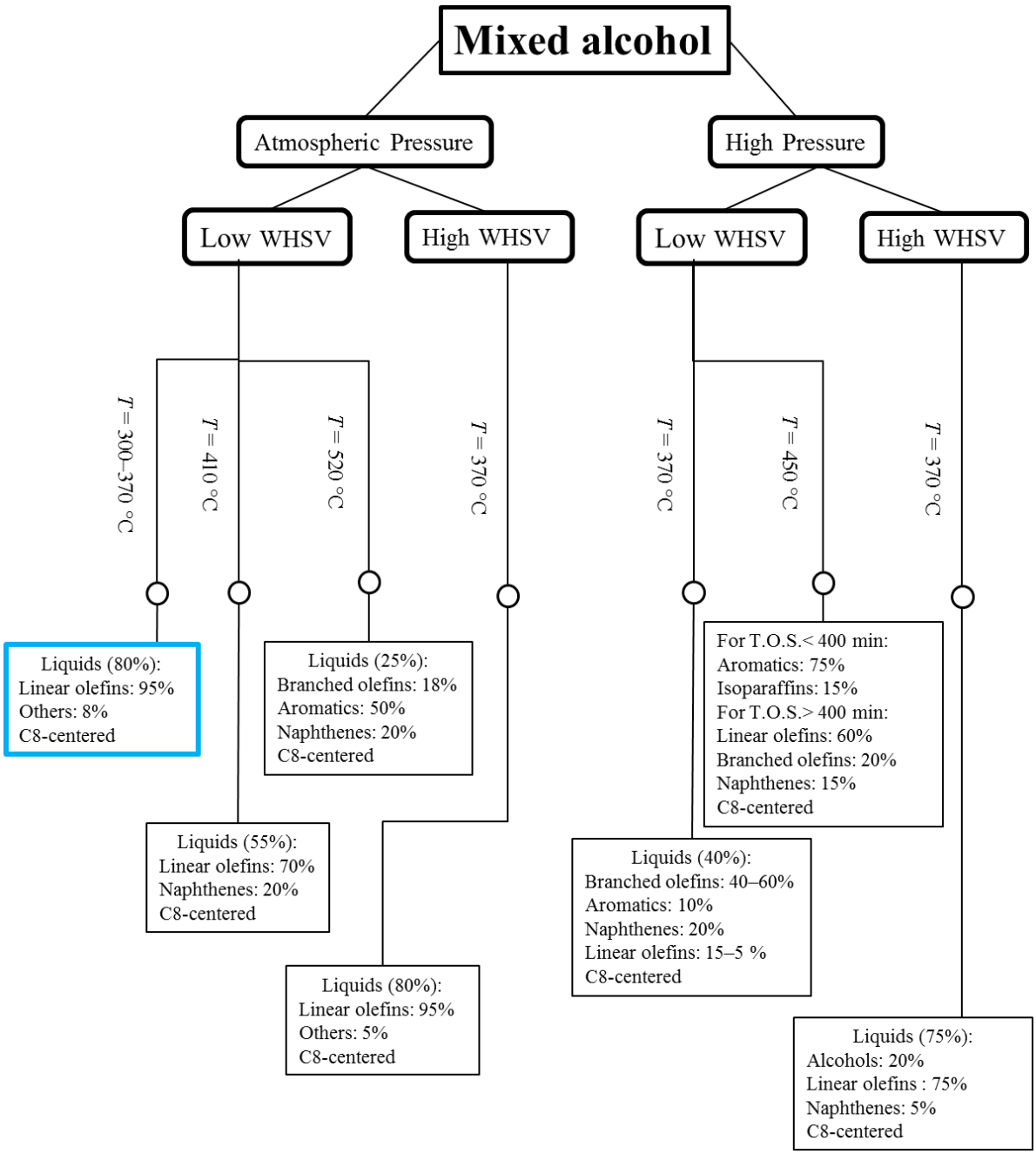

Figure 9-2. Tree diagram of mixed alcohol transformation to hydrocarbons at different reaction conditions of *P*, WHSV, and *T*.

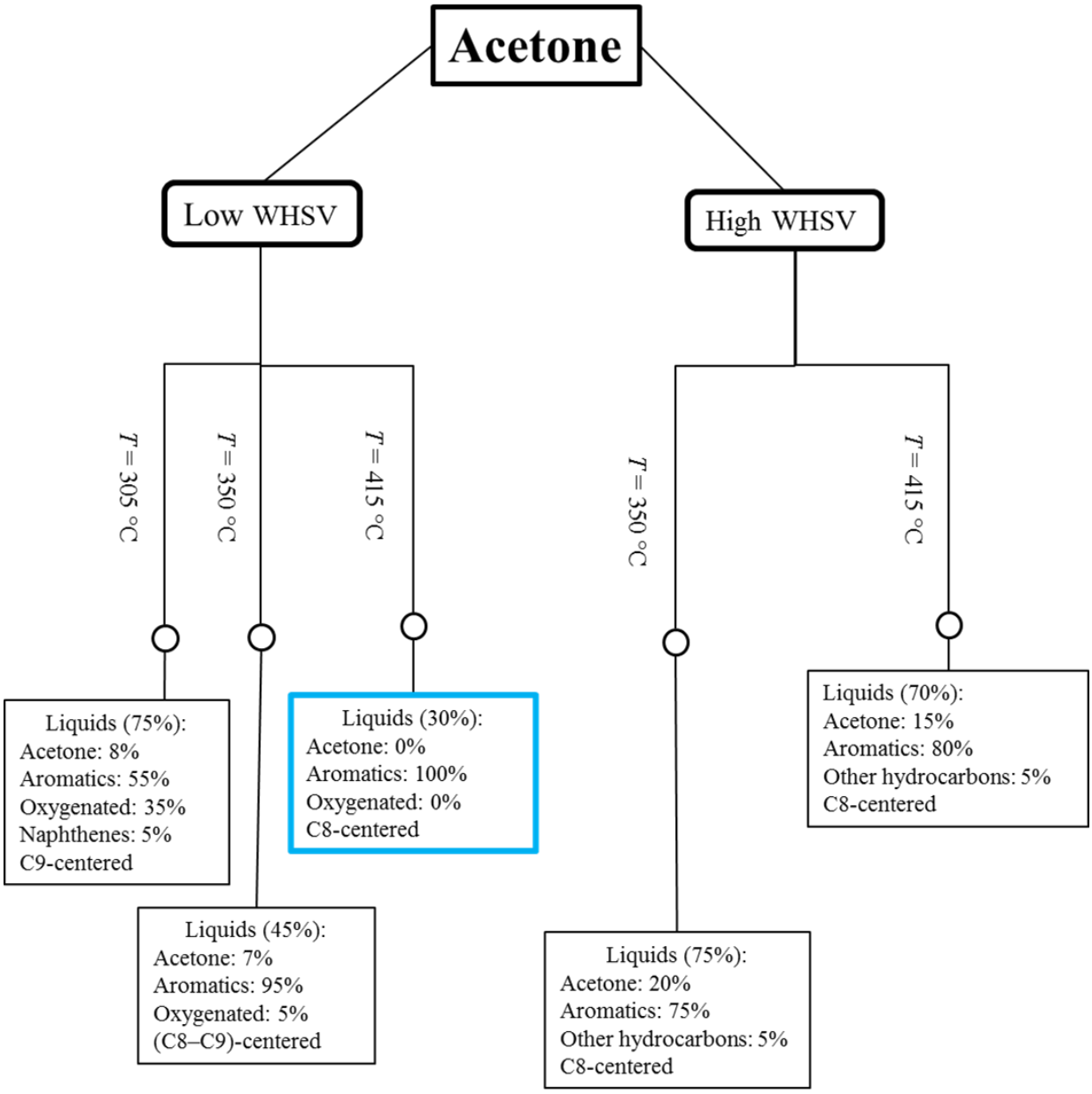

Figure 9-3. Tree diagram of acetone transformation to hydrocarbons at different reaction conditions of *P*, WHSV, and *T*.

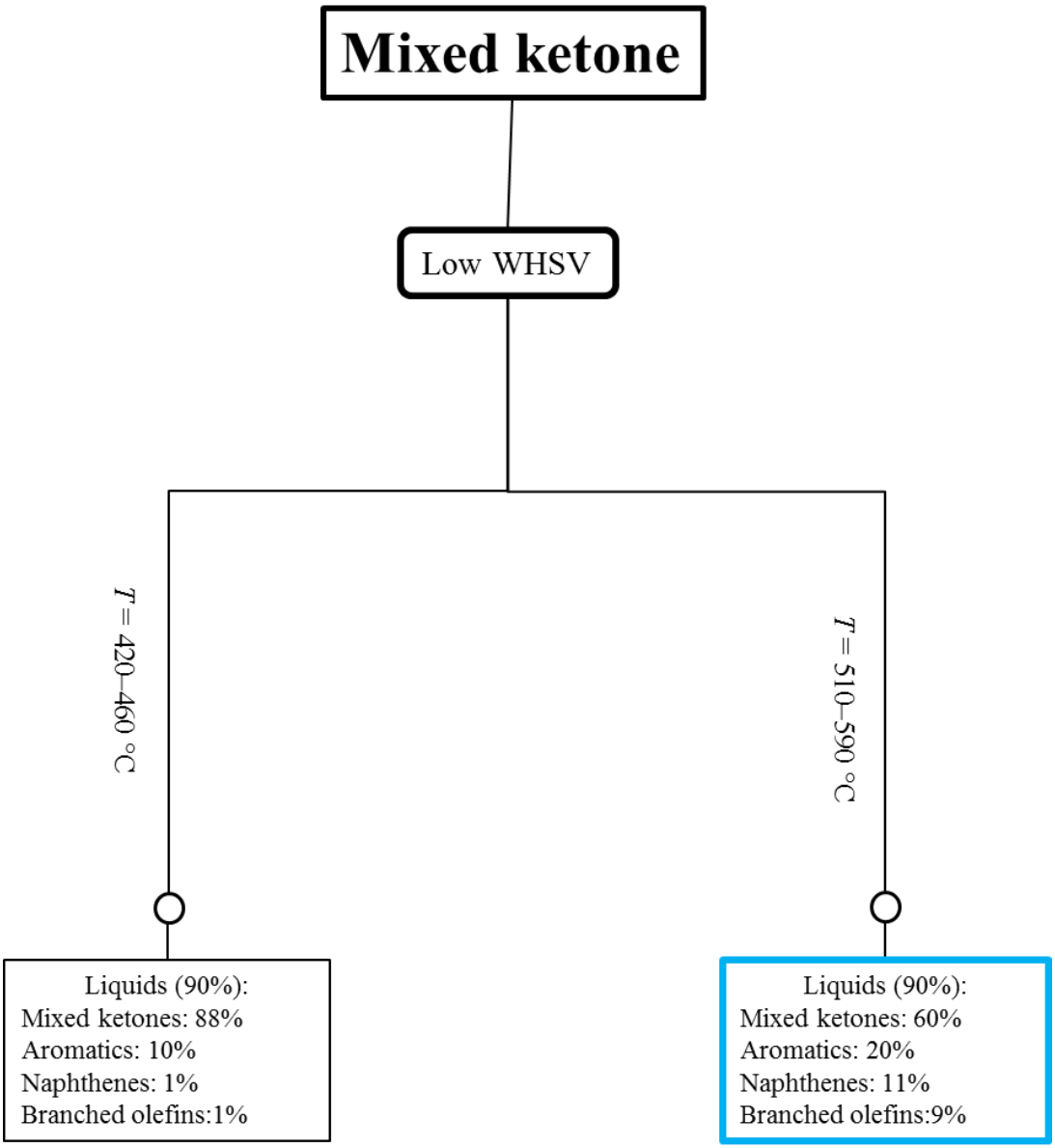

Figure 9-4. Tree diagram of mixed ketone transformation to hydrocarbons at different reaction conditions *P*, WHSV, and *T*.

REFERENCES

1. Pham V, Holtzapple M, El-Halwagi M. Techno-economic analysis of biomass to fuel conversion via the MixAlco process. Journal of Industrial Microbiology Biotechnology. 2010;37(11):1157–1168.
2. Holtzapple M, Davison R, Ross M, Aldrett-Lee S, Nagwani M, Lee C-M, Lee C, Adelson S, Kaar W, Gaskin D, Shirage H, Chang N-S, Chang V, Loescher M. Biomass conversion to mixed alcohol fuels using the MixAlco process. Applied Biochemistry and Biotechnology. 1999;79(1):609–631.
3. Granda C, Holtzapple M, Luce G, Searcy K, Mamrosh D. Carboxylate platform: The MixAlco process part 2: Process economics. Applied Biochemistry and Biotechnology. 2009;156(1–3):107–554.
4. Agler M, Wrenn B, Zinder S, Angenent L. Waste to bioproduct conversion with undefined mixed cultures: The carboxylate platform. Trends in Biotechnology. 2011;29(2):70–78.
5. Agbogbo F, Holtzapple M. Fermentation of rice straw/chicken manure to carboxylic acids using a mixed culture of marine mesophilic microorganisms. Applied Biochemistry and Biotechnology. 2006;132(1–3):997–1014.
6. Aiello-Mazzarri C, Coward G, Agbogbo F, Holtzapple M. Conversion of municipal solid waste into carboxylic acids by anaerobic countercurrent fermentation – effect of using intermediate lime treatment. Applied Biochemistry and Biotechnology. 2005;127(2):79–93.

7. Domke S, Aiello-Mazzarri C, Holtzapple M. Mixed acid fermentation of paper fines and industrial biosludge. Bioresource Technology. 2004;91(1):41–51.
8. Thanakoses P, Mostafa N, Holtzapple M. Conversion of sugarcane bagasse to carboxylic acids using a mixed culture of mesophilic microorganisms. Applied Biochemistry and Biotechnology. 2003;105:523–546.
9. Holtzapple M, Granda C. Carboxylate platform: The MixAlco process part 1: Comparison of three biomass conversion platforms. Applied Biochemistry and Biotechnology. 2009;156(1–3):95–536.
10. Kalghatgi-Gautam T. 2003; U.S. Patent 6,565,617.
11. Taco-Vasquez S, Holtzapple M. Transformation of Acetone and Isopropanol to Hydrocarbons. Berlin: LAP LAMBERT Academic Publishing. Berlin, 2012: 76–84.
12. Mayfield H. JP-8 Composition and Variability Report. Armstrong Laboratories, Florida, 1996.
13. Chang C, Silvestri A. The conversion of methanol and other O-compounds to hydrocarbons over zeolite catalysts. Journal of Catalysis, 1977;(47):249–259.
14. Stocker, M. Methanol-to-hydrocarbons: Catalytic materials and their behavior. Microporous and Mesoporous Materials. 1999;29(1–2):3–48.
15. Wu X, Abraha M, Anthony R. Methanol conversion on SAPO-34: Reaction condition for fixed-bed reactor. Applied Catalysis. A, General. 2004;260(1):63–69.

16. Chang C. Hydrocarbons from methanol (2nd edition). New York: Marcel Dekker, Inc., 1983.
17. Komarewsky V, Uhlick S, and Murray M. Catalytic Dehydration of 1-Hexanol and 1-Octanol. Journal of the American Chemical Society. 1945;67 (4):557-558
18. Meier, W, Olson D, Baerlocher, Ch. Atlas of Zeolite Structure Types, Elsevier, 4th edition, (1996). New York.
19. Anderson J, Mole T, and Christov V. Mechanism of some conversions over ZSM-5 catalyst. Journal of Catalysis, 1980, 61, 477.
20. Fuhse J, Friedhelm B. Conversion of organic oxygen compounds and their mixtures on HZSM-5. Chem. Eng. Technol. 1987;10:323–329.
21. Aguayo, A., Gayubo, A., Tarrio, A., Atutxa, A., & Bilbao, J. Study of operating variables in the transformation of aqueous ethanol into hydrocarbons on an HZSM-5 zeolite. Journal of Chemical Technology and Biotechnology. 2002;7(2):211–216. doi:10.1002/jctb.540
22. Gaigneaux E. International Symposium on the Scientific Bases for the Preparation of Heterogeneous Catalysts (10th : 2010 : Louvain-la-Neuve, Belgium). In Gaigneaux E. (Ed.), Scientific bases for the preparation of heterogeneous catalysts: Proceedings of the 10th International Symposium, Louvain-la-Neuve, Belgium, July (1st ed.). Amsterdam.
23. Yoon J. W, Chang J, Lee H, Kim T, Jhung S H. Trimerization of isobutene over a zeolite Beta catalyst. Journal of Catalysis. 2007;245(1):253–256.

24. Gayubo A, Aguayo A, Atutxa A, Aguado R, Bilbao J. Transformation of oxygenated components of biomass pyrolysis oil on a HZSM-5 zeolite. I alcohols and phenols. Kinetics, Catalysis and Reaction Engineering. 2004;43:2610–2618.
25. Guisnet M, Magnoux P. Coking and deactivation of zeolites: Influence of the Pore Structure. Applied Catalysis. 1989;54(1):1–27.
26. Chang C, Lang W, Smith R. The conversion of methanol and other O-compounds to hydrocarbons over zeolite catalysts: II. Pressure effects. Journal of Catalysis. 1979;56(2):169-173.
27. Mentzel U, Shunmugavel S, Hruby S, Christensen CH, Holm M. High yield of liquid range olefins obtained by converting i-propanol over zeolite H-ZSM-5. Journal American Chemical Society. 2009;131(46):17009-17013.
28. Tabak S, Krambeck F, Garwood W. Conversion of propylene and butylene over ZSM-5 catalyst. AIChE J. 1986;32(9):1526-1531.
29. Salvapatini S, Ramanamurty V, Janardanarao M. Selectivity catalytic self-condensation of acetone. Journal of Molecular Catalysis. 1989;54, 9–30.
30. Gayubo A. Transformation of oxygenate components of biomass pyrolysis oil on a HZSM-5 zeolite. H. Aldehydes, ketones, and acids. Industrial & Engineering Chemistry Research. 2004;43(11):2619-2626.
31. Sanati M, Hornell C, Jaras S. The oligomerization of alkenes by heterogeneous catalysts. In: Vol 14. The Royal Society of Chemistry; 1999:236-288.

32. Gliński M, Kijeński J, Jakubowski A. Ketones from monocarboxylic acids: Catalytic ketonization over oxide systems. Applied Catalysis A: General. 1995;128(2):209-217.
33. Frerich J. Methanol-to-hydrocarbons: process technology. Microporous and Mesoporous Materials. 1999;29(1–2):49-66.

APPENDIX A: GAS CHROMATOGRAPHIC ANALYSIS

Gas chromatography (GC) is a tool used to determine the components and their concentrations in a mixture. A GC employs carrier gas, columns, and detectors. The carrier gas transports the sample into the column where the sample is separated by molecular weight and other properties. The detector identifies the amount of a component exiting the column by sending out an electronic signal that appears as a peak in the chromatograph.

Two detectors were employed: thermal conductivity detector (TCD) and flame ionization detector (FID). The TCD signal is related to the thermal conductivity of the gas and is proportional to the mole fraction of the component. It does not decompose the sample. In contrast, the FID signal is a function of the mass of the component. The sample is burned at the detector causing it to decompose producing ions and electrons that can conduct electricity through the flame. FID not only needs a carrier gas, but also air (or oxygen) and hydrogen to provide a constant flame.

The GC response factor is used to convert a GC peak area to an analytical value (e.g., mole or weight percent). For this experiment, the GC response factors are used to convert a GC peak area to a mole percent.

$$\text{mol \% Species } i = (\text{response factor of } i) \times (\text{GC peak area of } i)$$

Tables A-1 list the response factors for compounds detected on TCD and FID detectors.

TCD detects CO, CO_2, N_2, light hydrocarbons (up to C_4), water, methanol, and dimethyl ether. FID detects C5+ hydrocarbons. Theoretically, the sum of concentrations on TCD and FID should be 100 ± 2 %. Figures A-1 and A-2 show typical chromatographs on TCD and FID, respectively.

The GC has six 30-m mega-bore capillary columns: one methyl silicone HP-1, two HP Plot Q, HP Mole Sieve, one HP Plot Alumna, and one 5% phenyl methyl silicone HP-5 (Agilent Technologies, Santa Barbara, California). All columns have about 40- to 50-µm-thick adsorption phases. The GC has three valves (Figure A-3) that split the carrier gas into six columns, which better separates the samples and consequently gives more accurate results.

Table A-1. TCD and FID response factors.

Compound	TCD Response Factor (mol %/area)	Compound	FID Response Factor (mol%/area)
H_2O	0.006406	Cyclopentene	7.11E-05
DME	0.002976	Cyclopentane	6.64E-05
Methanol	0.003842	Isopentane	6.40E-05
Ethylene	0.004402	Pentane	6.46E-05
Propylene	0.003276	Methyl pentene	5.41E-05
Isobutylene	0.002577	Methyl pentane	5.36E-05
Butene-1	0.002609	Hexene	5.82E-05
Methane	0.005919	Cyclohexene	5.95E-05
Ethane	0.004127	Cyclohexane	5.69E-05
Propane	0.003276	Benzene	5.26E-05
Butane	0.002486	Methyl pentene	5.36E-05
CO	0.004402	Methyl pentane	5.41E-05
CO_2	0.005031	Heptene	4.94E-05
O_2	0.005283	Heptane	4.83E-05
N_2	0.005031	Toluene	4.91E-05
Isobutane	0.002577	Methyl cyclohexane	4.88E-05
		Methyl hexane	4.84E-05
		Octene	4.19E-05
		Ethyl benzene	4.42E-05
		0-Xylene	4.47E-05
		Methyl heptane	4.19E-05
		Mesitylene	4.11E-05
		C4 Benzene	3.61E-05
		N decane	3.47E-05
		C5 Benzene	3.27E-05

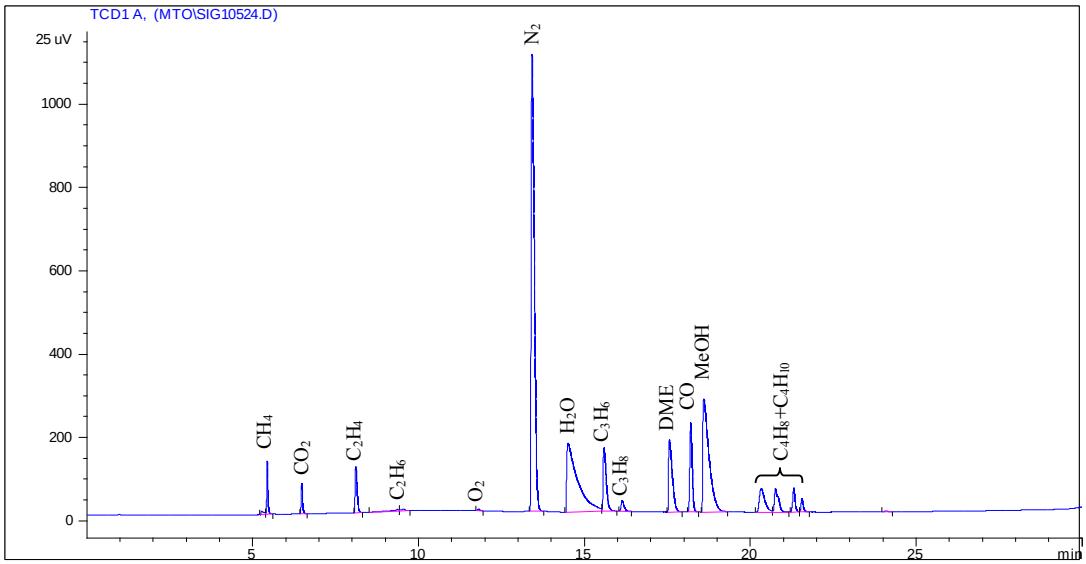

Figure A-1. Representation of a TCD chromatography chart.

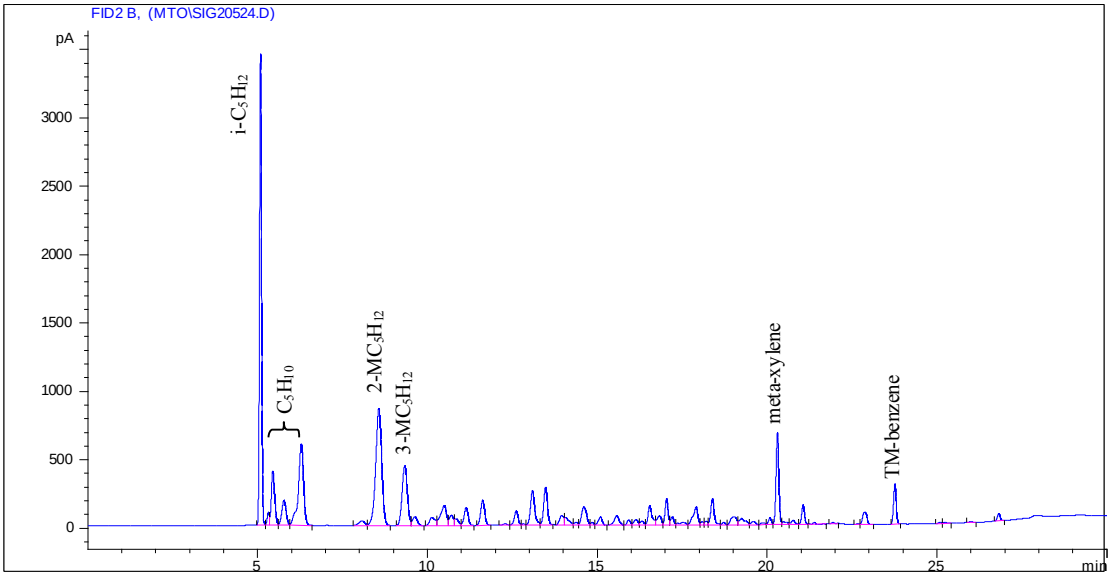

Figure A-2. Representation of a FID chromatography chart.

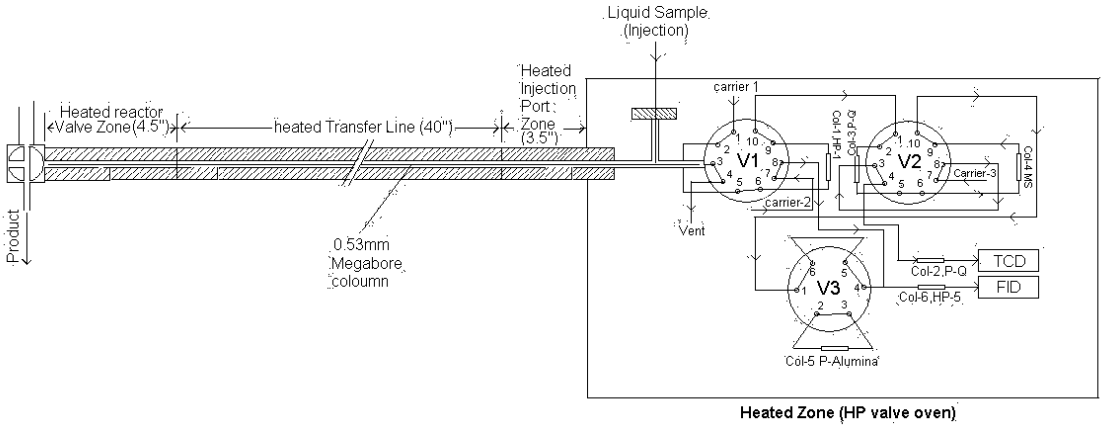

Figure A-3. GC valves and column scheme.

APPENDIX B: COMPOUND ANALYSIS OF COMMERCIAL GASOLINES AND JET FUEL

Table B-1 lists the conventional fuel names and components resulting from the refining of crude oil. This dissertation focuses on gasoline and jet fuel (or kerosene).

Figures B-1 to B-3 show component analysis of commercial gasolines from a local Shell gas station taken in February 2009. Tables B-2 to B-4 show the most abundant components in gasoline, which accounts for 80 wt% of the total hydrocarbon in the mixture. Three types of gasoline were tested: regular, plus, and power. In the three types of gasoline, the most abundant component is C8, which increases as the gasoline grade improves. For example, the C8 concentration in regular gasoline is 20% whereas the concentration of C8 in power gasoline is 40%. In higher grades, the aromatics decrease and isoparaffins increase. In all gasoline types, the paraffin concentration is around 12%. In gasolines, the most abundant hydrocarbons are aromatics, paraffins, and isoparaffins.

Table B-1. Conventions of fuel names and composition (I. Kroschwitz,; M. Howe-Grant, Kirk-Othmer Encyclopedia of Chemical Technology, Wiley & Sons, New York, 4th ed., 1996).

Name	Synonyms	Components
Fuel gas		C1–C2
LPG		C3–C4
Gasoline		C5-C12
Naphtha		C8–C12
Kerosene	Jet Fuel	C9–C14
Diesel	Fuel oil	C13–C17
Middle distillates	Light gas oil	C10–C20
Soft wax		C19–C23
Medium wax		C24–C35
Hard wax		C35+

Table B-2. Most abundant compounds in commercial regular gasoline from a Shell gas station taken in February 2009.

Paraffins (g C/100 g C liquid)		Isoparaffins (g C/100 g C liquid)		Aromatics (g C/100 g C liquid)	
hexane	3	pentane, 2-methyl	3.8	benzene, 1,4-dimethyl	12.3
pentane	2.8	butane, 2-methyl	3.4	benzene, 1-ethyl-4-methyl	8.4
butane	1.6	butane, 2,2,3,3-tetramethyl	3	benzene, 1,2,3-trimethyl	7.3
heptane	1.4	pentane, 3-methyl	2.4	benzene, methyl	6.5
		hexane, 3-methyl	2.1	benzene	3.8
		octane, 4-methyl	1.6	benzene, ethyl	3.6
		pentane, 2,3,4-trimethyl	1.6	benzene, 1-methyl-3-(1-methylethyl)	3
Naphthenes	6	hexane, 2,4-dimethyl	1.5	benzene, 1-methyl-3-propyl	1.4
		butane, 2,2-dimethyl	0.8	benzene, 1,2,4,5-tetramethyl	0.9
				benzene, propyl	0.9
others	4.2		4.8		7.9
Total	13		25		56

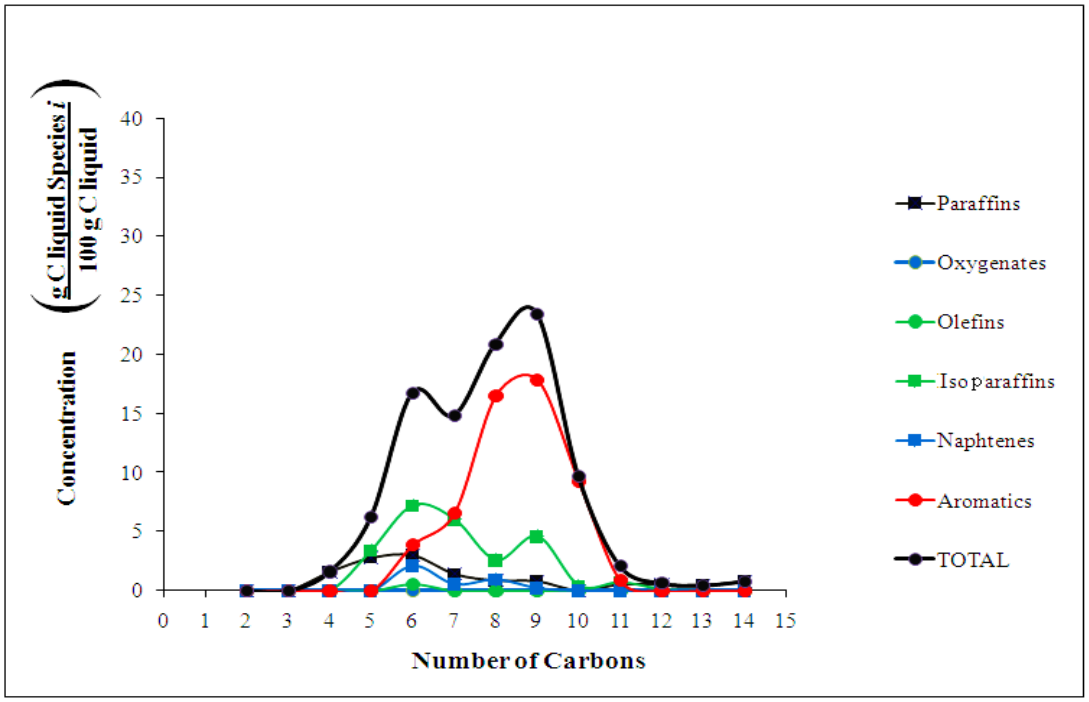

Figure B-1. Carbon distribution of commercial regular gasoline from a Shell gas station taken in February 2009.

Table B-3. Most abundant compounds of a commercial plus gasoline from a Shell gas station taken in February 2009.

Paraffins (g C/100 g C liquid)		Isoparaffins (g C/100 g C liquid)		Aromatics (g C/100 g C liquid)	
pentane	4.3	butane, 2-methyl	5.2	benzene, 1,3-dimethyl	16.5
butane	4.1	pentane, 2-methyl	4.8	benzene, methyl	14.5
		butane, 2,2,3,3-tetramethyl	4.4	benzene	4.7
		pentane, 3-methyl	2.8	benzene, ethyl	3.6
		pentane, 2,3,4-trimethyl	2.5	benzene, 1-ethyl-4-methyl	3.5
Naphthenes	7	heptane, 4-methyl	2	benzene, 1,3,5-trimethyl	3.4
		hexane, 3-methyl	1.8		
		hexane, 2,4-dimethyl	1.8		
others	3.6		1.7		7.8
Total	12		27		54

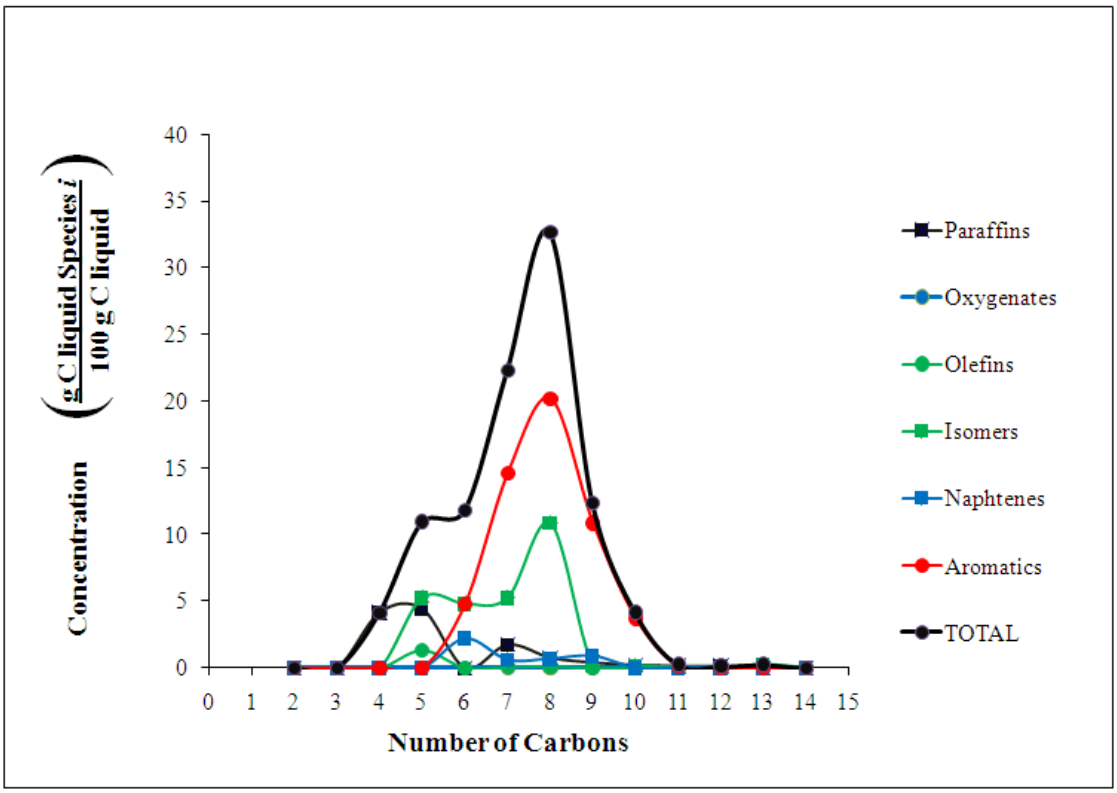

Figure B-2. Carbon distribution of commercial plus gasoline from a Shell gas station taken in February 2009.

Table B-4. Most abundant compounds of a commercial power gasoline from a Shell gas station taken in February 2009.

Paraffins (g C/100 g C liquid)		Isoparaffins (g C/100 g C liquid)		Aromatics (g C/100 g C liquid)	
butane	5.7	pentane, 2,3,4-trimethyl	11.4	benzene, 1,4-dimethyl-	18.3
heptane	1.8	pentane, 2,2,4-trimethyl	8.9	benzene	5.5
		pentane, 2-methyl	5	benzene, 1,3,5-trimethyl-	4
		pentane, 2,4-dimethyl	5	benzene, 1-ethyl-4-methyl	3.6
Naphthenes		1,6-heptadiyne	4.8		
		butane, 2-methyl	3.2		
		pentane, 2,4-dimethyl	2.6		
others	3.5		6.1		10.6
Total	11		47		42

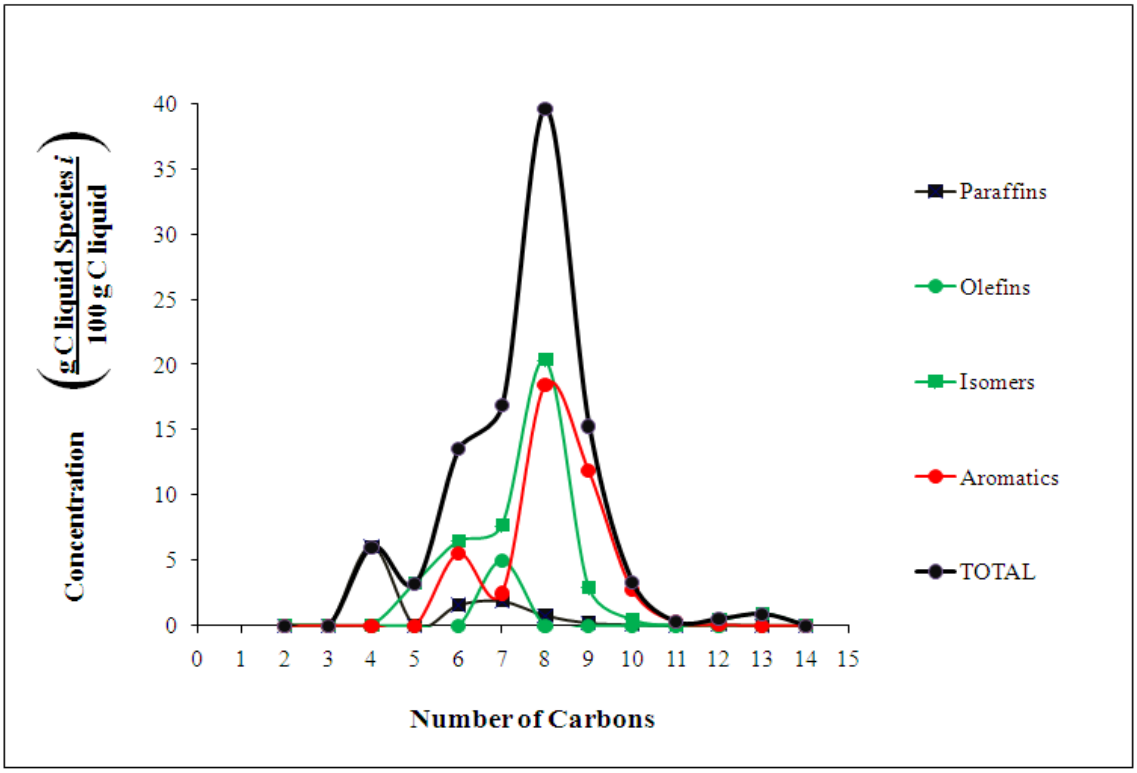

Figure B-3. Carbon distribution of commercial power gasoline from a Shell gas station taken in February 2009.

Jet fuel or aviation turbine fuel (ATF) is a type of aviation fuel designed for use in aircraft powered by gas-turbine engines. Table B-5 shows the composition of the most abundant hydrocarbons found in a jet fuel sample analyzed by LOGOS Technologies, Inc. (2011). Figures B-4 and B-5 show the carbon distribution of commercial jet fuel for two samples: (1) laboratory analysis of LOGOS Technologies, Inc (2011) and (2) ARMSTRONG laboratories Florida (1996). For both figures, the most abundant hydrocarbons are paraffins, isoparaffins, and aromatics. Table B-6 shows the comparison between jet fuel compositions. For both analyses, paraffins are the most abundant. LOGOS jet fuel contains 54 wt% paraffins whereas ARMSTRONG contains 37 wt%.

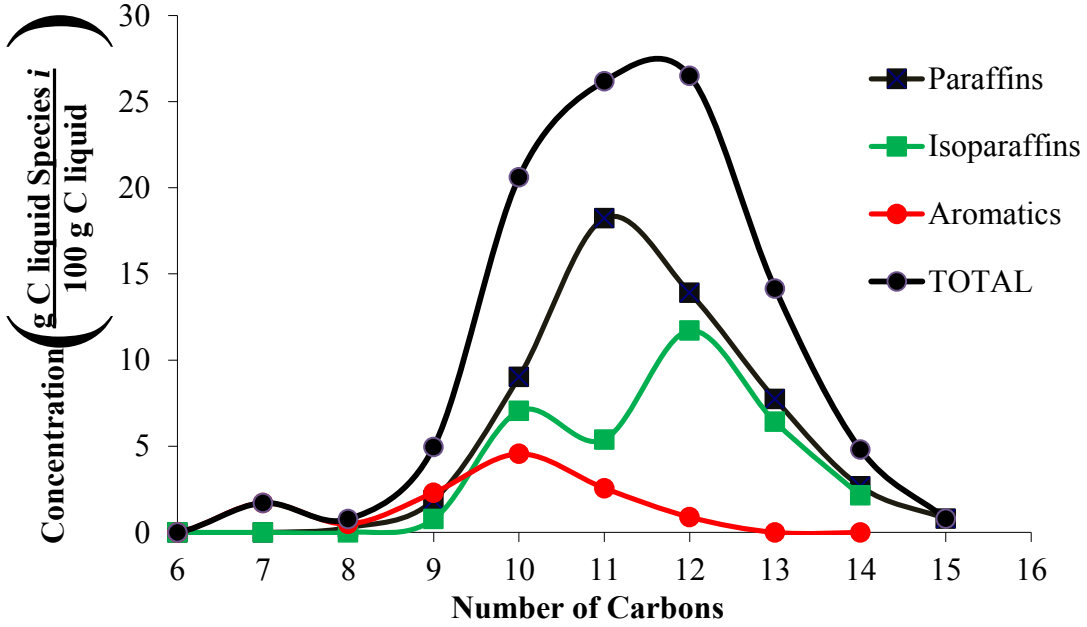

Figure B-4. Carbon distribution of commercial jet fuel by LOGOS laboratory taken in September 2011

Table B-5. Most abundant hydrocarbons in a jet fuel from LOGOS Technologies, Inc.

Compound	Concentration (wt %)	Type	Carbon number
Undecane	18.22	Paraffin	11
Dodecane	13.9	Paraffin	12
Decane	9.01	Paraffin	10
Tridecane	7.73	Paraffin	13
Undecane, 4-methyl	3.52	Isoparaffin	12
Decane, 3-methyl-	3.5	Isoparaffin	11
Undecane, 4-methyl	3.04	Isoparaffin	12
C7+3 or C9+1	2.8	Isoparaffin	10
Tetradecane	2.67	Paraffin	14
Undecane, 2-methyl	2.03	Isoparaffin	12
Undecane, 2,6-dimethyl	1.94	Isoparaffin	13
Decane, 2-methyl-	1.89	Isoparaffin	11
Nonane	1.88	Paraffin	9
Dodecane, methyl	1.69	Isoparaffin	13
Dodecane, dimethyl	1.59	Isoparaffin	14
Decane, dimethyl	1.57	Isoparaffin	12
Undecane, methyl	1.54	Isoparaffin	12
Undecane, dimethyl	1.41	Isoparaffin	13
Dodecane, methyl	1.37	Isoparaffin	13
Aromatics	12.5	Aromatics	8–12
Others	6.7	----------	--------
Total	100		

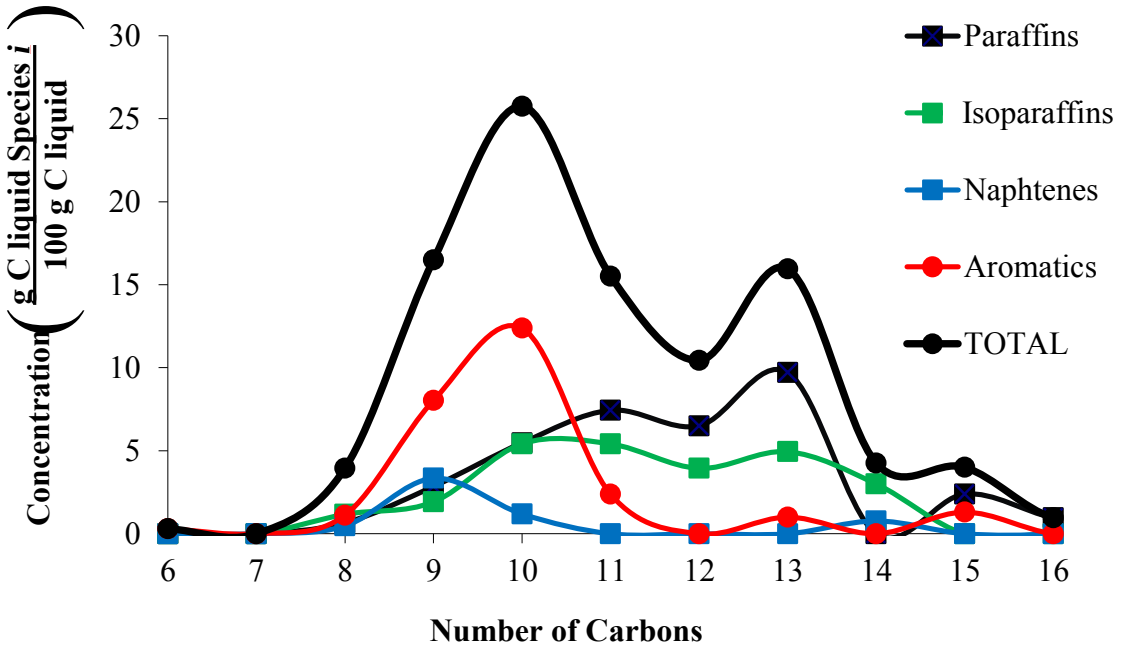

Figure B-5. Carbon distribution of commercial jet fuel (Adaptation of JP-8 Composition and Variability, MAYFIELD Howard, 1996).

Table B-6. Jet fuel distribution comparison between jet fuel sample from LOGOS laboratory and MAYFIELD**.**

	Concentration LOGOS (wt %)	Average Carbon Number LOGOS	Concentration ARMSTRONG (wt %)	Average Carbon Number ARMSTRONG
Paraffins	54.5	11.49	37.0	11.90
Isoparaffins	33.5	11.67	28.0	11.60
Aromatics	12.5	9.67	27.0	10.00
Naphthenes	0	--------	7.0	9.00
Total	100.0	11.58	100.0	10.98

APPENDIX C: INPUT SUMMARY FOR PRODUCT ANALYSIS TO CLASSIFY THE CONCENTRATION INTO CARBON NUMBER AND TYPE OF PRODUCT IN MATLAB

```
clear all;
close all;
clc;
input='u:\MA1.xlsx';%%%Excel input file
output='u:\MA1a.xlsx';%%%Excel output file
[C type]=xlsread(input,'f20:g72');%%%Type and Carbon number columns
Area=xlsread(input,'c20:c72');%%%Concentration Column
[x,y]=size(C)
n=1;
AreaRes(1)=Area(1);
CRes(1)=C(1);
typeRes(1)=type(1);
for t=2:x
   if (C(t)==C(t-1))
      AreaRes(n)=Area(t)+AreaRes(n);
      CRes(n)=C(t);
      typeRes(n)=type(t);
   else
      n=n+1;
      AreaRes(n)=Area(t);
      CRes(n)=C(t)
      typeRes(n)=type(t);
      %n=n+1;
   end
end
[x,y]=size(AreaRes);
finalA=num2str(y);
sizeAC=['a1:b',finalA];
sizet=['c1:c',finalA];
success=xlswrite(output,[AreaRes;CRes]','sheet1',sizeAC);
success=xlswrite(output,typeRes','sheet1',sizet);
```

APPENDIX D: INPUT SUMMARY FOR PRODUCT ANALYSIS TO CLASSIFY THE CONCENTRATION INTO CARBON NUMBER AND TYPE OF PRODUCT IN MATLAB

```
Min  =  (XA*ARA + XB*ARB - ARG)^2 + (XA*LOA + XB*LOB - LOG)^2 +
(XA*BOA + XB*BOB - BOG)^2 + (XA*NPA + XB*NPB - NPG)^2 ;
ARA = 7;
ARB = 71.5;
ARG = 64;
LOA = 72;
LOB = 0;
LOG = 5.5;
BOA = 16;
BOB = 16.2;
BOG = 30.3;
NPA = 2.3;
NPB = 12.2;
NPG = 3;
ARBG = XA*ARA + XB*ARB;
LOBG = XA*LOA + XB*LOB;
BOBG = XA*BOA + XB*BOB;
NPBG = XA*NPA + XB*NPG;

!XA*ARA + XB*ARB +  XA*LOA + XB*LOB +  XA*BOA + XB*BOB + XA*NPA +
XB*NPB = 100;

XA + XB = 1;
END
```

APPENDIX E: TOTAL YIELD OF ISOPROPANOL REACTION OVER HZSM-5

This appendix presents mass balances for the isopropanol reactions. The basis for each table is 100 grams of isopropanol feed.

Table E.1 Product distribution for gases and liquids for isopropanol reaction (Experiment I1).

Catalyst		***T***		***P***		**WHSV**	
HZSM-5 (280)		300°C		101 kPa		1.3 h^{-1}	
Gas		Liquid					
		Hydrocarbons		Aqueous			
CO_2	0.00	C5	5.52	H_2O	30.38		
CO	0.00	C6	8.00	Isop.	0.00		
C1	0.07	**C6	0.00				
C2	0.14	C7	8.73				
*C2	1.08	C8	7.12				
C3	2.31	C9	5.24				
*C3	3.41	C10	2.50				
C4	14.00	C11	1.10				
*C4	7.90	C12	0.88				
		C13	0.91				
Total	28.91	+	40.01	+	30.38		99.30

*Olefin
** Benzene

Table E.2 Product distribution for gases and liquids for isopropanol reaction (Experiment I2).

Catalyst		***T***		***P***		**WHSV**	
HZSM-5 (280)		320°C		101 kPa		1.3 h^{-1}	
Gas		Liquid					
		Hydrocarbons		Aqueous			
CO_2	0.00	C5	1.93	H_2O	30.38		
CO	0.00	C6	6.18	Isop.	0.00		
C1	0.07	**C6	0.00				
C2	0.14	C7	10.55				
*C2	0.79	C8	10.71				
C3	1.48	C9	4.93				
*C3	5.24	C10	3.54				
C4	12.73	C11	1.09				
*C4	7.13	C12	1.20				
		C13	0.91				
Total	27.57	+	41.06	+	30.38		99.00

*Olefin
** Benzene

Table E.3 Product distribution for gases and liquids for isopropanol reaction (Experiment I3).

Catalyst		***T***		***P***		**WHSV**	
HZSM-5 (280)		370°C		101 kPa		1.3 h^{-1}	
Gas		Liquid					
		Hydrocarbons		Aqueous			
CO_2	0.00	C5	5.52	H_2O	30.38		
CO	0.00	C6	8.00	Isop.	0.00		
C1	0.07	**C6	0.00				
C2	0.14	C7	8.73				
*C2	1.08	C8	7.12				
C3	2.31	C9	5.24				
*C3	3.41	C10	2.50				
C4	14.00	C11	1.10				
*C4	7.90	C12	0.88				
		C13	0.91				
Total	28.91	+	40.01	+	30.38		99.30

Table E.4 Product distribution for gases and liquids for isopropanol reaction (Experiment I4).

Catalyst		***T***		***P***		**WHSV**
HZSM-5 (280)		410°C		101 kPa		1.3 h^{-1}
Gas		Liquid				
		Hydrocarbons		Aqueous		
CO_2	0.19	C5	3.54	H_2O	30.16	
CO	0.00	C6	5.35	Isop.	0.00	
C1	0.14	**C6	0.00			
C2	0.28	C7	6.46			
*C2	2.06	C8	6.57			
C3	7.66	C9	3.86			
*C3	2.78	C10	1.82			
C4	16.54	C11	0.98			
*C4	8.32	C12	0.93			
		C13	0.92			
Total	37.98	+	30.43	+	30.16	98.57

*Olefin
** Benzene

Table E.5 Product distribution for gases and liquids for isopropanol reaction (Experiment I5).

Catalyst		***T***		***P***		**WHSV**
HZSM-5 (280)		370°C		101 kPa		0.52 h^{-1}
Gas		Liquid				
		Hydrocarbons		Aqueous		
CO_2	0.18	C5	3.09	H_2O	30.16	
CO	0.02	C6	2.84	Isop.	0.00	
C1	0.09	**C6	0.00			
C2	0.19	C7	7.66			
*C2	1.94	C8	7.11			
C3	3.73	C9	8.78			
*C3	0.74	C10	4.87			
C4	14.34	C11	2.26			
*C4	8.61	C12	1.68			
		C13	0.92			
Total	29.84	+	39.20	+	30.16	99.21

Table E.6 Product distribution for gases and liquids for isopropanol reaction (Experiment I6).

Catalyst		***T***		***P***		**WHSV**
HZSM-5 (280)		370°C		101 kPa		1.9 h^{-1}
Gas		Liquid				
		Hydrocarbons		Aqueous		
CO_2	0.00	C5	5.52	H_2O	30.38	
CO	0.00	C6	8.00	Isop.	0.00	
C1	0.07	**C6	0.00			
C2	0.14	C7	8.73			
*C2	1.08	C8	7.12			
C3	2.31	C9	5.24			
*C3	3.41	C10	2.50			
C4	14.00	C11	1.10			
*C4	7.90	C12	0.88			
		C13	0.91			
Total	28.91	+	40.01	+	30.38	99.30

*Olefin
** Benzene

Table E.7 Product distribution for gases and liquids for isopropanol reaction (Experiment I7).

Catalyst		***T***		***P***		**WHSV**
HZSM-5 (280)		370°C		101 kPa		7.5 h^{-1}
		Liquid				
		Hydrocarbons		Aqueous		
CO_2	0.00	C5	2.64	H_2O	30.24	
CO	0.00	C6	11.18	Isop.	0.00	
C1	0.07	**C6	0.28			
C2	0.14	C7	13.01			
*C2	0.87	C8	9.38			
C3	0.87	C9	2.76			
*C3	7.04	C10	1.69			
C4	9.46	C11	0.84			
*C4	6.79	C12	0.84			
		C13	0.91			
Total	25.23	+	43.54	+	30.24	99.01

Table E.8 Product distribution for gases and liquids for isopropanol reaction (Experiment I8).

Catalyst		***T***		***P***		**WHSV**
HZSM-5 (280)		370°C		101 kPa		11.2 h^{-1}
Gas		Liquid				
		Hydrocarbons		Aqueous		
CO_2	0.00	C5	3.25	H_2O	30.38	
CO	0.00	C6	10.84	Isop.	0.00	
C1	0.07	**C6	0.00			
C2	0.14	C7	4.55			
*C2	0.55	C8	9.16			
C3	0.92	C9	4.18			
*C3	9.52	C10	2.40			
C4	12.07	C11	1.20			
*C4	8.71	C12	0.84			
		C13	0.91			
Total	31.99	+	37.34	+	30.38	99.70

*Olefin
** Benzene

APPENDIX F: TOTAL YIELD OF ACETONE REACTION OVER HZSM-5

A mass balance analysis of the acetone reaction experiments is presented. One hundred grams of acetone is chosen as a basis for the product distribution. The products are divided into gases and liquids. The liquid products are divided in hydrocarbons and aqueous products. The conditions for each experiment are shown before each result table. The type of catalysts for these experiments are HZSM-5 (80) and HZSM-5 (280)

Table F.1 Product distribution for gases and liquids for acetone reaction (Experiment A1).

Catalyst		***T***		***P***	**WHSV**		**H_2 Ratio (mol H_2 / mol acetone)**
HZSM-5 (80)		305°C		101 kPa	1.3 h^{-1}		0
Gas		Liquid					
		Hydrocarbons			Aqueous		
CO_2	1.81	C5	1.26		H_2O	26.41	
CO	0.46	C6	2.33		Acetone	6.62	
C1	0.22	**C6	0.32				
C2	0.00	C7	5.78				
*C2	1.13	C8	8.85				
C3	0.82	C9	22.19				
*C3	0.96	C10	5.53				
C4	7.10	C11	1.63				
*C4	2.63	C12	1.99				
		C13	1.94				
Total	15.13	+	51.84		+	33.03	100.00

*Olefin
** Benzene

Table F.2 Product distribution for gases and liquids for acetone reaction (Experiment A2).

Catalyst		***T***		***P***	**WHSV**		**H_2 Ratio (mol H_2 / mol acetone)**
HZSM-5 (80)		350°C		101 kPa	1.3 h^{-1}		0
Gas		Liquid					
		Hydrocarbons			Aqueous		
CO_2	16.23	C5	0.57		H_2O	14.61	
CO	2.60	C6	0.40		Acetone	5.59	
C1	0.35	**C6	0.92				
C2	0.58	C7	4.64				
*C2	2.30	C8	8.52				
C3	3.68	C9	10.25				
*C3	5.81	C10	3.52				
C4	9.63	C11	1.75				
*C4	5.66	C12	1.22				
		C13	1.16				
Total	46.85	+	32.95		+	20.20	100.00

*Olefin ** Benzene

Table F.3 Product distribution for gases and liquids for acetone reaction (Experiment A3).

Catalyst		***T***		***P***	**WHSV**		**H_2 Ratio (mol H_2 / mol acetone)**
HZSM-5 (80)		350°C		101 kPa	2.63 h^{-1}		0
Gas		Liquid					
		Hydrocarbons			Aqueous		
CO_2	0.85	C5	0.28		H_2O	25.26	
CO	0.00	C6	1.62		Acetone	15.43	
C1	0.06	**C6	1.47				
C2	0.00	C7	7.73				
*C2	0.34	C8	11.16				
C3	0.17	C9	18.58				
*C3	0.32	C10	6.11				
C4	4.73	C11	2.98				
*C4	0.45	C12	1.23				
		C13	1.24				
Total	6.92	+	52.39		+	40.69	100.00

Table F.4 Product distribution for gases and liquids for acetone reaction (Experiment A4).

Catalyst		***T***		***P***	**WHSV**		**H_2 Ratio (mol H_2 / mol acetone)**
HZSM-5 (80)		350°C		101 kPa	3.95 h^{-1}		0
		Liquid					
Gas		Hydrocarbons			Aqueous		
CO_2	2.48	C5	0.64		H_2O	21.15	
CO	0.51	C6	0.63		Acetone	18.32	
C1	0.12	**C6	0.71				
C2	0.00	C7	5.79				
*C2	0.66	C8	14.11				
C3	0.79	C9	19.11				
*C3	0.61	C10	6.24				
C4	2.06	C11	2.43				
*C4	1.38	C12	1.33				
		C13	0.92				
Total	8.61	+	51.92		+	39.47	100.00

Table F.5 Product distribution for gases and liquids for acetone reaction (Experiment A5). .

Catalyst		***T***		***P***	**WHSV**		**H_2 Ratio (mol H_2 / mol acetone)**
HZSM-5 (80)		350°C		101 kPa	5.30 h^{-1}		0
		Liquid					
Gas		Hydrocarbons			Aqueous		
CO_2	0.07	C5	0.51		H_2O	23.63	
CO	0.02	C6	1.24		Acetone	22.17	
C1	0.06	**C6	0.67				
C2	0.00	C7	6.38				
*C2	0.16	C8	11.57				
C3	0.20	C9	16.69				
*C3	0.21	C10	8.26				
C4	0.74	C11	3.76				
*C4	0.55	C12	1.90				
		C13	1.21				
Total	2.01	+	52.18		+	45.80	100.00

Table F.6 Product distribution for gases and liquids for acetone reaction (Experiment A6).

Catalyst		***T***		***P***	**WHSV**		**H_2 Ratio (mol H_2 / mol acetone)**
HZSM-5 (80)		415°C		101 kPa	1.3 h^{-1}		0
Gas		Liquid					
		Hydrocarbon			Aqueous		
CO_2	21.27	C5	0.47		H_2O	11.98	
CO	3.59	C6	0.00		Acetone	0.00	
C1	0.99	**C6	1.42				
C2	0.68	C7	3.47				
*C2	1.45	C8	7.62				
C3	3.33	C9	4.57				
*C3	15.88	C10	2.13				
C4	11.54	C11	1.18				
*C4	6.20	C12	1.14				
		C13	1.07				
Total	64.93	+	23.09		+	11.98	100.00

Table F.7 Product distribution for gases and liquids for acetone reaction (Experiment A7).

Catalyst		***T***		***P***	**WHSV**		**H_2 Ratio (mol H_2 / mol acetone)**
HZSM-5 (80)		415°C		101 kPa	1.3 h^{-1}		0
Gas		Liquid					
		Hydrocarbons			Aqueous		
CO_2	13.58	C5	1.06		H_2O	19.31	
CO	1.74	C6	0.46		Acetone	0.00	
C1	1.00	**C6	2.07				
C2	0.58	C7	6.12				
*C2	0.88	C8	13.69				
C3	9.83	C9	9.76				
*C3	1.04	C10	3.64				
C4	6.29	C11	1.85				
*C4	4.00	C12	1.91				
		C13	1.19				
Total	38.95	+	41.74		+	19.31	100.00

Table F.8 Product distribution for gases and liquids for acetone reaction (Experiment A8).

Catalyst		***T***		***P***	**WHSV**		**H_2 Ratio (mol H_2 / mol acetone)**
HZSM-5 (80)		415°C		101 kPa	3.95 h^{-1}		0
Gas		Liquid					
		Hydrocarbons			Aqueous		
CO_2	10.70	C5	0.30		H_2O	21.73	
CO	1.64	C6	0.39		Acetone	0.00	
C1	0.19	**C6	1.82				
C2	0.13	C7	8.29				
*C2	2.02	C8	15.87				
C3	3.53	C9	12.50				
*C3	3.31	C10	3.71				
C4	6.08	C11	1.68				
*C4	3.87	C12	1.13				
		C13	1.11				
Total	31.47	+	46.79		+	21.73	100.00

*Olefin
** Benzene

Table F.9 Product distribution for gases and liquids for acetone reaction (Experiment A9).

Catalyst		***T***		***P***	**WHSV**		**H_2 Ratio (mol H_2 / mol acetone)**
HZSM-5 (80)		415°C		101 kPa	5.27 h^{-1}		0
Gas		Liquid					
		Hydrocarbons			Aqueous		
CO_2	8.22	C5	1.26		H_2O	22.17	
CO	1.26	C6	1.15		Acetone	4.84	
C1	0.16	**C6	1.43				
C2	0.10	C7	8.46				
*C2	1.58	C8	15.03				
C3	2.75	C9	13.75				
*C3	2.59	C10	3.69				
C4	4.78	C11	1.57				
*C4	3.08	C12	1.19				
		C13	0.95				
Total	24.51	+	48.48		+	27.01	100.00

Table F.10 Product distribution for gases and liquids for acetone reaction (Experiment A10).

Catalyst		***T***		***P***	**WHSV**		**H_2 Ratio (mol H_2 / mol acetone)**
HZSM-5 (80)		415°C		101 kPa	6.58 h^{-1}		0
Gas		Liquid					
		Hydrocarbons			Aqueous		
CO_2	0.85	C5	0.28		H_2O	25.27	
CO	0.00	C6	0.88		Acetone	15.43	
C1	0.06	**C6	1.53				
C2	0.00	C7	9.27				
*C2	0.34	C8	16.64				
C3	0.17	C9	16.33				
*C3	0.32	C10	3.60				
C4	4.73	C11	1.88				
*C4	0.45	C12	1.11				
		C13	0.86				
Total	6.92	+	52.38		+	40.70	100.00

*Olefin
** Benzene

Table F.11 Product distribution for gases and liquids for acetone reaction (Experiment A11).

Catalyst		***T***		***P***	**WHSV**		**H_2 Ratio (mol H_2 / mol acetone)**
HZSM-5 (80)		415°C		101 kPa	7.9 h^{-1}		0
Gas		Liquid					
		Hydrocarbons			Aqueous		
CO_2	9.01	C5	0.46		H_2O	19.51	
CO	0.71	C6	0.94		Acetone	11.25	
C1	0.14	**C6	0.85				
C2	0.00	C7	7.46				
*C2	2.09	C8	12.17				
C3	0.80	C9	16.18				
*C3	0.99	C10	4.23				
C4	6.04	C11	1.91				
*C4	3.10	C12	1.09				
		C13	1.07				
Total	22.87	+	46.36		+	30.77	100.00

Table F.12 Product distribution for gases and liquids for acetone reaction (Experiment A12).

Catalyst	***T***	***P***	**WHSV**	**H_2 Ratio (mol H_2 / mol acetone)**
HZSM-5 (80)	415°C	101 kPa	1.3 h^{-1}	0.34

Gas		Liquid				
		Hydrocarbons		Aqueous		
CO_2	13.00	C5	0.41	H_2O	19.86	
CO	1.78	C6	0.00	Acetone	0.00	
C1	0.52	**C6	2.34			
C2	0.43	C7	9.58			
*C2	0.78	C8	12.06			
C3	1.74	C9	8.86			
*C3	10.40	C10	3.04			
C4	6.44	C11	2.07			
*C4	4.04	C12	1.51			
		C13	1.16			
Total	39.12	+	41.02	+	19.86	100.00

Table F.13 Product distribution for gases and liquids for acetone reaction (Experiment A13).

Catalyst	***T***	***P***	**WHSV**	**H_2 Ratio (mol H_2 / mol acetone)**
HZSM-5 (80)	415°C	101 kPa	2.63 h^{-1}	0.34

Gas		Liquid				
		Hydrocarbons		Aqueous		
CO_2	0.67	C5	1.14	H_2O	30.30	
CO	0.39	C6	1.21	Acetone	0.00	
C1	0.05	**C6	2.82			
C2	0.00	C7	7.99			
*C2	0.13	C8	10.44			
C3	0.48	C9	27.17			
*C3	0.16	C10	7.96			
C4	0.64	C11	3.13			
*C4	0.92	C12	2.57			
		C13	1.81			
Total	3.45	+	66.25	+	30.30	100.00

Table F.14 Product distribution for gases and liquids for acetone reaction (Experiment A14).

Catalyst		***T***		***P***	**WHSV**		**H_2 Ratio (mol H_2 / mol acetone)**
HZSM-5 (80)		415°C		101 kPa	3.95 h^{-1}		0.34
Gas		Liquid					
		Hydrocarbons			Aqueous		
CO_2	2.22	C5	0.27		H_2O	29.36	
CO	0.23	C6	0.32		Acetone	0.00	
C1	0.08	**C6	2.30				
C2	0.00	C7	12.31				
*C2	0.56	C8	20.65				
C3	0.51	C9	16.35				
*C3	0.58	C10	4.63				
C4	2.46	C11	2.69				
*C4	1.52	C12	1.64				
		C13	1.33				
Total	8.16	+	62.49		+	29.36	100.00

Table F.15 Product distribution for gases and liquids for acetone reaction (Experiment A15).

Catalyst		***T***		***P***	**WHSV**		**H_2 Ratio (mol H_2 / mol acetone)**
HZSM-5 (80)		415°C		101 kPa	1.3 h^{-1}		1
Gas		Liquid					
		Hydrocarbons			Aqueous		
CO_2	6.66	C5	0.45		H_2O	25.55	
CO	0.91	C6	0.26		Acetone	0.00	
C1	0.26	**C6	2.16				
C2	0.26	C7	11.32				
*C2	0.71	C8	17.58				
C3	0.97	C9	11.96				
*C3	4.89	C10	4.29				
C4	3.62	C11	2.85				
*C4	2.38	C12	1.77				
		C13	1.14				
Total	20.67	+	53.79		+	25.55	100.00

Table F.16 Product distribution for gases and liquids for acetone reaction (Experiment A16).

Catalyst		***T***		***P***	**WHSV**		**H_2 Ratio (mol H_2 / mol acetone)**
HZSM-5 (80)		415°C		101 kPa	2.63 h^{-1}		1
Gas		Liquid					
		Hydrocarbons			Aqueous		
CO_2	6.52	C5	0.76		H_2O	25.69	
CO	0.86	C6	0.63		Acetone	0.00	
C1	0.18	**C6	2.38				
C2	0.13	C7	13.70				
*C2	1.41	C8	13.30				
C3	2.24	C9	17.09				
*C3	2.14	C10	3.44				
C4	4.20	C11	1.07				
*C4	2.83	C12	0.67				
		C13	0.73				
Total	20.52	+	53.78		+	25.69	100.00

*Olefin ** Benzene

Table F.17 Product distribution for gases and liquids for acetone reaction (Experiment A17).

Catalyst		***T***		***P***	**WHSV**		**mol H_2 / mol Acetone**
HZSM-5 (80)		415°C		101 kPa	3.95 h^{-1}		1
Gas		Liquid					
		Hydrocarbons			Aqueous		
CO_2	0.15	C5	0.59		H_2O	31.12	
CO	0.04	C6	0.66		Acetone	0.00	
C1	0.07	**C6	1.23				
C2	0.00	C7	11.62				
*C2	0.19	C8	21.52				
C3	0.21	C9	19.94				
*C3	0.22	C10	6.55				
C4	0.95	C11	1.71				
*C4	0.59	C12	1.37				
		C13	1.28				
Total	2.40	+	66.48		+	31.12	100.00

Table F.18 Product distribution for gases and liquids for acetone reaction (Experiment A18).

Catalyst		***T***	***P***	**WHSV**		**H_2 Ratio (mol H_2 / mol acetone)**
HZSM-5 (280)		415°C	101 kPa	1.3 h^{-1}		0
Gas		Liquid				
		Hydrocarbons		Aqueous		
CO_2	4.45	C5	1.38	H_2O	27.47	
CO	0.47	C6	1.07	Acetone	0.00	
C1	0.23	**C6	1.73			
C2	0.20	C7	9.54			
*C2	1.04	C8	18.06			
C3	1.30	C9	15.04			
*C3	1.59	C10	6.70			
C4	2.48	C11	2.03			
*C4	1.80	C12	1.63			
		C13	1.79			
Total	13.55	+	58.97	+	27.47	100.00

Table F.19 Product distribution for gases and liquids for acetone reaction (Experiment A19).

Catalyst		***T***	***P***	**WHSV**		**H_2 Ratio (mol H_2 / mol acetone)**
HZSM-5 (280)		415°C	101 kPa	2.63 h^{-1}		0
Gas		Liquid				
		Hydrocarbons		Aqueous		
CO_2	6.62	C5	1.51	H_2O	25.46	
CO	0.73	C6	0.89	Acetone	0.00	
C1	0.14	**C6	1.39			
C2	0.24	C7	9.12			
*C2	1.83	C8	17.72			
C3	1.21	C9	14.13			
*C3	1.99	C10	3.87			
C4	4.71	C11	2.30			
*C4	3.51	C12	1.50			
		C13	1.11			
Total	20.99	+	53.55	+	25.46	100.00

Table F.20 Product distribution for gases and liquids for acetone reaction (Experiment A20).

Catalyst		***T***		***P***	**WHSV**		**H_2 Ratio (mol H_2 / mol acetone)**
HZSM-5 (280)		415°C		101 kPa	3.95 h^{-1}		0
		Liquid					
Gas		Hydrocarbons			Aqueous		
CO_2	1.51	C5	0.66		H_2O	25.71	
CO	0.08	C6	1.02		Acetone	11.17	
C1	0.07	**C6	1.34				
C2	0.00	C7	8.58				
*C2	0.26	C8	17.31				
C3	0.26	C9	19.45				
*C3	0.39	C10	4.20				
C4	2.71	C11	2.14				
*C4	0.92	C12	1.25				
		C13	0.97				
Total	6.20	+	56.92		+	36.88	100.00

Table F.21 Product distribution for gases and liquids for acetone reaction (Experiment A21).

Catalyst		***T***		***P***	**WHSV**		**H_2 Ratio (mol H_2 / mol acetone)**
HZSM-5 (280)		415°C		101 kPa	5.97 h^{-1}		0
		Liquid					
Gas		Hydrocarbons			Aqueous		
CO_2	3.36	C5	0.52		H_2O	24.11	
CO	0.25	C6	1.98		Acetone	10.31	
C1	0.09	**C6	1.14				
C2	0.00	C7	7.84				
*C2	0.70	C8	11.03				
C3	0.44	C9	21.87				
*C3	1.54	C10	4.85				
C4	4.01	C11	2.29				
*C4	1.82	C12	1.00				
		C13	0.85				
Total	12.21	+	53.37		+	34.42	100.00

Table F.22 Product distribution for gases and liquids for acetone reaction (Experiment A24).

Catalyst	***T***	***P***	**WHSV**	**H_2 Ratio (mol H_2 / mol acetone)**
HZSM-5 (280)	415°C	101 kPa	1.3 h^{-1}	0.5

Gas		Liquid				
		Hydrocarbons		Aqueous		
CO_2	7.41	C5	0.66	H_2O	24.26	
CO	0.80	C6	0.84	Acetone	0.00	
C1	0.30	**C6	1.01			
C2	0.07	C7	8.65			
*C2	1.81	C8	17.97			
C3	1.57	C9	17.17			
*C3	2.13	C10	5.22			
C4	3.08	C11	1.50			
*C4	2.83	C12	1.50			
		C13	1.25			
Total	19.99	+	55.75	+	24.26	100.00

Table F.23 Product distribution for gases and liquids for acetone reaction (Experiment A25).

Catalyst	***T***	***P***	**WHSV**	**H_2 Ratio (mol H_2 / mol acetone)**
HZSM-5 (280)	415°C	101 kPa	2.63 h^{-1}	0.5

Gas		Liquid				
		Hydrocarbons		Aqueous		
CO_2	5.98	C5	0.78	H_2O	25.55	
CO	0.54	C6	0.99	Acetone	0.00	
C1	0.24	**C6	0.89			
C2	0.00	C7	8.56			
*C2	1.40	C8	14.26			
C3	0.85	C9	17.16			
*C3	2.01	C10	7.09			
C4	4.58	C11	1.67			
*C4	3.17	C12	3.26			
		C13	1.02			
Total	18.77	+	55.68	+	25.55	100.00

Table F.24 Product distribution for gases and liquids for acetone reaction (Experiment A27).

Catalyst		***T***		***P***	**WHSV**		**H_2 Ratio (mol H_2 / mol acetone)**
HZSM-5 (280)		415°C		101 kPa	1.3 h^{-1}		1
		Liquid					
Gas		Hydrocarbons			Aqueous		
CO_2	7.07	C5	1.04		H_2O	25.01	
CO	0.82	C6	1.28		Acetone	0.00	
C1	0.34	**C6	1.58				
C2	0.09	C7	10.08				
*C2	1.46	C8	15.24				
C3	1.88	C9	14.23				
*C3	2.14	C10	5.97				
C4	3.55	C11	2.90				
*C4	2.54	C12	1.31				
		C13	1.45				
Total	19.90	+	55.09		+	25.01	100.00

Table F.25 Product distribution for gases and liquids for acetone reaction (Experiment A23).

Catalyst		***T***		***P***	**WHSV**		**H_2 Ratio (mol H_2 / mol acetone)**
HZSM-5 (280)		415°C		101 kPa	1.3 h^{-1}		0.34
		Liquid					
Gas		Hydrocarbons			Aqueous		
CO_2	1.20	C5	1.06		H_2O	30.17	
CO	0.38	C6	1.51		Acetone	0.00	
C1	0.56	**C6	1.69				
C2	0.17	C7	9.82				
*C2	2.30	C8	13.07				
C3	3.82	C9	9.94				
*C3	4.38	C10	6.54				
C4	5.41	C11	1.61				
*C4	3.77	C12	1.31				
		C13	1.31				
Total	21.97	+	47.86		+	30.17	100.00

Table F.26 Product distribution for gases and liquids for acetone reaction (Experiment A30).

Catalyst	***T***	***P***	**WHSV**	**H_2 Ratio (mol H_2 / mol acetone)**
HZSM-5 (280)	415°C	6.8 atm	1.3 h^{-1}	0

Gas		Liquid				
		Hydrocarbons		Aqueous		
CO_2	11.57	C5	0.30	H_2O	20.72	
CO	2.12	C6	0.17	Acetone	0.00	
C1	1.61	**C6	2.18			
C2	0.61	C7	10.21			
*C2	0.42	C8	11.15			
C3	1.23	C9	14.93			
*C3	0.77	C10	5.29			
C4	6.70	C11	2.07			
*C4	4.42	C12	1.94			
		C13	1.58			
Total	29.46	+	49.81	+	20.72	100.00

Table F.27 Product distribution for gases and liquids for acetone reaction (Experiment A31).

Catalyst	***T***	***P***	**WHSV**	**H_2 Ratio (mol H_2 / mol acetone)**
HZSM-5 (280)	415°C	6.8 atm	3.95 h^{-1}	0

Gas		Liquid				
		Hydrocarbons		Aqueous		
CO_2	11.59	C5	0.71	H_2O	18.36	
CO	2.40	C6	0.70	Acetone	5.71	
C1	0.70	**C6	0.87			
C2	0.17	C7	5.99			
*C2	1.16	C8	12.26			
C3	3.18	C9	16.28			
*C3	0.91	C10	5.31			
C4	5.55	C11	2.05			
*C4	3.25	C12	1.57			
		C13	1.28			
Total	28.92	+	47.02	+	24.07	100.00

Table F.28 Product distribution for gases and liquids for acetone reaction (Experiment A32).

Catalyst	***T***	***P***	**WHSV**	**H_2 Ratio (mol H_2 / mol acetone)**
HZSM-5 (280)	415°C	6.8 atm	5.53 h^{-1}	0

Gas		Liquid				
		Hydrocarbons		Aqueous		
CO_2	4.19	C5	3.24	H_2O	24.76	
CO	0.34	C6	1.67	Acetone	7.75	
C1	0.11	**C6	0.64			
C2	0.00	C7	6.17			
*C2	0.47	C8	8.70			
C3	0.28	C9	17.38			
*C3	0.88	C10	7.69			
C4	9.17	C11	2.55			
*C4	1.46	C12	1.12			
		C13	1.42			
Total	16.92	+	50.57	+	32.52	100.00

Table F.29 Product distribution for gases and liquids for acetone reaction (Experiment A32).

Catalyst	***T***	***P***	**WHSV**	**H_2 Ratio (mol H_2 / mol acetone)**
HZSM-5 (280)	415°C	6.8 atm	5.53 h^{-1}	0

Gas		Liquid				
		Hydrocarbon		Aqueous		
CO_2	6.23	C5	1.50	H_2O	21.31	
CO	0.42	C6	2.00	Acetone	13.29	
C1	0.14	**C6	0.90			
C2	0.17	C7	4.77			
*C2	0.95	C8	9.19			
C3	0.30	C9	12.62			
*C3	1.24	C10	4.36			
C4	13.21	C11	1.31			
*C4	3.04	C12	1.47			
		C13	1.58			
Total	25.69	+	39.70	+	34.60	100.00

Table F.30 Product distribution for gases and liquids for acetone reaction (Experiment A33).

Catalyst		***T***		***P***	**WHSV**		**H_2 Ratio (mol H_2 / mol acetone)**
HZSM-5 (280)		415°C		6.8 atm	9.48 h^{-1}		0
Gas		Liquid					
		Hydrocarbons			Aqueous		
CO_2	1.70	C5	1.78		H_2O	22.19	
CO	0.17	C6	2.20		Acetone	21.72	
C1	0.08	**C6	0.84				
C2	0.00	C7	5.57				
*C2	0.27	C8	8.84				
C3	0.26	C9	16.13				
*C3	0.60	C10	6.50				
C4	4.45	C11	1.57				
*C4	1.41	C12	2.72				
		C13	0.99				
Total	8.95	+	47.13		+	43.92	100.00

*Olefin
** Benzene

Table F.31 Product distribution for gases and liquids for acetone reaction (Experiment A34).

Catalyst		***T***		***P***	**WHSV**		**H_2 Ratio (mol H_2 / mol acetone)**
HZSM-5 (280)		415°C		6.8 atm	11.85 h^{-1}		0
Gas		Liquid					
		Hydrocarbons			Aqueous		
CO_2	2.52	C5	0.45		H_2O	17.06	
CO	0.00	C6	0.87		Acetone	34.69	
C1	0.06	**C6	1.04				
C2	0.00	C7	4.29				
*C2	0.13	C8	7.39				
C3	0.19	C9	12.70				
*C3	0.19	C10	4.84				
C4	8.52	C11	1.55				
*C4	0.85	C12	1.33				
		C13	1.32				
Total	12.46	+	35.78		+	51.75	100.00